2008

Mannaric Acid and Mannaric Acid Polyamides: Synthesis and Characterization

Chrissie Ann Carpenter
The University of Montana

MANNARIC ACID AND MANNARIC ACID POLYAMIDES:

SYNTHESIS AND CHARACTERIZATION

By

CHRISSIE ANN CARPENTER

B.A. Chemistry, Carroll College, Helena, Montana, USA, 2002

Dissertation

Presented in partial fulfillment of the requirements
for the degree of

Doctor of Philosophy
in Chemistry

The University of Montana
Missoula, MT

29 September 2008

Approved by:

Dr. David A. Strobel, Dean
Graduate School

Dr. Donald E. Kiely, Chairperson
Chemistry

Dr. Merilyn Manley-Harris
Chemistry

Dr. Christopher P. Palmer
Chemistry

Dr. Holly Thompson
Chemistry

Dr. Andrew Ware
Physics

Carpenter, Chrissie A., Ph.D., Fall 2008 Chemistry

Mannaric Acid and Mannaric Acid Polyamides: Synthesis and Characterization

Chairperson: Donald E. Kiely

D-Mannose, an aldohexose and a C-2 epimer of the common monosaccharide D-glucose, occurs in a pyranose ring form as a component of a variety of plant polysaccharides and is the third most abundant naturally occurring aldohexose after D-glucose and D-galactose, respectively. Historically, D-mannaric acid has been prepared by the nitric acid oxidation of D-mannose. The first published report comes from Haworth *et al.* in 1944 with D-mannaric acid isolated as crystalline D-mannaro-1,4:6,3-dilactone. Nitric acid has been employed for the conversion of aldoses to aldaric acid for decades because it is such a potent oxidant. A new method for the nitric acid oxidation of D-mannose has been developed using a Mettler Toledo RC-1 Labmax reactor. The reaction is monitored with GC-MS and IC to ensure complete oxidation. D-mannaric acid which has been isolated as a new derivative, *N,N*'-dimethyl-D-mannaramide, in a yield of 52%. Characterization of *N,N*'-dimethyl-D-mannaramide was accomplished with GC-MS, ^{1}H and ^{13}C NMR, elemental analysis, and X-ray crystallography.

D-mannaric acid has four chiral centers and a C-2 axis of symmetry but no plane of symmetry and consequently is a chiral molecule. Because of the C-2 axis of symmetry and chirality, polyamides derived from D-mannaric acid are chiral and stereoregular. D-Mannaric acid has been used here as an aldaric acid monomer for a new method of synthesizing polyhydroxypolyamides, PHPAs, based on a stoichiometrically balanced 1:1 ratio of aldaric acid: diamine. Alkylenediammonium salts of D-mannaric acid with varying alkyl chain lengths were synthesized and used as the starting material to give polyamides whose number average molecular weights were determined by ^{1}H NMR end group analysis. All polyamides synthesized were subjected to a post-polymerization in hopes of increasing their size. As with the pre-polymers, the number average molecular weights of polyamides formed from post-polymerizations were determined by ^{1}H NMR end group analysis. X-ray crystal analysis was carried out on octamethylenediammonium D-mannarate to better understand the conformation of the D-mannaryl unit of poly(alkylene D-mannaramides).

Computational analysis has been carried out for D-glucaramides and its derivatives, but has never been attempted for D-mannaric acid or any derivatives thereof. In this work, MM3(96) computational analysis was performed on D-mannaric acid, its dimethyl ester, and three amide derivatives to learn more about the shapes and conformations of these molecules in solution with the hope of better understanding the polymerization reaction and gaining some insight into the three dimensional structures of the resultant polymers.

Acknowledgements

First and foremost I would like to thank Dr. Donald E. Kiely, my Ph.D. advisor and mentor. Dr. Kiely accepted me into his lab, presented me with my research project, and has advised and supported me, both financially and emotionally, for the past five years. For his encouragement and belief in my abilities I will always be thankful.

Dr. Merilyn Manley-Harris has also been instrumental in my graduate career. In both the Shafizadeh Center and in her laboratory at the University of Waikato, Dr. Manley-Harris has been a teacher, a mentor and a friend. I thank her for her support and for making my time in New Zealand absolutely amazing.

My parents, Jere and Debbie Carpenter, and my sister, Whitney Moen, along with the rest of my family deserve a special acknowledgement and thanks. Without their love, encouragement, and support I would not be where I am today.

I want to thank everyone in the Shafizadeh Center; Kirk Hash, Sr., Michael Hinton, Kylie Kramer, and Tyler Smith for making my time here enjoyable.

Thank you to everyone on my Ph.D. committee for their guidance and time; Dr. Holly Thompson, Dr. Chris Palmer, Dr. Andrew Ware, and Dr. Merilyn Manley-Harris.

This research was supported by funding from the United States Department of Agriculture Cooperative Research, Education, and Extension Service.

Table of Contents

List of Tables

List of Figures

Chapter 1

Chapter 3

List of Schemes

Chapter 1

Chatper 2

List of Abbreviations

4-AcNH-TEMPO	4-Acetamido-2,2,6,6-tetramethylpiperidine 1-oxyl
DABCO	1,4-diazabicyclo[2.2.2]octane
D_2O	Deuterated Water
D.I. H_2O	Deionized Water
dp	Degree of Polymerization
DMSO	Dimethyl Sulfoxide
DMSO-d_6	Deuterated Dimethyl Sulfoxide
EtOH	Ethanol
Et_3N	Triethylamine
GC-MS	Gas Chromatography/Mass Spectrometry
HNO_3	Nitric Acid
IC	Ion Chromatography
MeOH	Methanol
$NaNO_2$	Sodium Nitrite
NaOMe	Sodium Methoxide
NMR	Nuclear Magnetic Resonance
PHPAs	Polyhydroxypolyamides
TFA	Trifluoroacetic Acid
TFA-d_1	Deuterated Trifluoroacetic Acid

Dissertation Overview

This focus of this dissertation is the chemistry of the naturally occurring aldohexose D-mannose and derivatives thereof. The dissertation is organized into three main body chapters: 1) D-Mannaric Acid: Variations in the Nitric Acid Oxidation of D-Mannose, 2) Synthesis of Some Poly(D-mannaramides) from their Corresponding Diammonium Salts, and 3) MM3(96) Conformational Analysis of D-Mannaric Acid and Some Ester and Amide Derivatives as Models for the D-Mannaryl Unit of Poly(Alkylene D-Mannaramides). These chapters are designed to stand alone and each has its own introduction, literature review, and summary. The final chapter is a brief conclusion to summarize all the findings and also to highlight possible areas of further research. References are organized by chapter and all are found at the end of this work.

Chapter 1

D-Mannaric Acid: Variations in the Nitric Acid Oxidation of D-Mannose

1.1 Introduction

1.1.1 D-Mannose

D-Mannose is an aldohexose and a C-2 epimer of the common monosaccharide D-glucose, Figure 1.[1]

D-mannose D-glucose

Figure 1. Acyclic structures of D-mannose and D-glucose showing the difference in stereochemistry at C_2

D-Mannose occurs in a pyranose ring form as a component of a variety of plant polysaccharides and is the third most abundant naturally occurring aldohexose after D-glucose and D-galactose, respectively.[1] The monosaccharide was first synthesized by Emil Fischer in 1887 by nitric acid oxidation of D-mannitol and later isolated from the acid hydrolysis of the polysaccharide mannan.[1]

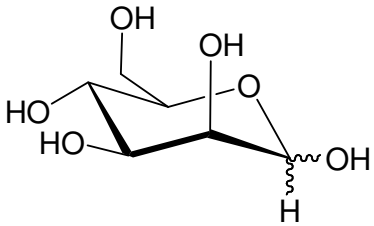

Figure 2. α/β-D-mannopyranose (**1**)

1.1.2 Oxidation of D-Mannose and Isolation of D-Mannaric Acid

Historically, D-mannaric acid (**2**) has been prepared by the nitric acid oxidation of D-mannose (**1**). The first published report comes from Haworth *et al.* in 1944 with **2** isolated as crystalline D-mannaro-1,4:6,3-dilactone (**3**).[2]

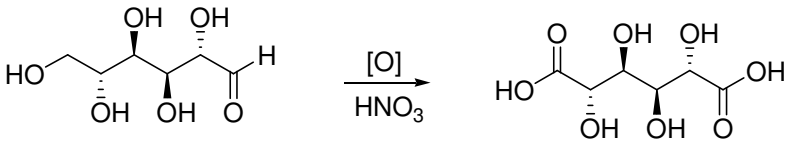

(1) **(2)**

Scheme 1. Nitric acid oxidation of D-mannose (**1**) to D-mannaric acid (**2**)

Oxidation was achieved in 4 hours at 55 °C, the oxidation mixture was concentrated to dryness at 80 °C, and the crude product triturated with ethanol-ether to give **3** in a yield of 25.9 %. Employing even more severe oxidation conditions (4 hours at 60 °C followed by 30 min at 85 °C), **3** was isolated in a slightly better yield of 31.0%.[2] Given such severe oxidation conditions it is clear that **2** is a reasonably stable molecule to further oxidation. More recently, Kiely and Ponder reported a 61.8% yield **3** after HNO_3 oxidation of **1** with $NaNO_2$ as a catalyst followed by extraction of nitric acid with isopropyl ether.[3]

Nitric acid has been employed for the conversion of aldoses to aldaric acid for decades because it is such a potent oxidant.[4] However, the mechanism of the nitric acid oxidation is not well understood, and the true nature of the oxidant is not known. It has been suggested that the actual oxidant may be nitrous acid, which, in the presence of nitric oxide, is in an equilibrium with nitric acid, Equation 1.1.[4]

$$HNO_3\ (l) + 2\ NO\ (g) + H_2O\ (l) \rightleftharpoons 3\ HNO_2\ (l) \qquad (\mathbf{1.1})$$

A generally accepted view of the oxidation mechanism is that the alcohol function forms an intermediate nitrate or nitrite ester followed by β-elimination to generate a carbonyl function and nitrogen dioxide or nitric oxide, respectively.[4] With reducing sugars, it is thought that the anomeric hydroxyl group is oxidized directly to a lactone carbonyl oxygen.[4] Equilibria between various lactone forms and the acyclic form are established quickly under such strongly aqueous acidic conditions.[4] The use of a nitrite salt, such as sodium nitrite, has been reported to initiate the oxidation.[3, 5, 6]

Nitrogen dioxide is produced as a reduction product of the oxidation and is involved in two important aqueous equilibria, one with nitric acid and nitrous acid and the other with nitric acid and nitric oxide, Equations 1.2 and 1.3. Nitrogen dioxide therefore generates nitric acid as well as nitric oxide and nitrous acid. Nitric oxide is also a further reduction product of the oxidation and readily forms nitrogen dioxide in the presence of oxygen, Equation 1.4. Nitrogen dioxide can then regenerate nitric and nitrous acids, as previously stated. Other relevant transformations include conversion of nitrous acid into nitric acid, nitric oxide, and water; coupling of nitrogen dioxide with nitric oxide under equilibria conditions to give dinitrogen trioxide, and dimerization of nitrogen dioxide give dinitrogen tetraoxide, Equations 1.5, 1.6 and 1.7. In short, various NOx gases are formed directly from the nitric acid oxidation or generated from reactions and equilibria thereof, but ultimately regenerate nitric acid in concert with oxygen oxidation of nitric oxide to nitrogen dioxide. While previous benchtop nitric acid oxidation methods with **1** have been successful, control of the reaction is challenging because the reaction is highly exothermic and can be violent.[7] Containing NOx gases in a closed vessel and using them to regenerate nitric acid and further the oxidation would

offer a significant improvement to benchtop methods where these gases were simply released into the atmosphere.

$$2\ NO_2\ (g) + H_2O\ (l) \rightleftharpoons HNO_3\ (l) + HNO_2\ (l) \quad (\mathbf{1.2})$$

$$3\ NO_2\ (g) + H_2O\ (l) \rightleftharpoons 2\ HNO_3\ (l) + NO\ (g) \quad (\mathbf{1.3})$$

$$2\ NO\ (g) + O_2\ (g) \longrightarrow 2\ NO_2\ (g) \quad (\mathbf{1.4})$$

$$3\ HNO_2\ (l) \longrightarrow HNO_3\ (l) + 2\ NO\ (g) + H_2O\ (l) \quad (\mathbf{1.5})$$

$$NO\ (g) + NO_2\ (g) \rightleftharpoons N_2O_3\ (g) \quad (\mathbf{1.6})$$

$$2\ NO_2\ (g) \rightleftharpoons N_2O_4\ (g) \quad (\mathbf{1.7})$$

NOx gases formed and released throughout the oxidation process can form smog in the atmosphere, a significant form of air pollution. NOx gases also react with atmospheric moisture to form a component of acid rain. The U.S. EPA regulates emissions of NOx gases as does the Department for Environment, Food and Rural Affairs in the UK. In 1997 the Kyoto Protocol classified N_2O, one of the NOx gases, as a greenhouse gas. Containing these NOx gases and recycling them to regenerate nitric acid and further the oxidation would eliminate pollution affects of such oxidations and offer improved air quality as compared with simply releasing them into the atmosphere.

The amount of nitric acid used to oxidize monosaccharides has been varied according to different reports. While three moles of nitric acid are theoretically needed to oxidize one mole of sugar, an 8:1 ratio was used by Haworth *et al*. in the benchtop oxidation of **1**.[2] Later Mehltretter stated that in the oxidation of glucose a 4 : 1 molar ratio of nitric acid to monosaccharide was preferred.[5] Kiely *et al*. reported nitric acid to sugar molar ratios of 3:1[6] and 4:1, which subsequently gave the best reported yield of **3.**[3]

Oxidation of aldoses to aldaric acids has also been reported using both bromine and chlorine as terminal oxidants with 4-AcNH-TEMPO as a catalyst.[8] It was reported that terminal oxidants, chlorine and bromine in this case, oxidize only the anomeric hydroxyl and primary alcohol groups and leave secondary alcohol groups untouched. With chlorine as the terminal oxidant, D-glucose oxidation gave a yield of 80 % D-glucaric acid.[8] Successful oxidations were completed for D-glucose, D-galactose and D-mannose with bromine as the terminal oxidant with yields of 90% and 70% reported for D-glucaric and D-galactaric acid, respectively. D-Mannaric acid was isolated as its crude disodium salt contaminated with 15 % tartarate and 10 % unidentified product.[8]

Other D-mannose oxidation methods have been employed in which the final product was not mannaric acid. For example, silver oxide in the presence of potassium hydroxide was used to oxidize D-mannose and other monosaccharides, the oxidation producing carbon dioxide, oxalic acid, formic acid, and glycolic acid.[9] It has been reported that oxidations of D-mannose with tetramethylammonium chlorochromate in aqueous acetic acid gives arabinose and formic acid.[10] Oxidations with oxygen as the oxidant using metal catalysts such as gold, platinum, and nickel in the form of titanium dioxide and aluminum trioxide have been reported; the oxidations leading predominantly to D-mannonic acid.[11] In some such oxidations, D-mannose is present in the final product as well as a relatively small amount of D-mannaric acid.[12]

1.1.3 Some Properties of D-Mannaric acid and D-Mannaro-1,4:6,3-dilactone

D-Mannaric acid has four *S*-designated chiral centers and a C-2 axis of symmetry, but has no plane of symmetry and is a chiral molecule. When displayed in an extended

conformation, D-mannaric acid, unlike D-glucaric acid, is free of destabilizing 1,3-parallel hydroxyl group eclipsing steric interactions, Figure 3.

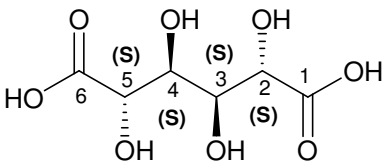

D-mannaric acid

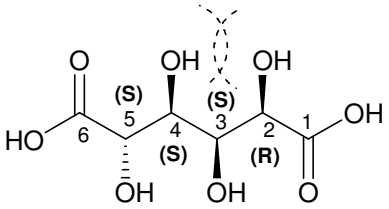

D-glucaric acid

Figure 3. Extended conformation of D-mannaric acid and D-glucaric acid

Under reduced pressure and with heating D-mannaric acid readily undergoes dehydration to form a dilactone molecule, *i.e*. D-mannaro-1,4:6,3-dilactone (**3**). Mannarodilactone is stable in that its five-membered lactone rings are only slowly hydrolyzed in water at neutral pH. The dilactone is a crystalline molecule in contrast to acyclic D-mannaric acid which, as of yet, has not been reported as crystalline.[7] Mannarodilactone is base labile and undergoes β-elimination reactions to give enol and/or enol-ether products.[7]

Meso-Galactaric acid, like diastereomeric D-mannaric acid, lacks destabilizing 1,3-parallel hydroxyl group eclipsing steric interactions in an extended conformation. Results from an X-ray crystal structure study showed that *meso*-galactaric acid adopts an extended conformation in the solid state.[13] By comparison, D-glucaric acid, with destabilizing 1,3-parallel hydroxyl group eclipsing steric interactions in an extended conformation, crystallizes in a bent or sickle conformation.[14] Based upon the conformational comparisons to *meso*-galactaric acid and D-glucaric acid it is reasoned that the acyclic form of D-mannaric acid may be dominated by an extended conformation.

1.1.4 X-ray Crystallography

X-ray crystallography is the most common experimental method to obtain a detailed picture of a molecule in the solid state. It is accomplished by interpretation of the diffracted x-rays from identical molecules in an ordered array. This technique also provides structural information such as molecule absolute configuration, bond lengths and angles, and symmetry of the molecule.[15, 16] There are, however, some limitations to x-ray crystallography analysis. Single-crystal x-ray crystallography requires a crystal of good quality and size, but the requirements for a good quality of crystal vary with the compound to be analyzed. Some compounds cannot be crystallized and for the compounds that can be crystallized there is variation in the ease of crystallization. Finding the appropriate conditions to produce good crystals of a specific molecule often requires many careful trials and may be considered more art than science.[16] Furthermore, there is no way to consistently and reliably predict crystal structures.[17]

A crystal consists of atoms arranged in a pattern repeated in three dimensions.[18] The unit cell is the simplest and smallest volume element that is completely representative of the whole crystal, Figure 4.[16]

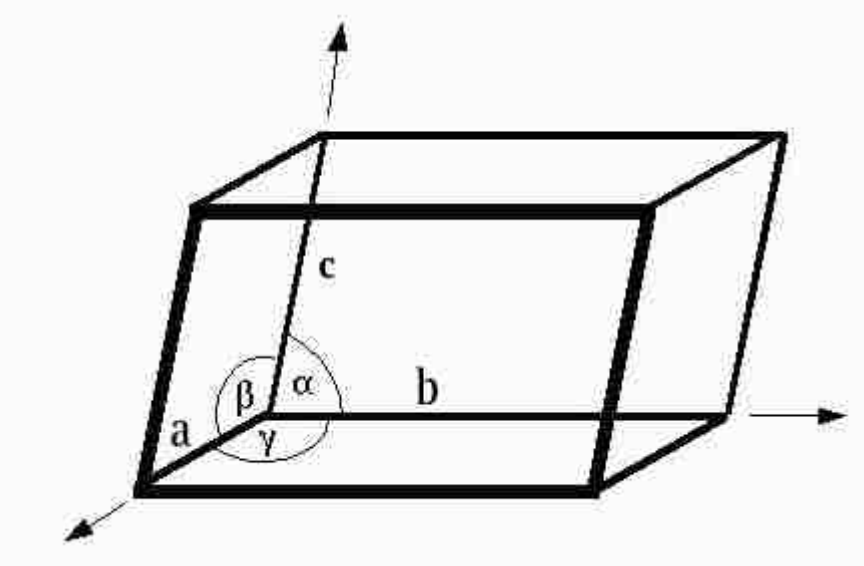

Figure 4. Depiction of a unit cell showing length and angle parameters

If the exact content of the unit cell is known, the whole crystal system can be imagined as an efficiently packed array of many unit cells stacked beside and on top of each other.[16] The length of the unit cell is described by the vectors a, b, and c corresponding to the Cartesian coordinates z, x, and y respectively. The angles of the unit cell are described by the parameters α, β. and γ.[15] The location of an atom within the unit cell is given in terms of the length and angle coordinates.[16]

1.1.5 Aims of This Research

- Improve on previous benchtop nitric acid oxidation methods with D-mannose, making them more effective and efficient under less severe conditions
- Regenerate nitric acid aided by continuous oxidation of NO to NO_2
- Crystallize a derivative of D-mannaric acid for x-ray crystallographic analysis to better understand the conformation of the mannaryl unit

- Isolate D-mannaric acid as a stable derivative with increased yields for use in the synthesis of stereoregular, chiral polyhydroxypolyamides.

1.2 Results and Discussion

1.2.1 Oxidation

Reaction Conditions

In an effort to control the highly exothermic nature of the nitric acid oxidation of D-mannose, and therefore increase product yields and limit formation of unwanted by-products, oxidations were carried out in a Mettler Toledo RC-1 Labmax reactor. The reactor is well suited for this application as it is designed as a computer controlled temperature/pressure controlled closed-system reactor. As a closed-system reactor, all NOx gases generated are contained in the reaction vessel. To aid in the regeneration of nitric acid from these gases, the oxidation was carried out under a positive pressure by addition of oxygen gas which rapidly oxidizes nitric oxide to nitrogen dioxide. Nitrogen dioxide then regenerates nitric acid through a series of reactions (Equations 1.1-1.7) and serves to further the oxidation. As with benchtop oxidations, a nitrite salt, sodium nitrite, was used to initiate the nitric acid oxidation.

The initial oxidation conditions employed for the oxidation of D-mannose were patterned after those reported for D-glucose oxidations[19] An experimental schematic for the oxidation, Oxidation Experimental Method 1, is provided in Figure 5. The stars indicate when samples were taken for GC-MS analysis.

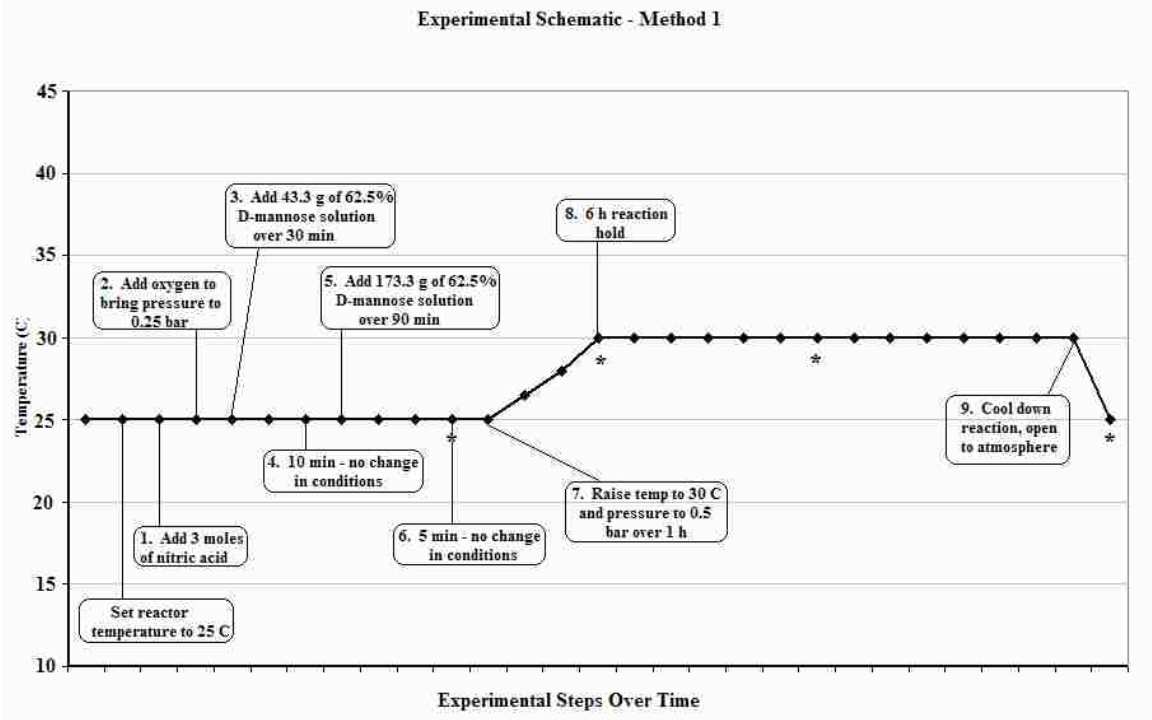

Figure 5. Experimental Schematic of Oxidation Method 1, 4:1 Molar Ratio Oxidation at 25 °C.

During the course of the oxidation, samples were taken and analyzed by GC-MS as their per-*O*-trimethylsilyl derivatives. Results from the GC-MS analysis showed that D-mannose was still present after the second dosing step (D-mannose addition step), 79%, but by the end of the reaction both D-mannonic acid and D-mannaric acid had been formed to some extent. In comparison, oxidation of D-glucose employing the same experimental protocol showed no unreacted D-glucose at the end of dosing and a final product mixture that was dominated by D-glucaric acid, 86% based on integration. These results suggest that both the first oxidation of the anomeric hydroxyl group and the second oxidation of the C-6 primary alcohol function were more difficult to achieve for D-mannose as compared to D-glucose.

Modifications were then made to Oxidation Experimental Method 1 to develop a new method for the complete oxidation of D-mannose. The first experimental

modification, Oxidation Method 2, included an increase in temperature in both the dosing steps (30 °C) as well as the reaction hold step (40 °C). This method provided somewhat better results as there was no mannose present after dosing, but the oxidation was still not complete at the end of the designated reaction time. Based on integration results 80% of the final reaction mixture was D-mannaric acid.

The next experimental modification, Oxidation Method 3, involved carrying out the oxidation as outlined in Figure 6; concentrating the reaction mixture to a thick syrup under reduced pressure, dissolving the syrup in an amount of nitric acid equal to that used in the beginning of the procedure, and putting the solution back into the LabMax reactor for a second reaction hold (Step 11) under the same conditions as the first reaction hold. In summary, two nitric acid oxidative steps (both with a 4:1 molar ratio of acid/sugar) were employed in this method. This modification provided a product mixture consisting of 100% D-mannaric acid and no D-mannose. Thus, the use of additional nitric acid and a second reaction hold provided the necessary energy for complete oxidation of D-mannose. Figure 6 shows the experimental schematic for Experimental Oxidation Method 3. The stars indicate when samples were taken for GC-MS analysis.

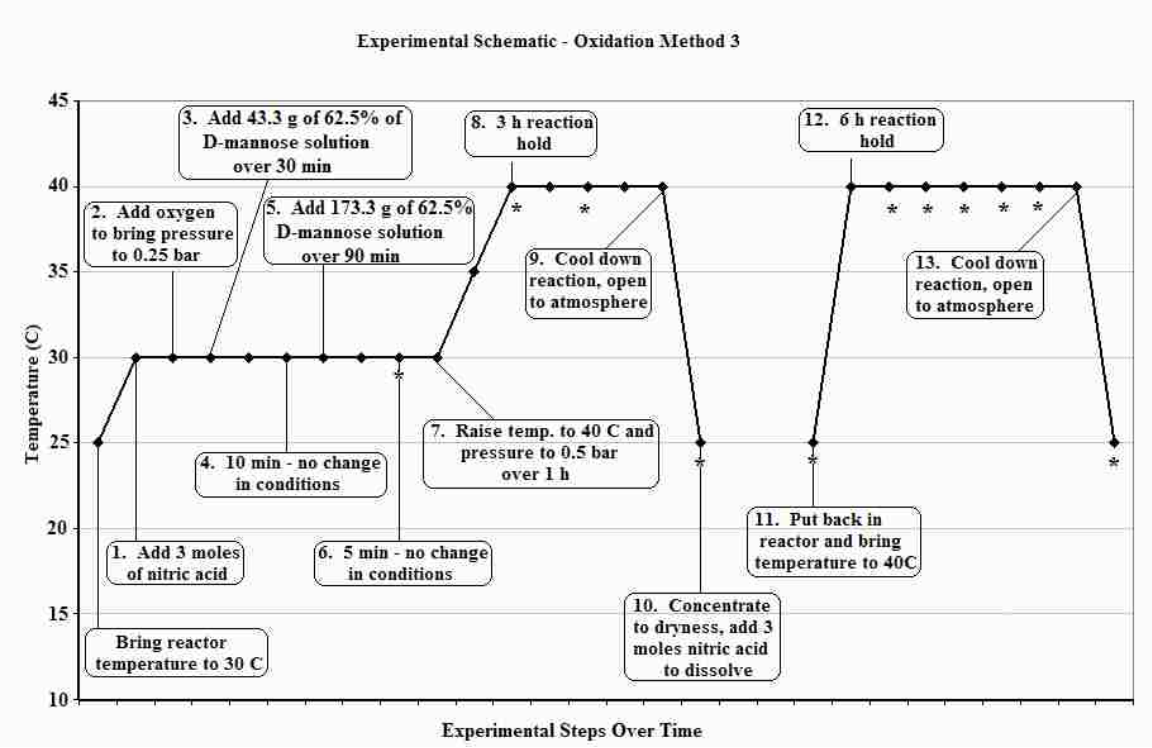

Figure 6. Experimental Schematic of Oxidation Method 3, 4:1 Molar Ratio Oxidation at 30 °C.

While Oxidation Method 3 provided a reaction mixture consisting of 100% of the desired product, D-mannaric acid, it was a lengthy and somewhat cumbersome procedure. Thus, a further experimental modification, Oxidation Method 4, was carried out using an increased amount of nitric acid (5 moles) to give a molar ratio of 6.67:1 nitric acid:D-mannose. The reaction was carried out under the same conditions as Experimental Oxidation Method 3 but was only applied once. GC-MS data showed that the oxidation was complete and no mannonic acid remained. Oxidation Method 4 not only provided the desired product but it eliminated the concentration step, the need for additional nitric acid, and the second reaction hold. Based on these results, Experimental Oxidation Method 4 (6.67:1 molar ratio nitric acid to D-mannose) was chosen as the preferred

oxidation method. Figure 7 shows the experimental schematic for Oxidation Method 4. The stars indicate when samples were taken for GC-MS analysis.

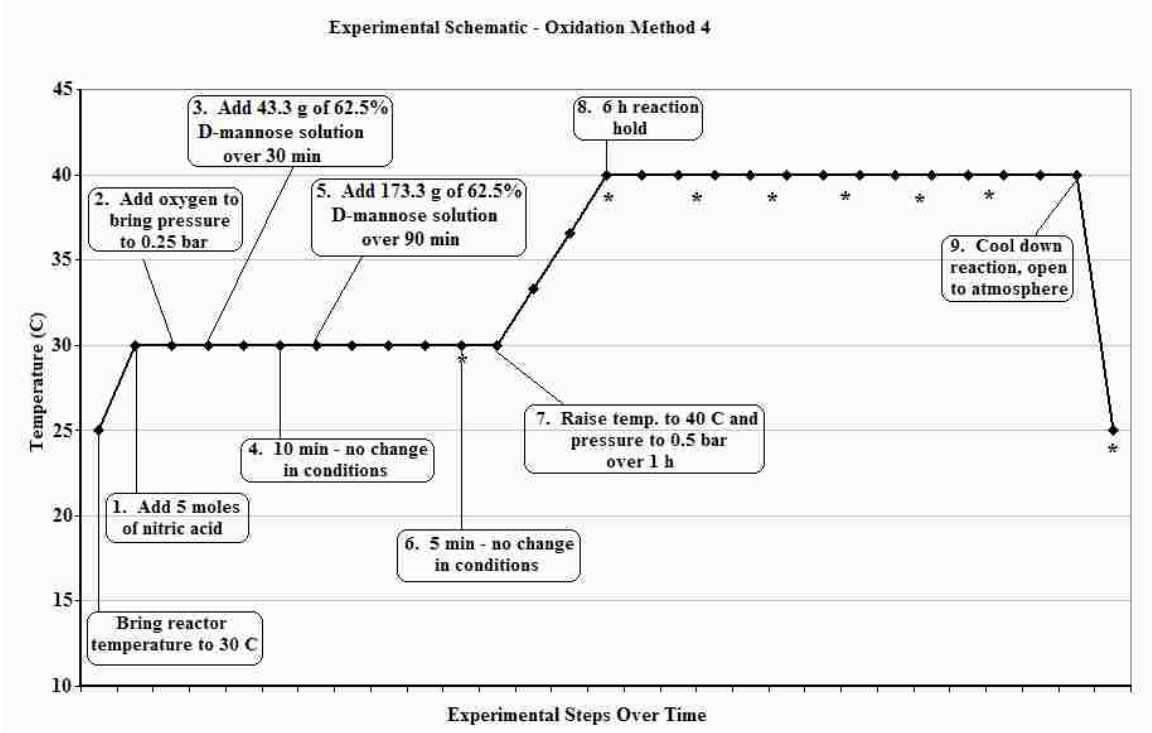

Figure 7. Experimental Schematic of Oxidation Method 4, 6.67:1 Molar Ratio Oxidation at 30 °C.

GC-MS Monitoring of Reaction

All samples were analyzed as their per-*O*-trimethylsilyl derivatives. GC-MS Method 1 is a GC-MS temperature program used routinely in this laboratory for carbohydrate analysis and it was initially employed for D-mannose oxidation mixture analysis. However, it was determined that peaks from the two main products formed, D-mannonic acid and D-mannaric acid, overlapped in the GC using Method 1 and as baseline separation of the aldonic and aldaric acid is necessary to evaluate the course of an oxidation, a new temperature program with a much slower temperature ramp was developed, GC-MS Method 2. Using this method D-mannonic and D-mannaric acid

could be separated as two peaks with baseline resolution. Hereafter GC-MS Method 2 was used for GC-MS analysis of all oxidation samples. Some of the results contained herein were obtained with GC-MS Method 1; however, most were obtained with GC-MS Method 2.

D-Mannaric acid and D-mannonic acid are clearly differentiated by their mass fragmentation patterns, Figures 11 and 12. Many of the middle to small mass range fragments are the same but the $[M - 15]^+$ peaks, arising from a loss of CH_3 from a TMS group, are unique to each species; for D-mannaric acid *m/z* = 627 and for D-mannonic *m/z* = 613.[20] These mass fragments were used for compound identification purposes.

The largest peak in the mass fragmentation is pattern of both mannonic and mannaric acid is *m/z* = 333 and it is formed from the loss of TMSOH from m\z = 423.[21] To account for this intensity a rearrangement is suggested in which the TMS group from C4 migrates to the carbonyl oxygen of C1 in conjunction with loss of C5, C6 and corresponding functional groups; this gives a m\z = 423.[21] This is followed by loss of TMSOH from C2 to give the very favorable m\z = 333 ion with resonance stabilization.[21] A McClafferty rearrangement involving migration of the C2 TMS group to the C1 carbonyl oxygen followed by fragmentation between C2 and C3 accounts for the characteristic peak at m\z = 292.[20] It is noted that the peaks m\z = 73 and m\z = 147 are characteristic of per-*O*-trimethylsilyl derivatives of carbohydrates.[21]

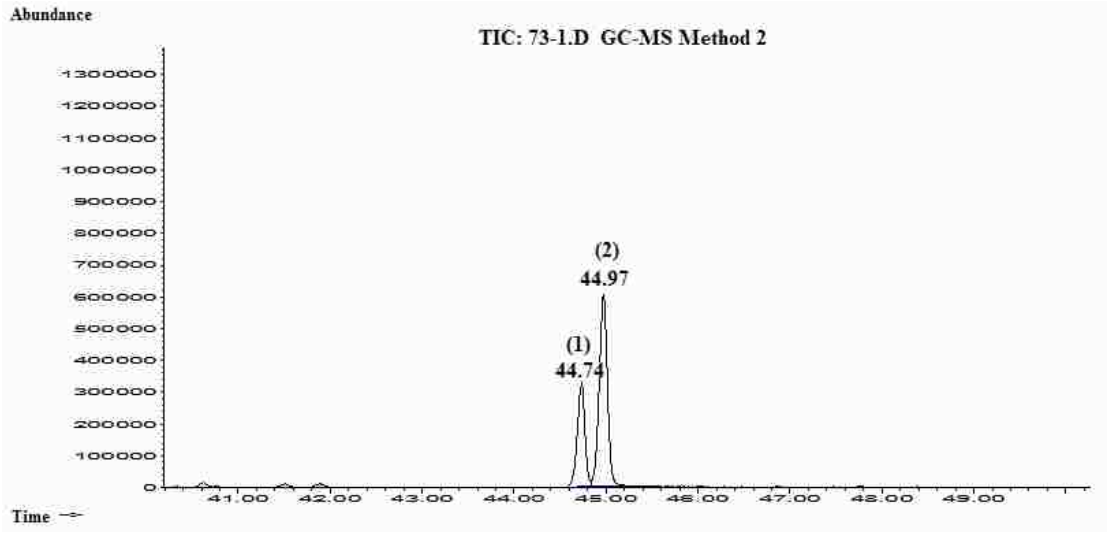

Figure 8. Gas chromatogram of an oxidation mixture using GC-MS Method 2 showing separation of peak 1, per-*O*-TMS-D-mannaric acid, and peak 2, per-*O*-TMS-D-mannonic acid

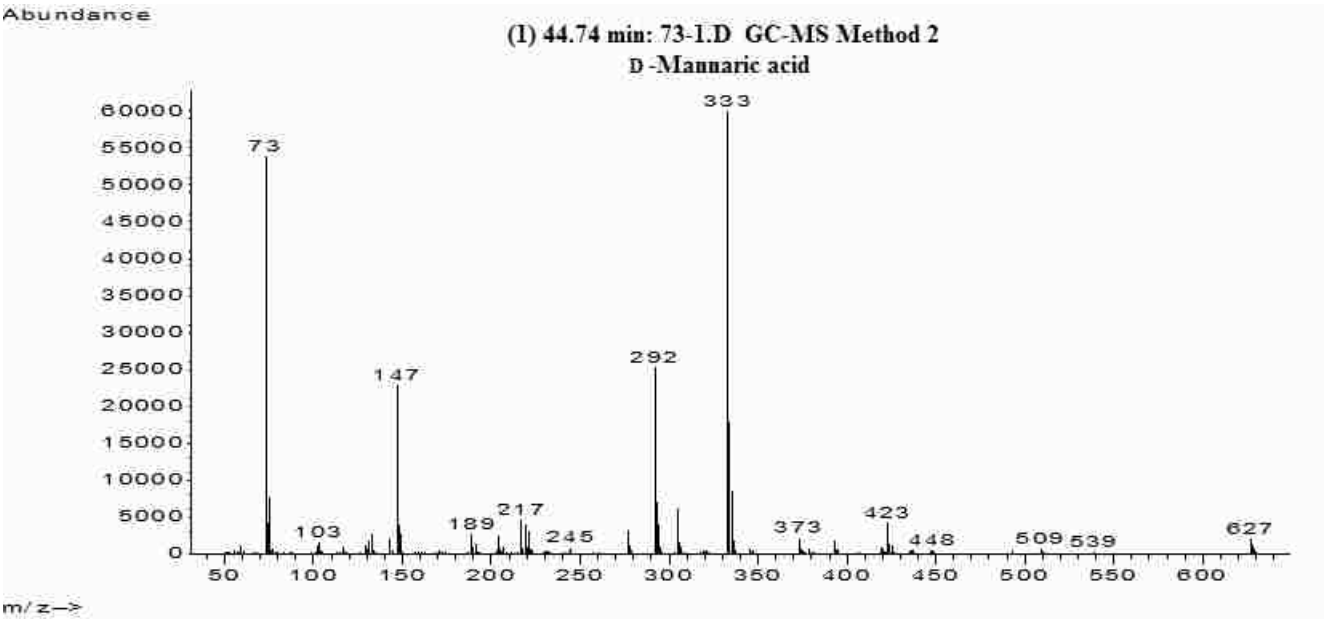

Figure 9. Mass spectrum of peak 1, per-*O*-TMS-D-mannaric acid, with retention time 44.74 min

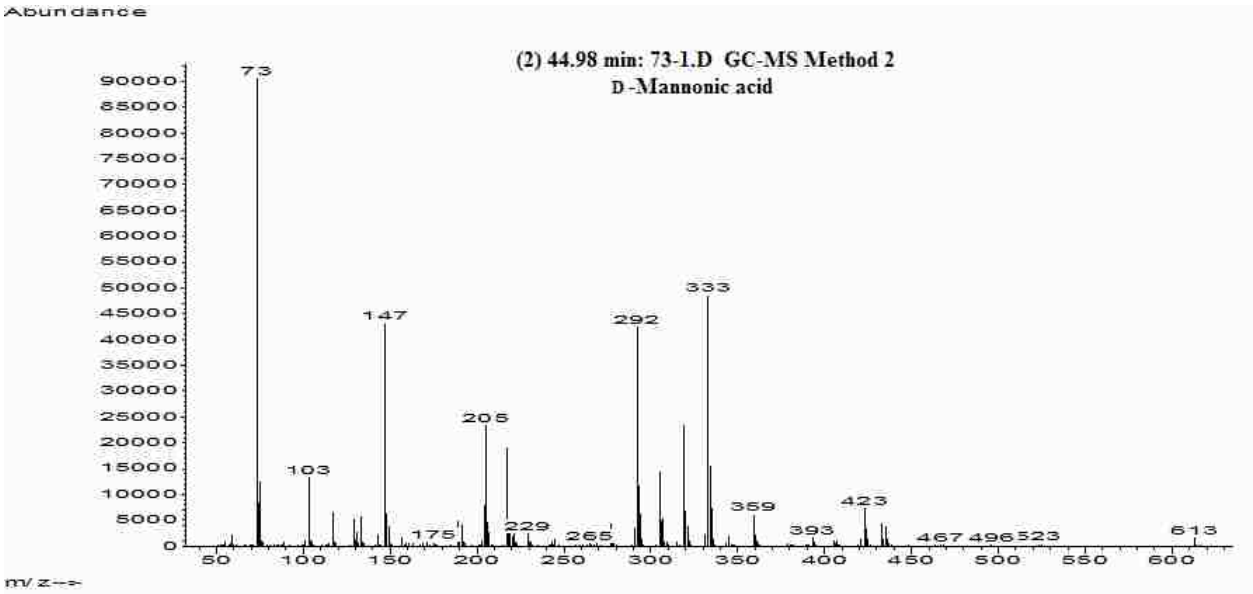

Figure 10. Mass spectrum of peak 2, per-O-TMS- D-mannonic acid, with retention time 44.98 min

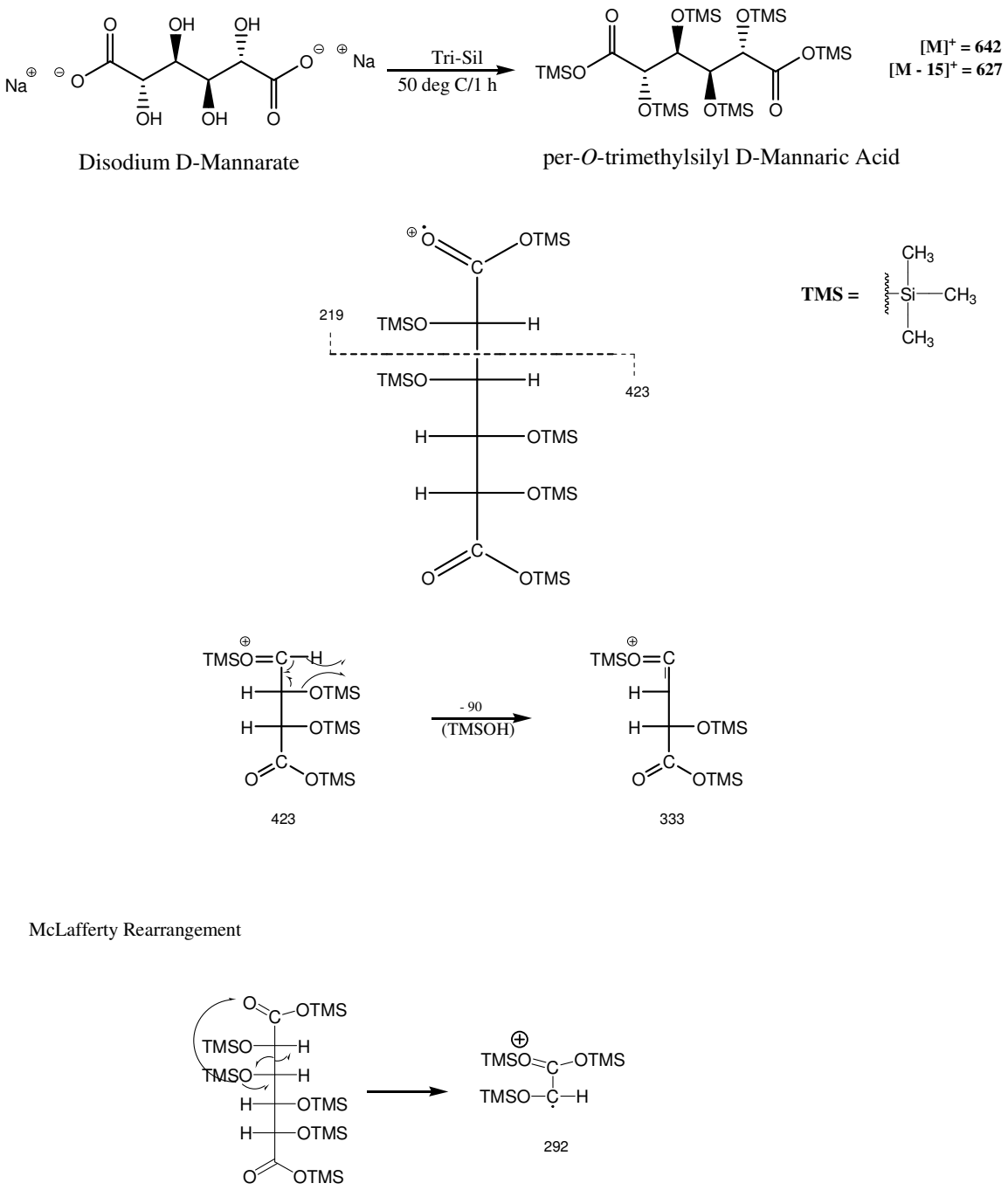

Figure 11. Important mass fragmentations for per-O-trimethylsilyl D-mannaric acid including a McLafferty Rearrangement[20]

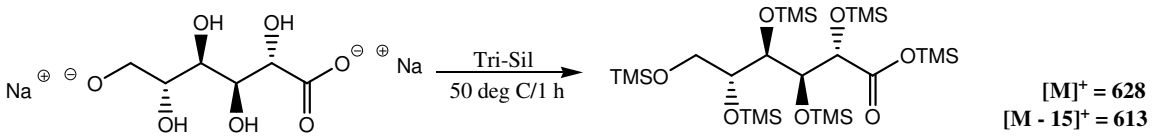

Disodium D-Mannonate per-*O*-trimethylsilyl D-Mannonic Acid

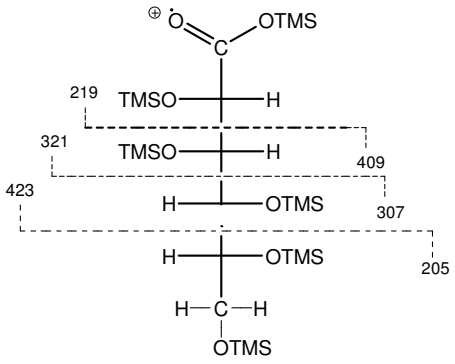

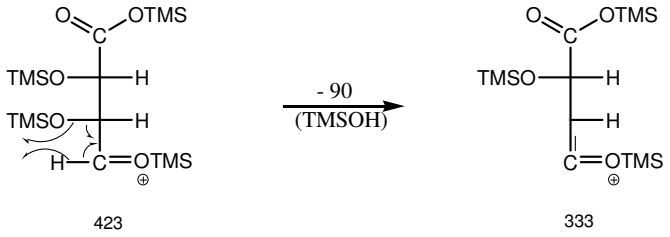

423 333

McLafferty Rearrangement

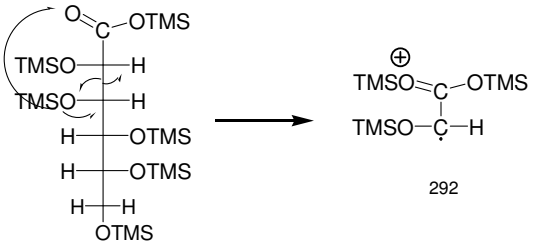

292

Figure 12. Important mass fragmentations for per-O-trimethylsilyl D-mannonic acid including a McLafferty Rearrangement[20]

1.2.2 Isolation of D-mannaric-1,4:6,3-dilactone (3) from the Oxidation of D-Mannose *via* Disodium D-mannarate and a Nanofiltration Step

Mannaric acid has been previously isolated as its dilactone, D-mannaro-1,4:6,3-dilactone (**3**), after concentration of the syrupy acidic product mixture.[2,3] An alternative route to the dilactone isolation was undertaken in order to minimize the amount of nitric acid present in the final product mixture and to facilitate more efficient crystallization of D-mannaro-1,4:6,3-dilactone (**3**). The route evaluated involved treating the crude product mixture with sodium hydroxide to neutralize residual nitric acid plus generate disodium D-mannarate. The salt solution was then passed through a nanofilter, with the permeate holding the bulk of the sodium nitrate and the retentate holding most of the disodium D-mannarate and other minor hydroxy acid sodium salts. Scheme 2 shows the overall reaction scheme for the oxidation of **1** and the isolation of **3** employing a nanofiltration purification step. As disodium D-mannarate (**5**) was the targeted starting material for further chemistry, discussed in detail in Chapter 3, its preparation required sodium hydroxide hydrolysis of **3.** D-Mannaro-1,4:6,3-dilactone (**3)** is base labile and susceptible to unwanted β-elimination reactions to produce enol and/or enol ether by-products. These side reactions lowered product yield with isolated yield only 34%, caused coloration of the material, and rendered this route to the **5** impractical.

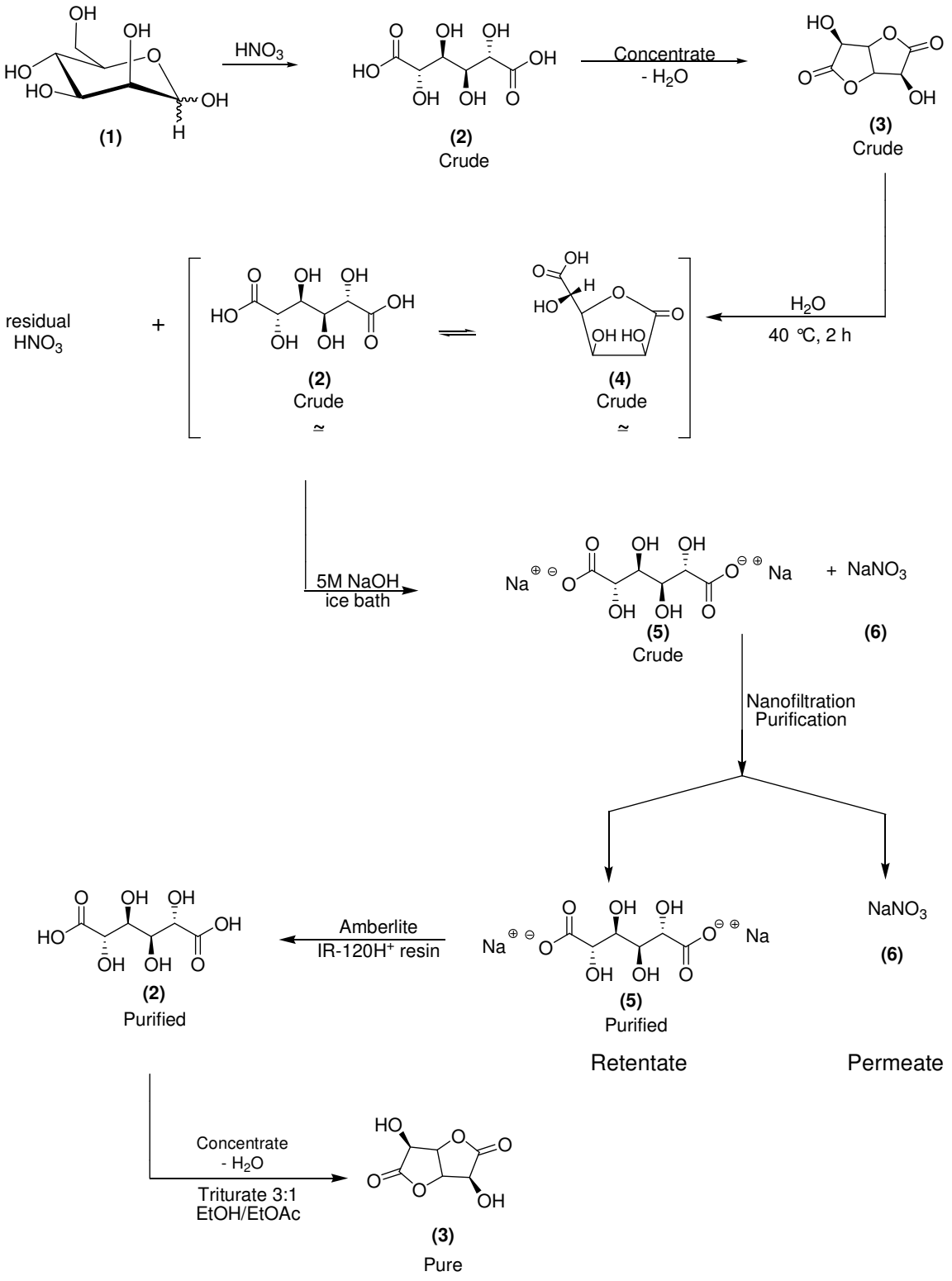

Scheme 2. Nitric acid oxidation of D-mannose – nanofiltration purification method

^{1}H and ^{13}C NMR Characterization of D-mannaric-1,4:6,3-dilactone

The assigned ^{1}H and ^{13}C NMR were consistent with a literature report, Figure 16 and 17.[22] It is worth noting that only two signals are seen because the H2 and H5 are equivalent (5.31 ppm) as are H3 and H4 (4.98 ppm), $J_{2,3} = J_{4,5} = 5.86$ Hz. There is no vicinal coupling between magnetically equivalent protons H3 and H4.

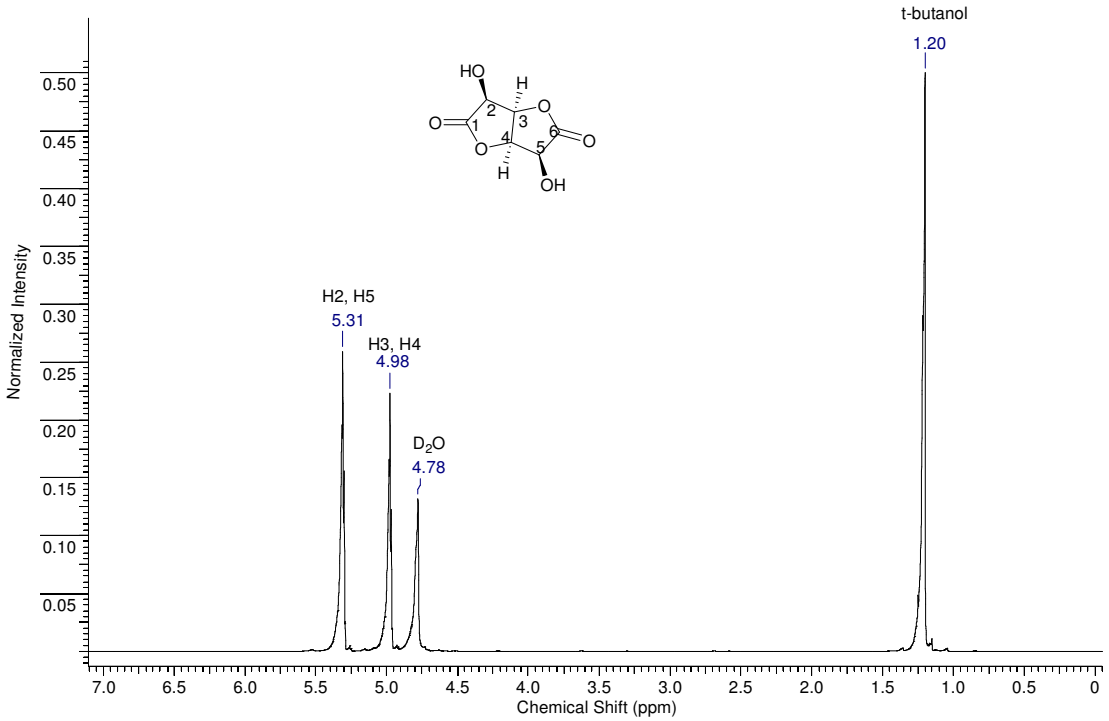

Figure 13. Assigned ^{1}H NMR spectrum of **3** in D_2O

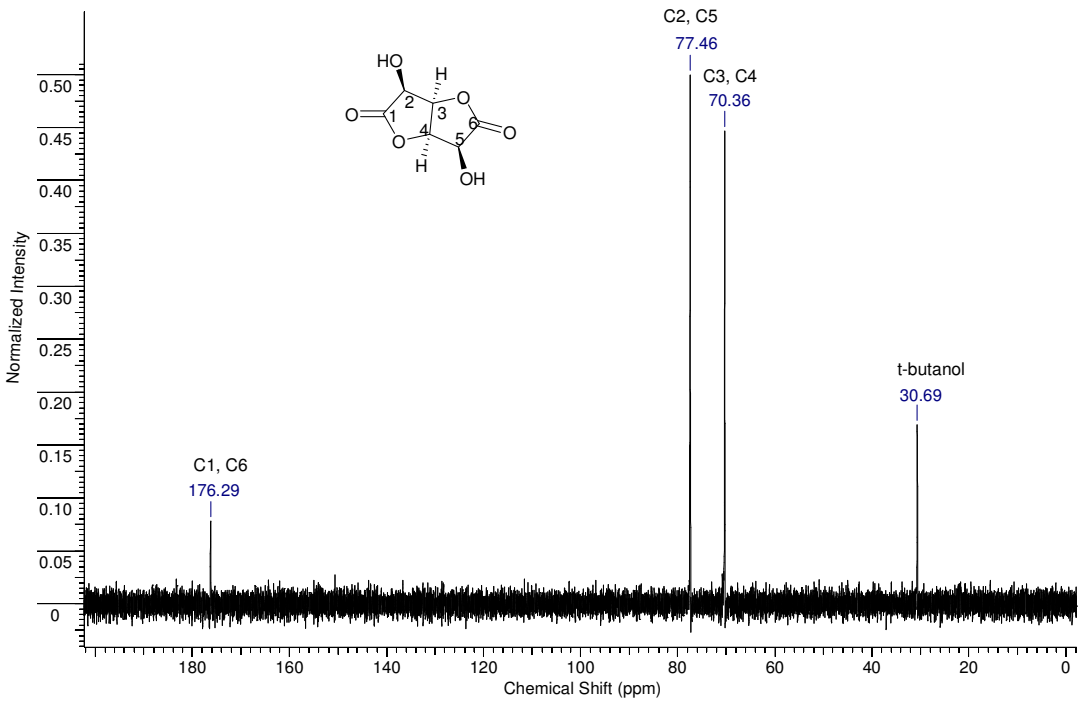

Figure 14. Assigned ^{13}C NMR spectrum of **3** in D_2O

1.2.3 Isolation of *N,N´*-dimethyl-D-mannaramide (9) from the Oxidation of D-Mannose

A suitable route to disodium D-mannarate (**5)** was undertaken that avoided the direct sodium hydroxide hydrolysis of **3**, Scheme 3, and proceeded through an acyclic diamide, *N,N´*-dimethyl-D-mannaramide (**9**). It was reasoned that such a route would minimize β-elimination reactions and colored product formation associated with base hydrolysis of **3**. This was accomplished by esterification of **3**, Scheme 3, with methanolic hydrogen chloride to give a mixture of the methyl ester lactone (**7**) and acyclic dimethyl mannarate (**8**). Aminolysis of **7** and **8** with methylamine in methanol provided acyclic diamide **9**. This isolation procedure turned out to be the preferred method for isolation of a mannaric acid derivative with isolated yields of 52.9% for **9.** Furthermore, sodium hydroxide hydrolysis of **9** to form **5** proceeded with quantitative yield.

A diffusion dialysis modification to remove nitric acid from the oxidation mixture prior to isolation of **9** was also used in hopes of isolating the diamide in higher yield. However, methanol work-up provided an isolated yield of only 30.9% and work-up with absolute ethanol only 35.2%. The greater product recovery from absolute ethanol over methanol is consistent with my observation that derivatives of mannaric acid are much less soluble in ethanol than methanol. However, more ethanol is required to obtain a solution from the concentrated mannaric acid (thick syrup). In fact, only with the addition of acetyl chloride with stirring did the mixture dissolve.

Using the diffusion dialysis method took more time and provided decreased yields compared with isolation of **9** directly from an oxidation mixture. However, the IC data showed the presence of carbohydrate acids in the reclaimed acid and some nitric acid in the product stream. Given that ca. 66% of mannarate was present in the product stream (IC) the 30.9% and 35.2% yields above correlate to percent yields of 52.3% and 60.0% for methanol and absolute ethanol diffusion dialysis work-up, respectively. It is possible that further development of the diffusion dialysis separation could provide better separation of nitric acid and mannaric acid and would improve the recycling of nitric acid for further use.

Scheme 3 shows the conversion route of a crude oxidation mixture to directly to **9** and conversion employing the diffusion dialysis modification.

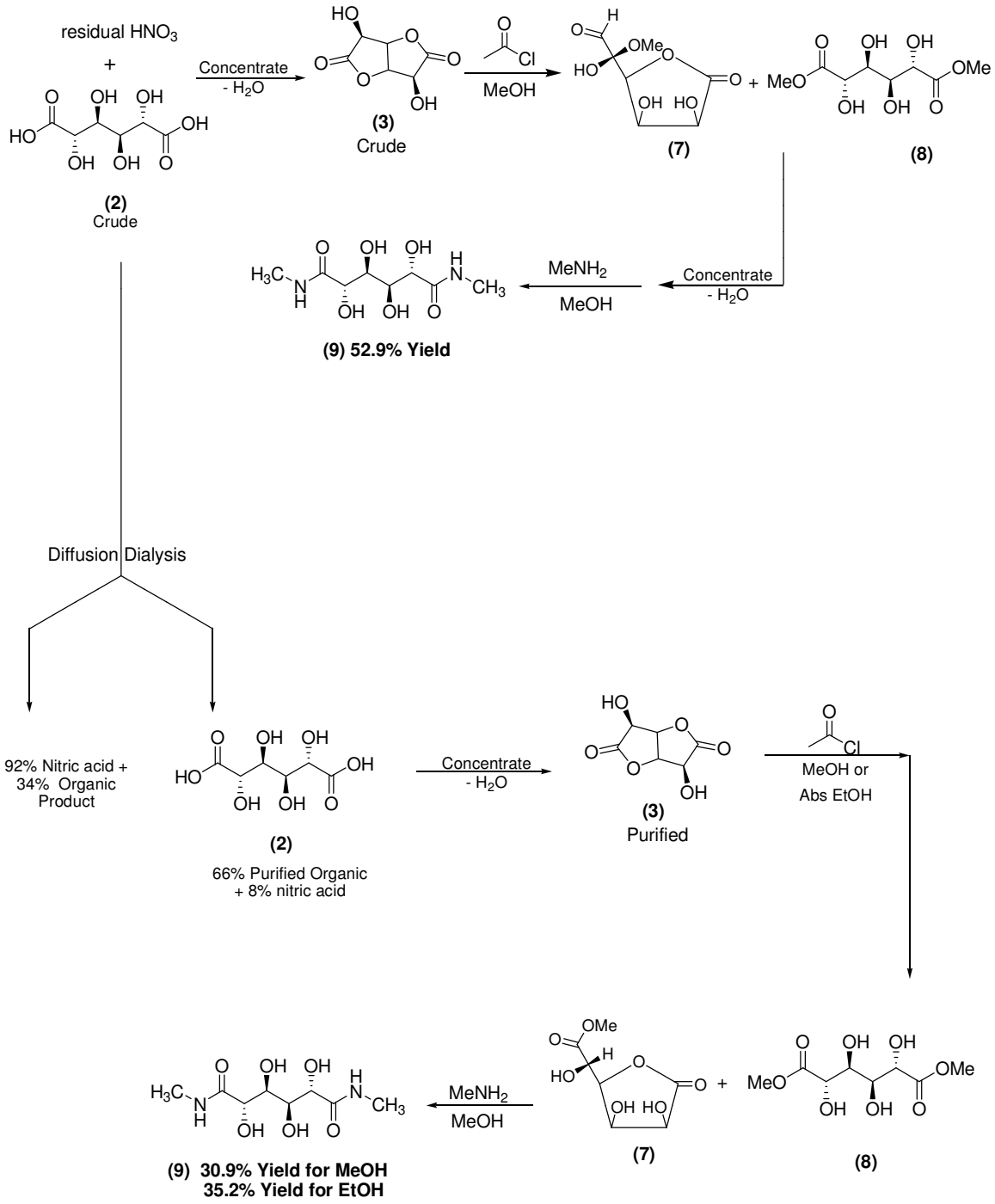

Scheme 3. Isolation of *N,N´*-dimethyl-D-mannaramide (**9**) from a crude oxidation mixture with 52.9% yield and employing a diffusion dialysis modification with 30.9-35.2% yield.

IC of Reaction

Ion chromatography was used as a qualitative tool to monitor the progress of diffusion dialysis. The goal of the diffusion dialysis modification was to completely separate the carbohydrate portion of the oxidation from the nitric acid portion. Diffusion dialysis was used to remove nitric acid as an alternative to the previous nanofiltration method in which the crude oxidation product mixture was treated with sodium hydroxide to neutralize residual nitric acid plus generate disodium D-mannarate. Diffusion dialysis eliminates the need for sodium hydroxide, a significant improvement, and affords the possibility of a much cleaner isolation of the target product, possibly with improved yields. The feedstock solution contained nitrate, mannarate, tartarate, and oxalate based on IC analysis. The enriched oxidized carbohydrate product, or the product collective pot, represented ca. 66% of total carbohydrate product and 8% nitric acid from the feedstock solution and contained nitric, mannaric, tartaric, and oxalic acid and an unknown based on IC analysis. The reclaimed acid collective pot accounted for ca. 92% of the nitric acid plus 34% organic acids as D-mannaric, tartaric, and oxalic acids and a small amount of unknown product. IC analysis shows that further method development is necessary to improve separations of nitric acid from organic acids. However, the diffusion dialysis method still offers considerable improvement on the previous method for removing nitric acid which included concentration under reduced pressure or a nanofiltration modification. Figures 13, 14, and 15 show the IC of the feedstock solution, the organic acid collective pot, and the reclaimed acid collective pot, respectively.

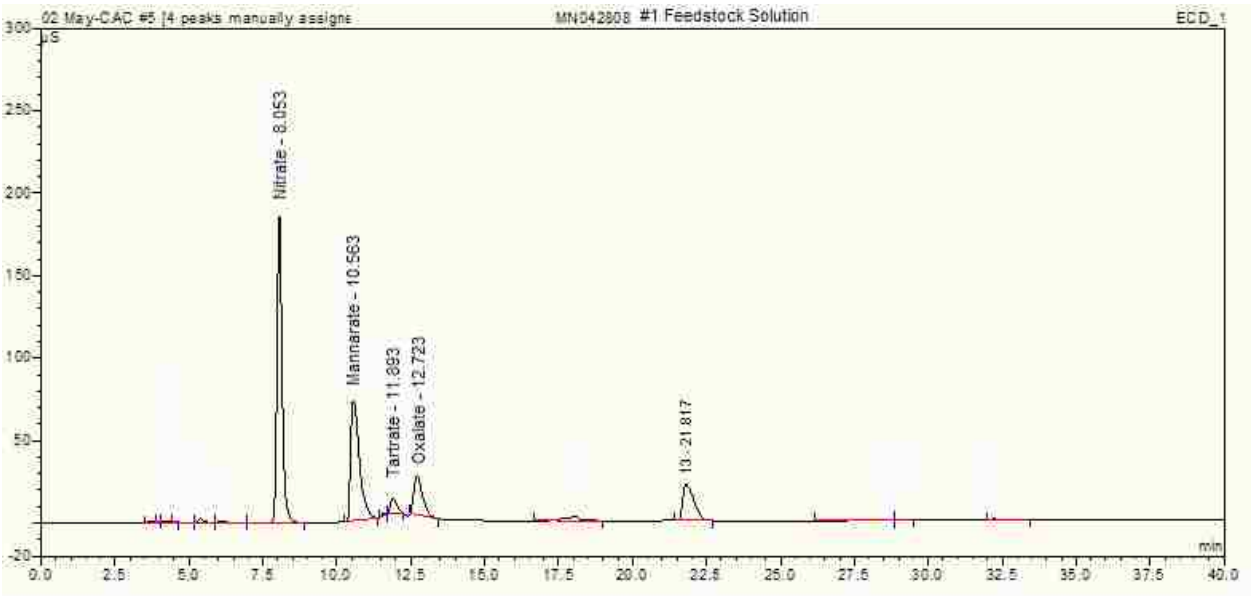

Figure 15. Ion chromatogram of an oxidation diffusion dialysis feedstock solution

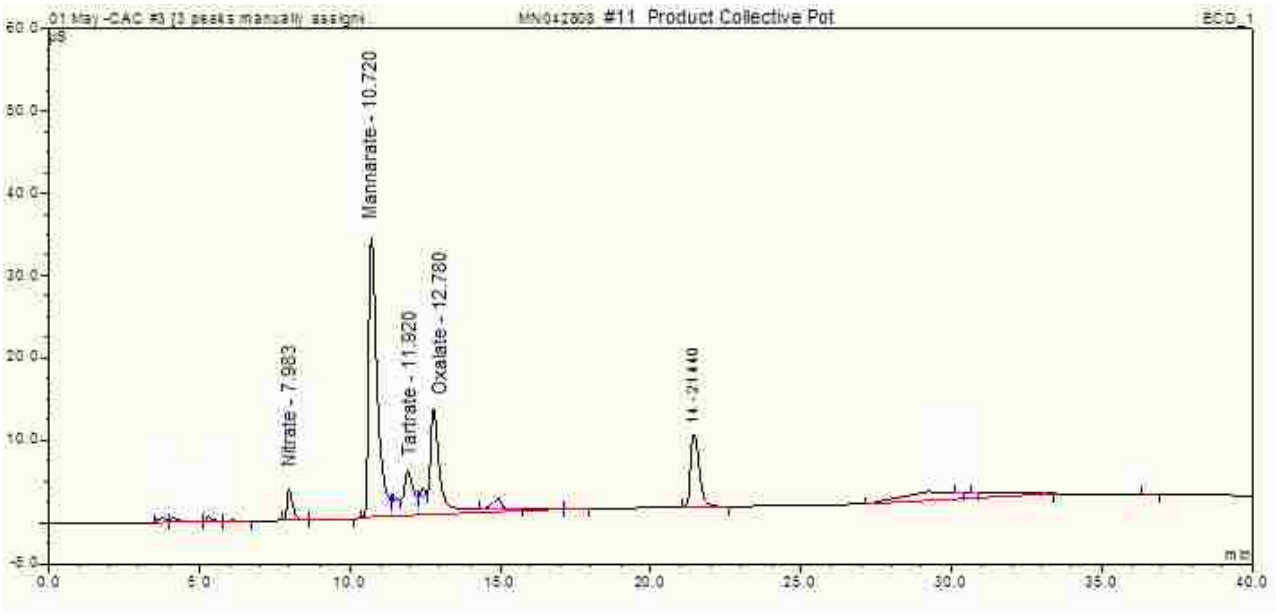

Figure 16. Ion chromatogram of the diffusion dialysis final organic acid collective pot from an oxidation mixture.

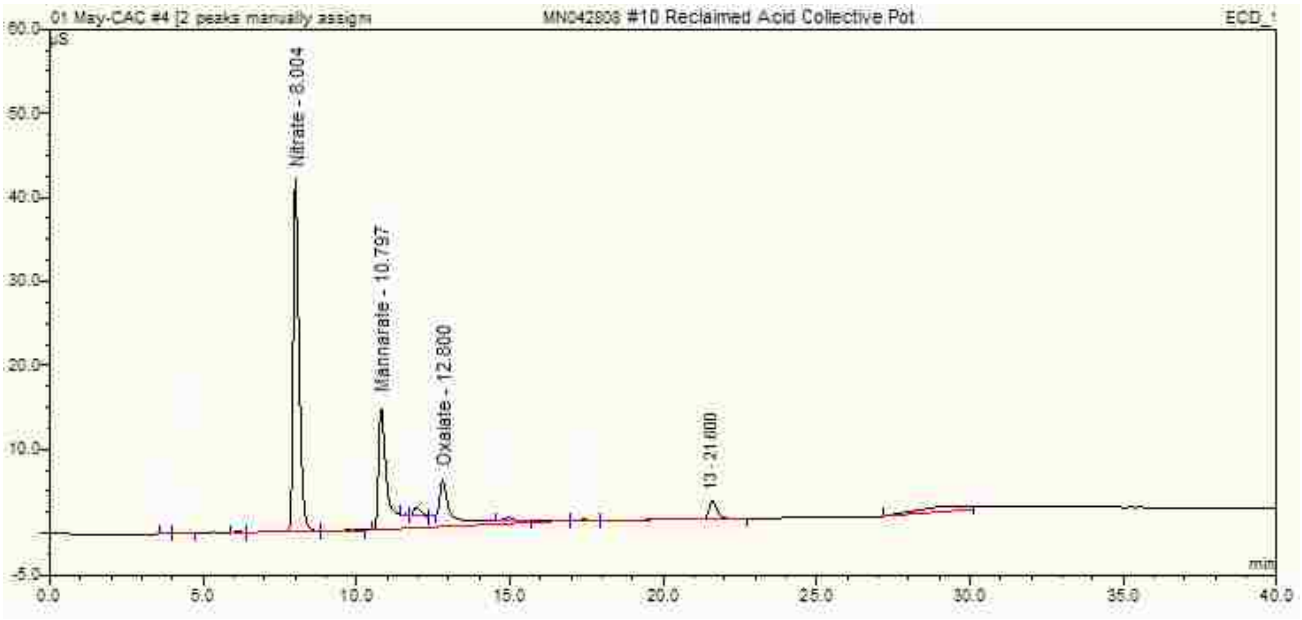

Figure 17. Ion chromatogram of the diffusion dialysis final reclaimed acid collective pot from an oxidation mixture.

Commentary on Mass Spectral Fragments from per-*O*-TMS- *N,N´*-dimethyl-D-mannaramide (9)

GC-MS was used in the characterization of isolated *N,N´*-dimethyl-D-mannaramide and to also determine its purity. The "nitrogen rule" states that a molecule of even-numbered molecular weight must have either no nitrogen present or an even number of nitrogens; an odd-numbered molecular weight requires an odd number of nitrogen.[20] The first part of the rule is the case for mannonic and mannaric acid, with no nitrogen present, as well as for *N,N´*-dimethyl-D-mannaramide, with two nitrogen present. The $[M]^+$ of all three molecules therefore have an even-numbered mass. A corollary to the "nitrogen rule" states that fragmentation at a single bond from an even-numbered molecular ion gives an odd-numbered ion fragment; however, if a molecule that contains two nitrogens breaks at a single bond to give a fragment with only one nitrogen then that fragment will be even-numbered.[20] When *N,N´*-dimethyl-D-

mannaramide fragments, each fragment contains only one nitrogen. This explains why the fragments resulting from the mannonic and mannaric acid are odd-numbered and the fragments resulting from *N,N´*-dimethyl-D-mannaramide are even-numbered.

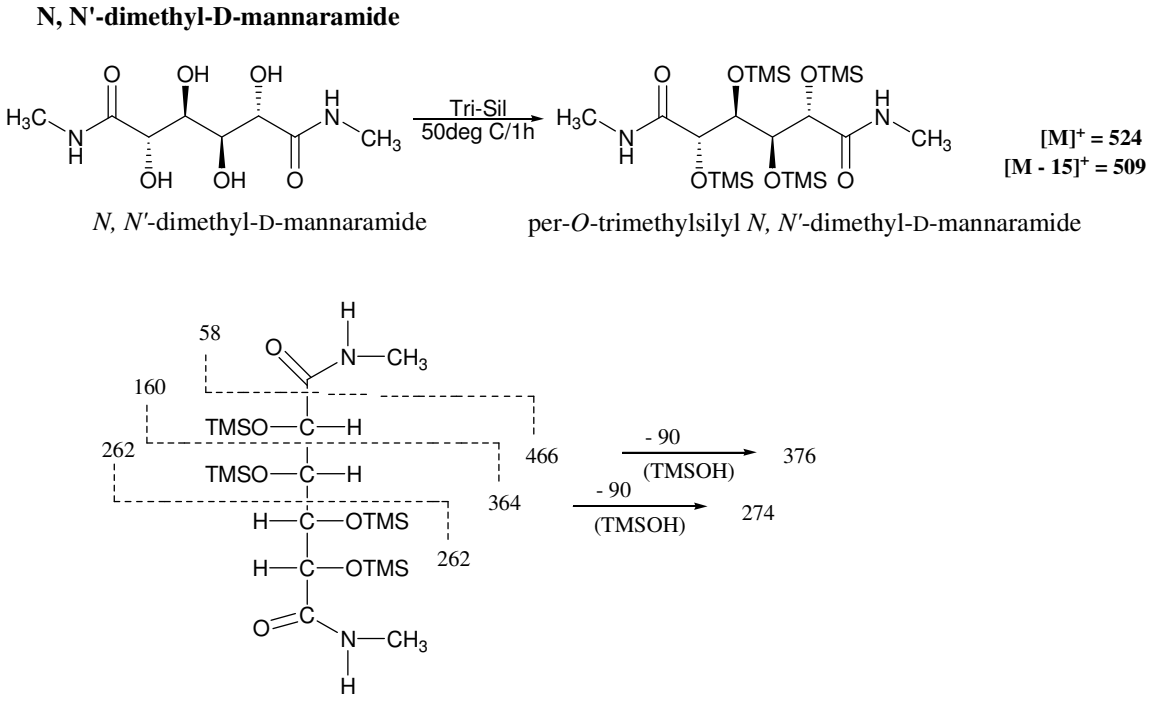

Figure 18. Fragmentation pattern of *N,N´*-dimethyl-D-mannaramide

^{1}H and ^{13}C NMR Characterization of *N,N´*-dimethyl-D-mannaramide (9)

NMR was also used to characterize isolated *N,N´*-dimethyl-D-mannaramide. Figure 19 shows the ^{13}C NMR spectra and Figure 20 shows the ^{1}H NMR spectra of *N,N´*-dimethyl-D-mannaramide in DMSO-*d6*. The molecule is symmetrical and therefore only four signals were observed in its ^{13}C NMR spectra; the equivalent terminal *N*-methyl carbons (25.32 ppm), C1 and C6 (173.87 ppm), C2 and C5 (71.57 ppm), and C3 and C4 (71.01 ppm). The assignment of C1-6 was consistent with that of the ^{13}C acyclic diacid spectrum in D_2O.[23] The ^{1}H NMR spectra shows three signals; the equivalent H2 and H5 protons (5.31 ppm), the H3 and H4 protons (4.98 ppm), $J_{2,3} = J_{4,5} = 5.86$ Hz, and the 1´

and 2´ methyl protons (2.74 ppm). There is no coupling between magnetically equivalent H3 and H4 protons.

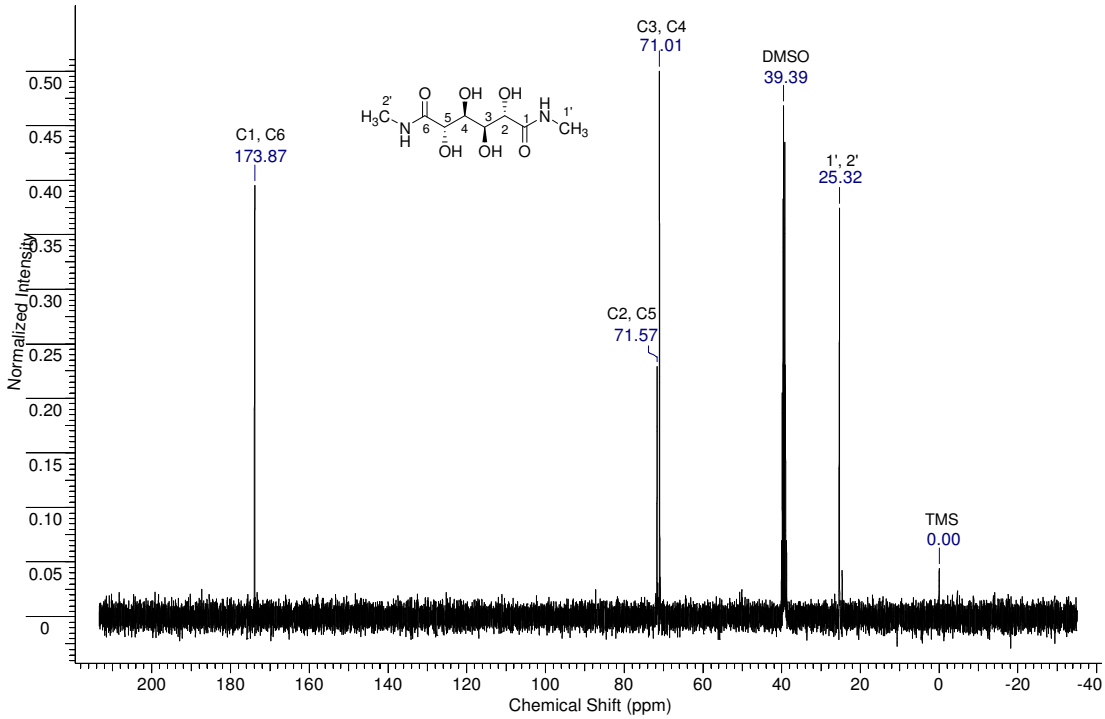

Figure 19. Assigned ^{13}C spectrum of **9** in DMSO-$_{d6}$.

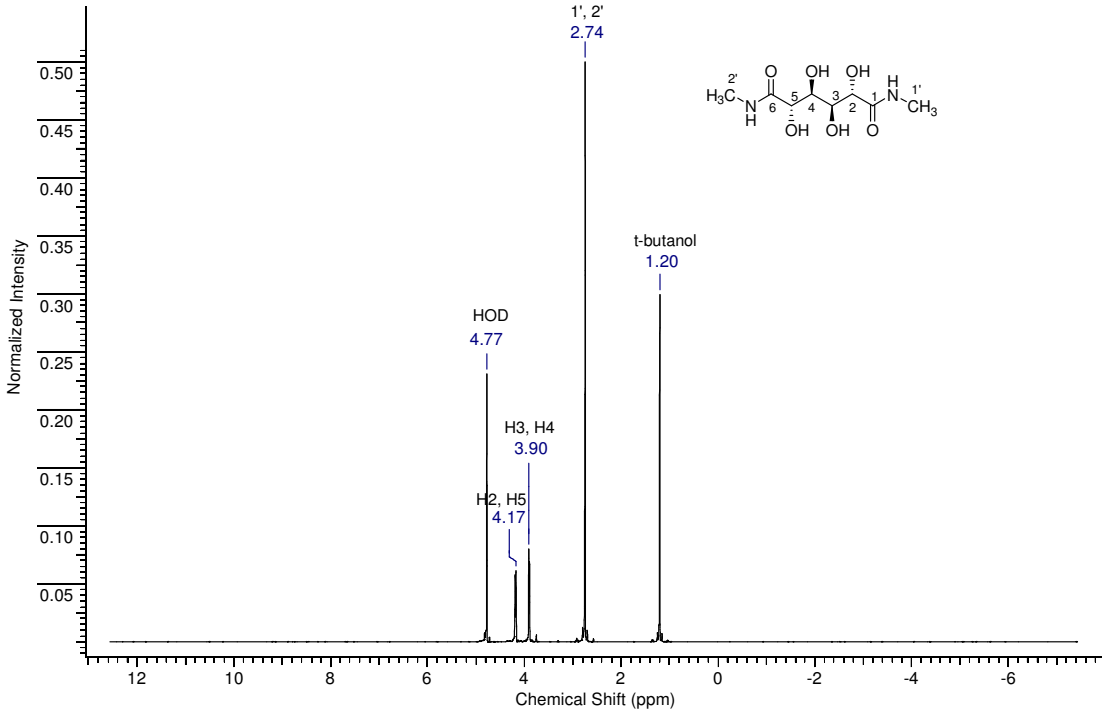

Figure 20. Assigned ^{1}H spectrum of **9** in D_2O

X-ray Crystallographic Analysis of *N, N'*-dimethyl-D-mannaramide (9)

N,N´-dimethyl-D-mannaramide (**9**) was successfully recrystallized from water to produce crystals of good quality and size for single-crystal x-ray crystal structure analysis. This is a new stable derivative of D-mannaric acid is the starting material for synthesis of poly(alkylene D-mannaramides). This molecule was recrystallized not only for characterization purposes, but also to gain a better understanding of the conformation of the mannaryl unit, as D-mannaric acid is not a crystalline molecule. Figure 21 shows the labeling of atoms in the x-ray crystal structure. Selected bond angles are reported in table 2. The unit cell associated with the crystal structure, with dashed lines representing hydrogen bonding, is shown in Figure 22.

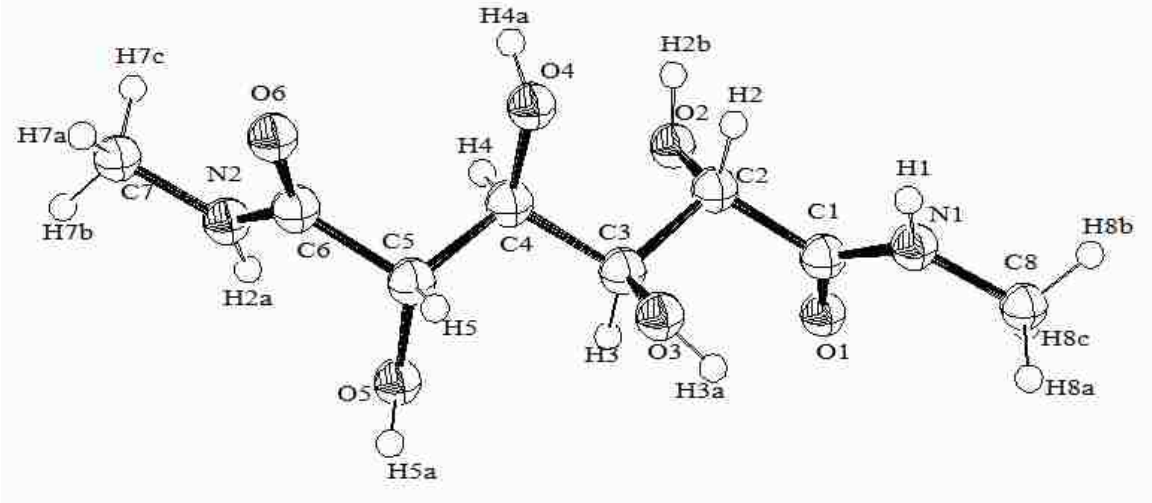

Figure 21. Ortep drawing showing the labeling of the atoms in the crystal structure of *N,N´*-dimethyl-D-mannaramide (**9**)

Table 1. Selected torsion angles from the crystal structure of *N,N´*-dimethyl-D-mannaramide (**9**)

Backbone	**Torsion Angle**
N(1)-C(1)-C(2)-C(3)	-102.03(14)
C(1)-C(2)-C(3)-C(4)	-176.82(12)
C(2)-C(3)-C(4)-C(5)	-177.15(11)
C(3)-C(4)-C(5)-C(6)	-176.63(12)
C(4)-C(5)-C(6)-N(2)	94.84(15)
C(2)-C(1)-N(1)-C(8)	179.03(14)
C(5)-C(6)-N(2)-C(7)	-178.64(15)
O(1)-C(1)-C(2)-C(3)	78.44(17)
O(2)-C(2)-C(3)-C(4)	-59.44(15)
O(3)-C(3)-C(4)-C(5)	-57.75(15)
O(4)-C(4)-C(5)-C(6)	64.21(15)
O(5)-C(5)-C(6)-N(2)	-25.11(18)
O(1)-C(1)-C(2)-O(2)	-40.35(17)
O(2)-C(2)-C(3)-O(3)	-176.12(12)
O(3)-C(3)-C(4)-O(4)	60.76(15)
O(4)-C(4)-C(5)-O(5)	-174.57(12)
O(5)-C(5)-C(6)-O(6)	156.78(14)
N(1)-C(1)-C(2)-O(2)	139.18(13)
C(1)-C(2)-C(3)-O(3)	66.50(16)
C(2)-C(3)-C(4)-O(4)	-58.64(15)
C(3)-C(4)-C(5)-O(5)	-55.40(15)
C(4)-C(5)-C(6)-O(6)	-83.27(17)

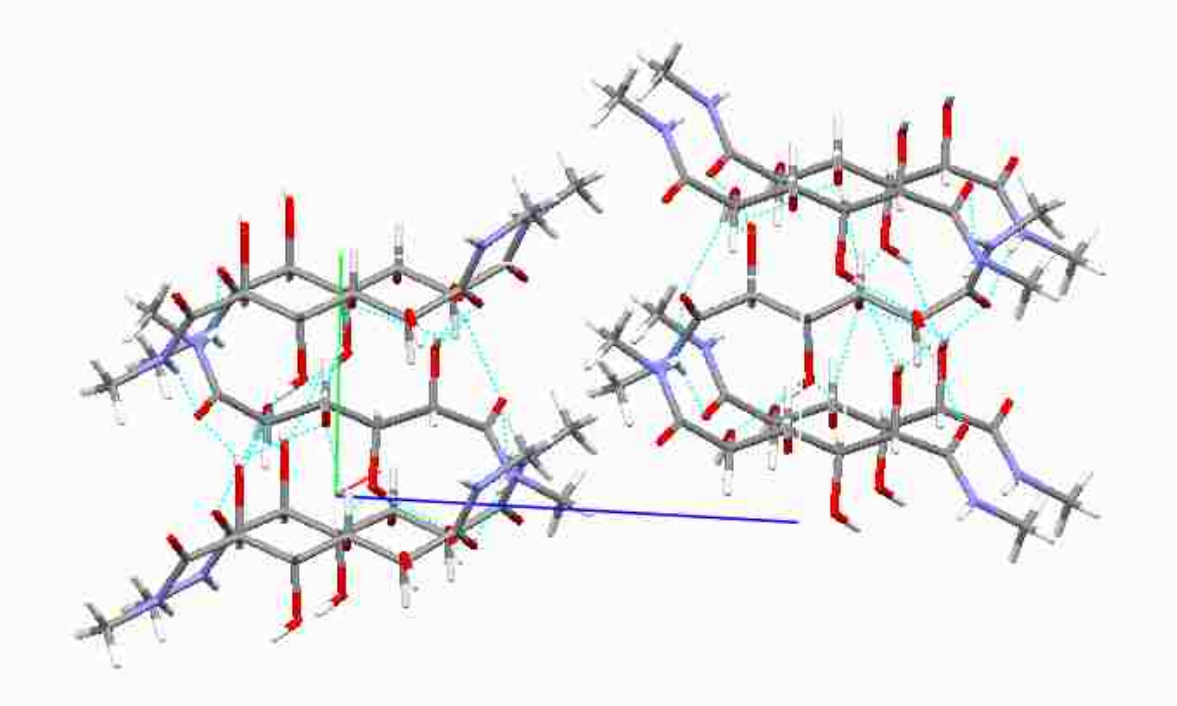

Figure 22. Mercury drawing of the unit cell of *N,N´*-dimethyl-D-mannaramide as viewed perpendicular to the ac-plane showing the hydrogen bonding associated with the crystal structure.

N,N´-dimethyl-D-mannaramide (**9**) adopts an extended conformation in the crystalline state, free of destabilizing 1,3-parallel hydroxyl group eclipsing steric interactions. The molecule also crystallized in sheets perpendicular to the ac plane of the unit cell. While there are no intramolecular hydrogen bonds present, there is a network of intermolecular hydrogen bonds that involve carbonyl oxygen and amide N-H groups. Hydrogen bonding occurs between C1-O1···H2A-N2 (2.072 Å), C1-O1···H5A-O5-C5 (2.142 Å), C6-O6···H1-N1 (2.098 Å), and C6-O6···H2B-O2-C2 (1.994 Å). The extended conformation of crystalline (**9**) is consistent with a structure devoid of parallel 1,3-hydroxy group steric interactions and is also almost identical to that of *N,N´*-dimethyl-D-glucaramide.[24] All x-ray crystallographic data for *N,N´*-dimethyl-D-mannaramide (**9**) can be found in the appendix of this dissertation.

1.2.4 Summary

An improved method for the nitric acid oxidation of D-mannose has been developed. The method employed a Mettler Toledo RC-1 Labmax reactor, which was well suited for the nitric acid oxidation as it is designed as a computer controlled temperature/pressure controlled closed-system reactor. As a closed-system reactor, all NOx gases generated in the reaction were contained in the reaction vessel. The most effective and efficient oxidation method was determined to be Oxidation Method 4, which was carried out using an excess amount of nitric acid (5 moles) to give a molar ratio of 6.67:1 nitric acid:D-mannose. GC-MS data showed that the oxidation was complete and no mannonic acid remained. Oxidation Method 4 provided the desired product and also required only a single oxidation procedure.

D-Mannaric acid was isolated as *N,N´*-dimethyl-D-mannaramide (**9**) with yields greater than 50%. The isolation of the acyclic diamide provided an alternative route to the synthesis of disodium D-mannarate (**5**) from D-mannaro-1,4:6,3-dilactone (**3**) avoided direct sodium hydroxide hydrolysis of **3** and accompanying β-elimination reactions and colored product formation**.** Additionally, isolated yields of **9** were much greater than isolated yields of **3** from the nitric acid oxidation of D-mannose.

N,N´-dimethyl-D-mannaramide (**9**) was recrystallized from water to produce crystals of good quality and size for single-crystal x-ray crystal structure analysis. The molecule adopts an extended conformation and crystallizes in sheets perpendicular to the ac-plane of the unit cell. The extended conformation of *N,N´*-dimethyl-D-mannaramide (**9**) is free of destabilizing 1,3-parallel hydroxyl group steric interactions, as predicted from the structure of D-mannaric acid. There are no intramolecular hydrogen bonds in **9**,

but intermolecular hydrogen bonding is present. The crystal structure of *N,N´*-dimethyl-D-mannaramide (**9**) provides a greater understanding of the D-mannaryl unit in solid state.

1.3 Experimental

Materials and General Methods

D-Mannose was purchased from Hofman International, ACS grade nitric acid (70 % w/w) and HPLC grade methanol from EMD Biosciences, Inc., ACS reagent grade sodium nitrite from Acros, Amberlite IR-120H cation exchange resin and methylamine (33% wt. in absolute ethanol) from Sigma-Aldrich, acetyl chloride (99+ %) from Alfa Aesar, sodium hydroxide DILUT-IT® analytical concentrate from J.T. Baker, and NMR solvents from Cambridge Isotope Laboratories, Inc.

Concentration of solutions was carried out under reduced pressure. Elemental analyses were preformed by Atlantic Microlab, Inc., Norcross, Georgia. The freeze-drier used was a LABCONCO Freezone 4.5. Millipore water was obtained from a Millipore Simplicity 185 system. Reverse osmosis (RO) water was generated in house. Melting points were obtained with a Fisher-Johns melting point apparatus.

Oxidation and work-up of D-Mannose

Oxidation of D-mannose was carried out using a Mettler Toledo RC-1 Labmax reactor. The reactor was fitted with a top-loading balance, a liquid feed pump, a Sierra oxygen flow valve, a mechanically driven stirring rod, a thermometer, a 2 L thermal jacketed flask, an FTS recirculating chiller, a pressure manifold fitted with pressure relief valves and a pressure gauge. Operation of the reactor was controlled using a personal computer with CamilleTG v1.2 software. Removal of nitric acid from solutions was

carried out under reduced pressure with a system consisting of a Buchi Rotovapor R-205, Buchi Vacuum Controller V-800, Buchi Heating Bath B-490, Brinkmann Model B-169 Vacuum Aspirator, and a Thermo Haake compact refrigerated circulator DC30-K20 in conjunction with a Thermo Haake EK45 immersion circulator cooling coil.

Nanofiltration

A nanofiltration unit was built in-house consisting of necessary valves, pump, lines, pressure gauge, and an appropriate membrane such as GE DL2540F using reverse osmosis (RO) purified water as a solvent.

Diffusion Dialysis

Diffusion dialysis was carried out on a Mech-Chem Diffusion Dialysis Acid Purification System laboratory scale Model AP-L05 consisting of two metering pumps, the first being the acid-reclaim pump and the second being the acid-reject pump.

Removal of nitric acid from oxidation mixtures was carried out using the Mech-Chem Diffusion Dialysis Acid Purification System. The acid reject pump was set at 30% (pump length) and 30% (pump seed) and the acid reclaim pump was set at 40% (pump length) and 40% (pump seed). The acid tank was filled with the diluted aqueous oxidation mixtures and the water tank was filled with reverse osmosis water. The acid purification unit was turned on with the pumps set as indicated and the process initiated. Over a period of 21 h the acid recovery stream and product recovery stream were collected and samples were taken for IC analysis. The acid recovery stream was enriched in nitric acid (reclaimed acid collective pot) and the product recovery stream was enriched in the oxidized carbohydrate portion (product collective pot).

Gas Chromatography/Mass Spectrometry of Trimethylsilyl Derivatives

GC-MS was performed on an Agilent 6890N Network GC System with an on-column injector fitted with a 5%-phenyl 95%-dimethylpolysiloxane column (Phenomenex ZB-5, 30 m x 32 mm x 0.25 μm) installed with direct interface to an Agilent 5973 Network MS Detector.

All samples for GC-MS analysis were worked up in the following manner: Coded sample (2 drops) was cooled (ice bath) and transferred to a 7 mL vial. The sample was made basic with sodium hydroxide (2M, 8 drops) and xylitol (30 mg/mL, 2 drops) was added as an qualitative internal standard. Samples were then concentrated to dryness on a freeze-drier.

Tri-Sil© Reagent (1.0 mL) was added to dried sample (10.0 mg) in a 7 mL vial and the mixture heated (50 °C, 1 h). During the silylation procedure solid residue remained and the supernatant was transferred (pipette) to heptane (3 mL). The heptane solution was centrifuged and the resulting supernatant removed for GC-MS analysis.

Samples were analyzed using one of two temperature program. GC-MS Method 1 = Begin 32 °C, + 12.5 °C/min to 250 °C, (hold 5 min), + 20°/min to 300 °C, (hold 5 min). Total acquisition time was 30.10 min. GC-MS Method 2 = Begin 40 °C, + 6.0 °C/min to 120 °C, + 2.0 °C/min to 210 °C, + 8.0 °C/min to 310 °C, (hold 10 min). Total acquisition time was 80.83 min.

Ion Chromatography

IC was performed on a Dionex ICS-2000 Ion Chromatography System consisting of a Dionex IonPac® AS II analytical column and a sodium hydroxide EluGen® cartridge in conjunction with Chromeleon software. Samples were analyzed using a 35mM sodium hydroxide isocratic elution method with a flow rate of 1.5 mL/min running with the

suppressor current at 186 mA. All IC method development was performed by Cara-Lee Davey from the University of Waikato, Hamilton, New Zealand.

Nuclear Magnetic Resonance

NMR spectra were recorded using a 400 MHz Varian *Unity Plus* spectrometer. Chemical shifts are expressed in parts per million relative to *t*-butyl alcohol (1.203 ppm) in D_2O as a solvent and tetramethylsilane (0.00 ppm) in DMSO-d_6 as a solvent. FIDs obtained were processed using ACD/SpecManager 1D NMR software.

1.3.1 Nitric Acid Oxidation of D-Mannose: Oxidation Protocols

Benchtop Method

D-Mannose (**1**, 10.04 g, 0.557 mmol) was added to concentrated nitric acid (70%, 50 mL, 800 mmol). The solution was heated with stirring in an oil bath (60 °C, 4 h). The temperature was raised to 85 °C and the solution was refluxed and stirred (0.5 h) before cooling to room temperature.

Oxidation Method 1 (4 : 1 Molar Ratio of Nitric Acid to D-Mannose at 25 °C)

The oxidation was carried out using the Labmax reactor. Reaction parameters for the oxidation were programmed in a series of stages: Stage 1. The reactor temperature was set at 25 °C, the stirring rod speed was set at 200 rpm (held constant through the remaining stages), concentrated nitric acid (70%, 3.00 mol, 187 mL) was added, the vessel was closed to the atmosphere, and time set for 1 min. Stage 2. Oxygen was added to bring the pressure to 0.25 bar and pressure maintained until the end of stage 6. Stage 3. D-mannose [43.3 g of an aqueous 62.5% solution containing sodium nitrite (8.7 mmol, 0.6 g)] was added over 30 min. Stage 4. A 10 min stabilization period under the same conditions. Stage 5. D-Mannose [173.9 g of an aqueous 62.2% solution containing

sodium nitrite (8.7 mmol, 0.6g)] was added over 90 min. Stage 6. A 5 min stabilization period was set under the same conditions. Stage 7. Reactor temperature was set to 30 °C and pressure to 0.5 bar over 1 h. Stage 8. Reaction conditions maintained over a 6 h reaction hold. Stage 9. Reaction mixture cooled to 25 °C over 10 min and the vessel opened to the atmosphere.

Oxidation Method 2 (4 : 1 Molar Ratio of Nitric Acid to D-Mannose at 30 °C)

The oxidation was carried out under the conditions described in Oxidation Method 1 (4:1 molar ratio nitric acid to D-mannose at 25 °C) with the following modifications: Stage 1. The reactor temperature was set at 30 °C, the stirring rod speed was set at 200 rpm (held constant through the remaining stages), concentrated nitric acid (70%, 3.00 mol, 187) was added, the vessel was closed to the atmosphere, and time set for 1 min.

Oxidation Method 3 (4 : 1 Molar Ratio of Nitric Acid to D-Mannose)

The oxidation was carried out under the conditions described in Oxidation Method 1 (4:1 molar ratio nitric acid to D-mannose at 25 °C) with the following modifications: Stage 1. The reactor temperature was set at 30 °C, the stirring rod speed was set at 200 rpm (held constant through the remaining stages), nitric acid (70%, 3.00 mol, 187 mL) was added, the vessel was closed to the atmosphere, and time set for 1 min. Stage 8. The reaction was held for 3 h. After stage 9, the reaction mixture was concentrated to a dry, foamy product. Concentrated nitric acid (3.00 mol, 187mL) and sodium nitrite (8.70 mmol, 0.6 g) were added with stirring to the concentrated reaction mixture. The mixture was put back into the reactor and held at 40 °C and 0.5 bar for an

additional 6 h. In the final step, the reaction was brought to 25 °C over 10 min and the vessel opened to the atmosphere.

Oxidation Method 4 (6.67 : 1 Molar Ratio of Nitric Acid to D-Mannose at 30 °C)

The oxidation was carried out under the conditions described in Oxidation Method 1 (4:1 molar ratio nitric acid to D-mannose at 25 °C) with the following modifications: Stage 1. The reactor temperature was set at 30 °C, the stirring rod speed was set at 200 rpm (held constant through the remaining stages), concentrated nitric acid (70%, 5.0 mol, 312.5 mL) was added, the vessel was closed to the atmosphere, and time set for 1 min. Stage 7. Reactor temperature was set to 40 °C and pressure to 0.5 bar over 1 h.

1.3.2 GC-MS Sample Analysis

GC-MS Sample Preparation

Samples were taken during the course of each oxidation for GC-MS analysis. Table 2 below indicates the points at which samples were collected for each oxidation method. The stars in Figures 5, 6, and 7 also indicate where samples were collected. Sodium hydroxide (2 M) was added to the samples to reach a basic pH and were then freeze-dried overnight. To the dried sample, Tri-Sil® was added and heated to 50 °C for 1 h to form the per-*O*-trimethylsilyl derivative. All samples were analyzed using GC-MS Method 2; GC-MS Method 1 was also employed for Oxidation Method 1 and Oxidation Method 2.

Table 2. GC-MS sample collection points for each of the indicated oxidation methods

Method 1 (25 ℃) 4:1 HNO3 to D-Mannose	Method 2 (30 ℃) 4:1 HNO_3 to D-Mannose	Method 3 (30 °C) 4:1 HNO_3 to D-Mannose	Method 4 (30 ℃) 6.67:1 HNO_3 to D-Mannose
End of stage 5	End of stage 5	End of stage 5	End of stage 5
End of stage 7	End of stage 7	End of stage 7	End of stage 7
1.5 h into stage 8	1 h into stage 8	1.5 h into stage 8	1 h into stage8
Final reaction mixture	2 h into stage 8	End of stage 8	2 h into stage 8
	Final reaction mixture	After 2nd HNO_3 add	3 h into stage 8
		1 h into stage 12	4 h into stage 8
		2 h into stage 12	5 h into stage 8
		3 h into stage 12	Final reaction mixture
		4 h into stage 12	
		5 h into stage 12	
		Final reaction mixture	

1.3.3 IC Sample Analysis

Samples were taken during the course of diffusion dialysis: 1) feedstock solution 0 h, 2) reclaimed acid 4 h, 3) product 4 h, 4) reclaimed acid 5 h, 5) product 5 h, 6) reclaimed acid 9 h, 7) product 9 h, 8) reclaimed acid 21 h, 9) product 21 h, 10) reclaimed acid collective pot, and 11) product collective pot. Samples were diluted 100-fold for analysis by IC.

1.3.4 Isolation of D-mannaro-1,4:6,3-dilactone (3) – Nanofiltration Purification Method

An oxidation mixture (Oxidation Method 3), taken directly from the Mettler Toledo Labmax reactor, was concentrated to a thick syrup at 40 °C. The syrup was dissolved in water (200 mL) the resulting solution concentrated to a thick syrup. The syrup was again dissolved in water (100 mL) and stirred (40 °C, 1.5 h). Sodium

hydroxide (5 M) was added (ice bath) to bring the solution to pH 9.5. The solution was diluted to a volume of 3,650 mL (RO water) and subjected to a nanofiltration protocol using an Osmonics DL2514 membrane (2.5" diameter, 14" length). When the permeate volume reached 500 mL, RO water (500 mL) was added to the feedstock. The typical rate of permeate flow was 65.15 mL/min. This was repeated until 3,000 mL of permeate had been collected and 3,000 mL of RO water had been added. The typical permeate flow rate when removing the last 500 mL was 43 mL/min. Filtration continued after the last 500 mL of RO water had been added to the feedstock and until the permeate flow slowed to a trickle. The retentate solution of enriched disodium mannarate (**5**) was concentrated to 200 mL and then treated with an excess of Amberlite IR-120 H^+ form resin for 1 h to give the aqueous diacid (**2**). The resin was removed by filtration and thoroughly rinsed with water. The solution was concentrated to a thick syrup, seeded with D-mannaro-1,4:6,3-dilactone, and dried under vacuum at room temperature using a vacuum pump for 24 h. The dried syrup was triturated with EtOH/EtOAc (3:1) to give solid D-mannaro-1,4:6,3-dilactone (**3**, 43.18 g, 248 mmol, 33.1%): mp 183-185 ºC, lit. mp 180-190 °C.[7] ^{1}H NMR (D_2O) δ4.9 (d, 2H, H-3, H-4) δ5.31 (d, 2H, H-2, H-5). ^{13}C NMR (D_2O) δ70.36 (C3, C4) δ77.46 (C2, C5) δ176.29 (C1, C6).

1.3.5 *N, N'*-dimethyl D-mannaramide Isolation Modification (9)

Benchtop Oxidation Method

The cooled benchtop oxidation mixture was concentrated to a thick syrup at 40 °C. The syrup was dissolved in water (100 mL) and the mixture concentrated to dryness at 40 °C; the water dilution and concentration procedures were repeated once. The final syrupy concentrate was dissolved in methanol (75 mL) and acetyl chloride (0.396 mL,

5.57 mmol) was added dropwise (ice bath) with stirring. The resulting solution was stirred at room temperature for 24 h after which it was concentrated to a thick syrup at 30 °C. The syrup residue was dissolved in methanol (75 mL) and concentrated again at 30 °C to remove residual HCl. The resulting syrupy residue was dissolved in methanol (75 mL) and methylamine (13.87 mL, 111 mmol) was added. This solution was stirred at room temperature (24 h) with a precipitate beginning to form within 30 min. The precipitate was removed by filtration, washed with methanol (3 x 10 mL), and dried under vacuum to give *N,N'*-dimethyl-D-mannaramide (**8**, 4.393 g, 18.6 mmol, 33.3%): mp 219-221 ºC. ^{1}H NMR (D_2O) δ 2.74 (s, 6H, NH-C**H**$_3$) δ3.90 (d, 2H, H-2, H-5, $J_{2,5}$ = 6.35 Hz) δ4.17 (d, 2H, H-3, H-4, $J_{3,4}$ = 5.86 Hz). ^{13}C NMR (DMSO-d_6) δ25.32 (NH-**C**H$_3$) δ71.01 (C3, C4) δ71.55 (C2, C5) δ173.86 (C1, C6). Anal. Calcd. for $C_8H_{16}N_2O_6$ (236.22): C, 40.68; H, 6.83; N, 11.86. Found: C, 40.97; H, 6.98; N, 11.79.

Oxidation Method 4 (9)

An oxidation mixture (Oxidation Method 4), taken directly from the Mettler Toledo Labmax reactor, was concentrated to a thick syrup at 40 °C. Water (200 mL) was added to dissolve the dried oxidation mixture and the solution concentrated to dryness at 40 °C. The water dilution and concentration procedure was repeated four times. The final concentrate was dissolved in methanol (500 mL) and acetyl chloride (2.67 mL, 37.5 mmol) was added dropwise (ice bath) with stirring. The resulting solution was stirred at room temperature (24 h) after which it was concentrated to a thick syrup (30 °C). The syrup residue was dissolved in methanol (200 mL) and the solution concentrated at 30 °C to remove residual HCl. The resulting syrup residue was redissolved in methanol (200 mL) and methylamine (187.98 mL, 1.51 mol) was added. As before, the solution was

stirred at room temperature (24 h) with a precipitate beginning to form within 30 min. The precipitate was removed by filtration, washed with methanol (3 x 10 mL), and dried under vacuum to give *N,N'*-dimethyl-D-mannaramide (**8**, 92.8 g, 393 mmol, 52.4%). ^{1}H NMR (D_2O) δ 2.74 (s, 6H, NH-C**H**$_3$) δ3.90 (d, 2H, H-2, H-5, $J_{2,5}$ = 6.35 Hz) δ4.17 (d, 2H, H-3, H-4, $J_{3,4}$ = 5.86 Hz). ^{13}C NMR (DMSO-d_6) δ25.31 (NH-**C**H$_3$) δ70.99 (C3, C4) δ71.54 (C2, C5) δ173.84 (C1, C6).

Diffusion Dialysis Modification

Two oxidation mixtures (both Oxidation Method 4) were combined and diluted to a volume of 2,000 mL (RO water). The Mech-Chem Diffusion Dialysis Acid Purification System acid reject pump was set at 30% (pump length) and 30% (pump seed) and the acid reclaim pump was set at 40% (pump length) and 40% (pump seed). The acid tank was filled with the diluted aqueous oxidation mixtures and the water tank was filled with RO water. The acid purification unit was turned on with the pumps set as indicated and the process initiated. Over a period of 21 h the acid recovery stream and product recovery stream were collected. The acid recovery stream was enriched in nitric acid (ca. 92%) and the product recovery stream contained was enriched in the oxidized D-mannose product (ca. 66%). The product recovery stream was concentrated to a thick syrup and then dissolved in water (500 mL). Based on IC analysis, the enriched oxidized carbohydrate product represented ca. 66% of total oxidized D-mannose product and 8% nitric acid from the feedstock solution. The solution was then divided into two equal aliquots, A and B which were processed with methanol and absolute ethanol, respectively.

Diffusion Dialysis Modification – Methanol Work-Up

Aliquot A was concentrated to a thick syrup; the resulting syrup was dissolved in methanol (600 mL) and acetyl chloride (26. 79 mL, 377 mmol) added dropwise (ice bath) with stirring. The resulting solution was stirred at room temperature for 24 h after which it was concentrated to a thick syrup under reduced pressure at 30 °C. The syrup was dissolved in methanol (600 mL), the addition of acetyl chloride with stirring was repeated as was concentration of the solution under reduced pressure. The syrupy residue was redissolved in methanol (200 mL) and concentrated again at 30 °C to remove residual HCl. The syrupy residue was dissolved in methanol (200 mL) and methylamine (187.976 mL, 1.51 mol) was added. This solution was stirred at room temperature (24 h) with a precipitate beginning to form within 30 min. The precipitate was removed by filtration, washed with methanol (3 x 10 mL), and dried under vacuum to give *N, N'*-dimethyl-D-mannaramide (**8**, 54.7 g, 232 mmol, 30.9%, 52.3% based on oxidized D-mannose product stream).

Diffusion Dialysis Modification – Absolute Ethanol Work-Up

Aliquot B was concentrated to a thick syrup; the resulting syrup was dissolved in abs ethanol (800 mL) and acetyl chloride (26. 79 mL, 377 mmol) added dropwise (ice bath) with stirring. The resulting solution was stirred at room temperature (24 h) after which it was concentrated to a thick syrup at 30 °C. The syrup was dissolved in abs ethanol (400 mL), and the addition of acetyl chloride with stirring was repeated as was concentration of the solution under reduced pressure process repeated. The syrupy residue was dissolved in abs. ethanol (400 mL) and concentrated again at 30 °C to remove residual HCl. Finally the syrupy residue was redissolved in absolute ethanol (400 mL) and methylamine (187.976 mL, 1.51 mol) was added. The solution was stirred at

room temperature (24 h) with a precipitate beginning to form within 30 min. The precipitate was removed by filtration, washed with abs ethanol (3 x 10 mL), and dried under vacuum to give *N,N'*-dimethyl-D-mannaramide (**8**, 62.4 g, 264 mmol, 35.2%, 60.0% based on oxidized D-mannose product stream).

1.3.6 *N,N´*-dimethyl-D-mannaramide X-ray Crystal Structure Analysis

All software used was from Bruker AXS, Inc. Data collection, indexing and initial cell refinements were all carried out using APEX software. Frame integration and final cell refinements were done using SAINT Version 6.45A software. Structure solution, refinement, graphics and generation of publication materials were performed by using SHELXTL V6.12 software.

A suitable crystal of *N,N´*-dimethyl-D-mannaramide was coated with Paratone N oil, suspended in a small fiber loop and placed in a cooled nitrogen gas stream at 173 K on a Bruker D8 APEX II CCD sealed tube diffractometer with graphite monochromated CuK_α (1.54178 Å) radiation. Data were measured using a series of combinations of phi and omega scans with 10 s frame exposures and 0.5^o frame widths.

The structure was solved using Direct methods and difference Fourier techniques (SHELXTL, V6.12, Bruker). Hydrogen atoms were placed their expected chemical positions using the HFIX command and were included in the final cycles of least squares with isotropic Uij 's related to the atom's ridden upon. All non-hydrogen atoms were refined anisotropically. Scattering factors and anomalous dispersion corrections are taken from the International Tables for X-ray Crystallography.

1.4 References

1. Stick, Robert V. *Carbohydrates: The Sweet Molecules of Life;* Academic Press: San Diego, CA, 2001.

2. Haworth, W. N.; Heslop, D.; Salt, E.; and Smith, F. Lactones of Mannosaccharic Acid. Part I. 2:5-Dimethyl-Δ-Mannosaccharo-3:6-lactone 1-Methyl Ester, an Analogue of Ascorbic Acid. *J. Chem. Soc.* **1944**, Part 1, 217-224.

3. Kiely, Donald E.; Ponder, Glenn. Nitric acid removal from oxidation products. US Patent 6,049,004, April 11, 2000.

4. Greene, John W. Nitric Acid and Nitrogen Dioxide. In *The Carbohydrates: Chemistry and Biochemistry*. Pigman, Ward; Horton, Derek; Wander, Joseph D. Eds. Volume 1B; Academic Press: New York, 1980; pp1135-1139.

5. Mehltretter, Charles H. Process of Making D-Saccharic Acid. US Patent 2,436,659, February 24, 1948.

6. Kiely, Donald E; Carter, Andy; Shrout, David P. Oxidation process. US Patent 5,599,997, Feb 4, 1997.

7. Staněk, Jaroslav; Černý, Miloslav; Kocourek, Jan; Pacák, Josef. Monosaccharide Dicarboxylic Acids. *The Monosaccharides*, Academic Press: New York, 1963; pp 741-752.

8. Merbouh, Nabyl; Bobbitt, James M.; Brückner, Christian, 4-Ac-TEMPO-Catalyzed Oxidation of Aldoses to Aldaric Acids Using Chlorine or Bromine as Terminal Oxidants. *J. Carbohydr. Chem.* **2002**, *21* (1&2), 65-67.

9. Busch, K.G.A.; Clark, J.W.; Genung, L.B.; Schroeder, E.F.; and Evans, W.L. The Mechanism of Carbohydrate Oxidation. XVIII. The Oxidation of Certain Sugars with Silver Oxide in the Presence of Potassium Hydroxide. *J. Org. Chem.* **1936**, *1*, 1-16.

10. Tomar, Ashish and Kumar, Arun. Kinetic and Mechanistic Study of the Oxidation of D-Mannose by Tetramethylammounium Chlorochromate in Aqueous Acetic Acid Medium. *Asian J. Chem.* **2006**, *18* (4), 3073-3080.

11. Mirescu, Agnes and Prübe, Ulf. A New Environmentally Friendly Method for the Preparation of Sugar Acids via Catalytic Oxidation on Gold Catalysts. *Appl. Catal., B.* **2007**, *70*, 644-652.

12. Parpot, P.; Santos, P.R.B.; and Bettencourt, A.P. Electro-oxidation of D-Mannose on Platinum, Gold, and Nickel Electrodes in Aqueous Medium. *J. Electroanal. Chem.* **2007**, *610*, 154-162.

13. Jeffrey, G.A.; Wood, R.A. The Crystal Structure of Galactaric Acid (Mucic Acid) at -147°: An Unusually Dense, Hydrogen-Bonded Structure. *Carbohydr. Res.* **1982**, *108* (2), 205-211.

14. Kiely, Donald E.; Denton, Travis T. Unpublished Results.

15. Douglas, Bodie, E. and Ho, Shih-Ming. *Structure and Chemistry of Crystalline Solids*; Springer Science+Business Media, Inc.: New York, 2006, pp 1-20.

16. Rhodes, Gale. *Crystallography Made Crystal Clear: A Guide for Users of Macromolecular Models*, Second Edition; Academic Press: New York, 1999; pp 1-8.

17. Dunitz, Jack D. Are Crystal Structures Predictable? *Chem. Comm.* **2003**, *5*, 545-548.

18. Sands, Douglas E. *Introduction to Crystallography*; W.A. Benjamin, Inc.: New York, 1969, pp 1-9.

19. Kiely, Donald, E.; Hash, Kirk, R. Method for the Preparation of Organic Acids via Oxidation Using Nitric Acid. International Patent Application Number PCT/US2007/017493, Feb 21, 2008.

20. Silverstein, Robert M.; Webster, Francis X. *Spectrometric Identification of Organic Compounds*, 6th ed; John Wiley & Sons, Inc.: New York, 1998.

21. Petersson, G. Mass Spectrometry of Hydroxyl Dicarboxylic Acids as Trimethylsilyl Derivatives. Rearrangement Fragmentations. *Org. Mass Spectrom.* **1972**, *6*, 565-576.

22. Ma, Junkun. Mannaric Acid Dilactone – Preparation and Some Reactions. M.S. Thesis, University of Alabama at Birmingham. 1997.

23. Van Duin, M.; Peters, J. A.; Kieboom, A. P. G.; Van Bekkum, H. Proton NMR Spectra of Carbohydrate-derived Polyhydroxycarboxylates. Magn. Reson. Chem. **1986**, *24* (9), 832-833.

24. Styron, Susan D.; French, Alfred D.; Friedrich, Joyce D.; Lake, Charles H.; Kiely, Donald E. MM3(96) Conformational Analysis of D-Glucaramide and X-Ray Crystal Structures of Three D-Glucaric Acid Derivatives – Models for Synthetic Poly(Alkylene D-Glucaramides). *J. Carbohydr. Chem.* **2002**, *21* (1&2), 27-51.

Chapter 2

Synthesis of Some Poly(Alkylene D-mannaramides) from their Corresponding Diammonium Salts

2.1 Introduction

2.1.1 History of Polymers

Polymers are large molecules made up of many smaller bound monomer units. The word polymer comes from the Greek *poly* "many" and *meros* "parts" whereas the word monomer is derived from the Greek *mono* "one".[1] Naturally-occurring polymers have been used for mellenia beginning with prehistoric people as food, clothing, tools, and shelters.[2] Today polymers, both natural and synthetic, are all around us and play a large role in our day to day lives in an ever expanding range of structural and functional materials.

Synthetic polymers were first produced in the 19th century beginning with vulcanized rubber and later polyvinyl chloride and polystyrene.[3] Today over 50 billion pounds of synthetic polymers are produced each year in the United States alone.[3] The polymer industry is growing at a rate faster than that of any other chemical industry with every reason to believe it will continue as long as oil reserves continue to be available.[3] However, polymers synthesized from renewable resources are becoming increasingly attractive as oil prices skyrocket to record highs and we face a possible future shortfall of this non-renewable resource.

Over 10 million tons of waste plastics are disposed of in the US and EC countries each year.[4] These materials, once discarded, persist in the environment without being degraded, causing both environmental and ecological concerns; the shortage of landfill

space, emissions from incineration, and entrapment and ingestion hazards.[4] Consequently, growing environmental concern and consciousness has created a potential market for biodegradable polymers.[4] Biodegradation is defined as "an event that takes place through the action of enzymes and/or chemical decomposition associated with living organisms (bacteria, fungi, etc.) and their secretion products.[4] A structural variety of biodegradable polymers are readily available from renewable resources and biodegrade within a reasonable time scale.[4] Among them are polysaccharides, which are derived from glycosidically linked monosaccharides and generally undergo biodegradation more rapidly than synthetic polymers.[5] Carbohydrates, which account for ca. 70% of dried plant material, are getting increasing attention as sources of possible useful biodegradable polymers.[5] For example, polystyrene packing peanuts are already being widely replaced with biodegradable starch peanuts.

2.1.2 Mechanisms of Polymerization

Wallace H. Carothers proposed that there were two types of polymerizations; addition and step-growth.[6] He proposed that addition polymers were made up of identical monomer units which contain the same number of atoms as the monomers. Step-growth, or condensation polymers, are made up of two or more monomer units and the repeat units contain fewer atoms than the monomer units due to loss of simpler molecules as byproducts of the polymerization process.[6] The terms addition and condensation polymerizations are still used today but the definitions of each have expanded since the time of Carothers.[3]

Addition (Chain-growth) Polymerization

Addition polymerization is characterized by the rapid addition of one monomer at a time to the growing polymer chain, and is therefore referred to as chain-growth polymerization. [7] Chain-growth polymers have the same number of atoms in the repeating unit as the monomer, usually an unsaturated molecule.[1, 7, 2] Such polymers are characterized by the formation of a reactive intermediate at the growing end of the polymer chain with intermediates typically being cations, anions, or free radicals.[1, 7] The polymerization is usually rapid and continues to propagate until termination forming polymers of high molecular weight.[3]

There are many examples of chain-growth polymers and one of the most common is polystyrene, a free radical polymer.[3] It was invented in 1937 and is used for a variety of applications such as lighting fixtures, housewares, toys, and food containers but its major use is as a packing material.[3] The synthesis of polystyrene is by a free radical polymerization as shown in Scheme 1.

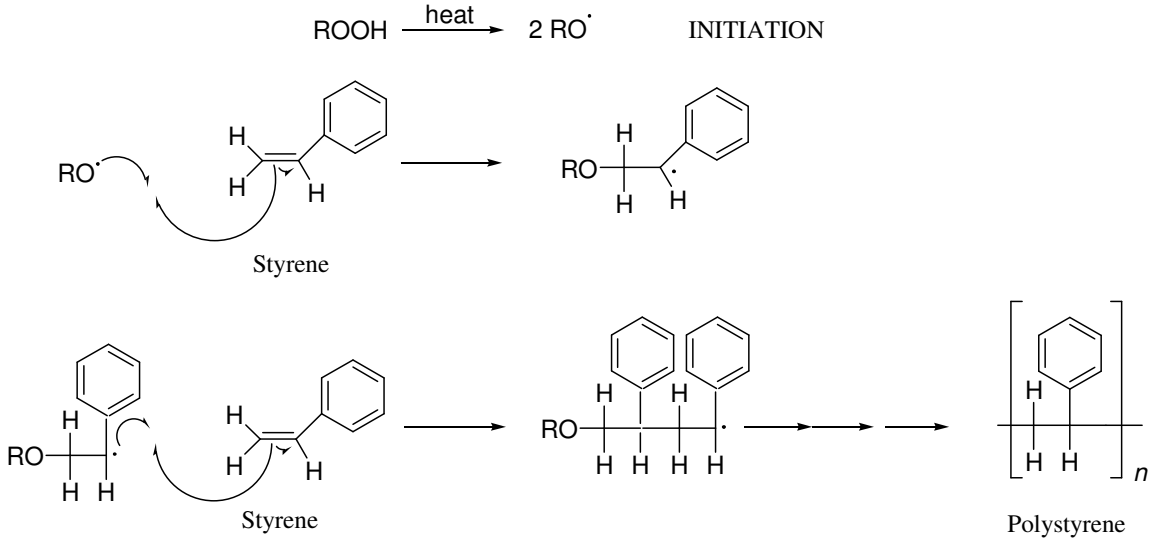

***Scheme 1*:** Free radical polymerization of styrene to form polystyrene.

Condensation (Step-growth) Polymerization

Condensation or step-growth polymerization results from the chemical union of many monomers in a series of individual steps and includes the elimination of simpler molecules (i.e. H_2O, HCl, NaCl, NH_3) with each step.[6] Carothers demonstrated in the 1930s that the chemistry of condensation polymers is essentially the same as classic condensations to yield esters, amides, etc.[3] The reactants of classic condensations have an active group on one end of the molecule (monofunctional) whereas monomers of condensation polymerization have an active group on both ends of the molecule (bifunctional).[2, 3] Individual molecules can react to form □ctamet (two monomers), trimers, tetramers, and so on. These oligomers can then react with other additional monomers or with other oligomers.[3] As the functional groups are consumed, the rate of polymerization decreases, while the molecular weight of these polymers increases slowly in a step-wise fashion, even at high levels of monomer conversion.[3, 7] The polymer continues to increase in molecular weight until the concentration of reactive groups is too low for the reaction to proceed at a significant rate.[7]

There are four major types of synthetic condensation polymers; polyamides, polyesters, polycarbonates, and polyurethanes.[1] Synthetic polyamides are commonly known as nylons and are synthesized by reacting diacid with diamine monomers.[7] Nylon fibers have good tensile strength and elasticity and are used to manufacture tire cord, clothing, rope, and carpeting to name but a few applications.[7] Molded nylon is used in a myriad of articles such as zippers, gears, brush bristles, and wire insulation. Nylon accounts for approximately 40% of all engineering plastics and 25% of total fiber

production.[7] The polymerization of hexamethylenediamine with adipic acid to form Nylon-6,6 is shown in Scheme 2 as an example of a condensation polymerization.

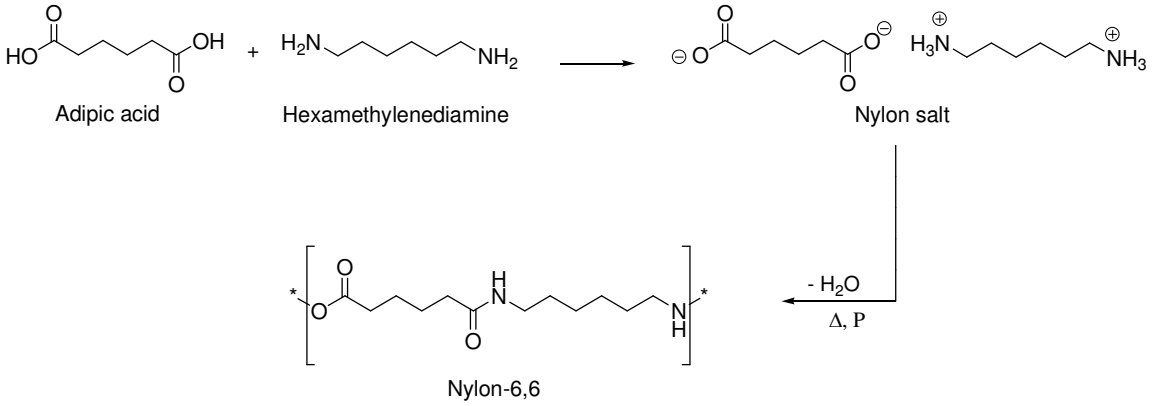

***Scheme 2*:** The synthesis of Nylon-6,6 from adipic acid and hexamethylenediamine via a diamine-dicarboxylic acid salt.

Polyesters are formed by the reaction of a diacid with a diol. They are found in almost permanent-press fabrics, tire cord, and the film Mylar® which was used to make the Echo satellite.[1] Polycarbonates are esters of carbonic acid. Lexan® is a carbonate bisphenol A condensation product and is used to make durable solid materials for uses such as bulletproof windows and crash helmets.[1] The last class of condensation polymers is polyurethanes, esters of carbamic acid. Because carbamic acid is unstable, polyurethanes are synthesized by reacting isocyanates with an alcohol or phenol.[1] Polyurethane polymers are structurally diverse with a wide number of applications that include fibers for swimsuits, elastomers for small industrial wheels, coatings for floors, and foam for pillows and cushions.

2.1.3 Describing the Size of Polymers

The size of a polymer can be described in a variety of ways. The first measure of polymer size is degree of polymerization, DP. This refers to the number of repeating units in a polymer, including end groups, and is related to both chain length and

molecular weight.[7] Most synthetic polymers are made up of chains of varying length, and therefore varying molecular weights, so the DP represents an average number.[7] The molecular weight of a polymer can be described as a number average or a weight average molecular weight.[3] The number average molecular weight (M*n*) is calculated using Equation 3.1, where M*i* is the molecular weight of the polymer molecules and N*i* is the number of polymer molecules.[3] For example, the M*n* of three molecules with molecular weights of 1.00 x 10^5, 2.00 x 10^5, and 3.00 x 10^5 is (6.00 x 10^5)/3 = 2.00 x 10^5, Equation 3.2.[3] M*n* can also be calculated by multiplying the DP by the molecular weight of the repeat unit, M*r*, as in Equation 3.3.[3]

$$Mn = \frac{W}{\sum Ni} = \frac{\sum Mi \times Ni}{\sum Ni} \tag{3.1}$$

$$Mn = \frac{(1.00\times10^5)(1) + (2.00\times10^5)(1) + (3.00\times10^5)(1)}{3} = 2.00\times10^5 \tag{3.2}$$

$$Mn = DP \times Mr \tag{3.3}$$

While Mn is dependent on the total number of particles, weight average molecular weight (M*w*) is more dependent on the number of heavier molecules present.[3] It is the second power average, shown mathematically in Equation 3.4.[3] For the example used in calculating M*n* (Equation 3.2) the M*w* is 2.33 x 10^5, Equation 3.5.[3]

$$Mw = \frac{\sum Mi^2 Ni}{\sum MiNi} \tag{3.4}$$

$$Mw = \frac{(1.00\times10^5)^2(1) + (2.00\times10^5)^2(1) + (3.00\times10^5)^2(1)}{(1.00\times10^5)(1) + (2.00\times10^5)(1) + (3.00\times10^5)(1)} = \frac{1.4\times10^{11}}{6.00\times10^5} = 2.33\times10^5 \quad \textbf{(3.5)}$$

In a monodisperse systems M*n* and M*w* are equal. In a polydisperse system M*w* is greater than M*n* and the ratio of M*w*/M*n* is a measure of the polydispersity and is called the polydispersity index.[3] A number of experimental techniques are used to determine M*n* and M*w* and include light scattering, microscopy, centrifugation, and end group analysis.[3]

2.1.4 Stereoregular Polymers

Stereoregular polymers are made up of identical, repeating chiral monomers. These polymers are stereoregular in comparison to stereorandom, or atactic, polymers in which there is no repeating orientation of the chiral monomer units. Classic examples of stereoregular polymers are isotactic or syndiotactic polymers. For example, isotactic polypropylene has all the pendant methyl groups on the same side of the polymer whereas syndiotactic polypropylene has alternate pendant methyl groups on the same side of the chain.

Nature also generates many stereoregular polymers. These include polysaccharides, such as cellulose and chitin, and polyamides such as polyalanine.[3] Stereoregular synthetic polymers are somewhat difficult to make and catalysts are typically needed for their formation.[3] Ziegler-Natta catalysts, used to catalyze olefin polymerization, are a combination of a transition metal compound from groups IV to VIII of the periodic table, such as $TiCl_4$, and an organometallic compound of a metal from groups I to III of the periodic table, such as diethyaluminum chloride.[3] *Cis*-polyisoprene, *cis*-poly-1,4-butadiene, and polypropylene are a few examples of polymers synthesized with Ziegler-Natta catalysts.[3] Copper and palladium are used to catalyze

the polymerization of α-carbonyl-stabilized carbenes from diazocarbonyl compounds to give stereoregular polycarbenes.[8] More recently the stereoselective polymerization of carbenes from ethyl diazoacetate was reported.[8] Stereoregular polyquinonimines have been synthesized via a condensation polymerization in the presence of TiCl4 and DABCO.[9] Stereoregular polymers are often attractive target molecules as high-strength materials with a high degree of crystallinity.[3]

2.1.5 Polyamides

Nylon was first synthesized by Wallace H. Carothers, working for E.I. du Pont de Nemours (now DuPont®), in 1935 by reacting adipic acid, a six carbon diacid, with hexamethylenediamine to form poly(hexamethylene adipamide).[10] Because both the diacid and the diamine had six carbons each, the new molecule was named Nylon-6,6. Nylon-6,6 was first prepared by the direct addition of hexamethylenediamine to adipic acid; the polymerization took place "quite readily" and was complete conditions that involved heating the reaction to 280-290 °C, giving polymers with molecular weights suitable for producing excellent quality synthetic silk.[11] However, the ratio of diamine to diacid is critical both initially and at various stages of the reaction.[11] If an excess of diamine is present the diacid will be capped at either end with the diamine, whereas use of excess acid generates an oligomer with acid functionality at both ends.[11] To produce a high molecular weight polymer stoichiometrically equivalent amounts of diamine and diacid must be used.[11] Carothers found it advantageous to prepare the polyamide from the diamine-dicarboxylic acid salt rather than directly from the diacid and diamine.[12] The salt provided an exact 1:1 molar ratio of diacid to diamine with the added benefit of

eliminating impurities present in both the original diacid and diamine.[12] The salts were also easier to handle, store, and ship.[12]

Following Carothers basic research at DuPont, nylons became marketable after World War II and are now some of the most important synthetic polymers worldwide.[13]

2.1.6 Polyhydroxypolyamides

Polyhydroxypolyamides (PHPAs) are derived from aldaric acids and diamines and can also be labeled hydroxylated nylons. They are of the general structure shown in Figure 1. For these polymers to be commercially attractive few steps should be required in their synthesis, no aldaric acid protection/deprotection is needed, and extensive purification must be avoided.[14] These polyamides, with both hydrophobic and hydrophilic characteristics, exhibit unique properties but as of yet are not commercially available.

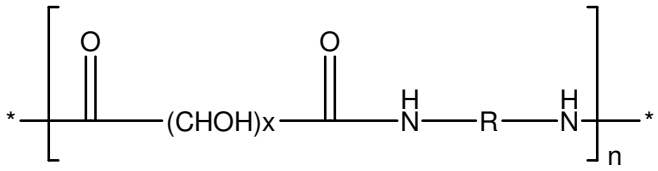

Figure 1: Generic polyhydroypolyamide or hydroxylated nylon

Polyamides from galactaric acid and a diamine were explored by Wolfrom *et al* in 1958.[15] Galactaric acid was first converted to the protected tetra-*O*-acetyl-galactaroyl dichloride and then condensed with a diamine in either benzene or methanolic sodium □ctamethy at room temperature.[15] These poly(galactaramides) were not soluble in common organic solvents.[15] The polymers generated in methanol were partially acetylated, and yields using benzene as a solvent were much greater than from methanolic sodium □ctamethy.[15] Carbohydrate polyamides have also been prepared by polycondensation of 1,6-diamino-1,6-dideoxy-*O*-allylenehexitols with aliphatic diacid

dichlorides.[16] Reported yields were modest and the acid catalyzed deprotection step caused some polymer decomposition.[16]

Ogata and co-workers further explored polycondensation reactions in the 1970s. They found that esterified galactaric acid rapidly undergoes polymerization with diamines at room temperature.[17] They also demonstrated that L-dimethyl tartarate, an α-hydroxy ester, was found to easily undergo polycondensation reactions with various aliphatic diamines in methanol to form polyamides at 30 °C, while aromatic diamines did not react under such mild conditions.[18] Ogata and Hosada postulated that the hydroxyl groups attract the diamine by way of hydrogen bonding thus increasing the local concentration of amine at the reaction site and facilitating the reaction.[18]

After the success of L-dimethyl tartarate polymerizations, Ogata undertook the polycondensation of diethyl 2,3,4,5-tetrahydroxyadipate (diethyl galactarate) with HMD.[19] The polymerizations also took place under mild conditions, 30 °C, compared with those of dimethyl adipate and HMD.[19] In addition, the reaction of diethyl 2,3,4,5-tetrahydroxyadipate and HMD proceeded much faster than that of L-diethyl tartarate and HMD confirming the enhancing effect of pendant hydroxyl groups.[19] The effect of solvent was also explored and polar solvents were found to enhance polycondensation reaction rates.[19] The best yields were reported with methanol as a solvent.[19]

Knowing that sugar lactones readily react with amines, Hoagland studied the mechanism involved in the aminolysis of diethyl galactarate.[20] He suspected the formation of intermediate lactones in the aminolysis and, employing ^{13}C NMR analysis, studied the reaction of diethyl galactarate and aminoethanol. He found that upon addition of the amine, the ester γ-monolactone formed quickly and was then slowly consumed by

the amine.[20] The resulting molecule is an amide-lactone, which is slowly consumed to give the acyclic diamide following second lactonization and aminolysis steps.[20] The acyclic ester-amide was not observed by NMR.[20] As five-membered γ-lactones react faster with nucleophiles than acyclic esters, the presence of such intermediate lactones explains why diethyl galactarate is more reactive with amines than diethyl adipate or diethyl tartarate.[20] Kiely and Viswanathan later expanded on this study by observing the aminolysis of D-glucaric esters with ^{1}H and ^{13}C NMR.[21] They observed the acyclic ester-amide and determined that the formation of the amide-lactone from the ester-lactone was not a concerted reaction.[21]

D-Glucaric acid based hydroxylated nylons were first prepared by Kiely *et. al.* from monopotassium D-glucarate and various diamines. The monopotassium salt was protonated with strong cation-exchange resin and dried to give a mixture of lactones.[14] The lactones were esterified with methanolic hydrogen chloride to give a mixture of dimethyl D-glucarate and methyl D-glucarate 1,4- and 6,3-monolactones. The diamine of choice was added to a methanol solution containing the D-glucaric acid esters and triethylamine.[14] Based on Hoagland's mechanistic study, triethylamine was added to ensure the base-induced amide-lactone to acyclic amide transformation would continue at an appreciable rate even near the end of the polymerization when the concentration of diamine was low.[14] This method gave yields of up to 96%.[14]

The initial poly(D-glucaramides) prepared by Kiely *et al*. were stereorandom polymers.[14] D-Glucaric acid is chiral, with four contiguous chiral centers, but is asymmetrical.[14] C1 is designated the "*head"* carbon and C6 is designated the "*tail"* carbon. This lack of symmetry introduced the possibility of different polymer

alignments, so called "*head to tail*" and "*tail to head*." Sodium D-glucarate 6,3-lactone was prepared from monopotassium D-glucarate and refluxed with even numbered aliphatic diamines in methanol.[22] This reaction produced sodium 6-[*N*-(amninoalkyl)]-D-glucaramides.[22] Each of the salts were then esterified with methanol hydrogen chloride and triethylamine added to initiate spontaneous polymerization and the formation of stereoregular *head,tail*-poly(alkylene D-glucaramides).[22] Later, the lithium salt of D-glucaro-6,3-lactone was mixed with a diamine in methanol and purified by gel permeation chromatography to give *head,tail* diamido-diacids.[23] The diamido-diacids were then esterified with methanolic hydrogen chloride in methanol and diamine added; this yielded alternating stereoregular *head,tail-tail,head*-poly(alkylene D-glucaramides).[23] This method however required multiple steps and purification of the intermediate compound.[23]

Higher molecular weight random polyhydroxypolyamides were more recently produced by the polymerization of a 1:1 stoichiometrically balanced esterified aldaric acid:alkylene diammonium salt.[24] The diammonium salt is analogous to the nylon salt used by Carothers to produce Nylon-6,6. A diamine was added to an aldaric acid in water to produce the diammonium salt. The aldaryl unit was then esterified in alcohol with an acid catalyst and the diester:diamide salt polymerized in the presence of a tertiary amine to form the random polymers labeled prepolymers.[24] The prepolymers were further polymerized in an appropriate solvent to form higher molecular weight polyhydroxypolyamides.[24]

2.1.7 Mannaramides

D-mannaric acid is a chiral tetrahydroxy adipic acid with four chiral centers, a C-2 axis of symmetry, but no plane of symmetry. Consequently, polyamides derived from D-mannaric acid are chiral and stereoregular.[25] A general structure of a poly(alkylene D-mannaramide) is shown in Figure 2.

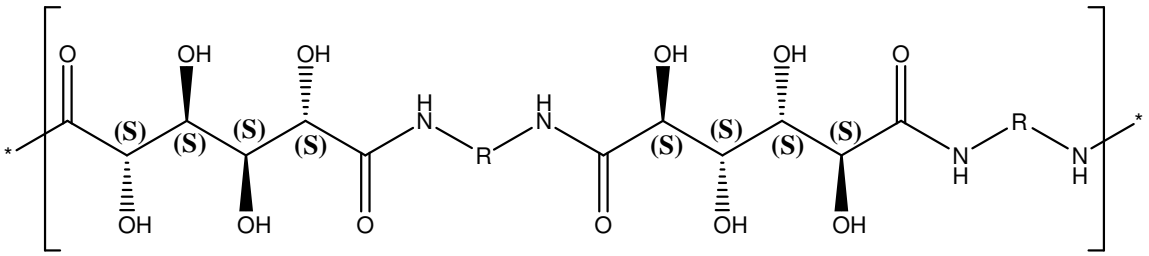

Figure 2: General structure of stereoregular poly(alkylene D-mannaramide)

Hashimoto and co-workers synthesized the first reported poly(alkylene D-mannaramides) from D-mannaro-1,4:6,3-dilactone and aliphatic diamines in DMSO at room temperature.[26] Yields were modest and both the yields and molecular weights of polymers formed were lower than the corresponding polymers formed from D-glucaro-1,4:6,3-dilactone.[26] This suggests that the ring-opening polyadditon of D-mannaro-1,4:6,3-dilactone with diamines is more difficult than with D-glucaro-1,4:6,3-dilactone.[26] It is worth noting that while the melting points of the poly(alkylene D-mannaramides) were lower than those of the corresponding nylons, they were greater than for the corresponding poly(alkylene D-glucaramides).[26]

Kiely *et al*. performed reactions similar to those performed by Hashimoto *et al*.[27] D-mannaro-1,4:6,3-dilactone was dissolved in methanol and a nearly equimolar amount of diamine was added.[27] Reaction mixtures became tan to brown and the resulting polyamides were colored similarly.[27] The polymers had low solubility in methanol and

the molecular weights were smaller than the corresponding polymers derived from D-glucaric acid and D-xylaric acid.[27]

The absence of 1,3-parallel hydroxyl group eclipsing steric interactions in an extended zigzag conformation of the mannaryl unit make this conformation a reasonable model for the repeating unit in the mannaramides.[27] Low solubility of the tetramethylene polyamide suggests intermolecular hydrogen bonding between mannaryl monomer units in parallel polymer chains, which is also observed for extended galactaryl units in galactaramides.[27] Low molecular weight values for poly(D-mannaramides) are consistent with extended polyamides with low methanol solubility when compared with molecular weight values from bent poly(D-glucaramides) and poly(xylaramides).[27]

Poly(alkylene D-mannaramides) were later prepared by Orgueira and Varela by dissolving D-mannaro-1,4:6,3-dilactone in methanol with triethylamine followed by the addition of a diamine.[25] White solids were obtained and purified by refluxing in methanol.[25] The reflux treatment lowered the yield but increased the molecular weights, as compared to polymers prepared by Kiely *et al*, probably by removing oligomers of low molecular weight.[25] The polycondensation of D-mannaro-1,4:6,3-dilactone with hexamethylenediamine was also attempted in *N,N*-dimethylformamide and DMSO, but polymers obtained were brown solids in low yield.[25]

2.1.8 Aims of this research

- Synthesize alkylenediammonium D-mannarate salts with stoichiometrically balanced 1:1 molar ratios of D-mannaric acid:diamine
- Use alkylenediammonium D-mannarate salts for the production of chiral, stereoregular and biodegradable poly(alkylene D-mannaramides)

- Determine the crystal structure of a salt of D-mannaric acid for possible insight into the conformation of the mannaryl unit of poly(alkylene D-mannaramides) in the solid state

2.2 Results and Discussion

2.2.1 Synthesis of Alkylenediammonium D-Mannarate Salts (5a-f)

Alkylenediammonium D-mannarate salts, **5a-f**, were synthesized from *N,N´*-dimethyl-D-mannaramide (**1**) (Chapter 1 p. 43-47) as shown in Scheme 3. The synthesis of **5a-f** was initiated by the base hydrolysis of *N,N´*-dimethyl-D-mannaramide (**1**) in aqueous solution using two equivalents of sodium hydroxide to give disodium D-mannarate (**2**).

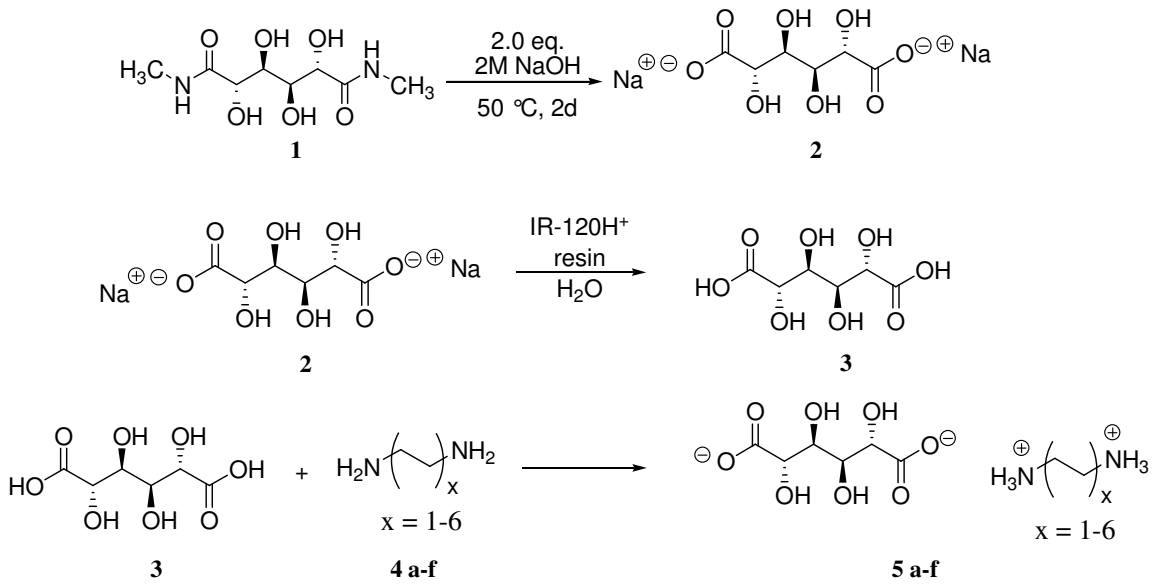

1 → 2 → 3 → 3 + 4 a-f → 5 a-f

***Scheme 3*:** Preparation of alkylenediammonium D-mannarate salts (**5a-f)** from *N,N´*-dimethyl-D-mannaramide (**1**)

Isolation of Disodium D-Mannarate

At room temperature base hydrolysis of **1** is a slow reaction and so the reaction mixture was heated to 50 °C for two days to accelerate the reaction. Concentration of the

reaction mixture followed by drying overnight under vacuum afforded a white solid which was triturated with methanol to remove residual sodium hydroxide. Insoluble, solid **2** was separated by vacuum filtration and characterized by GC-MS, IC, and ^{1}H NMR analysis. Disodium D-mannarate (**2)** was also analyzed by GC-MS as the per-*O*-trimethylsilyl derivative and seen as a single peak at 44.77 min, Figure 3, with a characteristic $[M-15]^{+}$ peak at *m/z* = 627, Figure 4. The peak at m\z = 333 is very abundant and formed from the loss of TMSOH from m\z = 423.[28] It is suggested that the intensity of m/z = 333 is also due to a fragmentation of m/z = 627 in which the TMS group from C4 migrates to the carbonyl oxygen of C1 and then loss of C5, C6 (m/z = 204) and corresponding functional groups; this gives a m\z = 423.[27] This is followed by loss of TMSOH from C2 to give the very favorable m\z = 333 ion with resonance stabilization.[28] A McClafferty rearrangement involving migration of the C2 TMS group to the C1 carbonyl oxygen followed by fragmentation between C2 and C3 and accounts for the characteristic peak at m\z = 292.[28] It should be noted that the peaks m\z = 73 and m\z = 147 are characteristic of per-*O*-trimethylsilyl derivatives of carbohydrates.[28] The important mass fragments of disodium D-mannarate are shown in Figure 4.

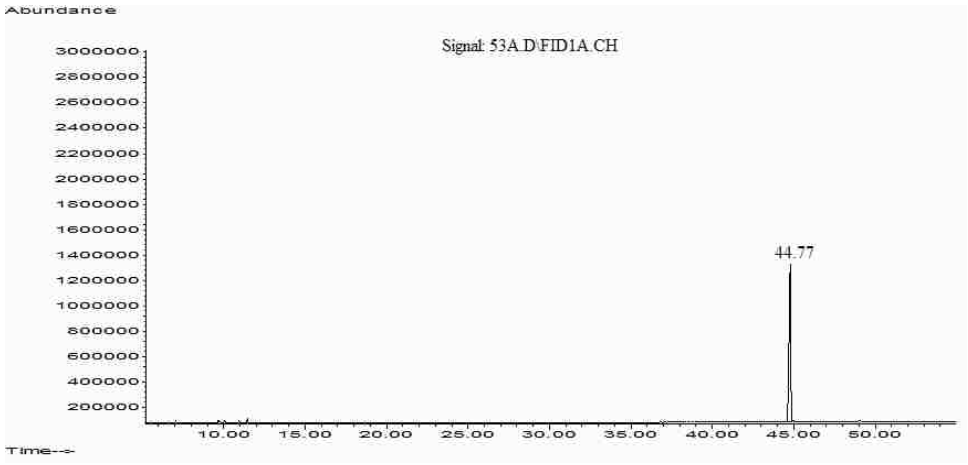

***Figure 3*:** Gas Chromatogram of **2** as the per-*O*-trimethylsilyl derivative.

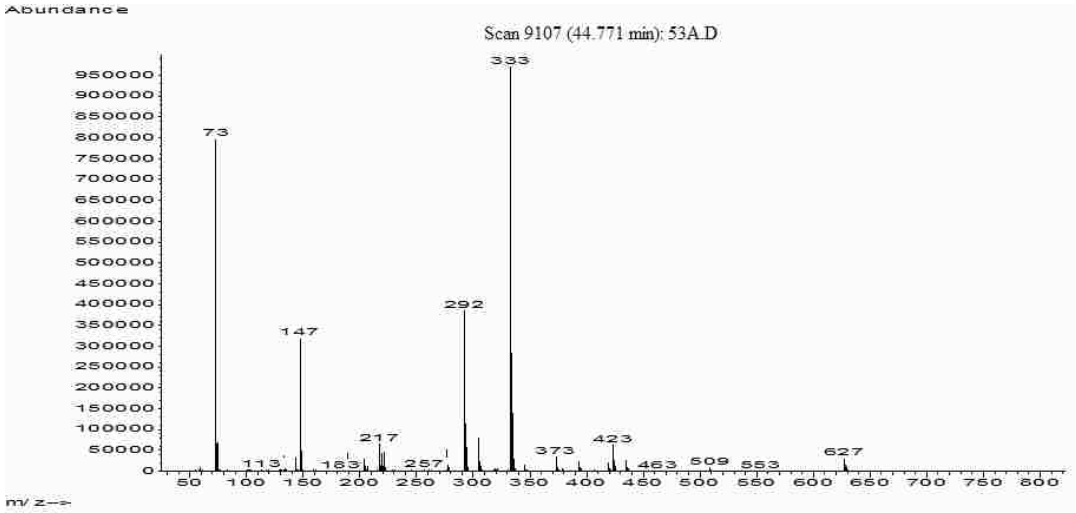

***Figure 4*:** Mass spectrum of the per-*O*-trimethylsilyl derivative of **2** showing $[M+15]^+$ of m/z = 627 showing prominent peaks at m/z = 292 and m\z = 333

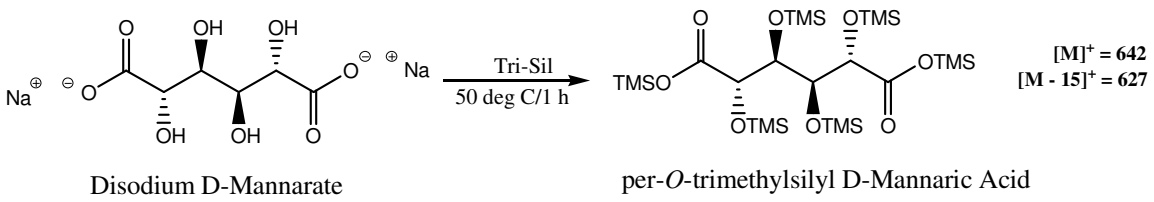

Disodium D-Mannarate

per-*O*-trimethylsilyl D-Mannaric Acid

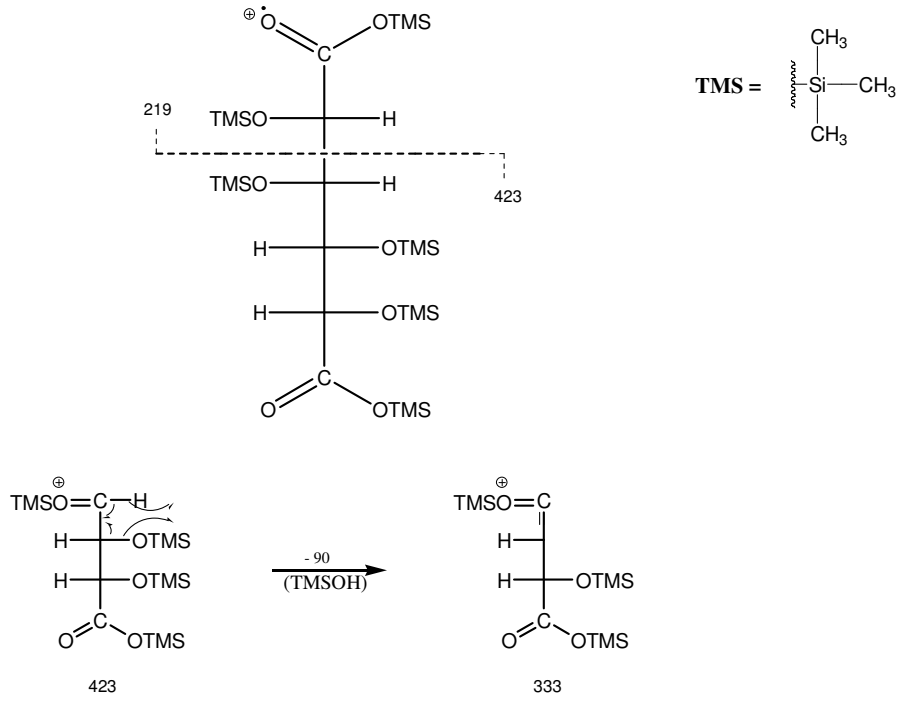

McLafferty Rearrangement

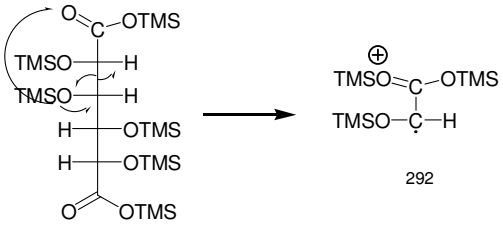

Figure 5. Important mass fragmentations for per-*O*-trimethylsilyl D-mannaric acid including the McLafferty Rearrangement

Disodium D-mannarate (**2)** was also seen as a single component by ion chromatography at retention time 10.964 min, Figure 6. The trailing peaks found just after the mannarate peak at 10.964 min are artifact peaks also found in blank samples. Because of the sodium

hydroxide eluent generator, the IC analyzes only for anions and therefore only one peak is observed for disodium D-mannarate.[30]

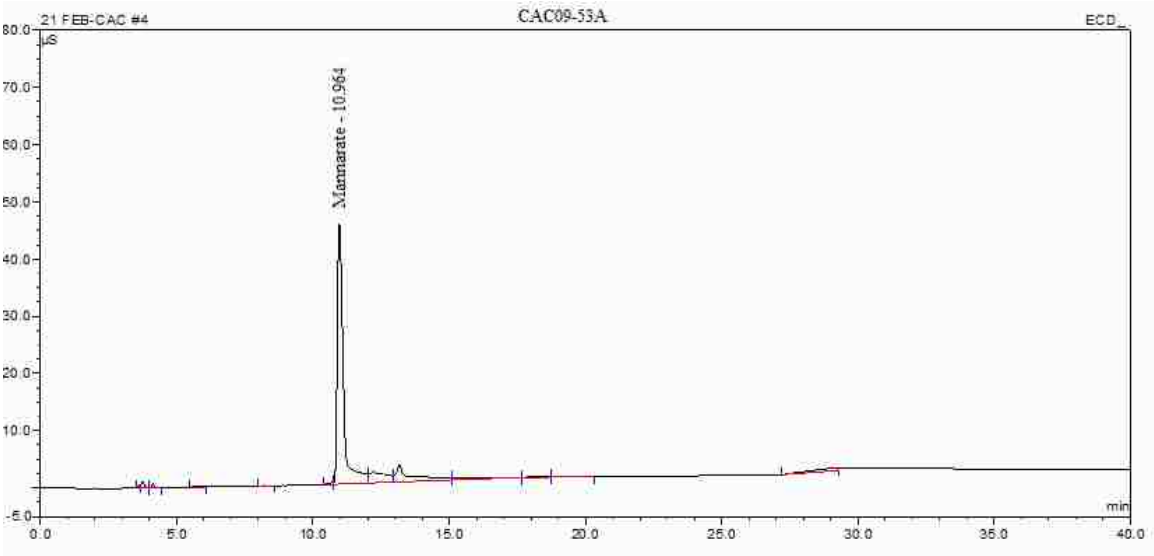

***Figure 6*:** Ion chromatogram of **2**

The assigned ^{1}H NMR spectrum of **2** was consistent with a literature assignment, Figure 7.[31] As with D-mannaro-1,4:6,3-dilactone H2 and H5 are equivalent protons as are H3 and H4. Consequently only two signals are observed; H2 and H5 at 4.05 ppm, H3 and H4 at 3.90 ppm with $J_{2,3} = J_{4,5} = 5.86$ Hz. The chemical shift between the two signals is relatively small (0.15 ppm or 60 Hz) and therefore instead of linear midpoints, or two signals with doublets of the same size, a "center of gravity" effect is observed.[29] As a result the two internal signals are slightly higher than the two outside signals. The coupling constants are not extremely large (5.86 Hz) and the effect is apparent but not pronounced.

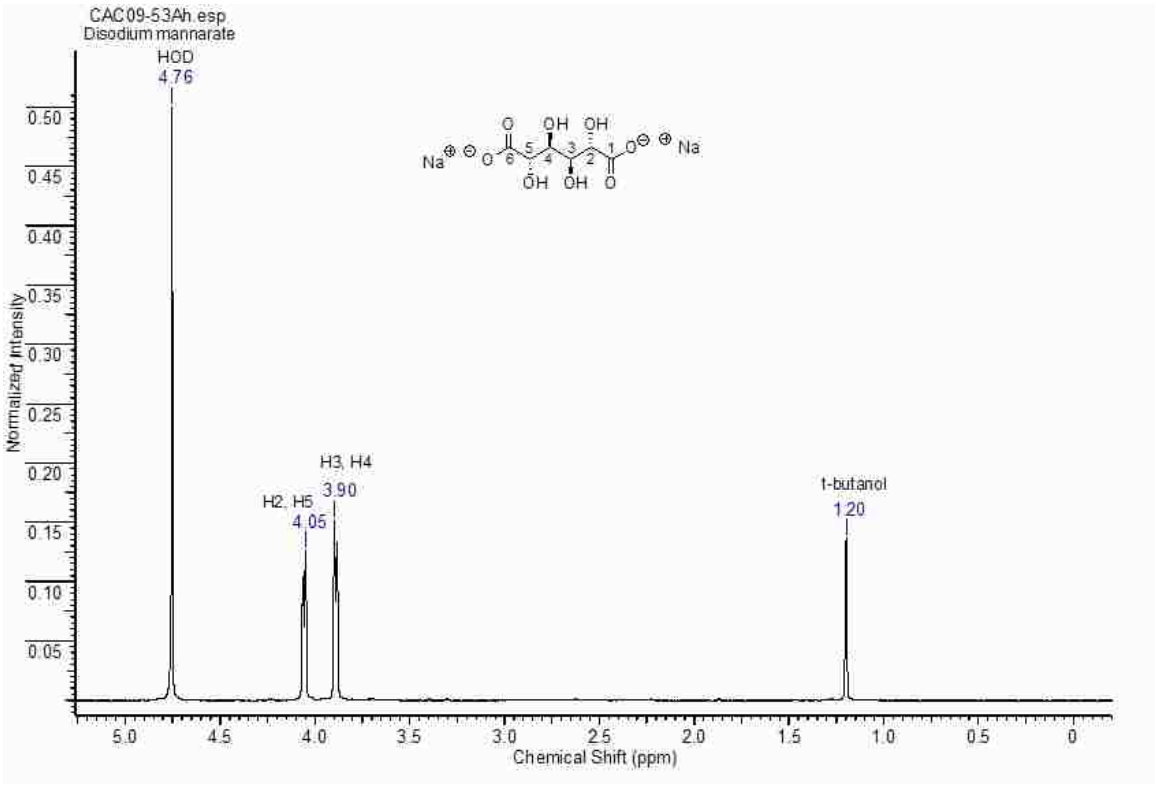

Figure7: Assigned ^{1}H NMR spectrum of **2** in D_2O showing doublets at 3.90 ppm and 4.05 ppm

Alkylenediammonium D-Mannarate Salts

Alkylenediammonium salts of D-mannaric acid (**5 a-f**) were then prepared by reacting **2** with a strong H^+ form cation exchange resin in water followed by addition of the diamine (**4 a-f**), Scheme 3. The resin was removed by filtration and the aqueous D-mannaric acid (**3**) added to a solution of diamine (slight excess) in water for all diamines with the exception of dodecamethylenediamine for which methanol was the solvent of choice. Each of the aqueous or methanol solutions was concentrated and the resulting thick syrup was dried under vacuum and then triturated with methanol to remove unreacted diamine. The product salts were isolated by vacuum filtration as white solids. After drying under vacuum, the salts were characterized by ^{1}H NMR and IC. Yields of the alkylenediammonium salts **5 a-f** are given in Table 1.

Table 1: Isolated % Yields of Alkylenediammonium Salts of D-Mannaric Acid

5 a-f	# of methylene groups in amine	Percent Yield
a	2	91.2
b	4	76.0
c	6	89.6
d	8	94.0
e	10	81.5
f	12	81.9

The ^{1}H NMR spectrum of hexamethylenediammonium mannarate (**5c**) is shown as a representative of alkylenediammonium salts, Figure 8.

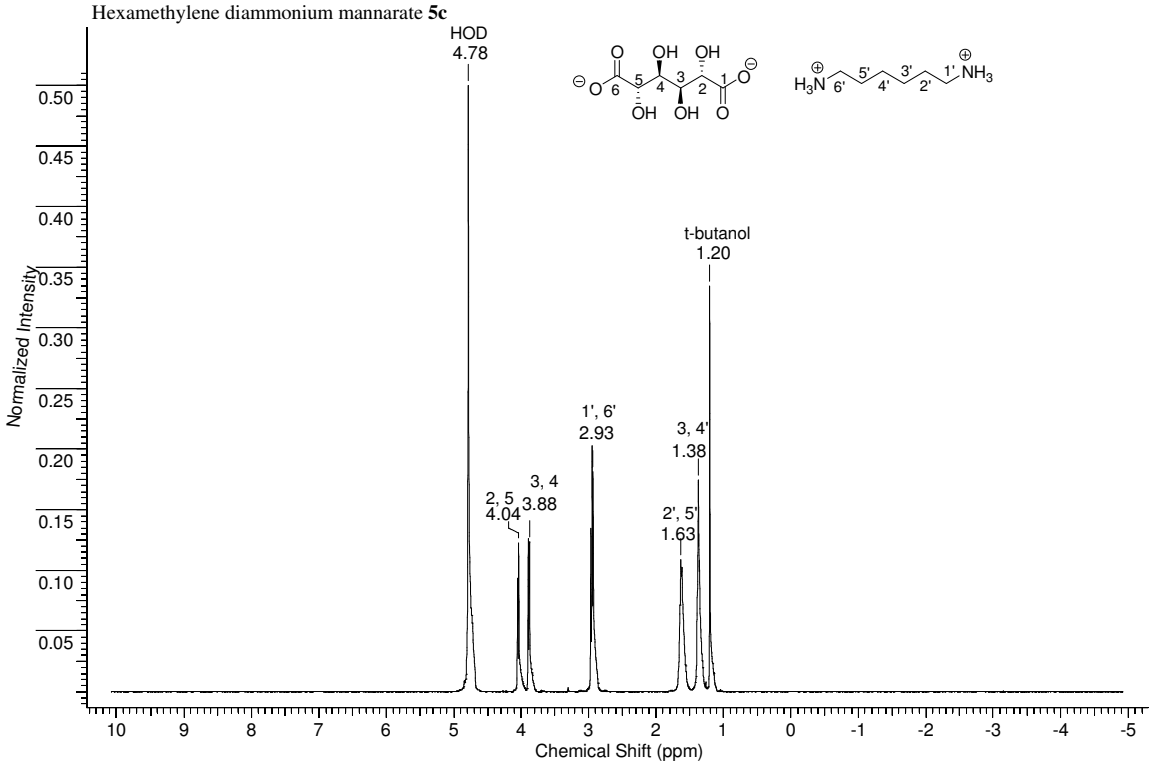

Figure 8: Assigned ^{1}H NMR spectrum **5c** in D_2O

All ^{1}H NMR spectra of the alkylenediammonium D-mannarate salts were recorded in D_2O. As with **2**, protons H2 and H5 are equivalent as are protons H3 and H4

of the D-mannaryl unit. With the hexamethylene unit three signals from equivalent 1´ and 6´, 2´ and 5´, and 3´ and 4´ respectively, are observed. Each of these signals is seen as an unresolved multiplet.

The ion chromatograms from **5a-f** were virtually identical showing a single peak for D-mannarate. The IC of **5c** with a retention time of 11.063 min is shown as an example, Figure 9.

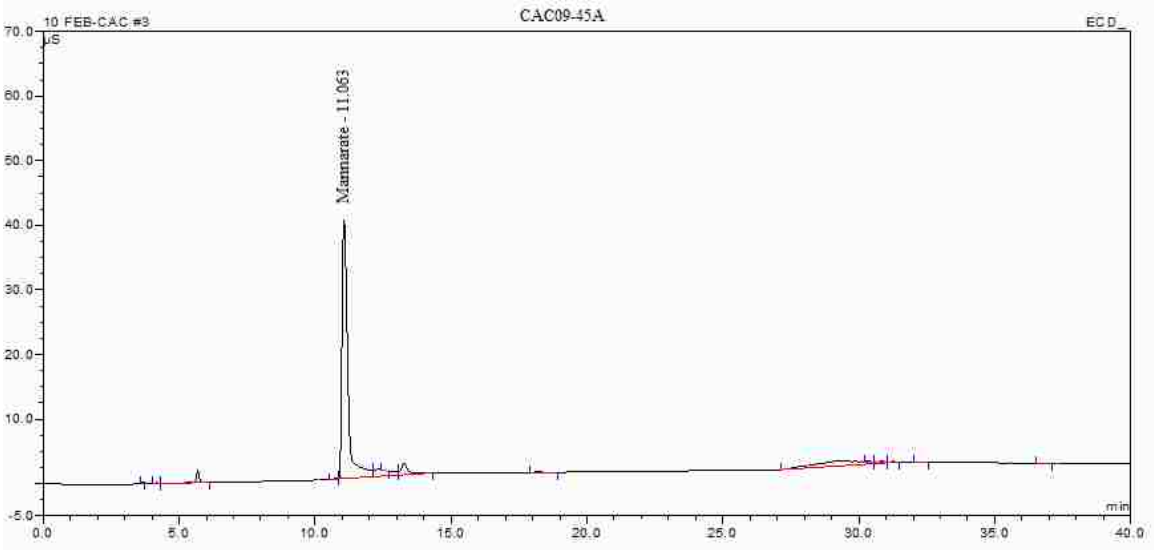

Figure 9: Ion chromatogram of **5c**

As with disodium D-mannarate, the peaks found trailing the mannarate peak are artifacts and found in the blank as well.

X-ray Crystallographic Analysis of Octamethylenediammonium D-Mannarate (5d)

Octamethylenediammonium mannarate (**5d**) was successfully recrystallized from water to produce crystals of good quality and size for single-crystal x-ray crystal structure analysis. This molecule was crystallized for possible structural and conformational correlation with the D-mannaryl unit in non-crystalline but solid poly(alkylene D-mannaramides). Figure 10 shows the labeling of atoms in the x-ray crystal structure.

Selected bond angles are reported in Table 2. The unit cell associated with the crystal structure is shown in Figure 11. Hydrogen bonds are represented by dashed lines.

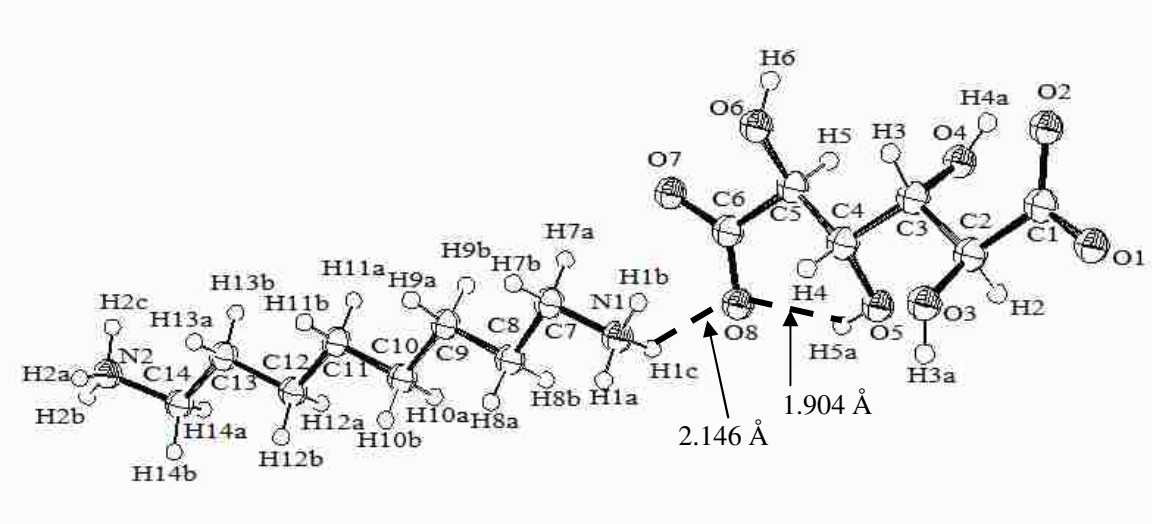

Figure 10: Ortep drawing showing the labeling of the atoms in the crystal structure of octamethylenediammonium D-mannarate showing the hydrogen bonding associated with the structure

Table 2: Selected torsion angles from the crystal structure of octamethylenediammonium D-mannarate (**6d**)

Backbone	**Torsion Angle**
O(1)-C(1)-C(2)-C(3)	176.41(13)
C(1)-C(2)-C(3)-C(4)	-175.45(10)
C(2)-C(3)-C(4)-C(5)	-176.70(11)
C(3)-C(4)-C(5)-C(6)	175.95(10)
C(4)-C(5)-C(6)-O(7)	157.82(12)
N(1)-C(7)-C(8)-C(9)	-176.63(11)
C(7)-C(8)-C(9)-C(10)	-175.75(12)
C(8)-C(9)-C(10)-C(11)	173.92(12)
C(9)-C(10)-C(11)-C(12)	179.76(12)
C(10)-C(11)-C(12)-C(13)	170.91(12)
C(11)-C(12)-C(13)-C(14)	-178.08(12)
C(12)-C(13)-C(14)-N(2)	168.71(12)
O(2)-C(1)-C(2)-O(3)	-127.91(15)
O(3)-C(2)-C(3)-O(4)	-172.64(10)
O(4)-C(3)-C(4)-O(5)	63.92(12)
O(5)-C(4)-C(5)-O(6)	178.35(10)
O(6)-C(5)-C(6)-O(8)	-145.00(12)
O(1)-C(1)-C(2)-O(3)	53.01(17)
O(6)-C(5)-C(6)-O(7)	36.47(16)

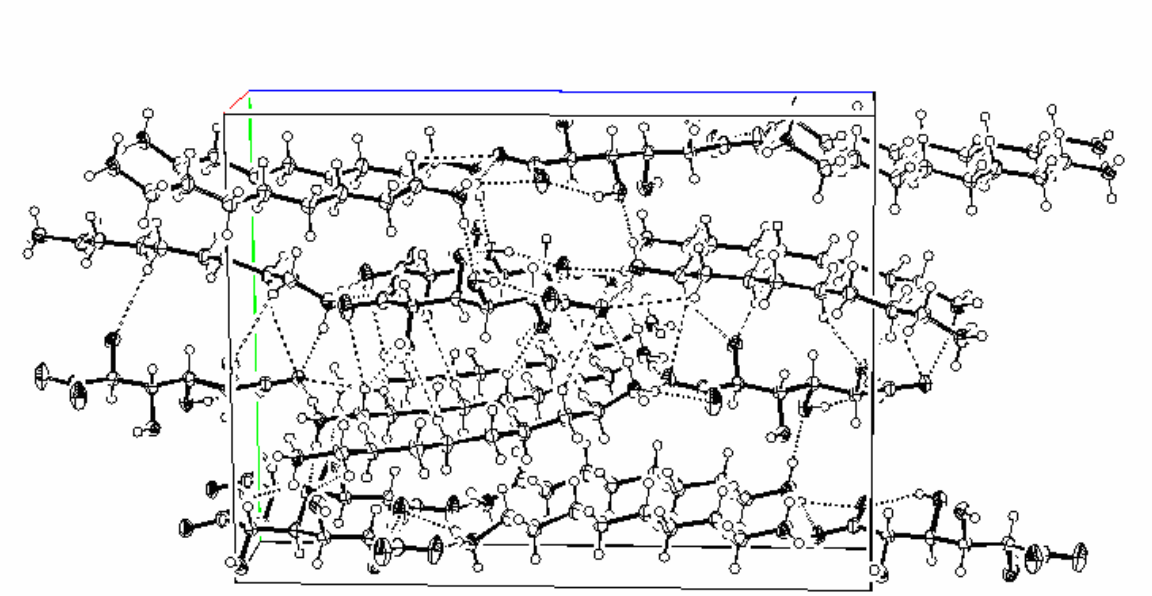

Figure 11: Ortep drawing of the unit cell associated with the crystal structure of octamethylenediammonium D-mannarate perpendicular to the bc-plane showing the hydrogen bonding associated with the system

Octamethylenediammonium mannarate (**5d**) adopts an extended conformation in the crystalline state and is free of destabilizing 1,3-parallel hydroxyl group eclipsing steric interactions which is consistent with a minimally sterically hindered model. The salt crystallizes in sheets perpendicular to the bc-plane of the unit cell and displays intramolecular hydrogen bonding as well as hydrogen bonding between terminal atoms of the cation and anion units and between somewhat parallel components of the salt. An intramolecular hydrogen bond is seen at C6-O8···H5a-O5-C4 (1.904 Å) and a hydrogen bond between the terminal cation and anion units at N1-H1C···O8-C6 (2.146 Å). Because the process of x-ray crystallographic analysis sees only one end of the molecule and the mannaryl unit is symmetric, it can be assumed that there is a corresponding hydrogen bond at C1-O2···H4A-O4-C3 of the same magnitude as the corresponding bond at the opposite end of the mannaryl unit (1.904 Å). There is also an extensive network of intermolecular hydrogen bonds; C1-O1···H2c-N2 (1.837 Å), C1-O2···H3a-O3-C2 (2.058

Å), C1-O2···H2b-N2 (2.058Å), C4-O5···H1c-N1 (1.901 Å), C6-O7···H1a-N1 (2.066 Å), C6-O7···H2a-N2 (1.946 Å), C6-O8···H5a-O5-C4 (1.904 Å), C6-O8···H1b-N1 (2.146 Å), and C6-O8···H6-O6-C5 (1.911 Å). All x-ray crystallographic data for Octamethylenediammonium mannarate (**5d**) can be found in the appendix of this dissertation.

2.2.2 Poly(alkylene D-mannaramide) Prepolymers (6 a-f)

Poly(alkylene D-mannaramide) polymers **6 a-f** were synthesized from the corresponding alkylenediammonium salts of D-mannaric acid **5 a-f** as shown in Scheme 5. These polymers are labeled as prepolymers **6a-f** as compared to postpolymers **7a-f** which originate from **6a-f** and will be described.

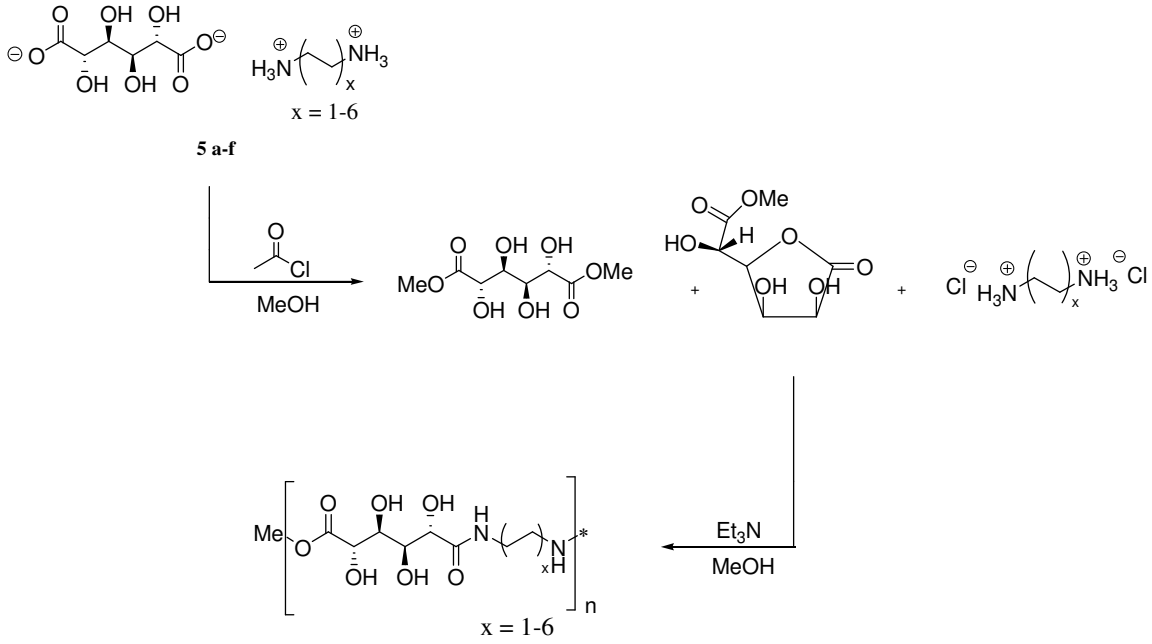

Scheme 4: Synthesis of poly(alkylene D-mannaramide) prepolymers **6 a-f** from diammonium salts of D-mannaric acid **5 a-f**

The diamines chosen (**4 a-f**) had 2, 4, 6, 8, 10, and 12 methylene groups, respectively. The C2, C4, and C6 diamines were polymerized with esterified mannaric

acid from D-mannaro-1,4:6,3-dilactone in the past but never with careful attention to diacid:diamine stoichiometric control.[25, 26] Each of the alkylenediammonium salts was esterified with methanolic hydrogen chloride to form active esters of mannaric acid as well as the corresponding alkylenediammonium dichlorides. The ester-salt mixture was then made basic with triethylamine which also served to promote polymerization by catalyzing the following reaction sequence:

diester→ester lactone→amide ester→amide lactone→diamide→polyamide

Use of triethylamine ensured that the polymerization continued at an appreciable rate throughout the reaction. This method was keeping with Hoagland's mechanistic study[20] and the previous results of Kiely *et al*.[21] After a reaction time of 24 hours, the polymers were isolated by vacuum filtration and dried under vacuum to give **6 a-f**. Additionally polymerizations were undertaken with **5c** in which the reaction time was extended to 2 weeks. The polymers isolated *via* this latter, modified method proved to be somewhat larger based on ^{1}H NMR end group analysis indicating a slow polymerization rate after initial and rapid polymer precipitation. Compared to poly(alkylene D-glucaramides) made in a similar fashion by Kiely *et al*, **6 a-f** were observed to be appreciably smaller. To further investigate poly(D-glucaramide) versus poly(D-mannaramide) formation some parallel polymerizations were carried out using hexamethylenediammonium D-glucarate and **5c** as starting materials. In all cases, the % yields and DPs were larger for the poly(hexamethyene D-glucaramide) prepolymers. Poly(hexamethylene D-glucaramide) was isolated with a percent yield of 75.7% and DP 4.96 compared to poly(hexamethylene D-mannaramide) with isolated yield 49.0% and DP 2.97. Based on the results of the 2 week polymerization and the parallel polymerizations, it appears that overall esterified D-

mannaric acid is less reactive to aminolysis than esterified D-glucaric acid and includes both diester and ester/lactone forms of the diacids.

^{1}H NMR Characterization

Prepolymers **6 a-f** were dissolved in TFA-$_d$ and characterized by ^{1}H NMR spectrometry. End group analysis was performed to provide polyamide DP values. In the NMR of the polyamides it is possible to readily distinguish the CH_2 protons α to the internal amide and the CH_2 protons α to a terminal amine. These protons were used in the determination, Figure 12. It is also possible to distinguish the CH_2 protons β to the internal amide and the CH_2 protons β to the terminal amine but these are less well resolved.

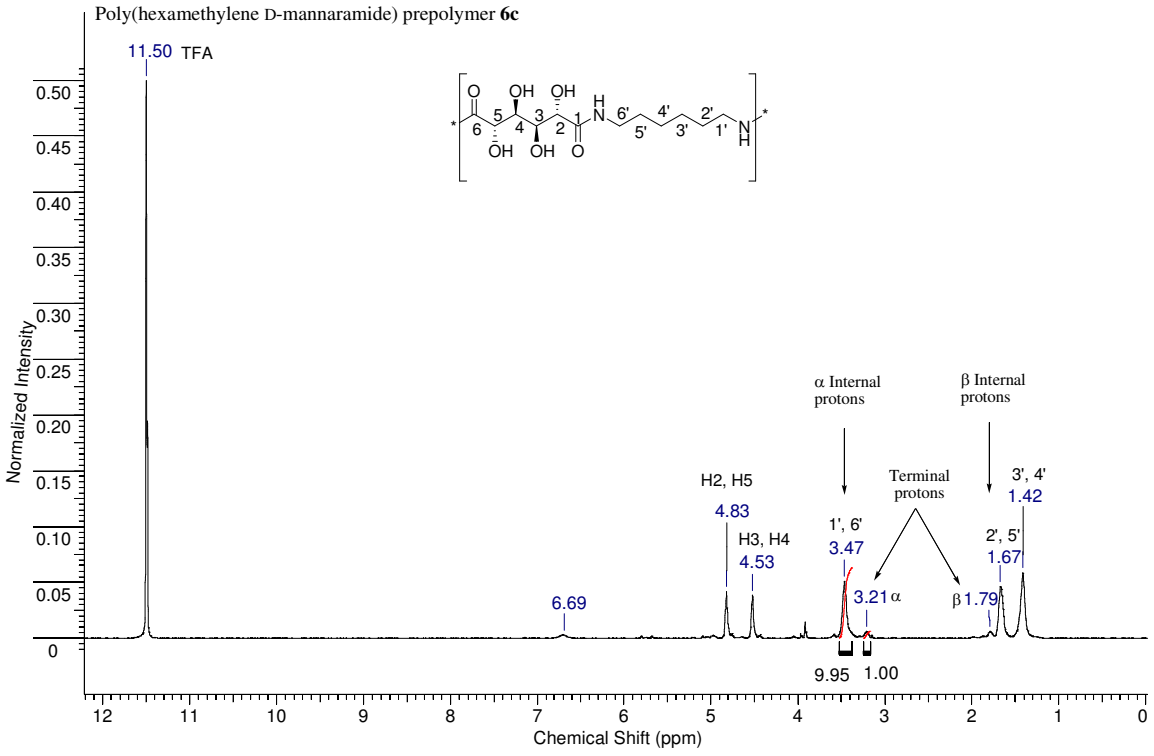

Figure 12: Assigned ^{1}H NMR spectrum of (**6c**) in TFA-$_{d6}$ with 2 week reaction time showing α and β internal and terminal protons

DP Calculation by ^{1}H NMR End Group Analysis

A formula for calculating DP was developed by Jarman based on the ratio of the integrated value of the CH_2 protons α to the amide to the integrated value of the CH_2 protons α to the amine.[32] The number of terminal and non-terminal protons were calculated for a range of theoretical DP values of poly(tetramethylene D-galactaramide) and the ratio determined.[32] The ratio of terminal to non-terminal protons was graphed against the DP to give a straight line.[32] The equation of the line was calculated (3.6) and rearranged to give the formula for calculating DP, Equation 3.7.[32]

$$Ratio = (2 \times DP) - 1 \quad (\mathbf{3.6})$$

$$DP = \frac{Ratio + 1}{2} \quad (\mathbf{3.7})$$

The CH_2 protons α to the terminal amine were assigned an integration value of 1.00 and the CH_2 protons α to the internal amide (non-terminal protons) were integrated relative to that value. Thus, the ratio of non-terminal to terminal protons was equal to the integrated value of the non-terminal protons. These values, for **6a-6f**, were used in Equation 3.7 to calculate DP values for prepolymers, Table 3. Results are comparable with the exception of poly(hexamethylene D-mannaramide) (**6c)** which was allowed to stir for 2 weeks and had DP 5.48. The larger size of **6c** indicates, as stated previously, that the rate of polymerization after initial polyamide precipitation is slow. It should be possible to make larger poly(alkylene D-mannaramide) prepolymers with the other alkyl chain lengths given longer reaction times.

Table 3: Poly(alkylene D-mannaramide) prepolymers calculated DP values and isolated % yields

Prepolymer Number	# of methylene groups in amine	Prepolymer DP	Percent Yield
6a	2	2.61	55.0
6b	4	3.14	38.1
6c	6	5.48	67.6
6d	8	3.51	48.2
6e	10	3.34	70.5
6f	12	3.31	59.9

2.2.3 Poly(alkylene D-mannaramide) Postpolymers

Poly(alkylene D-mannaramide) postpolymers (**7a-f**) were prepared from **6 a-f**, Scheme 5.

6 a-f x = 1-6 **7 a-f** x = 1-6

Scheme 5: Preparation of poly(alkylene D-mannaramide) postpolymers from poly(alkylene D-mannaramide) prepolymers

Prepolymers **6 a-f** were dissolved in DMSO/MeOH to increase their solubility, and triethylamine was added to promote the polymerization by ensuring the base catalyzed amide-lactone to acyclic amide transformation. The postpolymerization reactions were carried out at 40 °C. The elevated temperature was utilized for two reasons: 1) to further increase reactive prepolymer solubility and 2) to provide additional energy to increase polymerization rate. In all cases, methanol was added to the reaction mixture after 24 h to precipitate the postpolymer which was then isolated by vacuum filtration.

^{1}H NMR Characterization and Comparison to Poly(Alkylene D-mannaramide) Prepolymers

As with **6 a-f**, all poly(alkylene D-mannaramide) postpolymers (**7 a-f**) were dissolved in TFA-$_d$ and characterized by ^{1}H NMR. A representative ^{1}H NMR of poly(hexamethylene D-mannaramide) postpolymer (**7c**) is provided, Figure 13.

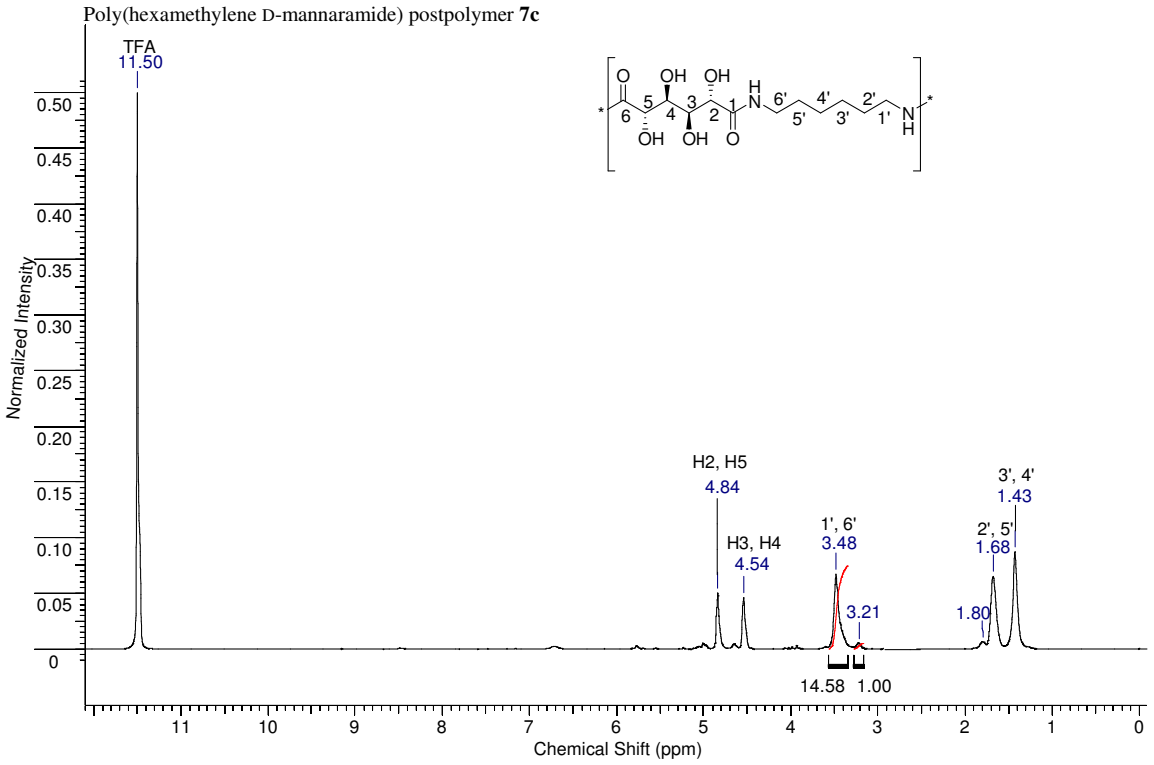

Figure 13: Assigned ^{1}H NMR spectrum of **7c** in TFA-$_d$.

End-group analysis was performed on each postpolymer and DPs calculated using Equation 3.7. In all cases, the postpolymers had markedly larger DPs than their corresponding prepolymers, Table 4. Clearly increasing reactive prepolymer solution concentration in DMSO/MeOH and raising the reaction temperature were effective in generating larger polyamides.

Table 4: Poly(alkylene D-mannaramide) postpolymers calculated DPs, % yields, and % increase from prepolymer DPs

Postpolymer Number	# of methylene groups in amine	Postpolymer DP	Percent Yield	Percent Increase
7a	2	5.22	91.4	100
7b	4	4.54	35.9	45
7c	6	7.79	50.1	42
7d	8	4.76	71.5	36
7e	10	4.36	79.3	31
7f	12	4.61	88.6	39

Table 4 shows that the C2 postpolymer increased by 100%. Interestingly poly(ethylene D-galactarate) prepolymer does not increase in size under comparable postpolymer reaction conditions; in fact they are found to be problematic and it is difficult to achieve a DP greater than 1.[33] However, the DP increase in going from prepolymer to postpolymer was less dramatic at 45% increase of poly(tetramethylene D-mannaramide). It was observed that generally as the length of the diamine aliphatic chain increased, the prepolymer to postpolymer increase became smaller. This may be due to solubility issues of larger polymers with longer aliphatic portions.

2.2.4 Summary

Disodium D-mannarate (**2**) was prepared by the base hydrolysis of *N,N´*-dimethyl-D-mannaramide (**1**) and used to prepare a series of alkylenediammonium D-mannarate salts (**5a-f**). These salts possess a stoichiometrically balanced 1:1 molar ratio of D-mannaric acid:diamine and were used to prepare a series of poly(alkylene D-mannaramide) prepolymers (**6a-f**) and postpolymers (**7a-f**). The postpolymers synthesized were determined to be larger then the prepolymers by ^{1}H NMR end group analysis. Side-by-side polymerizations of hexamethylenediammonium D-mannarate and hexamethylenediammonium D-glucarate resulted in poly(hexamethylene D-glucaramide)

prepolymers that were larger than poly(hexamethylene D-mannaramide) prepolymers and isolated in a greater percent yield. Poly(hexamethylene D-glucaramide) was isolated with a percent yield of 75.7% and DP 4.96 compared to poly(hexamethylene D-mannaramide) with isolated yield 49.0% and DP 2.97. To better understand the conformation of the D-mannaryl unit of poly(alkylene D-mannaramides), octamethylenediammonium D-mannarate (**5d**) was crystallized from water and subjected to single-crystal x-ray crystal structure analysis. The salt (**5d**) adopts an extended conformation in the crystalline state and the molecule is free of destabilizing 1,3-parallel hydroxyl group eclipsing steric interactions.

2.3 Experimental

Materials and General Methods

HPLC grade methanol was obtained from EMD Biosciences, Inc. and acetyl chloride (99+%) obtained from Alfa Aesar. Triethylamine (puriss. p.a. ≥99.5% GC), methylamine (33% wt. in absolute ethanol), and all diamines (98%) were purchased from Aldrich and used without further purification. Amberlite IR-120H cation exchange resin was purchased from Aldrich. Sodium hydroxide DILUT-IT® analytical concentrate was purchased from J.T. Baker. NMR solvents were obtained from Cambridge Isotope Laboratories, Inc.

Solvent concentrations were carried out under reduced pressure. Elemental analyses were preformed by Atlantic Microlab, Inc., Norcross, Georgia.

Gas Chromatography/Mass Spectrometry of Trimethylsilyl Derivatives

GC-MS was performed on an Agilent 6890N Network GC System with an on-column injector fitted with a 5%-phenyl 95%-dimethylpolysiloxane column (Phenomenex ZB-5, 30 m x 32 mm x 0.25 μm) installed with direct interface to an Agilent 5973 Network MS Detector.

All samples were worked up in the following manner: Tri-Sil© Reagent (1.0 mL) was added to dried sample (10.0 mg) in a 7 mL vial and the mixture heated at 60 °C for 1 h. The sample was allowed to cool to room temperature at which point some solid residue remained. The cloudy supernatant was transferred (pipette) to heptane (3 mL). The heptane solution was centrifuged and the resulting supernatant removed for GC/MS analysis.

Samples were analyzed using the following temperature program: Begin 40 °C, + 6.0 °C/min to 120 °C, + 2.0 °C/min to 210 °C, + 8.0 °C/min to 310 °C, (hold 10 min). Total acquisition time is 80.83 min.

Ion Chromatography

IC was performed on a Dionex ICS-2000 Ion Chromatography System consisting of a Dionex IonPac® AS II analytical column and a sodium hydroxide EluGen® cartridge in conjunction with Chromeleon software. Samples were analyzed using a 35mM sodium hydroxide isocratic elution method with a flow rate of 1.5 mL/min running with the suppressor current at 186 mA.

Nuclear Magnetic Resonance

NMR spectra were recorded using a 400 MHz Varian *Unity Plus* spectrometer. Chemical shifts are expressed in parts per million relative to *t*-butyl alcohol (1.203 ppm) in D_2O as a solvent and tetramethylsilane (0.00 ppm) in DMSO-d_6 as a solvent and

relative to the residual proton of TFA-d_1 (11.50 ppm). FIDs obtained were processed using ACD/SpecManager 1D NMR software.

2.3.1 Disodium D-Mannarate (2)

Sodium hydroxide [2M, 22.56 mL (burette), 450 mmol] was added dropwise to a solution of *N, N'*-dimethyl-D-mannaramide (**1**, 3.522 g, 1.50 mmol) dissolved in water (70 mL) and the resulting solution heated at 60 °C with stirring for 48 h. The solution was then concentrated under vacuum at room temperature and triturated with methanol. Disodium D-mannarate was isolated by vacuum filtration (**2**, 3.713 g, 1.46 mmol, 98 %). ^{1}H NMR (D_2O) δ4.07 (d, 2H, H-2, H-5, $J_{2,5}$ = 5.86 Hz) δ3.90 (d, 2H, H-3, H-4, $J_{3,4}$ = 5.86 Hz). Anal Calcd for $C_6H_8Na_2O_8 \cdot (H_2O)_2$ (290.13): C, 24.84; H, 4.17. Found: C, 24.62; H, 3.66. The disodium mannarate was observed as a single component at retention time 10.964 min by ion chromatography and 44.77 min by GC/MS ($[M-15]^+$ of the trimethylsilyl derivative *m/z* 627).

2.3.2 Alkylenediammonium D-Mannarate Salts (5a-f)

Ethylenediammonium D-mannarate **(5a)**

Disodium D-mannarate (**2**, 0.505 g, 1.99 mmol) was dissolved in a minimal amount of water (*ca* 3 mL) and the solution was added to a slurry of washed Amberlite IR-120 H^+ form resin (6 mL). The mixture was agitated by hand for 10 min. The resin was removed from the mixture by vacuum filtration and the filtrate added to ethylenediamine (**4a**, 134 μL, 2.0 mmol) dissolved in water. The resin was washed with water (3 x 5 mL) and the washings added to the ethylenediamine/D-mannaric acid solution which was then stirred at room temperature (20 h). The solution was concentrated, dried under vacuum at room temperature, and triturated with methanol to

give ethylenediammonium D-mannarate (**5a**, 0.489 g, 1.81 mmol, 91.2%). ^{1}H NMR (D_2O) δ4.05 (d, 2H, H-2, H-5, $J_{2,5} = J_{3,4}$ =5.86 Hz) δ3.90 (d, 2H, H-3, H-4) δ3.22 (s, 4H, N-C**H**$_2$). Anal Calcd for $C_8H_{18}N_2O_8 \cdot (H_2O)_{0.5}$ (279.25): C, 34.45; H, 6.85; N, 10.05. Found: C, 34.32; H, 6.14; N, 9.44. The ethylenediammonium mannarate was observed as a single component at retention time 11.010 min by ion chromatography.

Tetramethylenediammonium D-mannarate **(5b)**

The procedure to prepare **5a** was adapted as follows: disodium D-mannarate (**2**, 0.409 g, 1.61 mmol), Amberlite IR-120 H^+ form resin (5 mL), tetramethylenediamine (**4b**, 162 μL, 1.61 mmol), and dissolution in a minimal amount of water (*ca.* 3 mL). The solid product, tetramethylenediammonium D-mannarate (**5b**, 0.3639 g, 1.22 mmol, 75.9%), was isolated as described for **5a**. ^{1}H NMR (D_2O) δ4.06 (d, 2H, H-2, H-5) δ3.90 (d, 2H, H-3, H-4) δ2.99 (t, 4H, N-C**H**$_2$) δ1.71 (q, 4H, N-CH$_2$-C**H**$_2$). Anal Calcd for $C_{10}H_{22}N_2O_8 \cdot (H_2O)_{0.5}$ (307.30): C, 39.12; H, 7.54; N, 9.13. Found: C, 38.99; H, 7.23; N, 8.63. The tetramethylenediammonium D-mannarate was observed as a single component at retention time 11.010 min by ion chromatography.

Hexamethylenediammonium D-mannarate **(5c)**

The procedure to prepare **5a** was adapted as follows: disodium D-mannarate (**2**, 1.059 g, 4.17 mmol), Amberlite IR-120 H^+ form resin (15 mL), hexamethylenediamine (**4c**, 0.484 g, 4.17 mmol), and dissolved in a minimal amount of water (*ca* 5 mL). The solid product, hexamethylenediammonium mannarate (**5c**, 1.218 g, 3.73 mmol, 89.4%), was isolated as described for **5a**. ^{1}H NMR (D_2O) δ4.04 (d, 2H, H-2, H-5, $J_{2,5} = J_{3,4}$ =5.86 Hz) δ3.88 (d, 2H, H-3, H-4) δ2.95 (t, 4H, N-C**H**$_2$) δ1.63 (q, 4H, N-CH$_2$-C**H**$_2$) δ1.38 (s, 4H, N-CH$_2$-CH$_2$-C**H**$_2$). Anal Calcd for $C_{12}H_{26}N_2O_8 \cdot (H_2O)_{0.25}$ (330.74): C, 43.58; H,

8.08; N, 8.47. Found: C, 43.59; H, 8.06; N, 8.55. The hexamethylenediammonium mannarate was observed as a single component at retention time 11.063 min by ion chromatography.

Octamethylenediammonium D-mannarate **(5d)**

The procedure to prepare **5a** was adapted as follows: disodium D-mannarate (**2**, 0.462 g, 1.83 mmol), Amberlite IR-120 H^+ form resin (5 mL), octamethylenediamine (**4d**, 0.2643 g, 1.83 mmol), and dissolution in a minimal amount of water (*ca* 8 mL). The solid product, octamethylenediammonium D-mannarate (**5d**, 0.6099 g, 1.72 mmol, 94.0%), was isolated as described in **5a**. ^{1}H NMR (D_2O) δ4.05 (d, 2H, H-2, H-5, $J_{2,5}$ = $J_{3,4}$ =5.86 Hz) δ3.89 (d, 2H, H-3, H-4) δ2.94 (t, 4H, N-C**H**$_2$) δ1.60 (q, 4H, N-CH_2-C**H**$_2$) δ1.31 (s, 8H, N-CH_2-CH_2-C**H**$_2$). Anal Calcd for $C_{14}H_{30}N_2O_8$ (354.40): C, 47.45; H, 8.53; N, 7.90. Found: C, 47.33; H, 8.51; N, 7.96. The octamethylenediammonium D-mannarate was observed as a single component at retention time 11.017 min by ion chromatography.

Decamethylenediammonium D-mannarate **(5e)**

The procedure to prepare **5a** was adapted as follows: disodium D-mannarate (**2**, 2.240 g, 8.82 mmol), Amberlite IR-120 H^+ form resin (25 mL), decamethylenediamine (**4e**, 1.520 g, 8.82 mmol), and dissolution in a minimal amount of water (*ca* 8mL). The resin was washed with water (3 x 5 mL) and the washings added to the decamethylenediamine solution which was then stirred at room temperature (48 h). The solid product, decamethylenediammonium D-mannarate (**5e**, 0.6467 g, 1.69 mmol, 81.5%), was isolated as described in **5a**. ^{1}H NMR (D_2O) δ4.04 (d, 2H, H-2, H-5) δ3.88 (d, 2H, H-3, H-4, $J_{2,5}$ = $J_{3,4}$ =5.86 Hz) δ2.95 (t, 4H, N-C**H**$_2$) δ1.62 (q, 4H, N-CH_2-C**H**$_2$)

δ1.28 (s, 12H, N-CH_2-CH_2-C**H**$_2$). Anal Calcd for $C_{16}H_{34}N_2O_8$ (382.45): C, 50.25; H, 8.96; N, 7.32. Found: C, 50.76; H, 9.17; N, 7.70. The decamethylenediammonium D-mannarate was observed as a single component at retention time 11.117 min by ion chromatography.

Dodecamethylenediammonium D-mannarate **(5f)**

The procedure to prepare **5a** was adapted as follows: disodium D-mannarate (**2**, 1.234 g, 4.86 mmol), Amberlite IR-120 H^+ form resin (15 mL), dodecamethylenediamine (**4f**, 0.9737 g, 4.86 mmol), and dissolution in a minimal amount of methanol (*ca* 10 mL). The resin was washed with water (3 x 5 mL) and the washings added to the dodecamethylenediamine solution which was then stirred at room temperature (96 h). The solid product, dodecamethylenediammonium D-mannarate (**5f**, 1.634 g, 3.98 mmol, 81.9%), was isolated as described in **5a**. ^{1}H NMR (D_2O) δ4.13 (d, 2H, H-2, H-5, $J_{2,5}$ = $J_{3,4}$ =5.86 Hz) δ3.92 (d, 2H, H-3, H-4) δ2.94 (t, 2H, N-C**H**$_2$) δ1.61 (q, 2H, N-CH_2-C**H**$_2$) δ1.25 (s, 16H, N-CH_2-CH_2-C**H**$_2$). Anal Calcd for $C_{18}H_{38}N_2O_8 \cdot (H_2O)_{0.5}$ (419.51): C, 51.56; H, 9.37; N, 6.68. Found: C, 51.33; H, 8.99; N, 6.60. The dodecamethylenediammonium D-mannarate was observed as a single component at retention time 11.020 min by ion chromatography.

2.3.3 Poly(Alkylene D-mannaramide) Prepolymers (6a-f)

Poly(ethylene D-mannaramide) Prepolymer **(6a)**

Methanolic hydrogen chloride was prepared by the dropwise addition of acetyl chloride (0.750 mL, 10.5 mmol) to methanol (5 mL) with stirring (ice bath) for 10 min. Ethylenediammonium D-mannarate (**5a**, 0.497 g, 1.84 mmol) was added to the methanolic hydrogen chloride solution, the reaction mixture stirred at room temperature

(30 min) and sonicated (10 min). The resulting solution was concentrated and dried under vacuum to a solid at room temperature overnight. The solid was then dissolved in methanol (10 mL) to which triethylamine (0.8 mL, 5.75 mmol) was added. The solution was stirred (10 min) followed by addition of triethylamine (0.4 mL, 2.87 mmol) to a basic pH ≈ 10 (pH paper). The final solution was stirred at room temperature (1 h) and then at 65 °C (6 h). The precipitate that formed was removed by filtration, washed with methanol (3 x 5 mL), and dried under vacuum at room temperature to give poly(ethylene D-mannaramide) prepolymer as a white solid. [(**6a**, 0.237 g, 1.01 mmol, 55.0%, DP 2.32) ^{1}H NMR (TFA-d_1) δ 4.67 (d, 2H,H-2, H-5) δ4.43 (d, 2H, H-3, H-4) δ3.64 (s, CON-C**H**$_2$) δ3.46 (s, C**H**$_2$-NH$_2$)].

Poly(tetramethylene D-mannaramide) Prepolymer **(6b)**

The procedure to prepare **6a** was adapted for **6b** as follows: acetyl chloride (0.750 mL, 10.5 mmol), methanol (5 mL), stirring (ice bath) for 10 min, tetramethylenediammonium D-mannarate (**5b**, 0.5004 g, 1.68 mmol) added, stirring at room temperature (30 min) and sonication (10 min). The solution was concentrated and dried to a solid under vacuum at room temperature overnight, the solid was dissolved in methanol (30 mL), triethylamine (0.8 mL, 5.75 mmol) was added, solution stirred (10 min), triethylamine (0.4 mL, 2.87 mmol) added to give a solution pH ≈ 10 (pH paper). The solid product was isolated as for **6a** to give poly(tetramethylene D-mannaramide) prepolymer as a white solid. [(**6b**, 0.168 g, 6.39 mmol, 38.1%, DP 2.74). ^{1}H NMR (TFA-d_1) δ 4.80 (d, 2H, H-2, H-5) δ4.51 (d, 2H, H-3, H-4) δ3.51 (s, CON-C**H**$_2$) δ3.27 (s, C**H**$_2$-NH$_2$) δ 1.88 (C**H**$_2$-CH$_2$-NH$_2$) δ 1.74 (CON-CH$_2$-C**H**$_2$)].

Poly(hexamethylene D-mannaramide) Prepolymer **(6c)**

The procedure to prepare **6a** was adapted for **6c** as follows: acetyl chloride (1.50 mL, 21.1 mmol), methanol (10 mL), stirring (ice bath) for 10 min, hexamethylenediammonium D-mannarate (**5c**, 0.5118 g, 1.57 mmol) added, stirring at room temperature (30 min) and sonication (10 min). The solution was concentrated and dried to a solid under vacuum at room temperature overnight, the solid was dissolved in methanol (10 mL), triethylamine (0.82 mL, 5.88 mmol) was added, the solution stirred (10 min), triethylamine (0.82 mL, 5.88 mmol) added to give a solution pH ≈ 10 (pH paper). A precipitate formed within 20 min and the solution was allowed to stir for 14 d at room temperature. The solid product was isolated as for **6a** to give poly(hexamethylene D-mannaramide) prepolymer as a white solid. [(**6c**, 0.308 g, 1.06 mmol, 67.6%, DP 4.75). ^{1}H NMR (TFA-d_1) δ 4.82 (H2, H5) δ4.52 (H3, H4) δ3.44 (CON-C**H**$_2$) δ3.19 (C**H**$_2$-NH$_2$) δ 1.77 (C**H**$_2$-CH$_2$-NH$_2$) δ 1.64 (CON-CH$_2$-C**H**$_2$) δ 1.40 (CON-CH$_2$-CH$_2$-C**H**$_2$)].

Poly(octamethylene D-mannaramide) Prepolymer **(6d)**

The procedure to prepare **6a** was adapted for **6d** as follows: acetyl chloride (1.5 mL, 21.1mmol), methanol (10 mL), stirring (ice bath) for 10 min, □ctamethylenediammonium D-mannarate (**5d**, 0.506 g, 1.43 mmol) added, stirring at room temperature (30 min) and sonication (10 min). The solution was concentrated and dried to a solid under vacuum at room temperature overnight, the solid was dissolved in methanol (12 mL), triethylamine (0.75 mL, 5.39 mmol) was added, the solution stirred (10 min), triethylamine (0.75 mL, 5.39 mmol) added to give a solutuion pH ≈ 10 (pH paper). The solid product was isolated as for **6a** to give poly(octamethylene D-mannaramide) prepolymer as a white solid. [(**6d**, 0.270 g, 8.47 mmol, 48.2%, DP 3.21).

^{1}H NMR (TFA-d_1) δ 4.86 (H2, H5) δ4.55 (H3, H4) δ3.48 (CON-C**H**$_2$) δ3.22 (C**H**$_2$-NH$_2$) δ 1.77 (C**H**$_2$-CH$_2$-NH$_2$) δ 1.66 (CON-CH$_2$-C**H**$_2$) δ 1.37 (CON-CH$_2$-CH$_2$-C**H**$_2$)].

Poly(decamethylene D-mannaramide) Prepolymer **(6e)**

The procedure to prepare **6a** was adapted for **6e** as follows: acetyl chloride (0.750 mL, 10.5 mmol), methanol (5 mL), stirring (ice bath) for 10 min, decamethylenediammonium D-mannarate (**5e**, 0.498 g, 1.30 mmol) added, stirring at room temperature (30 min) and sonication (10 min). The solution was concentrated and dried to a solid under vacuum at room temperature overnight, the solid was dissolved in methanol (10 mL), triethylamine (0.5 mL, 3.60 mmol) was added, the solution stirred (10 min), triethylamine (0.3 mL, 2.16 mmol) added to give a solution pH ≈ 10 (pH paper). The solid product was isolated as for **6a** to give poly(decamethylene D-mannaramide) prepolymer as a white solid. [(**6e**, 0.318 g, 0.917 mmol, 70.5%, DP 2.74) ^{1}H NMR (TFA-d_1) δ 4.83 (H2, H5) δ4.52 (H3, H4) δ3.44 (CON-C**H**$_2$) δ3.17 (C**H**$_2$-NH$_2$) δ 1.74 (C**H**$_2$-CH$_2$-NH$_2$) δ 1.61 (CON-CH$_2$-C**H**$_2$) δ 1.29 (CON-CH$_2$-CH$_2$-C**H**$_2$)].

Poly(dodecamethylene D-mannaramide) Prepolymer **(6f)**

The procedure to prepare **6a** was adapted for **6f** as follows: acetyl chloride (1.5 mL, 21.1 mmol), methanol (10 mL), stirring (ice bath) for 10 min, dodecamethylenediammonium D-mannarate (**5f**, 0.504 g, 1.23 mmol) added, stirring at room temperature (30 min) and sonication (10 min). The solution was concentrated and dried to a solid under vacuum at room temperature overnight, the solid was then dissolved in methanol (10 mL), triethylamine (0.64 mL, 4.61 mmol) was added, the solution stirred (10 min), triethylamine (0.64 mL, 4.61 mmol) added give a solution pH ≈ 10 (pH paper). The solid product was isolated as in **6a** to give poly(dodecamethylene D-mannaramide) prepolymer

as a white solid. [(**6f**, 0.521 g, 1.27 mmol, 59.9%, DP 2.98) ^{1}H NMR (TFA-d_1) δ 4.85 (H2, H5) δ4.54 (H3, H4) δ3.47 (CON-C**H**$_2$) δ3.19 (C**H**$_2$-NH$_2$) δ 1.74 (C**H**$_2$-CH$_2$-NH$_2$) δ 1.64 (CON-CH$_2$-C**H**$_2$) δ 1.28 (CON-CH$_2$-CH$_2$-C**H**$_2$)].

2.3.4 Poly(alkylene D-mannaramide) Postpolymers (7a-f)

Poly(ethylene D-mannaramide) Postpolymer **(7a)**

Poly(ethylene D-mannaramide) prepolymer (**6a**, 0.209 g, 0.891 mmol) was dissolved in DMSO (10 mL, 40 °C) and triethylamine (0.310 mL, 2.23 mmol) and methanol (4 mL) were added. The solution was stirred (24 h, 40 °C) and then diluted with methanol (10 mL). The precipitate formed was removed by filtration, rinsed with methanol (3 x 5mL), and dried under vacuum at room temperature to give poly(ethylene D-mannaramide) postpolymer as a white solid. [(**7a**, 0.191 g, 0.814 mmol, 91.4%, DP 5.02). ^{1}H NMR (TFA-d_1) δ 4.69 (H2, H5) δ 4.43 (H3, H4) δ3.66 (CON-C**H**$_2$) δ3.47 (C**H**$_2$-NH$_2$)].

*Poly(tetramethylene D-mannaramide) Postpolymer (***7b)**

The procedure to prepare **7a** was adapted for **7b** as follows: poly(tetramethylene D-mannaramide) prepolymer (**6b**, 0.2248 g, 0.857 mmol), DMSO (10 mL, 40 °C), triethylamine (0.298 mL, 2.14 mmol), methanol (4 mL), the solution was stirred (24 h, 40 °C), and diluted with methanol (10 mL) to precipitate the polymer. The solid product was isolated as with **7a** to give poly(tetramethylene D-mannaramide) postpolymer as a white solid. [(**7a**, 0.081 g, 0.307 mmol, 35.9%, DP 4.24). (TFA-d_1) δ 4.78 (d, 2H, H-2, H-5) δ 4.50 (d, 2H, H-3, H-4) δ 3.48 (s, CON-C**H**$_2$) δ 3.26 (s, C**H**$_2$-NH$_2$) δ 1.85 (C**H**$_2$-CH$_2$-NH$_2$) δ 1.72 (CON-CH$_2$-C**H**$_2$)].

Poly(hexamethylene D-mannaramide) Postpolymer **(7c)**

The procedure to prepare **7a** was adapted for **7c** as follows: poly(hexamethylene D-mannaramide) prepolymer (**6c**, 0.2057 g, 0.697 mmol), DMSO (10 mL, 40 °C), triethylamine (0.246 mL, 1.77 mmol), methanol (4 mL), the solution was stirred (24 h, 40 °C), and diluted with methanol (10 mL) to precipitate the polymer. The solid product was isolated as with **7a** to give poly(hexamethylene D-mannaramide) postpolymer as a white solid. [(**7c**, 0.103 g, 0.355 mmol, 50.1%, DP 7.43). ^{1}H NMR (TFA-d_1) δ 4.84 (H2, H5) δ4.54 (H3, H4) δ 3.48 (CON-C**H**$_2$) δ 3.21 (C**H**$_2$-NH$_2$) δ 1.80 (C**H**$_2$-CH$_2$-NH$_2$) δ 1.68 (CON-CH$_2$-C**H**$_2$) δ 1.43 (CON-CH$_2$-CH$_2$-C**H**$_2$)].

Poly(octamethylene D-mannaramide) Postpolymer **(7d)**

The procedure to prepare **7a** was adapted for **7d** as follows: poly(octamethylene D-mannaramide) prepolymer (**6d**, 0.2658 g, 0.835 mmol), DMSO (3.0 mL, 40 °C), triethylamine (0.244 mL, 1.75 mmol), the solution was stirred (24 h, 40 °C), diluted with methanol (10 mL) to precipitate the polymer, and stirred (48 h, 40 °C). The solid product was isolated as with **7a** to give poly(octamethylene D-mannaramide) postpolymer as a white solid. [(**7d**, 0.190 g, 0.597 mmol, 71.5%, DP 4.35). ^{1}H NMR (TFA-d_1) δ 4.94 (H2, H5) δ 4.63 (H3, H4) δ 3.56 (CON-C**H**$_2$) δ 3.30 (C**H**$_2$-NH$_2$) δ 1.84 (C**H**$_2$-CH$_2$-NH$_2$) δ 1.74 (CON-CH$_2$-C**H**$_2$) δ 1.44 (CON-CH$_2$-CH$_2$-C**H**$_2$)].

Poly(decamethylene D-mannaramide) Postpolymer **(7e)**

The procedure to prepare **7a** was adapted for **7e** as follows: poly(decamethylene D-mannaramide) prepolymer (**6e**, 0.2115 g, 0.611 mmol), DMSO (13 mL, 40 °C), triethylamine (0.212 mL, 1.53 mmol), methanol (4 mL), the solution was stirred (24 h, 40 °C), and diluted with methanol (10 mL) to precipitate the polymer. The solid product

was isolated as with **7a** to give poly(decamethylene D-mannaramide) postpolymer as a white solid. [(**7a**, 0.168 g, 0.484 mmol, 79.3%, DP 4.16). ^{1}H NMR (TFA-d_1) δ 4.82 (H2, H5) δ4.51 (H3, H4) δ 3.44 (CON-C**H**$_2$) δ 3.17 (C**H**$_2$-NH$_2$) δ 1.72 (C**H**$_2$-CH$_2$-NH$_2$) δ 1.61 (CON-CH$_2$-C**H**$_2$) δ 1.29 (CON-CH$_2$-CH$_2$-C**H**$_2$)].

Poly(dodecamethylene D-mannaramide) Postpolymer **(7f)**

The procedure to prepare **7a** was adapted for **7f** as follows: poly(dodecamethylene D-mannaramide) prepolymer (**6f**, 0.2779 g, 0.742 mmol), DMSO (3 mL, 40 °C), triethylamine (0.217 mL, 1.56 mmol), the solution was stirred (24 h, 40 °C), diluted with methanol (10 mL) to precipitate the polymer, and stirred (48 h, 40 °C). The solid product was isolated as with **7a** to give poly(dodecamethylene D-mannaramide) postpolymer as a white solid. [(**7f**, 0.246 g, 0.657 mmol, 88.6%, DP 4.46). ^{1}H NMR (TFA-d_1) δ 4.85 (H2, H5) δ 4.54 (H3, H4) δ 3.46 (CON-C**H**$_2$) δ 3.20 (C**H**$_2$-NH$_2$) δ 1.74 (C**H**$_2$-CH$_2$-NH$_2$) δ 1.64 (CON-CH$_2$-C**H**$_2$) δ 1.27 (CON-CH$_2$-CH$_2$-C**H**$_2$)].

2.3.5 Octamethylenediammonium D-mannarate X-ray Crystal Structure Analysis

All software used was from Bruker AXS, Inc. Data collection, indexing and initial cell refinements were all carried out using APEX software. Frame integration and final cell refinements were done using SAINT Version 6.45A software. Structure solution, refinement, graphics and generation of publication materials were performed by using SHELXTL V6.12 software.

A suitable crystal of octamethylenediammonium D-mannarate was coated with Paratone N oil, suspended in a small fiber loop and placed in a cooled nitrogen gas stream at 173 K on a Bruker D8 APEX II CCD sealed tube diffractometer with graphite

monochromated CuK_α (1.54178 Å) radiation. Data were measured using a series of combinations of phi and omega scans with 10 s frame exposures and 0.5^o frame widths.

The structure was solved using Direct methods and difference Fourier techniques (SHELXTL, V6.12, Bruker). Hydrogen atoms were placed their expected chemical positions using the HFIX command and were included in the final cycles of least squares with isotropic Uij 's related to the atom's ridden upon. All non-hydrogen atoms were refined anisotropically. Scattering factors and anomalous dispersion corrections are taken from the International Tables for X-ray Crystallography.

2.4 References

1. Wade Jr., L.G. *Organic Chemistry*, 4th Edition; Prentice Hall: Upper Saddle River, NJ, 1999.

2. Billmeyer Jr., Fred W. *Synthetic Polymers: Building the Giant Molecule*; Doubleday & Company, Inc.: Garden City, NY, 1972.

3. Seymour, Raymond B.; Carraher, Charles E., Jr. *Polymer Chemistry: An Introduction*, 3rd Edition Revised and Expanded; Marcel Dekker, Inc.: New York, 1992.

4. Mohanty, A.K.; Misra, M.; Hinrichsen, G. Biofibres, Biodegradable Polymers, and Biocomposites: An overview. *Macromol. Mater. Eng.* **2000**, *276/277*, 1-24.

5. Dirlikov, Stoli K. Water Soluble Polymers. In *Agricultural and Synthetic Polymers: Biodegrability and Utilization*, Proceedings of the 197th National Meeting of the American Chemical Society, Dallas, TX, April 9-14, 1989; Glass, J.E.; Swift, G., Eds.; American Chemical Society: Washington, D.C., 1990.

6. Carothers, Wallace H. Studies on Polymerization and Ring Formation. I. An Introduction to the General Theory of Condensation Polymers. *J. Am. Chem. Soc.* **1929**, *51*, 2548-2559.

7. Stevens, Malcolm P. *Polymer Chemistry: An Introduction*, 3rd edition; Oxford University Press: New York, 1999.

8. Noels, Alfred F. Carbene Chemistry: Stereoregular Polymers from Diazo Compounds. *Angew. Chem. Int. Ed.* **2007**, *46*, 1208 – 1210.

9. Hall, H.K., Jr.; Padias, Anne B.; Boone, Harold W. Condensation Routes to Polyaniline and Its Analogs. *J. Polym. Sci., Part A: Polym. Chem.* **2007**, *45*, 4751-4763.

10. Smith, John K.; Houndshell, David A. Wallace H. Carothers and Fundamental Research at Du Pont. *Science*, **1985**, *229* (4712), 436-442.

11. Carothers, Wallace H. Linear Polyamides and their Production. US Patent 2,130,523, September 20, 1938.

12. Carothers, Wallace Hume. Diamine-Dicarboxylic Acid Salts and Process of Preparing Some. US Patent 2,130,947, September 20, 1938.

13. Thiem, Joachim; Bachmann, Frank. Carbohydrate-Derived Polyamides. *Trends Polym. Sci.* **1994**, *2* (12), 425-432.

14. Kiely, Donald E.; Chen, Liang; Lin, Tsu-Hsing. Hydroxylated Nylons Based on Unprotected Esterified D-Glucaric Acid by Simple Condensation Reactions. *J. Am. Chem. Soc*. **1994**, *116*, 571-578.

15. Wolfram, M. L.; Toy, Madeline S.; Chaney, Alan. Condensation Polymers from Tetra-*O*-acetylgalactaroyl Dichloride with Diamines. *J Am Chem Soc*. **1958**, *80*, 6328-6330.

16. Black, William A.P.; Falkirk, Eric T.; Dewar, Dalkeith; Rutherford, David. Carbohydrate Derived Polyamides. US Patent 3,225,012, December 21, 1965.

17. Ogata, N.; Sanui, K.; Iikima, K. Synthesis of Polyamides through Active Diesters. *J. Polym. Sci., Part A: Polym. Chem.* **1973**, *11*, 1095-1105.

18. Ogata, N.; Hosoda, Y. Synthesis of Hydrophilic Polyamide by Active Polycondensation. *J. Polym. Sci., Part C: Polym. Lett.* **1974**, *12*, 355-358

19. Ogata, Naoya; Sanui, Kohei; Hosoda, Yoshikazu; Nakamura, Hiroyuki. Active Polycondensation of Diethyl 2,3,4,5-Tetrahydroxyadipate with Diamines. *J. Polym. Sci., Part A: Polym. Chem*. **1976**, *14*, 783-792.

20. Hoagland, Peter D. The Formation of Intermediate Lactones During Aminolysis of Diethyl Galactarate. *Carbohydr. Res*. **1981**, *98*, 203-208.

21. Viswanathan, Arvind; Kiely, Donald E. Mechanisms for the Formation of Diamides and Polyamides by Aminolysis of D-Glucaric Acid Esters. *J. of Carbohydr. Chem*. **2003**, *22* (9), 903-918.

22. Chen, Liang; Kiely, Donald E. Synthesis of Stereoregular Head,Tail Hydroxylated Nylons Derived from D-Glucose. *J. Org. Chem*. **1996**, *61*, 5847-5851.

23. Styron, Susan D.; Kiely, Donald E.; Ponder, Glenn. Alternating Stereoregular *Head, Tail-Tail, Head*-Poly(Alkylene D-Glucaramides) Derived from a Homologous Series of Symmetrical Diamido-di-D-Glucaric Acid Monomers. *J. Carbohydr. Chem.* **2003**, *22* (2), 123-142.

24. Kiely, Donald E.; Kramer, Kylie; Zhang, Jinsong. Method for Preparing High Molecular Weight Random Polyhydroxypolyamides. US Patent 6,894,135, May 17, 2005.

25. Varela, Oscar; Orgueira, Hernan A. Synthesis of Chiral Polyamides from Carbohydrate-Derived Monomers. *Adv. Carbohydr. Chem. Biochem*. **2000**, 55, 137-174.

26. Hashimoto, Kazuhiko; Wibullucksanakui, Sirinat; Matsuura, Mitsuyasu; Okada, Masahiko. Macromolecular Synthesis from Saccharic Lactones. Ring-Opening

Polyaddition of D-Glucaro- and D-Mannaro-1,4:6,3-dilactones with Alkykenediamines. *J. Polym. Sci., Part A: Polym. Chem.* **1993**, *31*, 3141-3149.

27. Kiely, Donald E.; Chen, Liang; Lin, Tsu-Hsing. Synthetic Polyhydroxypolyamides from Galactaric, Xylaric, D-Glucaric, and D-Mannaric Acids and Alkylenediamine Monomers-Some Comparisons. *J. Polym. Sci., Part A: Polym. Chem.* **2000**, *38*, 594-603.

28. Petersson, G. Mass Spectrometry of Hydroxy Dicarboxylic Acids as Trimethylsilyl Derivatives. Rearrangement Fragmentations. *Org. Mass Spectrom.* **1972**, *6*, 565-576.

29. Silverstein, Robert M.; Webster, Francis X. *Spectrometric Identification of Organic Compounds*, 6th ed; John Wiley & Sons, Inc.: New York, 1998.

30. Dionex Corporation. ICS-2000 Ion Chromatography System Operator's Manual. Document No. 031857, Revision 03; Sunnyvale, CA, April 2006.

31. Van Duin, M.; Peters, J.A.; Kieboom, A.P.G.; Van Bekkum, H. ^{1}H NMR of Carbohydrate-Derived Polyhydroxycarboxylates. *Magn. Reson. Chem.* **1986**, *24* (9), 832-833.

32. Jarman, Bevan. Synthesis of Polyhydroxypolyamides Based on Galactaric Acid and X-Ray Crystal Analysis of Their Precursors. M.Sc. Thesis, University of Waikato, Hamilton, New Zealand, 2006.

33. Manley-Harris, Merilyn. Personal communication.

Chapter 3

MM3(96) Conformational Analysis of D-Mannaric Acid and Some Ester and Amide Derivatives as Models for the D-Mannaryl Monomer Unit of Poly(Alkylene D-Mannaramides)

3.1 Introduction

Poly(alkylene D-mannaramides) represent a class of carbohydrate-based synthetic polymers called polyhydroxypolyamides that have been studied to some extent by Hashimoto *et al* and more recently by Kiely *et al*.[1,2] These molecules are stereoregular polyamides and are derived in part from D-mannose, a renewable plant carbohydrate. In the work described here, MM3(96) computational analysis was performed on D-mannaric acid, its dimethyl ester, and three amide derivatives to learn more about the conformations of these molecules in solution with the hope of better understanding the polymerization reaction and gaining some insight into the three dimensional structures of the resultant polymers.

3.1.1 MM3(96)

MM3(96) is an empirical force field (molecular mechanics program) that has been successfully used for conformational analysis of cyclic forms of mono- and disaccharide molecules such as D-glucopyranose, fructose, sucrose, and maltose.[3,4,5] It has also been applied to acyclic carbohydrates which, compared to relatively constrained cyclic forms of carbohydrates, can exist in a vast number of conformations (> 14,000,000).[6, 7] MM3(96) has some limitations in that it does not provide a method for dealing with solvent and it does not account for chains of hydrogen bonding (donor-acceptor-donor-acceptor). It also does not incorporate an energy dependence of the orientation of the

acceptor hydroxyl groups.[6] However, MM3(96) does allow for changes in the dielectric constant and therefore altering the strength of hydrogen bonds. Increasing the dielectric constant simulates a more polar environment and decreases the influence of hydrogen bonding. A small dielectric constant simulates molecules in a vacuum or a non-polar solvent which is reflected in an increase in hydrogen bonding strength.

MM3(96) performs energy minimization calculations on input structures to find the nearest energy minimum. This nearest energy minimum is termed a local minimum or "well" and is not necessarily the global minimum. Carrying out simulations at high temperature generates higher energy conformers that can then be applied to the minimization routine. This process is called temperature shaking and is a way to make the computer program accept higher energy starting conformers in the search for multiple local energy minima as well as the overall global energy minimum.

3.1.2 Convergence

In general terms , the term convergence denotes the approach toward a definite value, as time goes on; or to a definite point, a common view or opinion, or toward a fixed or equilibrium state. In the context of this work, convergence is a means of modeling the tendency for populations of conformational families to stabilize over time. Establishing convergence of a simulation ensures that a valid representative data set has been obtained. Convergence is achieved when it has been established that all reasonable conformational space has been searched, a criterion that is of concern when a random search method is used. Criteria for convergence are as follows: 1) different initial conditions give the same result, 2) symmetric molecules show +/- gauche interactions equally populated, and 3) there is stability of average properties. As the degrees of

freedom of a molecule increase, the amount of conformational space to be searched also increases. In order to adequately establish convergence it is necessary to model at a high temperature to ensure that the simulation can jump from one region of conformational space to another. This is accomplished using a temperature shaking routine, as discussed previously. The number of steps needed to adequately search the conformational space is unique to each molecule studied.

3.1.3 MM3(96) Studies of D-Glucaric Acid Derivatives

As indicated in Chapter 2, D-glucaric acid is a C-2 epimer of D-mannaric acid. In an extended conformation D-glucaric acid possesses destabilizing 1,3-parallel hydroxyl group eclipsing steric interactions while the extended conformation of D-mannaric acid does not. Consequently, extended D-glucaric acid and its derivatives would be expected to adopt a sickle conformation to alleviate the 1,3-parallel hydroxyl group eclipsing steric interactions while D-mannaric acid and its derivatives would be expected to adopt an extended conformation. Full MM3(96) conformational analyses have been carried out for D-glucaramide, at dielectric constant 3.5 and 6.5[6], and used as a model based study for 2,3,4,5-tetra-*O*-acetyl-*N,N´*-dimethyl-D-glucaramide and some additional tetra-*O*-acyl-*N,N´*-dialkyl-D-glucaramides at dielectric constant 2.0.[7]

For the D-glucaramide study, nine torsional angles were varied, five in the backbone and four for the hydroxyl groups resulting in 3^9 (19,683) possible starting conformations.[6] Each conformation was fully energy-minimized using MM3's block diagonal/full matrix optimization option at both dielectric constants studied.[6]

At dielectric constant of 3.5 only ten different conformations were found within the range E_{min} to E_{min} + 1kcal/mol.[6] Of those conformations 45-50% of the population

were represented by a sickle conformation in which the 1,3-parallel hydroxyl group eclipsing steric interactions were alleviated.[6] However, two conformations did have one 1,3-parallel hydroxyl group eclipsing interactions. It is interesting to note that two conformations possessed two sets of hydroxyl groups with 1,3-parallel hydroxyl group interactions with one conformation in a fully extended conformation. It was suggested that conformations that have 1,3-parallel hydroxyl group eclipsing interactions are stabilized to some extent by intramolecular hydrogen bonding between alternating hydroxyl groups.[6]

At dielectric constant of 6.5, thirty-five conformations were found within the range of E_{min} to E_{min} + 1kcal/mol.[6] Of those conformations 52-59% of the population was void of 1,3-parallel hydroxyl group interactions.[6] Some conformers did display the 1,3-parallel hydroxyl group interactions (~28%) and a smaller number had two sets of hydroxyl groups with 1,3-parallel hydroxyl group eclipsing interactions (~13%).[6] It appears that at a higher dielectric constant intramolecular hydrogen bonding stabilizes 1,3-parallel hydroxyl group eclipsing interactions.[6]

In addition to D-glucaramide, 2,3,4,5-tetra-*O*-acetyl-*N,N´*-dimethyl-D-glucaramide and some tetra-*O*-acyl-*N,N´*-dialkyl-D-glucaramides were studied using MM3 conformational analysis. The simplest of these molecules, 2,3,4,5-tetra-*O*-acetyl-*N,N´*-dimethyl-D-glucaramide, had 15 variable torsion angles for a total of 3^{15} or 14,348,907 possible conformations, a conformer number that was too large for a full conformational search routine and required high-level computational ability.[7] A simplified "model building approach" was employed in which some of the torsion angles were manually defined using small model compounds, or building blocks, to simulate portions of the

larger molecules.[7, 8] For all molecules studied, four starting sickle rotamers were considered; they were derived from an extended conformation by a 120º counterclockwise rotation about the C3-C4 bond or a 120º clockwise or counterclockwise rotation about the C2-C3 and C4-C5 bonds.[7, 8] The model compounds considered were *N*-methylacetamide, *N*-methyl-2-acetoxypropanamide, methyl acetate, 2,3-diacetoxybutane, methyl propanate, methyl-2-methylpropanate,and *N*-ethylacetamide. For each of the acetoxy groups, 16 conformers were generated from each of the 4 starting rotamers giving 64 total rotamers for computational analysis.[7, 8] Each conformation was fully energy-minimized using MM3's block diagonal/full matrix optimization option at dielectric constant of 2.0.[7, 8] In all cases, the lowest energy conformers had no 1,3-parallel hydroxyl group eclipsing steric interactions present.[7, 8] All low energy conformers were in a sickle conformation suggesting that larger protecting groups force a molecule into conformations void of destabilizing 1,3-parallel hydroxyl group eclipsing steric interactions.

In the study reported here a significantly more powerful computational tool has been employed in the form of a Monte Carlo simulation in conjunction with MM3(96) as developed by Dr. Michael Dowd.[9]

3.1.4 Monte Carlo Simulation

In concert with the MM3(96) force field, a Monte Carlo simulation has been developed which randomly generates low-energy conformations of each molecule being analyzed.[9] The simulation determines if a new conformation is unique by comparing its torsion angles with torsion angles of all other previously identified conformations. The simulation was designed so that if one or more torsion angle differs by 2.5 degrees or

more the conformation is accepted as unique. The Cartesian coordinates of each unique conformation are saved along with the conformer number.

Total steric energy of each of the conformers generated is compared with previous accepted energy values. If a new conformer has a lower energy than the previous accepted value, the conformation is preserved as the next starting conformer in the study. If the energy value is greater than the previous accepted value a probability test is automatically applied. The temperature of the shaking process (T) is applied to Equation 4.1 where P is the probability, E is the difference in energy between the new conformer and the previously accepted conformer and R is ideal gas constant.[10]

$$P = \frac{-\Delta E}{RT} \qquad \textbf{(4.1)}$$

A random number generator produces a number between 0 and 1. When P is greater than the random number generated, the conformation is preserved as the next starting conformer in the study. Selecting a temperature value of 10,000 K is sufficient to make the probability near one. This allows for preserving lower energy conformations and finding additional local minima.[10]

3.2 Results and Discussion

3.2.1 Mimics for Poly(alkylene D-mannaramides)

D-Mannaric acid (**1**) and four derivatives thereof were subjected to MM3(96) conformational analysis using a block diagonal/full matrix optimization option. The D-mannaric acid derivatives studied were dimethyl D-mannarate (**2**), D-mannaramide (**3**), *N,N´*-dimethyl-D-mannaramide (**4**), and 2,3,4,5-tetra-*O*-acetyl-*N,N´*-dimethyl-D-mannaramide (**5**). These molecules were studied to determine their low energy

conformations and to gain insight into the possible conformations of the mannaryl unit in synthetic poly(alkylene D-mannaramides). The small mannaramide derivatives provide good mimics for the D-mannaryl unit of these polyamides because they incorporate the carbon backbone of the mannaryl unit as well as the amides bonds present in the polymer. The free acid and methyl ester were evaluated to separate the conformational contributions of the D-mannaryl unit itself from those of the D-mannaramide unit with possible intramolecular amide group centered hydrogen bonding contributions.

3.2.2 MM3(96) Conformational Analysis

Application of MM3(96) to comparatively rapid conformational analysis of mannaric acid molecules (**1-5**) has only recently become practical due to the availability of the Monte Carlo simulation written by Dr. Michael Dowd. Empirical data was used to determine individual force constants and equilibrium values for conformational geometries. In MM3(96), this is done by defining an atom type according to hybridization and molecular environment. Atom types used for this study are listed in Table 1.

Table 1: Atom types in MM3(96)

Atom	Type	Description	At Wt	LTG	LT3	LT4	LT5	ITP	MPL	CRD
1	C	sp3	12.000	0	0	0	0	0	0	0
3	C	sp2 carbonyl	12.000	0	0	0	0	0	3	0
5	H	except on N, O, S	1.008	0	0	0	0	0	0	0
9	N	sp2 carbonyl	14.003	0	0	0	0	0	9	0
28	H	H-N-C=O (amide)	1.008	0	0	0	0	0	0	0
75	O	O-H, O-C (carboxyl)	15.995	6	6	6	6	0	0	0
78	O	O=C-O-C (ester)	15.995	7	0	0	0	7	0	0
79	O	O=C-N< (amide)	15.995	7	0	0	0	7	0	0

At Wt = Atomic Weight (g/mol)
LTG = Replaceable Atom Type For General, Localized (LTYPEG)
LT3 = Replaceable Atom Type For 3-Mem, Localized (LTYPE3)
LT4 = Replaceable Atom Type For 4-Mem, Localized (LTYPE4)

LT5 = Replaceable Atom Type For 5-Mem, Localized (LTYPE5)
LTP = Replaceable Atom Type, Delocalized (LTYPEP)
MPL = Atom Having Out-Of-Plane Bending If Not Zero (KOUTP)
CRD = Atom Having G 4-Coordinate Bond If Not Zero (ITCOORD)

All bond angles and lengths were assumed to be constant and ideal. Torsion angle parameters associated with acetylated acyclic carbohydrates were not present in MM3(96) and therefore had to be input manually. The parameters were calculated and input according to the suggestion of Dr. Jenn-Huei Lii from Dr. Norman L. Allinger's laboratory at the University of Georgia.

3.2.3 Statistical Analysis

A representative population was generated from the lowest energy conformers using Equations 4.2 and 4.3.

$$Na / No = e^{(\Delta E / RT)} \tag{4.2}$$

$$Pa = \left[\frac{(Na / No)}{\sum (Ni / No)} \right] \times 100 \tag{4.3}$$

N*a*/N*o* is the molar ratio of some rotamer *a* to the most stable rotamer *o* with the difference in energy between the two rotamers equal to ΔE. R is the ideal gas constant and T the temperature. Pa represents the percent population of rotamer *a* among a total of *i* rotamers.[6] Summation of all values of P for *i* total rotamers will be equal to 100%.

Haasnoot's adaptation of the Karplus equation was used to calculate vicinal coupling constants for the protons of the mannaramide backbone.[11] Because the mannaryl unit is symmetrical, H2 and H5 are equivalent and H3 and H4 are equivalent for all unique conformations. Therefore theoretical average coupling constants $J_{2,3}$ and $J_{3,4}$ were calculated based on Equation 4.4.

$$J_{calculated} = \sum Xi \times Ji \quad (\mathbf{4.4})$$

X*i* is the percent population (Pa) of each rotamer and J*i* is the corresponding calculated coupling constant for that particular rotamer. Results were compared to actual ^{1}H NMR coupling constants in section 4.2.3, where applicable.

3.2.4 Establishing Convergence

Convergence of the computational model was established by originating simulations from seven conformations of each molecule. Achieving the same result for each conformation using MM3(96) ensures that all conformational space for each molecule has been searched. The computational analysis produces a conformational set considered to be representative of the entire population and is composed of conformations that are accessible in solution. This is tested by extending a computational run to ensure that no additional low-energy structures are found. The conformer populations were calculated according to a Boltzmann distribution. Because this conformational set is assumed to be representative of the entire population the numbers are standardized so that the population of all conformers is equal to 100%.

3.2.5 Conformational Analysis

D-Mannaric acid (**1**) and derivatives 2-5 were subjected to conformational analysis, Figure 1.

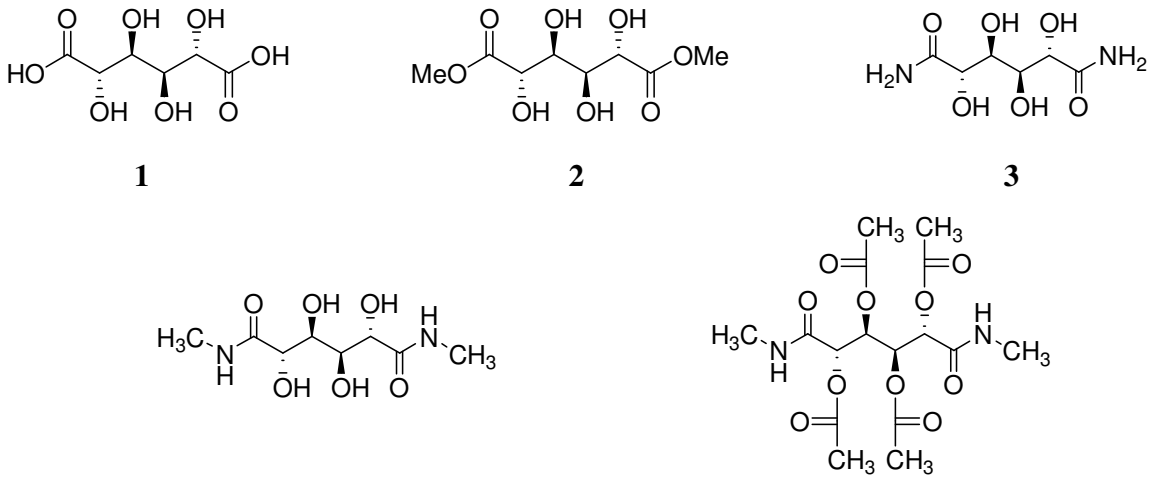

Figure 1: D-Mannaric acid and derivatives that were subjected to MM3(96) conformational analysis

Torsion angles were varied in the analysis to explore the conformation of these compounds; 13 angles for **5** and 9 for **1-4**. The nine common torsion angles varied included five along the carbon backbone and four for the hydroxyl groups; the additional four came from rotation of the acetyl group. The Monte Carlo program randomly selects a torsion angle and an angle increment (δ) between 60° < δ< 300° to vary. Conformational analysis was carried out using the block diagonal minimization/full matrix optimization routine of MM3(96) at dielectric constant of 3.5. 2,3,4,5-tetra-*O*-acetyl-*N,N´*-dimethyl mannaramide (**5**) was also analyzed at dielectric constant of 1.5. The energies of the resulting minimized conformations were sorted in order of lowest final steric energy to highest final steric energy. The reported percent population is based on the percent population analyzed by MM3(96) conformational analysis. The standardized percent population represents the percent present of each conformational family if 100% of the population had been analyzed.

D-Mannaric Acid (1) and Dimethyl D-Mannarate (2)

The atoms of each molecule were numbered for identification, Figures 2 and 3.

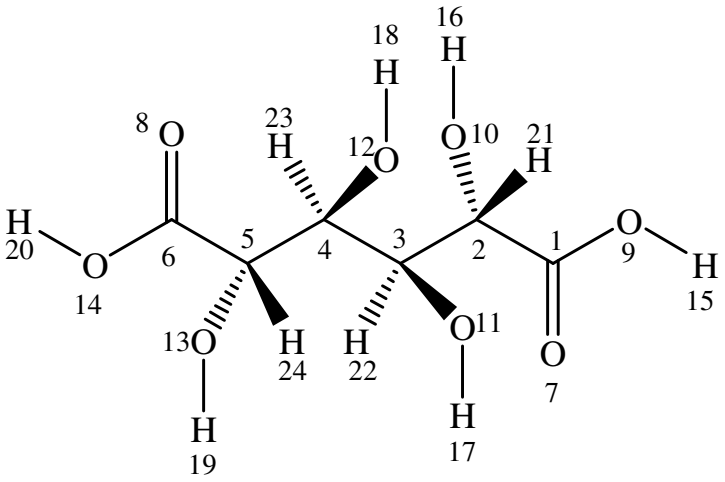

Figure 2: Numbering scheme for D-mannaric acid (**1**)

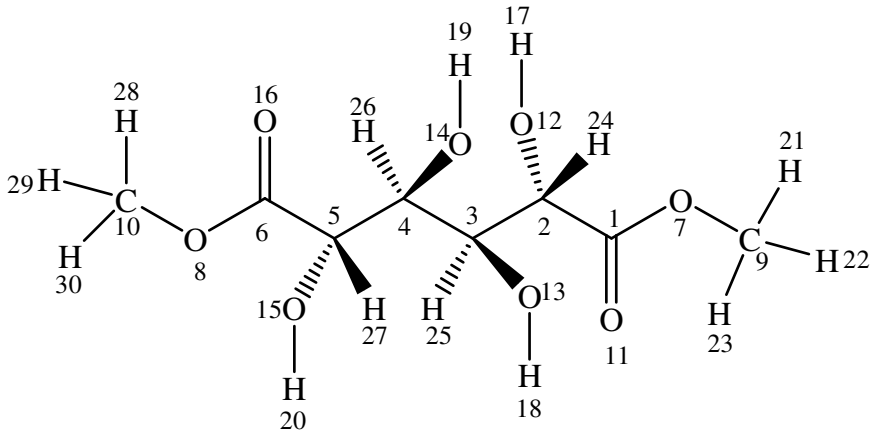

Figure 3: Numbering scheme for dimethyl D-mannarate (**2**)

The results from computational analysis of D-mannaric acid and dimethyl D-mannarate at dielectric constant 3.5 are summarized in Table 2 and Table 3 respectively. These tables list percent population and the low energy value of each conformer family generated in this analysis.

Table 2: Complete list of conformers found using MM3(96) conformational analysis and their contributions to the overall population for D-mannaric acid (**1**)

D-Mannaric acid (1) at dielectric constant 3.5				
Conformer Family	**Conformer Label**	**Low Energy (kcal/mol)**	**Percent Population**	**Standardized % Population**
$_2G^+{}_3G^+{}_4G^+$	**1a**	10.1483	30.83	39.89
$_2G^+{}_4G^-$	**1b**	11.0197	13.95	18.05
$_2G^-{}_4G^-$	**1c**	11.1208	8.46	10.95
$_2G^+{}_4G^+$	**1d**	10.8163	8.30	10.74
$_2G^+$	**1e**	11.3681	6.89	8.91
$_2G^-$	**1f**	11.0919	5.24	6.78
$_2G^+{}_3G^+$	**1g**	11.8881	2.72	3.52
Extended	**1h**	12.3628	0.89	1.16
Total			77.28	100.00

Table 3: Complete list of conformers found using MM3(96) conformational analysis and their contributions to the overall population for dimethyl D-mannarate (**2**)

Dimethyl D-mannarate (2) at dielectric constant 3.5				
Conformer Family	**Conformer Label**	**Low Energy (kcal/mol)**	**Percent Population**	**Standardized % Population**
$_2G^+{}_3G^+{}_4G^+$	**2a**	10.7883	49.91	60.02
$_2G^+{}_4G^-$	**2b**	11.7097	9.60	11.54
$_2G^+{}_4G^+$	**2c**	11.5083	6.90	8.30
$_2G^-{}_4G^-$	**2d**	12.0914	4.67	5.61
$_2G^+$	**2e**	11.9704	5.36	6.45
$_2G^-$	**2f**	12.2119	4.29	5.16
$_2G^+{}_3G^+$	**2g**	12.5297	1.48	1.78
$_2G^+{}_3G^+{}_4G^-$	**2h**	13.2778	0.43	0.51
Extended	**2i**	13.1144	0.52	0.62
Total			83.15	100.00

The computational analysis determined that the lowest energy conformers of mannaric acid and dimethyl mannarate that were of the same $_2G^+{}_3G^+{}_4G^+$ conformer

family, Figure 4, **1a** and Figure 4, **2a** and account for 39.20% and 60.02% of the overall population, respectively. The corresponding torsion angles varied and the angles calculated for the lowest energy conformers are displayed in Table 4. This family is characterized by the lack of intramolecular hydrogen bonding and a sickle conformation of the carbon backbone. In addition, the hydroxyl groups on both mannaric acid and dimethyl mannarate appear on the same side of the molecule. This gives each of the molecules a hydrophobic and hydrophilic face.

Because mannaric acid and dimethyl mannarate do not have destabilizing 1,3-parallel hydroxyl group eclipsing steric interactions while in an extended conformation, this conformational family was expected to represent the lowest energy conformational family for both molecules. However, from the results of this study this is not the case. In fact, the extended conformation of mannaric acid and dimethyl mannarate accounts for only 1.14% and 0.62% of the populations, respectively, indicative of a much higher energy conformation than expected.

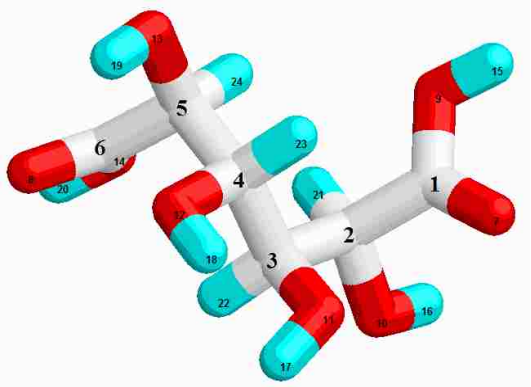

1a

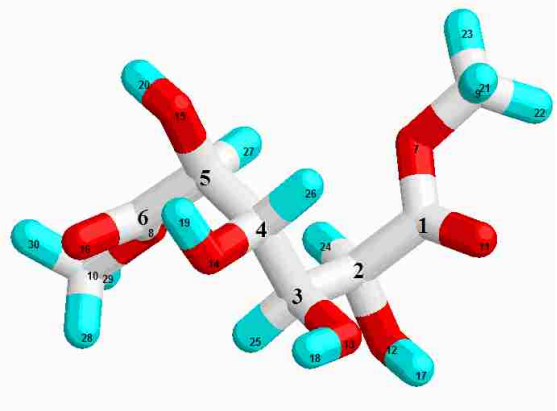

2a

Figure 4: ${}_2G^+{}_3G^+{}_4G^+$ lowest energy conformers of mannaric acid (1a) and dimethyl mannarate (2a) showing the hydroxyl groups all on one side of both molecules.

Table 4: Torsion angles varied and calculated angles for the lowest energy conformers of D-mannaric acid (1a) and dimethyl D-mannarate (2a)

Torsion Angle	**1a**	**Torsion Angle**	**2a**
O(9)-C(1)-C(2)-C(3)	-112.5	O(7)-C(1)-C(2)-C(3)	-109.4
C(1)-C(2)-C(3)-C(4)	59.8	C(1)-C(2)-C(3)-C(4)	58.5
C(2)-C(3)-C(4)-C(5)	62.3	C(2)-C(3)-C(4)-C(5)	61.9
C(3)-C(4)-C(5)-C(6)	59.0	C(3)-C(4)-C(5)-C(6)	59.3
C(4)-C(5)-C(6)-O(14)	-110.4	C(4)-C(5)-C(6)-O(8)	-111.4
H(21)-C(2)-O(10)-H(16)	64.5	H(24)-C(2)-O(12)-H(17)	179.7
H(22)-C(3)-O(11)-H(17)	66.8	H(25)-C(3)-O(13)-H(18)	-63.6
H(23)-C(4)-O(12)-H(18)	-63.6	H(26)-C(4)-O(14)-H(19)	67.5
H(24)-C(5)-O(13)-H(19)	-179.8	H(27)-C(5)-O(15)-H(20)	65.8

While the ${}_2G^+{}_3G^+{}_4G^+$ conformer family was the lowest energy conformer family and made a significant contribution to the overall populations for both D-mannaric acid and dimethyl D-mannarate, at least three other conformational families were important, as noted in Tables 2 and 3, respectively. It is interesting to note that the dominant contributors of the conformer families for both molecules are the same with the exception being that the ${}_2G^+{}_3G^+{}_4G^-$ conformer family is only present in dimethyl D-mannarate, but in a minor amount. The four conformer families that make the largest contributions to the overall population are shown in Figures 5 and 6 for D-mannaric acid (**1**) and dimethyl D-mannarate (**2**), respectively.

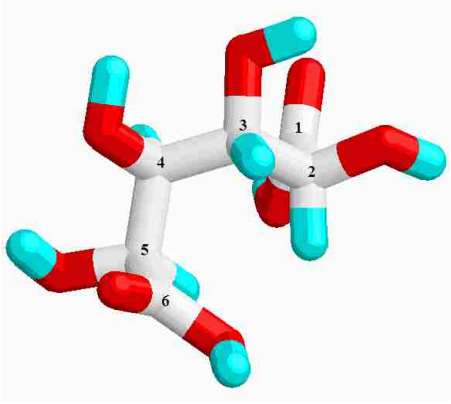

1a
$_2G^+{}_3G^+{}_4G^+$, 39.89%

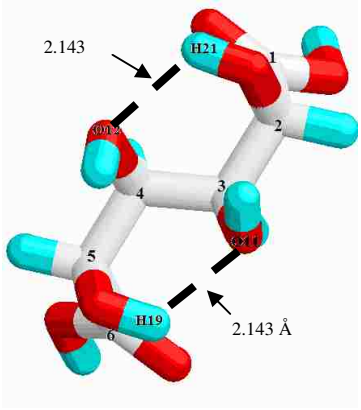

1c
$_2G^-{}_4G^-$, 10.95%

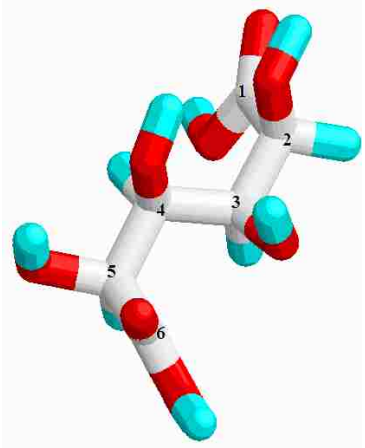

1b
$_2G^+{}_4G^-$, 18.05%

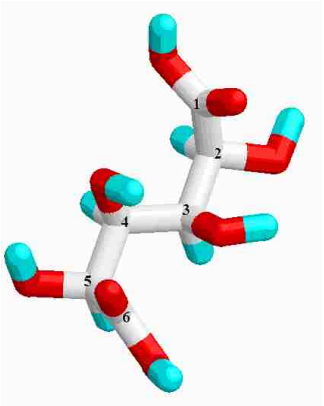

1d
$_2G^+{}_4G^+$, 10.74%

Figure 5: The four conformational families of D-mannaric acid making the largest contributions to the overall population all shown with the carbon backbone numbered

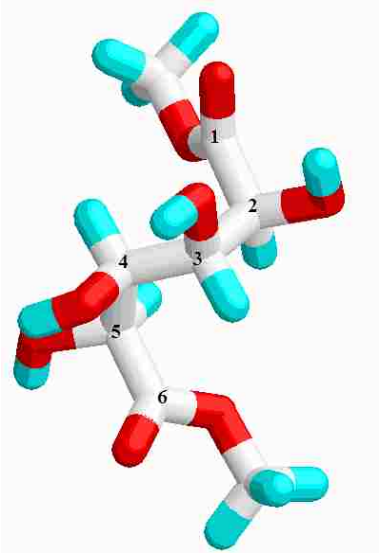

2a
$_2G^+{}_3G^+{}_4G^+$60.02%

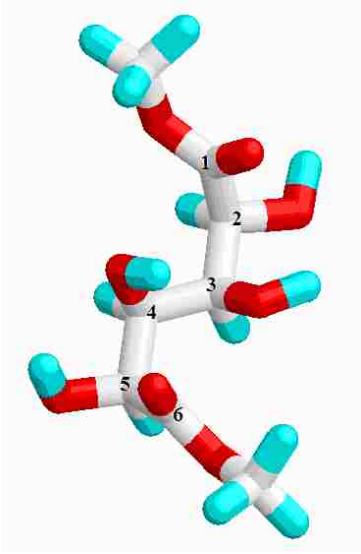

2c
$_2G^+{}_4G^+$, 8.30%

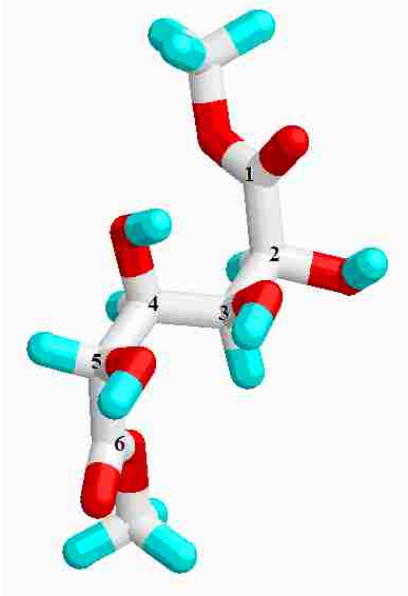

2b
$_2G^+{}_4G^-$, 11.54%

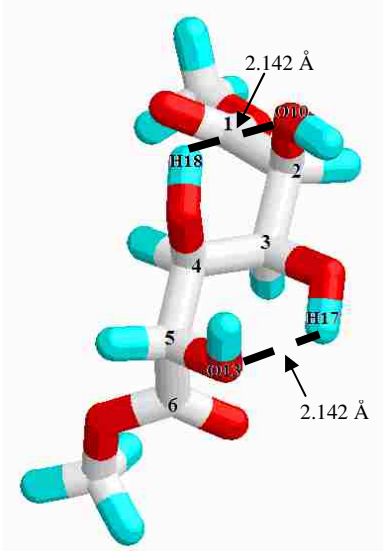

2d
$_2G^-{}_4G^-$, 5.61%

Figure 6: The four conformational families of dimethyl D-mannarate making the largest contributions to the overall population all shown with the carbon backbone numbered

The torsion angles of the backbone carbons for the four conformational families of each are all very similar, with only slight variations. The major differences arise from the torsion angles of the hydroxyl groups. Conformer family $_2G^+_4G^-$, **1b** and **2b**, has one set of 1,3-parallel hydroxyl group eclipsing steric interactions. Hydroxyl group torsion angles alternate between ~60° and ~170° and no hydrogen bonding is present. Conformer family $_2G^-_4G^-$, **1c** and **2d**, has two sets of 1,3-parallel hydroxyl group eclipsing steric interactions. All hydroxyl group torsion angles are ~165° with evidence of intramolecular hydrogen bonding. For D-mannaric acid (**1c**) hydrogen bonds are present at C3-O11···H19-O13 (2.143 Å) and C4-O12···H16-O10 (2.143 Å); for dimethyl D-mannarate (**2d**) hydrogen bonds are present at C2-O10···H18-O12 (2.142 Å) and C5-O13···H17-O11 (2.142 Å). Thus, for both D-mannaric acid and dimethyl D-mannarate conformational destabilization from parallel hydroxyl groups is offset to some extent by stabilizing intramolecular hydrogen bonding as noted. Interestingly, the hydrogen bond lengths in **1c** and **2d** differ by only 0.001 Å. The last of the larger contributors is conformational family $_2G^+_4G^+$, **1d** and **2c**. This family has no 1,3-parallel hydroxyl group eclipsing steric interactions and no intramolecular hydrogen bonding. The torsion angles between the hydroxyl group oxygens for C2 and C3 are ~60°, those between the oxygens for C4 and C5 are ~170°.

D-Mannaramide (3), *N,N´*-dimethyl-D-mannaramide (4), and 2,3,4,5-tetra-*O*-acetyl-*N,N´*-dimethyl-D-mannaramide (5)

The numbering schemes for mannaramide (**3**), *N,N´*-dimethyl mannaramide (**4**), and 2,3,4,5-tetra-*O*-acetyl-*N,N´*-dimethyl-D-mannaramide (**5**) are shown in Figures 7, 8, and 9.

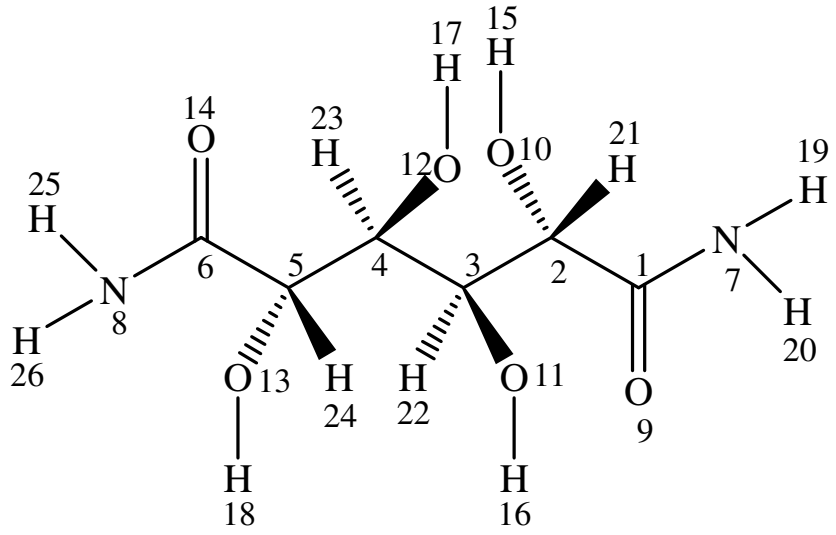

Figure 7: Numbering scheme for D-mannaramide (**3**)

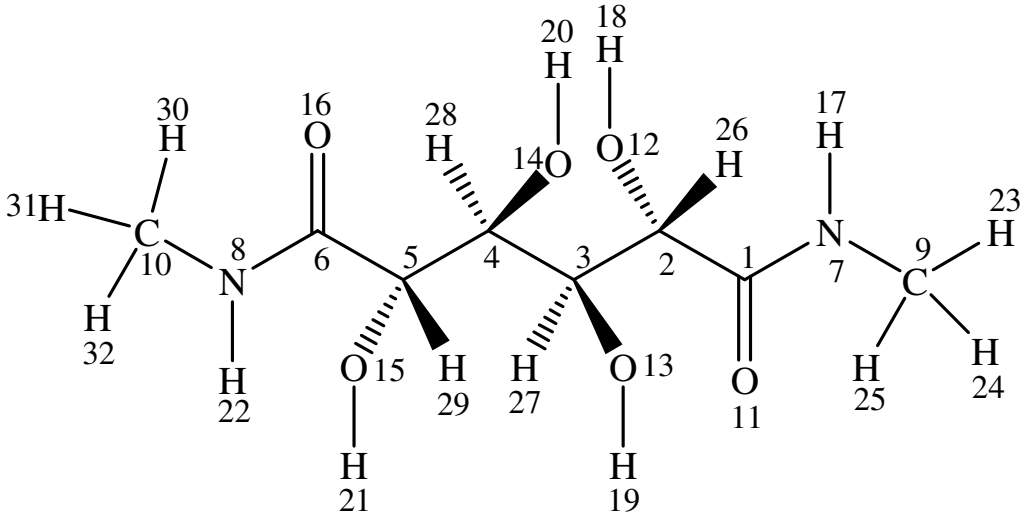

Figure 8: Numbering scheme for *N,N´*-dimethyl-D-mannaramide (**4**)

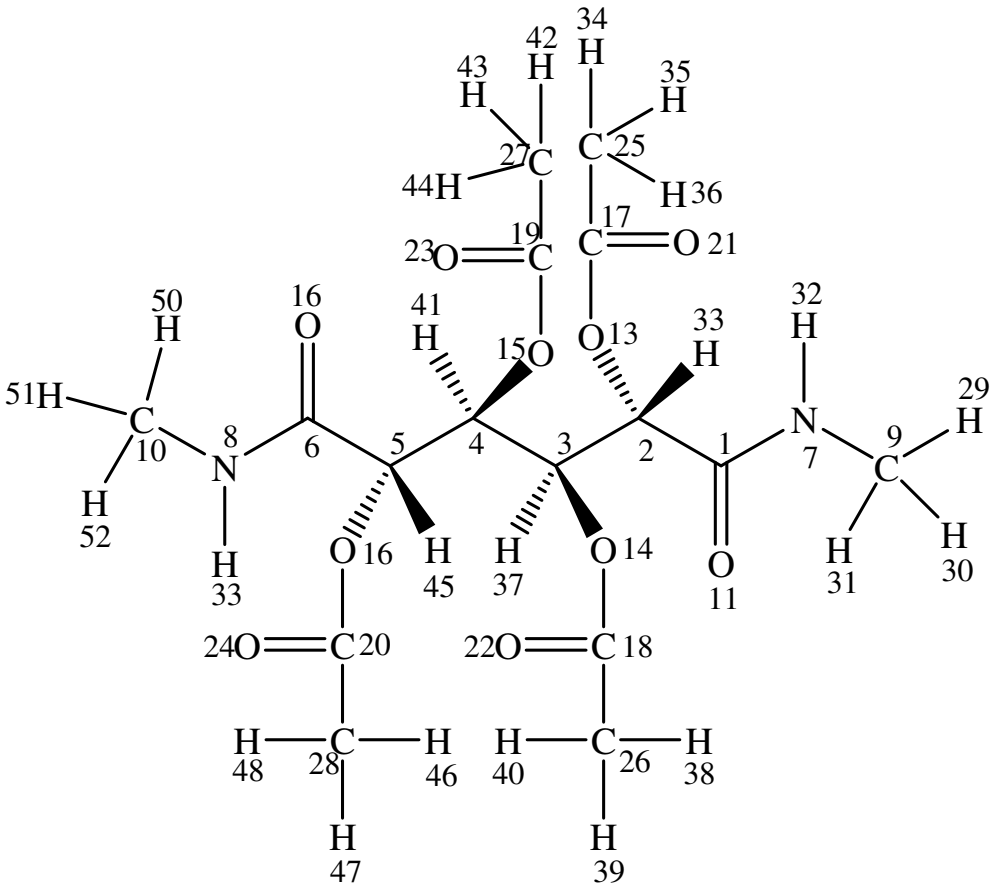

Figure 9: Numbering scheme for 2,3,4,5-tetra-*O*-acetyl- *N,N´*-dimethyl-D-mannaramide (**5**)

The results from computational analysis of D-mannaramide and *N,N´*-dimethyl-D-mannaramide are summarized in Tables 5 and 6. The computational results from 2,3,4,5-tetra-*O*-acetyl-*N,N´*-dimethyl-D-mannarate at dielectric constants 1.5 and 3.5 are summarized in Table 7 and Table 8, respectively. These tables list percent population and the low energy value of each conformer family generated in this analysis.

Table 5: Conformers found using MM3(96) conformational analysis and their contributions to the overall population for D-mannaramide (**3**)

D-Mannaramide (3) at dielectric constant 3.5				
Conformer Family	**Conformer Label**	**Low Energy (kcal/mol)**	**Percent Population**	**Standardized % Population**
$_2G^-{}_4G^-$	**3a**	3.9905	29.18	33.21
$_2G^+{}_3G^+{}_4G^+$	**3b**	5.2183	23.09	26.29
$_2G^+{}_4G^-$	**3c**	5.2813	21.01	23.92
$_2G^-$	**3d**	5.533	9.16	10.42
$_2G^-{}_3G^+{}_4G^+$	**3e**	5.7241	3.88	4.42
Extended	**3f**	6.178	0.85	0.96
$_2G^+{}_3G^+$	**3g**	6.8683	0.69	0.78
Total			87.86	100.00

Table 6: Conformers found using MM3(96) conformational analysis and their contributions to the overall population for *N,N´*-dimethyl-D-mannaramide (**4**)

***N,N*'-dimethyl-D-mannaramide (4) at dielectric constant 3.5**				
Conformer Family	**Conformer Label**	**Low Energy (kcal/mol)**	**Percent Population**	**Standardized % Population**
$_2G^-{}_4G^-$	**4a**	2.7281	35.82	41.00
$_2G^+{}_3G^+{}_4G^+$	**4b**	3.7648	29.77	34.07
$_2G^+{}_4G^-$	**4c**	3.8374	15.24	17.45
$_2G^-$	**4d**	4.3772	3.77	4.31
$_2G^-{}_3G^+{}_4G^+$	**4e**	4.3056	2.33	2.66
Extended	**4f**	5.0234	0.45	0.51
Total			87.36	100.00

Table 7: Conformers found using MM3(96) conformational analysis and their contributions to the overall population for 2,3,4,5-tetra-*O*-acetyl-*N,N´*-dimethyl-D-mannaramide (**5**) at dielectric constant 1.5

2,3,4,5-tetra-*O*-acetyl-*N,N*'-dimethyl-D-mannaramide (5) at dielectric constant 1.5				
Conformer Family	**Conformer Label**	**Low Energy (kcal/mol)**	**Percent Population**	**Standardized % Population**
$_2G^-{}_4G^-$	**5a**	3.2203	67.82	68.17
$_2G^-{}_4G^+$	**5b**	4.4478	13.75	13.82
$_2G^-$	**5c**	4.9856	9.60	9.65
$_2G^-{}_3G^+{}_4G^+$	**5d**	5.0777	3.76	3.78
$_2G^-{}_3G^-{}_4G^+$	**5e**	5.1641	2.84	2.86
Extended	**5f**	5.0208	1.49	1.50
$_2G^+{}_4G^+$	**5g**	5.3484	0.23	0.23
Total			99.48	100.00

Table 8: Conformers found using MM3(96) conformational analysis and their contributions to the overall population for 2,3,4,5-tetra-*O*-acetyl-*N,N´*-dimethyl-D-mannaramide (**5**) at dielectric constant 3.5

2,3,4,5-tetra-*O*-acetyl- *N,N*'-dimethyl-D-mannaramide (5) at dielectric constant 3.5				
Conformer Family	**Conformer Label**	**Low Energy (kcal/mol)**	**Percent Population**	**Standardized % Population**
$_2G^-{}_4G^-$	**5a (3.5)**	9.6829	32.83	36.47
$_2G^+{}_4G$-	**5b (3.5)**	10.4663	26.94	29.92
$_2G^-{}_3G^+{}_4G^+$	**5c (3.5)**	10.961	17.86	19.84
$_2G^-$	**5d (3.5)**	11.0146	10.63	11.81
$_2G^-{}_3G^+{}_4G^+$	**5e (3.5)**	11.2513	1.15	1.27
$_2G^-{}_4G^+$	**5f (3.5)**	11.0268	0.63	0.70
Total			90.03	100.00

Computational analysis of mannaramide (**3**), *N,N´*-dimethyl mannaramide (**4**), and 2,3,4,5-tetra-*O*-acetyl-*N,N´*-dimethyl mannaramide (**5**) (at dielectric constant 1.5 and 3.5) generated the same $_2G^-{}_4G^-$ lowest energy conformational family for all three molecules. This conformer family is characterized by destabilizing 1,3-parallel hydroxyl group

eclipsing steric interactions and accompanying intramolecular hydrogen bonds. Oxygens bonded to C2-C5 in all of the lowest energy conformers are on the same face of the molecule. In addition, the oxygens on C2 and C4 of these conformers are approximately 90° to the oxygens on C3 and C5.

Each of the molecules also exhibits amide intramolecular hydrogen bonding between the N7 amide proton and the oxygen on C2 and another hydrogen bond between the N8 amide proton and the oxygen on C5. Additionally, both D-mannaramide and *N,N´*-dimethyl-D-mannaramide display hydrogen bonds between 1,3-parallel hydroxyl groups; C5-O13···H16-O11-C3 and C2-O10···H17-O12-C4 for D-mannaramide (**3a**) and C5-O15···H19-O13-C3 and C2-O12···H20-O14-C4 for *N,N´*-dimethyl-D-mannaramide (**4a**).

Figures 10-12 show the $_2G^-{}_4G^-$ lowest energy conformers of these molecules. Lines between atoms represent the site of hydrogen bonding. The corresponding torsion angles varied and the angles calculated for the lowest energy conformers are presented in Table 9.

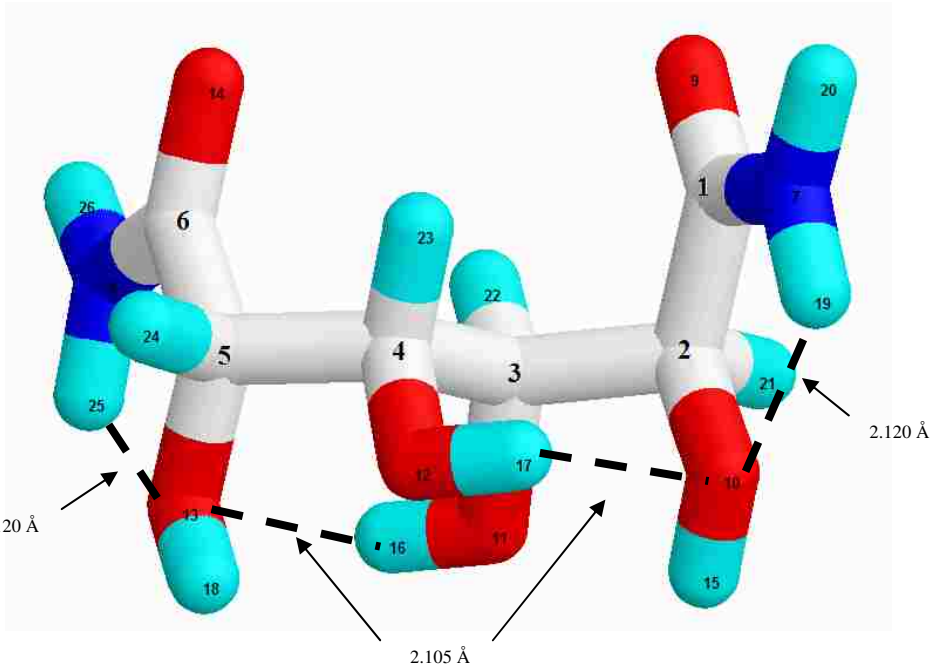

Figure 10: $_2G^-{}_4G^-$ lowest energy conformer of D-mannaramide (**3a**) accounting for 33.21% of the overall population

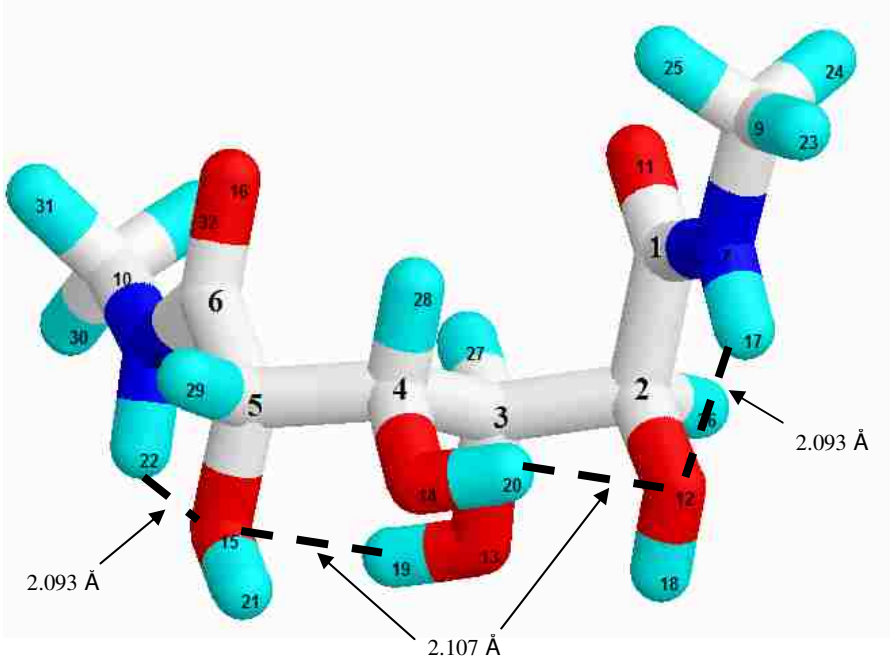

Figure 11: $_2G^-{}_4G^-$ lowest energy conformer of *N,N´*-dimethyl-D- mannaramide (**4a**) accounting for 41.09% of the overall population

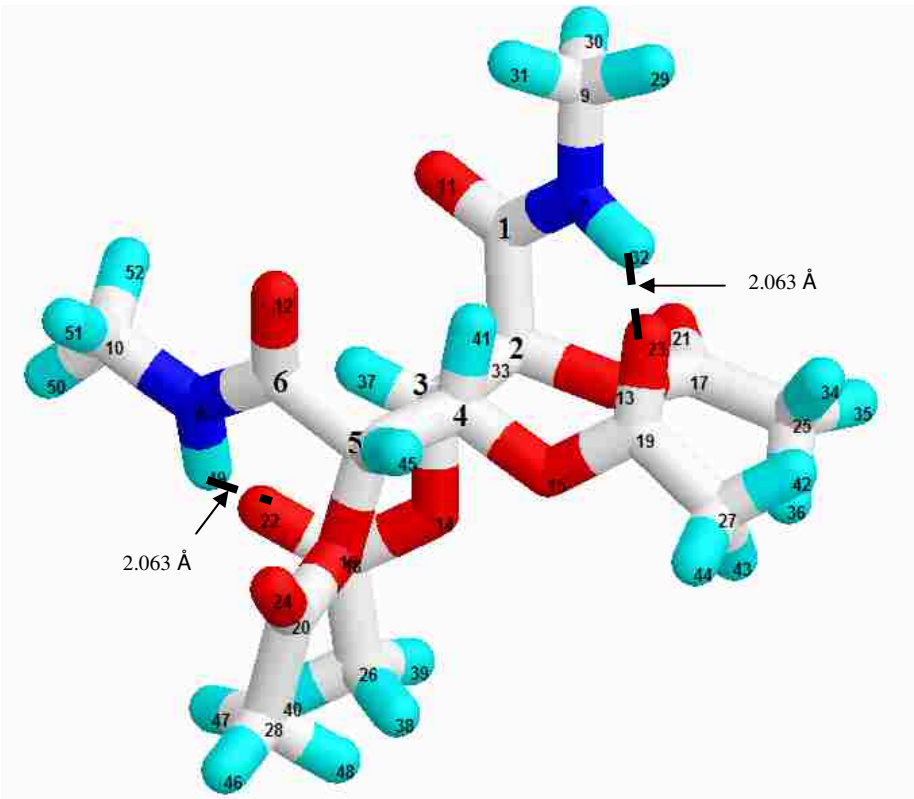

Figure 12: $_2G^-{}_4G^-$ lowest energy conformer of 2,3,4,5-tetra-*O*-acetyl *N,N´*-dimethyl-D-mannaramide (**5a**) at dielectric constant 1.5 accounting for 58.52% of the overall population.

Table 9: Torsion angles varied for D-mannaramide (**3**) and *N,N´*-dimethyl-D-mannaramide (**4**), and 2,3,4,5-tetra-*O*-acetyl-*N,N´*-dimethyl-D-mannaramide at dielectric constants 1.5 and 3.5 (**5**, **5 (3.5)**) with calculated angles for the lowest energy conformers of each

Torsion Angle	**3a**	**Torsion Angle**	**4a**	**Torsion Angle**	**5a**	**5a (3.5)**
N(7)-C(1)-C(2)-C(3)	125.4	N(7)-C(1)-C(2)-C(3)	123.8	N(7)-C(1)-C(2)-C(3)	97.5	107.1
C(1)-C(2)-C(3)-C(4)	-60.2	C(1)-C(2)-C(3)-C(4)	-60	C(1)-C(2)-C(3)-C(4)	-67.4	-59.6
C(2)-C(3)-C(4)-C(5)	175.4	C(2)-C(3)-C(4)-C(5)	175.4	C(2)-C(3)-C(4)-C(5)	168.2	179.2
C(3)-C(4)-C(5)-C(6)	-60.2	C(3)-C(4)-C(5)-C(6)	-60	C(3)-C(4)-C(5)-C(6)	-67.5	-59.6
C(4)-C(5)-C(6)-N(8)	125.4	C(4)-C(5)-C(6)-N(8)	123.8	C(4)-C(5)-C(6)-N(8)	97.5	107.1
H(21)-C(2)-O(10)-H(15)	-59.2	H(26)-C(2)-O(12)-H(18)	-59.2	H(33)-C(2)-O(13)-C(17)	39.3	-24.2
H(22)-C(3)-O(11)-H(16)	-56.8	H(27)-C(3)-O(13)-H(19)	-56.7	H(37)-C(3)-O(14)-C(18)	-4.8	36.0
H(23)-C(4)-O(12)-H(17)	-56.8	H(28)-C(4)-O(14)-H(20)	-56.7	H(41)-C(4)-O(15)-C(19)	-4.8	36.0
H(24)-C(5)-O(13)-H(18)	-59.2	H(29)-C(5)-O(15)-H(21)	-59.2	H(45)-C(5)-O(16)-C(20)	39.3	-24.2
O(10)-C(2)-C(3)-O(11)	-60.5	O(12)-C(2)-C(3)-O(13)	-60.5	O(13)-C(2)-C(3)-O(14)	-66.8	-61.2
O(11)-C(3)-C(4)-O(12)	56.3	O(13)-C(3)-C(4)-O(14)	56.3	O(14)-C(3)-C(4)-O(15)	47.8	63.1
O(12)-C(4)-C(5)-O(13)	-60.5	O(14)-C(4)-C(5)-O(15)	-60.5	O(15)-C(4)-C(5)-O(16)	-66.8	-61.2
H(21)-C(2)-C(3)-H(22)	-57.8	H(26)-C(2)-C(3)-H(27)	-57.7	H(33)-C(2)-C(3)-H(37)	-65.7	-58.2
H(22)-C(3)-C(4)-H(23)	-65.5	H(27)-C(3)-C(4)-H(28)	-65.5	H(37)-C(3)-C(4)-H(41)	-70.5	-59.9
H(23)-C(4)-C(5)-H(24)	-57.8	H(28)-C(4)-C(5)-H(29)	-57.7	H(41)-C(4)-C(5)-H(45)	-65.7	-58.1
				C(2)-O(13)-C(17)-C(25)	179.8	-178.0
				C(3)-O(14)-C(18)-C(26)	177.3	179.4
				C(4)-O(15)-C(19)-C(27)	177.3	179.4
				C(5)-O(16)-C(20)-C(28)	179.8	-178.0

The four conformer families that make the largest contributions to the overall population are shown in Figures 13 and 14 for D-mannaramide (**3**) and *N,N´*-dimethyl D-mannaramide (**4**), respectively. Hydrogen bonds are shown by dashed lines with corresponding bond lengths.

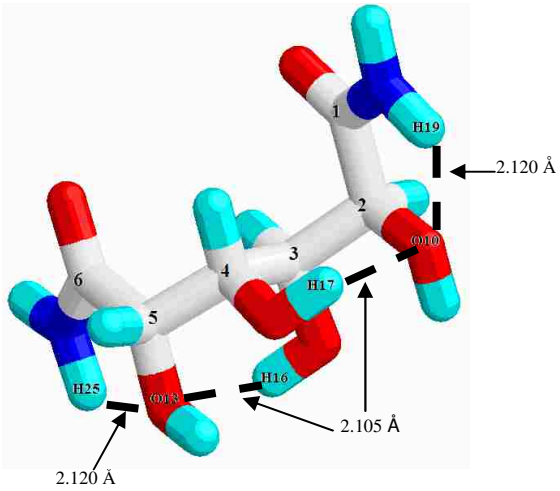

3a
$_2G^-{}_4G^-$, 33.21%

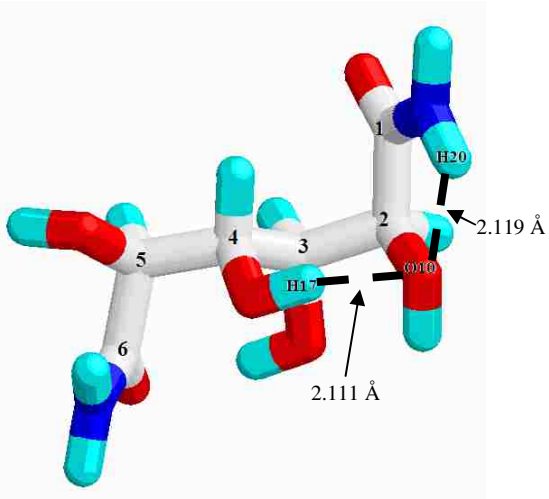

3c
$_2G^+{}_4G^-$, 23.92%

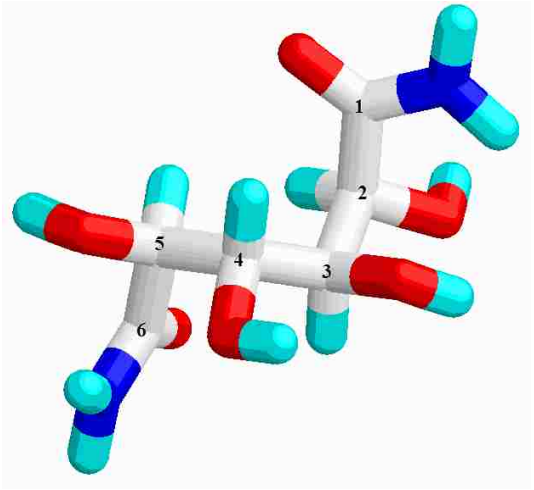

3b
$_2G^+{}_3G^+{}_4G^+$, 26.29%

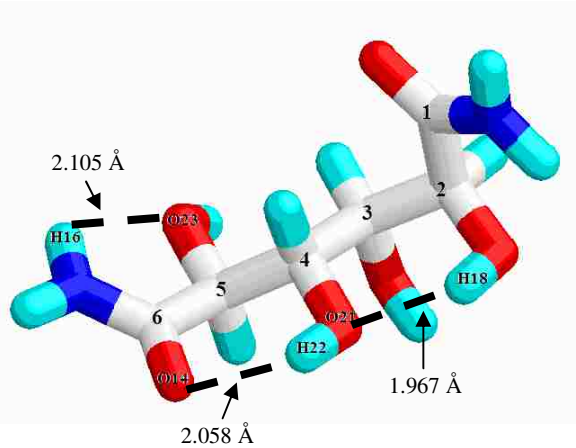

3d
$_2G^-$, 10.42%

Figure 13: The four conformational families of D-mannaramide making the largest contributions to the overall population all shown with the carbon backbone numbered

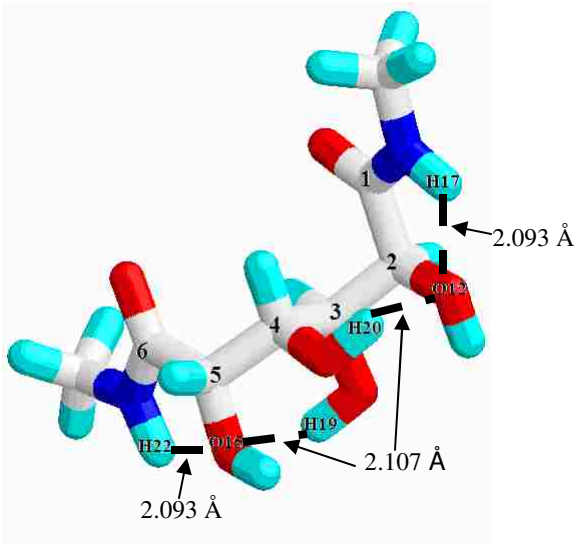

4a
$_2G^-{}_4G^-$, 41.0%

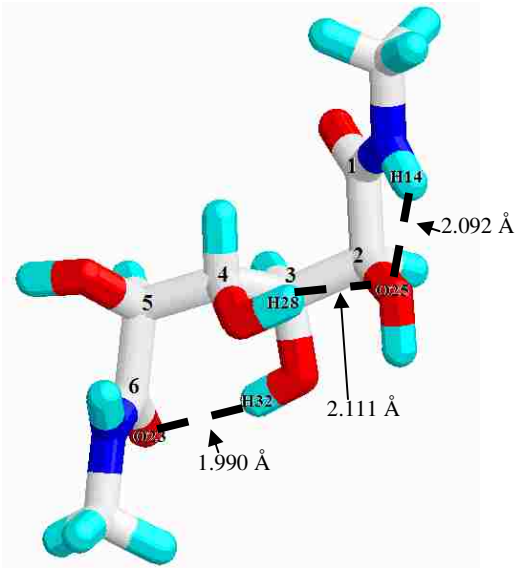

4c
$_2G^-{}_4G^+$, 17.45%

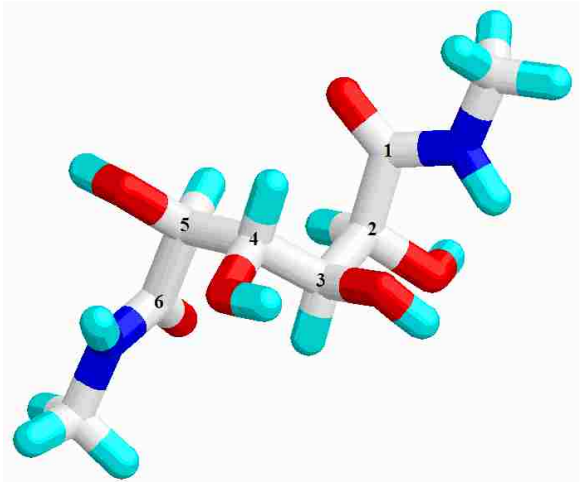

4b
$_2G^+{}_3G^+{}_4G^+$, 34.07%

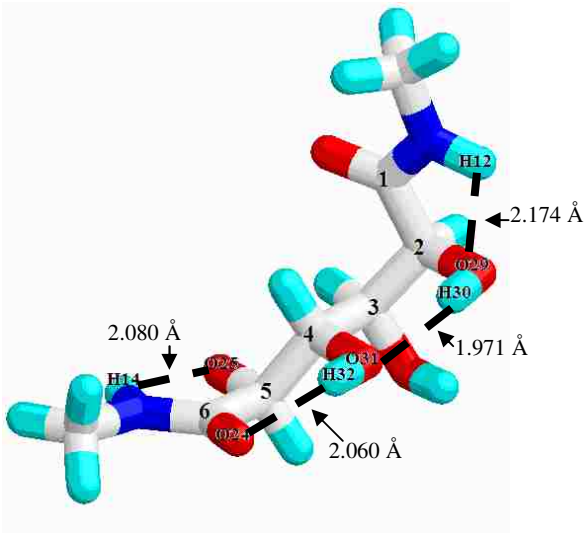

4d
$_2G^-$, 4.31%

Figure 14: The four conformational families of *N,N´*-dimethyl-D-mannaramide making the largest contributions to the overall population all shown with the carbon backbone numbered

It is clear from the D-mannaric acid (**1**) and dimethyl D-mannarate (**2**) computational results that the lowest energy conformers of these molecules are strongly driven by relief from 1,3-parallel oxygen steric interactions. In contrast, intramolecular hydrogen bonding contributions form amide N-H protons drives the conformational

preferences of molecules (**3**-**5**). The resulting lowest energy conformers (**3a** and **4a**) and slightly higher energy conformers **3b**, **3d**, **4b**, and **4d** originating from **3** and **4**, respectively, are further stabilized by intramolecular hydrogen bonds between 1,3-parallel hydroxyl groups. This importance of amide intramolecular hydrogen bonds in **3**-**5** is further emphasized by the dominance of low energy $_2G^-{}_4G^-$ conformer for **5** (**5a** at 68.19%), with parallel, somewhat bulky 1,3-acetoxy groups, and no additional hydrogen bonding contributions. In short, intramolecular amide based hydrogen bonding plays a major role in determining the conformational distribution of molecules of types **3**-**5** based upon these molecular mechanics computational methods, and may also play a similar role on the solution conformations of such molecules. A striking feature of all the molecules evaluated (**1**-**5**) is that the expected important contribution from extended conformers are insignificant and very surprising.

The four conformer families that make the largest contribution to the overall population for 2,3,4,5-tetra-*O*-acetyl-*N,N´*-dimethyl-D-mannaramide (**5**) at dielectric constant 1.5 and 3.5 are shown in Figure 15 and 16, respectively. Hydrogen bonds are shown by dashed lines with corresponding bond lengths.

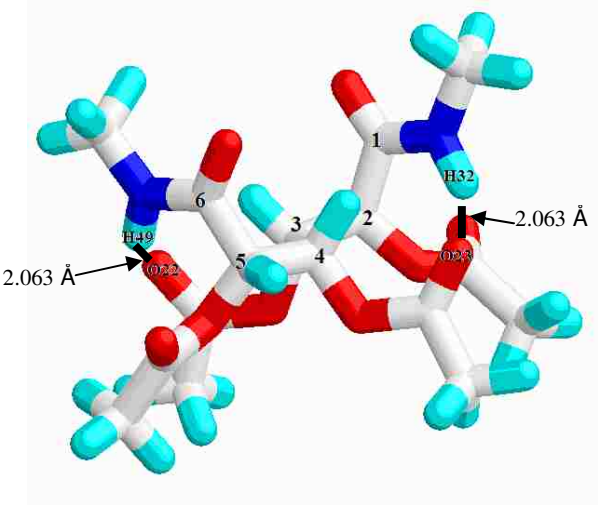

5a
$_2G^-{}_4G^-$, 68.17%

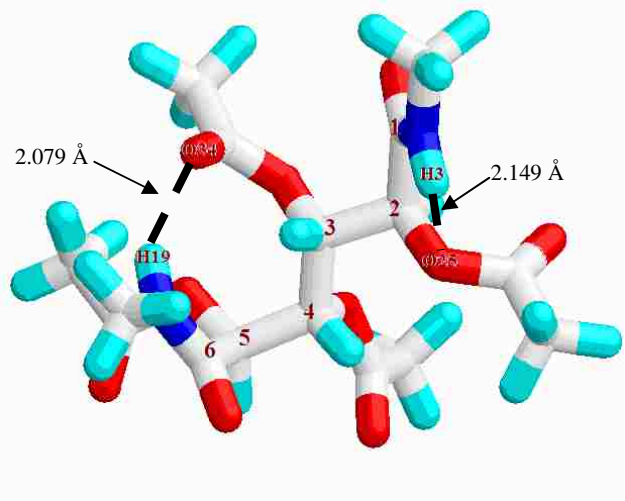

5c
$_2G^-$, 9.65%

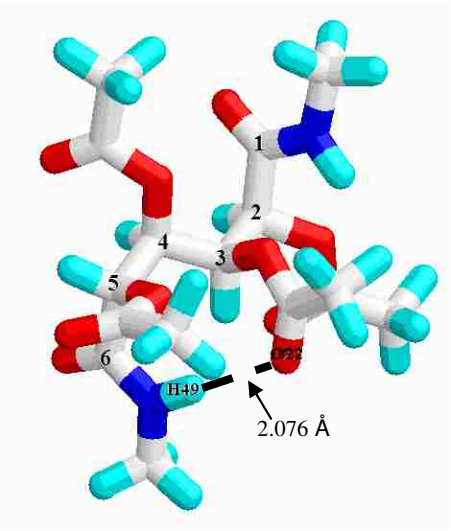

5b
$_2G^+{}_4G^-$, 13.82%

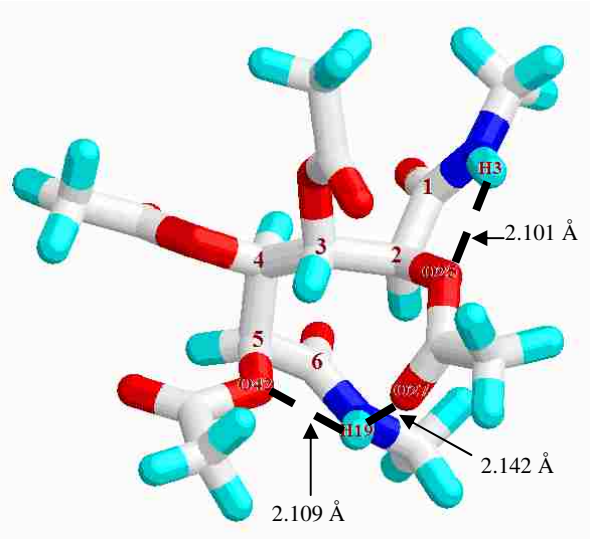

5d
$_2G^-{}_3G^+{}_4G^+$, 3.78%

Figure 15: The four conformational families of 2,3,4,5-tetra-*O*-acetyl-*N,N´*-dimethyl-D-mannaramide at dielectric constant 1.5 making the largest contributions to the overall population all shown with the carbon backbone numbered

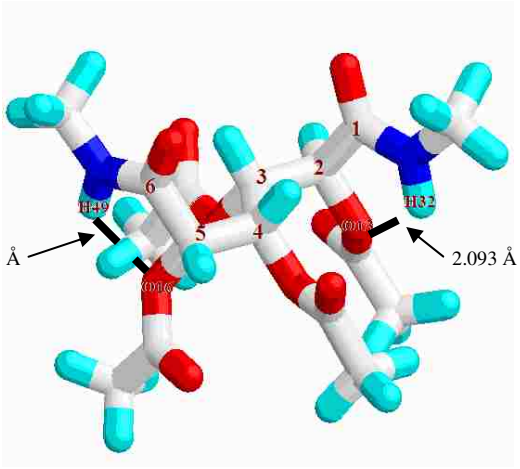

5a(3.5)
$_2G^-{}_4G^-$, 36.47%

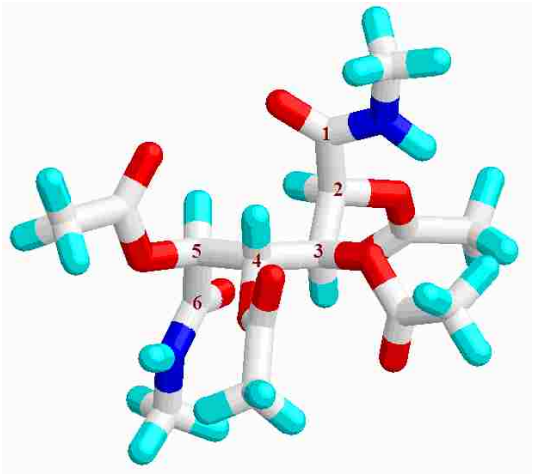

5c(3.5)
$_2G^+{}_3G^+{}_4G^+$, 19.84%

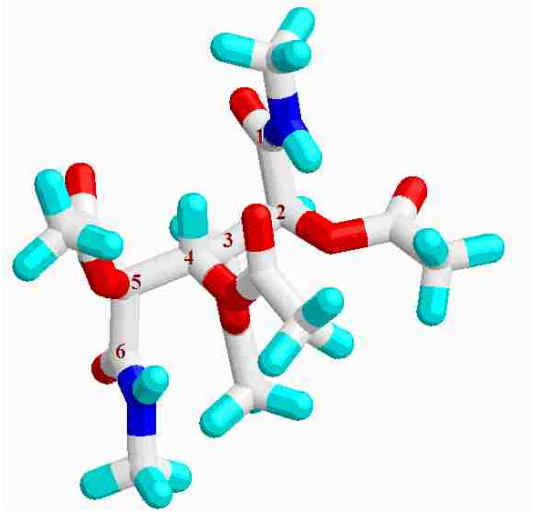

5b(3.5)
$_2G^+{}_4G^-$, 29.92%

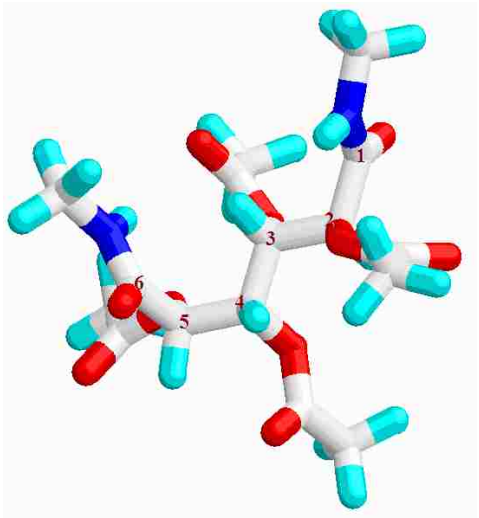

5d(3.5)
$_2G^-$, 11.81%

Figure 16: The four conformational families of 2,3,4,5-tetra-*O*-acetyl-*N,N´*-dimethyl-D-mannaramide at dielectric constant 3.5 making the largest contributions to the overall population all shown with the carbon backbone numbered

Three of the four most populated conformer families of 2,3,4,5-tetra-*O*-acetyl-*N,N´*-dimethyl-D-mannaramide at dielectric constant 3.5 [**5(3.5)**] are also present in **3**, **4**, and **5**. One family, $_2G^+{}_3G^+{}_4G^+$, does not appear for the other amide molecules but happens to be the lowest energy conformer for both D-mannaric acid (**1**) and dimethyl-D-mannaramide (**2**). Both the second and fourth most populated conformer families, $_2G^+{}_4G^-$ and $_2G^-$, have one set of 1,3-paralled hydroxyl group steric interactions while the third most populated conformer family has none. Only **5a(3.5)** has hydrogen bonding. 2,3,4,5-tetra-*O*-acetyl-*N,N´*-dimethyl-D-mannaramide was modeled at dielectric constant of 3.5, simulating a more polar solvent, for completeness. However, due to the hydrophobic nature of the molecule, the results found are unlikely to make a large contribution to experimental results.

A final noteworthy general observation from this study is that the lowest energy conformation of **3**-**5**, $_2G^-{}_4G^-$, all have symmetrical S-shaped structures with terminal amide functions in offset parallel planes. This view of the $_2G^-{}_4G^-$ conformer family is shown for D-mannaramide in Figure 17. Whether or not this conformation dominates poly(alkylene D-mannaramides) remains to be determined but is an observation worthy of further investigation.

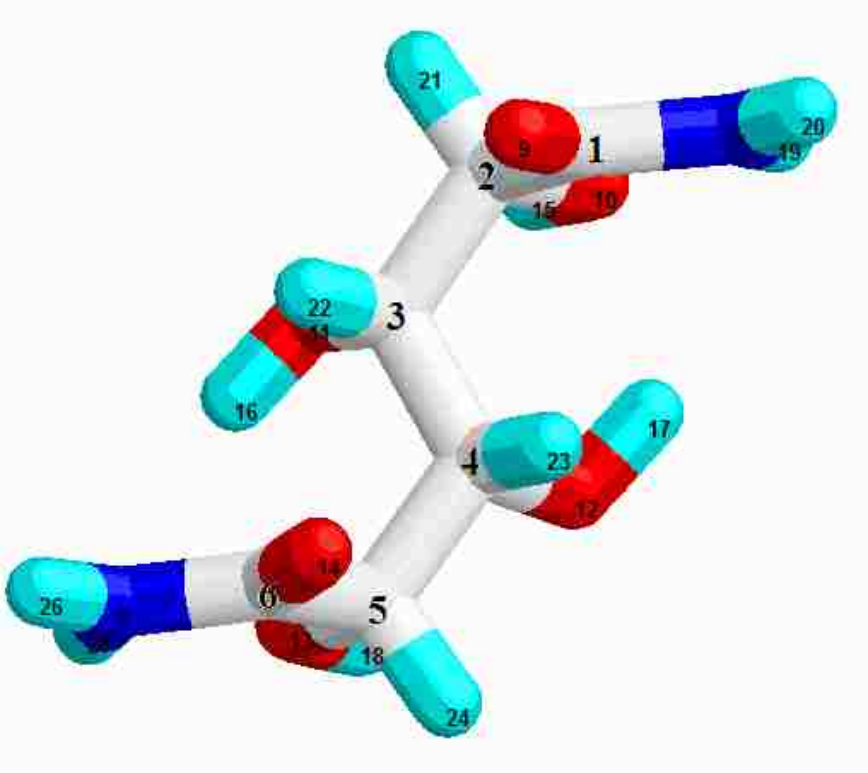

Figure 17: The lowest energy conformer of D-mannaramide (**3a**) showing the S-like shape and offset parallel amides

3.2.6 Comparison of Calculated and Experimental Coupling Constants

Coupling constants were calculated for all molecules analyzed using MM3(96) as part of the computational program and employed Karplus equations as modified by Haasnoot *et al.*[11] These values were compared with experimentally determined coupling constants from ^{1}H NMR analysis when possible, Table 10. The spectrum of disodium D-mannarate (simulating D-mannaric acid) and *N,N´*-dimethyl-D-mannaramide were both obtained in D_2O and coupling constants determined. The values calculated from computational results for $J_{2,3}$ and $J_{4,5}$ were much smaller than the experimentally determined values for both molecules, suggesting that the modeling does not effectively simulate the average conformational characteristics. The magnitude of the

experimentally determined coupling constants clearly suggests a greater contribution from vicinal-anti protons than suggested from the lower valued computationally generated couplings. The calculated coupling constants are averages based on the entire population analyzed and therefore all conformers found.

Table 10: Comparison of experimental and computational coupling constants for D-mannaric acid and *N,N´*-dimethyl-D-mannaramide

	Experimental		Computational	
Molecule	$J_{2,3}$	$J_{4,5}$	$J_{2,3}$	$J_{4,5}$
D-Mannaric acid (disodium salt)	5.86	5.86	3.39	3.35
N,N´-dimethyl-D-mannaramide	6.35	5.86	2.65	2.61

3.2.7 Summary

Table 11 summarizes the results for the lowest energy conformational family of **1-5** and also indicates total steric energy and the standardized % population of that family. Also listed is the standardized percent population of the lowest energy conformer for the first kcal/mol analyzed for each molecule.

Table 11: Lowest energy conformers and corresponding energy and standardized percent population for all molecules analyzed

Molecule	**Lowest Energy Conformer**	**Energy as (kcal/mol)**	**Standardized Percent Population**	**1 kcal/mol Percent Population**
D-Mannaric acid	${}_2G^+\ {}_3G^+\ {}_4G^+$	10.15	39.20	71.72
Dimethyl D-mannarate	${}_2G^+\ {}_3G^+\ {}_4G^+$	10.79	60.02	89.07
D-Mannaramide	${}_2G^-\ {}_4G^-$	3.99	33.21	100
N,N´-dimethyl-D-mannaramide	${}_2G^-\ {}_4G^-$	2.73	41.09	100
2,3,4,5-tetra-*O*-acetyl-*N,N´*-dimethyl-D-mannaramide @ 1.5	${}_2G^-\ {}_4G^-$	3.22	58.52	100
2,3,4,5-tetra-*O*-acetyl-*N,N´*-dimethyl-D-mannaramide @ 3.5	${}_2G^-\ {}_4G^-$	9.68	36.47	79.21

The lowest energy conformer for both D-mannaric acid (**1**) and dimethyl D-mannarate (**2**) is $_2G^+{}_3G^+{}_4G^+$ and displays no intramolecular hydrogen bonding. The lowest energy conformer of D-mannaramide (**3**), *N,N´*-dimethyl-D-mannaramide (**4**), and 2,3,4,5-tetra-*O*-acetyl- *N,N´*-dimethyl-D-mannaramide [**5** and **5**(**3.5**)] is $_2G^-{}_4G^-$. Intramolecular hydrogen bonding involving the amide N-H functions is evident in all four of these low energy conformers and appears to be a major stabilizing force with all three molecules. These conformations also display sterically unfavorable parallel 1,3-hydroxyl groups and which, in the case of **3** and **4**, that conformational instability is offset to some extent by intramolecular O-H···O-H hydrogen bonding. The lowest energy $_2G^+{}_3G^+{}_4G^+$ conformation of **1** and **2** appears more compact and dense than that of the lowest energy $_2G^-{}_4G^-$ conformation of **3**-**5**, but neither conformational family was predicted on the basis of stable steric considerations because they lack of destabilizing 1,3-parallel hydroxyl group eclipsing steric interactions in **1**-**5**. $J_{2,3}$ and $J_{4,5}$ coupling constants calculated from MM3(96) don't match closely with experimentally determined values, but they still provide some insight into the angular distribution of vicinal protons in these molecules.

3.3 Experimental

Six rotamers of each of the molecules **1**-**5** were built in Alchemy 2000 and input as coordinate files into MM3(96). Energy change optimizations were terminated using the default Alchemy 2000 value of 0.0003*n where n is the number of atoms. All conformers were fully energy-minimized at a low energy value of 300 K using MM3's block diagonal/full matrix optimization option at dielectric constant 3.5. 2,3,4,5-tetra-*O*-acetyl-*N,N´*-dimethyl-D-mannaramide (**5**) was also calculated at dielectric constant of 1.5.

Torsion parameters, or force constants, for the sequence of an ester group adjacent to an amide (9-3-1-75), Table 1, was input in the constant file of MM3(96) as the constant file of MM3(96) as V1 = -2.157, V2 = -0.592, and V3 = 0.466. The sequence of an ester group adjacent to a carbonyl (3-1-75-3), Table 1, was input as the constant file of MM3(96) as V1 = 0.7246, V2 = -0.6033, and V3 = 0.2583. For all molecules, with the exception of per-*O*-acetylated-*N,N´*-dimethyl-d-mannaramide, nine torsional angles were varied; five in the carbon backbone and four for the hydroxyl groups. For 2,3,4,5-tetra-*O*-acetyl-*N,N´*-dimethyl-D-mannaramide (**5**) 13 torsion angles were varied; five in the carbon backbone, eight associated with the ester functionality. Shaking was invoked to a user specified value of 10,000 K after the number of search steps reached 20 times the number of torsion angles being varied and shaking continues for 2 times the number of angles being varied. This amounts to 18 steps during shaking and 180 steps between shaking. A total number of 60,000 steps were performed for each molecule investigated.

The Monte Carlo program is written as a UNIX script that coordinates multiple subroutines with MM3(96). In general a coordinate file (MM3 file) is input into the simulation. The control file contains most of the information needed by the search. This includes torsion angles to vary, the number of program steps, and conditions for "temperature shaking" of the molecule. In addition, it contains information to monitor search progress including current step number and number of conformers found. To begin the search the input structure is used as is. The program randomly selects a torsion angle and an angle increment (δ) between $60° < \delta < 300°$ to vary. The resulting conformation is input into MM3(96) for energy minimization. After successful minimization, several decisions are made. First, the script determines if the output

conformation is a true local minima or a transition state by looking for imaginary vibrational frequencies. If the structure is not a true minimum, the program is redirected to the end of the current step, a new structure is generated, and the optimization is repeated. If a true minimum is found, the energy of the structure is compared with the energy of the base structure (Eb). If the energy is lower than Eb, the structure is substituted as the new base structure for the search. If the energy is higher, then a Metropolis function is calculated using Equation 4.5 where ΔE = Ei-Eb.

$$Pi = e^{\frac{-\Delta E}{R \times ST}} \quad (\mathbf{4.5})$$

The function is calculated and compared to a randomly generated number between 0 and 1 (RN). If Pi < RN, the structure and its energy are taken as the new starting point in the search. If Pi > RN the base structure and its energy is retained. The output conformation is also compared to all other previously found conformers and deemed to be a new conformer if any one torsion angle differs from all other previously found conformers by more than 2.5º. If the conformation is new it is added to the group of new found conformers. This process is defined as a step. This new conformer is then used as the coordinate file to be input back into the simulation and is treated in exactly the same manner as before. After a user defined number of steps has occurred, the simulation undergoes a temperature shaking process. The temperature shaking process enables the program to vary more than one torsion angle of a conformer before being input back into the simulation. The number of steps in the temperature shaking process is user defined and corresponds to the number of times a torsion angle is randomly selected and varied. All unrealistic conformations produced during this process fail to optimize in MM3(96) and are discarded. The simulation then inputs the coordinate file in that step and the

process is repeated. The simulation terminates itself after a user defined number of steps have been reached.

The program also contains a module to calculate hydrogen-hydrogen coupling constants from the Karplus equations of Haasnoot *et al*.[11] Implementation of this routine is achieved through the control file. The coupling constant information is tabulated in a separate summary file.

3.4 References

1. Hashimoto, Kazuhiko; Wibullucksanakui, Sirinat; Matsuura, Mitsuyasu; Okada, Masahiko. Macromolecular Synthesis from Saccharic Lactones. Ring-Opening Polyaddition of D-Glucaro- and D-Mannaro-1,4:6,3-dilactones with Alkykenediamines. *J. Polym. Sci., Part A: Polym. Chem.* **1993**, *31*, 3141-3149.

2. Kiely, Donald E.; Chen, Liang; Lin, Tsu-Hsing. Synthetic Polyhydroxypolyamides from Galactaric, Xylaric, D-Glucaric, and D-Mannaric Acids and Alkylenediamine Monomers-Some Comparisons. *J. Polym. Sci., Part A: Polym. Chem.* **2000**, *38*, 594-603.

3. Barrows, Susan E.; Dulles, Frederic, J.; Cramer, Christopher, J.; French, Alfred D.; Truhlar, Donald G. Relative Stability of Alternative Chair Forms and Hydroxymethyl Conformations of β-D-Glucopyranose. *Carbohydr. Res*. **1995**, *276*, 219-251.

4. French, Alfred D.; Dowd, Michael K. Exploration of Disaccharide Conformations by Molecular Mechanics. *J. Mol. Struct. (Theochem)*. **1993**, *286*, 183-201.

5. Dowd, Michael K.; Reilly, Peter J.; French, Alfred D. Molecular Modeling of Two Disaccharides Containing Fructopyranose Linked to Glucopyranose. *J. Carbohydr. Chem*. **1993**, *12* (4&5), 449-457.

6. Styron, Susan D.; French, Alfred D.; Friedrich, Joyce D.; Lake, Charles H.; Kiely, Donald E. MM3(96) Conformational Analysis of D-Glucaramide and X-Ray Crystal Structures of Three d-Glucaric Acid Derivatives – Models for Synthetic Poly(Alkylene D-Glucaramides). *J. Carbohydr. Chem*. **2002**, *21* (1&2), 27-51.

7. Zhang, Jinsong; Kiely, Donald E.; Hardcastle, Kenneth I. MM3 Conformational Analysis and X-Ray Crystal Structure of 2,3,4,5-Tetra-*O*-Acetyl-*N,N´*-Dimethyl-D-Glucaramide as a Conformational Model for the D-Glucaryl Unit of Poly(Alkylene 2,3,4,5-Tetra-*O*-Acetyl-D-Glucaramides). *J. Carbohydr. Chem*. **2006**, *25*, 633-659.

8. Zhang, Jinsong; Kiely, Donald E. Application of a Model Building Approach to Molecular Mechanics (MM3) for Calculating Low-Energy Conformations of Tetra-*O*-Acyl-*N,N´*-Dialkyl-D-Glucaramides. *J. Carbohydr. Chem*. **2006**, *25*, 697-711.

9. Mike Dowd

10. Metropolis, N.; Rosenbluth, A.W.; Rosenbluth, M.N.; Teller, A.H.; Teller, E. Equation of State Calculations by Fast Computing Mechanics. *J. Chem. Phys*. **1953**, *21*, 1087-1092.

11. Haasnoot, C.A.G.; De Leeuw, F.A.A.M.; Altona, C. The Relationship Between Proton-Proton NMR Coupling Constants and Substituent Electronegativies – I. An

Empirical Generalization of the Karplus Equation. *Tetrahedron*. **1980**, *36* (19), 2783-2792.

Chapter 4

Conclusion

An improved method for the nitric acid oxidation of D-mannose has been developed. The method employed a Mettler Toledo RC-1 Labmax reactor, which was well suited for the nitric acid oxidation as it is designed as a temperature/pressure controlled closed-system reactor operated by computer. The most effective and efficient oxidation method was determined to be Oxidation Method 4, which was carried out using an increased amount of nitric acid (5 moles) to give a molar ratio of 6.67:1 nitric acid:D-mannose. Oxidation Method 4 not only provided the desired product but required only a single oxidation procedure.

D-Mannaric acid was isolated as *N,N´*-dimethyl-D-mannaramide with yields greater than 50%. The of *N,N´*-dimethyl-D-mannaramide provided an alternative route to the synthesis of disodium D-mannarate. *N,N´*-dimethyl-D-mannaramide was recrystallized from water to produce crystals of good quality and size for single-crystal x-ray crystal structure analysis. The molecule adopts an extended conformation free of destabilizing 1,3-parallel hydroxyl group steric interactions. There are no intramolecular hydrogen bonds in *N,N´*-dimethyl-D-mannaramide, but intermolecular hydrogen bonding is present. The crystal structure of *N,N´*-dimethyl-D-mannaramide (**9**) provides a greater understanding of the D-mannaryl unit in solid state.

Disodium D-mannarate was prepared by the base hydrolysis of *N,N´*-dimethyl-D-mannaramide and used to prepare a series of alkylene diammonium D-mannarate salts. The alkylenediammonium D-mannarate salts possess a stoichiometrically balanced 1:1 molar ratio of D-mannaric acid:diamine and were used to prepare a series of

poly(alkylene D-mannaramide) prepolymers and postpolymers with number average molecular weights determined by ^{1}H NMR end group analysis. To better understand the conformation of the D-mannaryl unit of poly(alkylene D-mannaramides), octamethylenediammonium mannarate was recrystallized from water and subjected to single-crystal x-ray crystal structure analysis. Octamethylenediammonium mannarate adopts an extended conformation in the crystalline state and, as with *N,N´*-dimethyl-D-mannaramide, the molecule is free of destabilizing 1,3-parallel hydroxyl group eclipsing steric interactions.

MM3(96) computational analysis was performed on D-mannaric acid, its dimethyl ester, and three amide derivatives to learn more about the shapes and conformations of these molecules in solution with the hope of better understanding the polymerization reaction and gaining some insight into the three dimensional structures of the resultant polymers. The lowest energy conformer for both D-mannaric acid and dimethyl D-mannarate is $_2G^+{}_3G^+{}_4G^+$. This conformation is not dominated by hydrogen bonding. The lowest energy conformer of mannaramide, *N,N´*-dimethyl mannaramide, and 2,3,4,5-tetra-*O*-acetyl- *N,N´*-dimethyl mannaramide is $_2G^-{}_4G^-$. This conformational family is characterized by hydrogen bonding but results suggest that hydrogen bonding alone does not dictate the lowest energy conformation. The $_2G^+{}_3G^+{}_4G^+$ conformation is more compact and dense than that of the $_2G^-{}_4G^-$ conformation, but neither were the extended conformations predicted. $J_{2,3}$ and $J_{4,5}$ coupling constants calculated from MM3(96) underestimated experimental values and may not effectively simulate the average conformational characteristics but still provide a better understanding of the shapes and conformations that may be present in solution for the mannaric acid derivatives.

There are many areas of this research that would benefit from additional research. A method for the nitric acid oxidation of D-mannose using the Mettler Toledo LabMax® has been developed but is not optimized. An optimized procedure could provide better isolated percent yields of *N,N´*-dimethyl-D-mannaramide. Additional method development of the diffusion dialysis isolation modification could provide better separation of nitric acid and organic acids and would also provide better isolated percent yields of *N,N´*-dimethyl-D-mannaramide. This work provided two x-ray crystal structures of D-mannaric acid derivatives. There were molecules for which crystallization was not attempted; dipotassium D-mannarate, decamethylenediammonium D-mannarate, or dodecamethylenediammonium D-mannarate. It may also be possible to grow crystals suitable for x-ray crystal structure analysis from these molecules and gain better understanding of the D-mannaryl unit in the solid state. Preliminary research shows that a longer polymerization time increases the DP of poly(hexamethylene D-mannaramides). It may also be possible to increase the size of other poly(alkylene D-mannaramides) given a longer reaction time as well. With increasing computational ability, it may be possible to model poly(alkylene D-mannaramides) in the future to get a better understanding of the conformation of this class of polymers and compare results with those presented in this work.

Chapter 5

Appendix

5.1 Oxidation Experimental Method 1 Analyzed by GC-MS Method 1

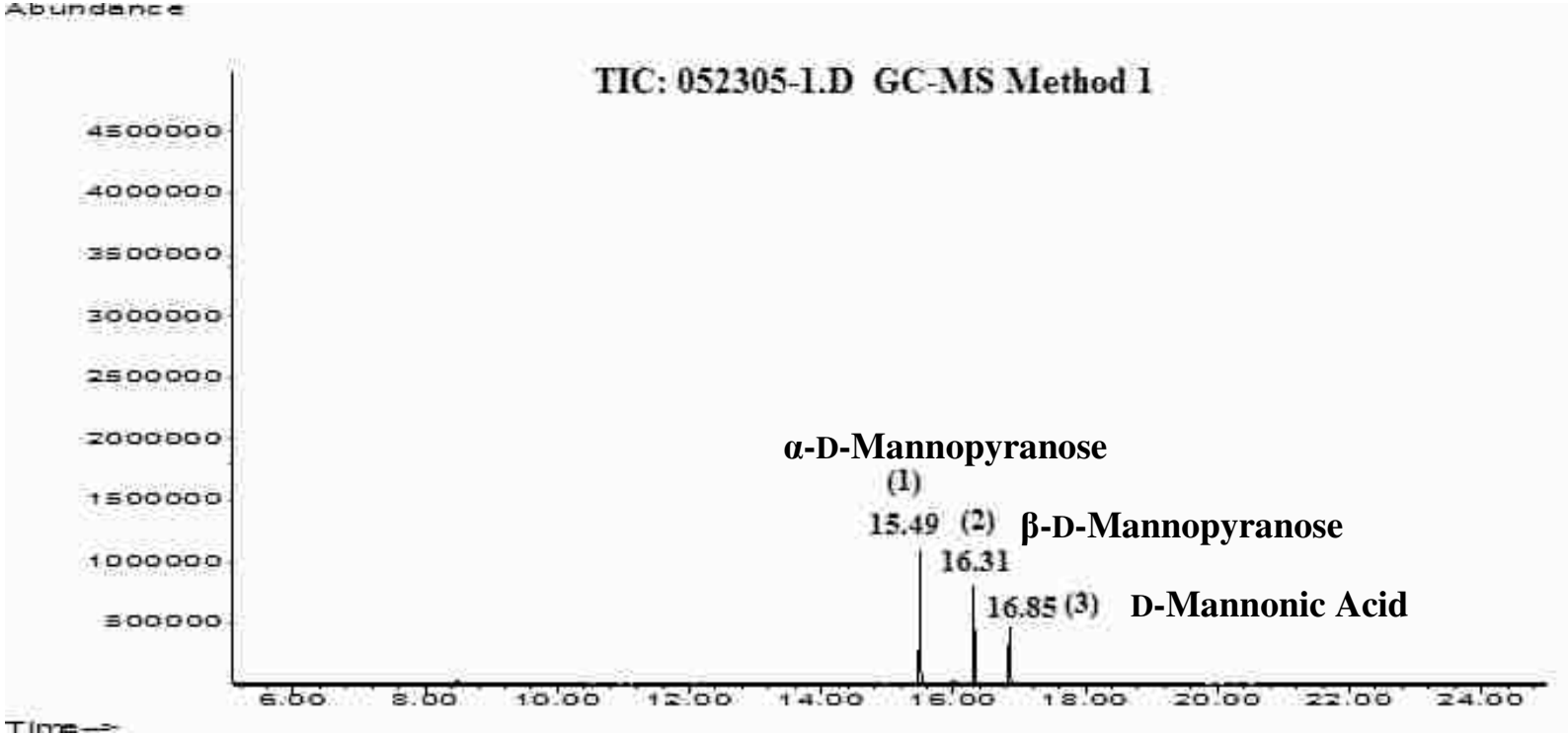

5.1.1 TIC after the second addition of D-mannose solution (step 5)

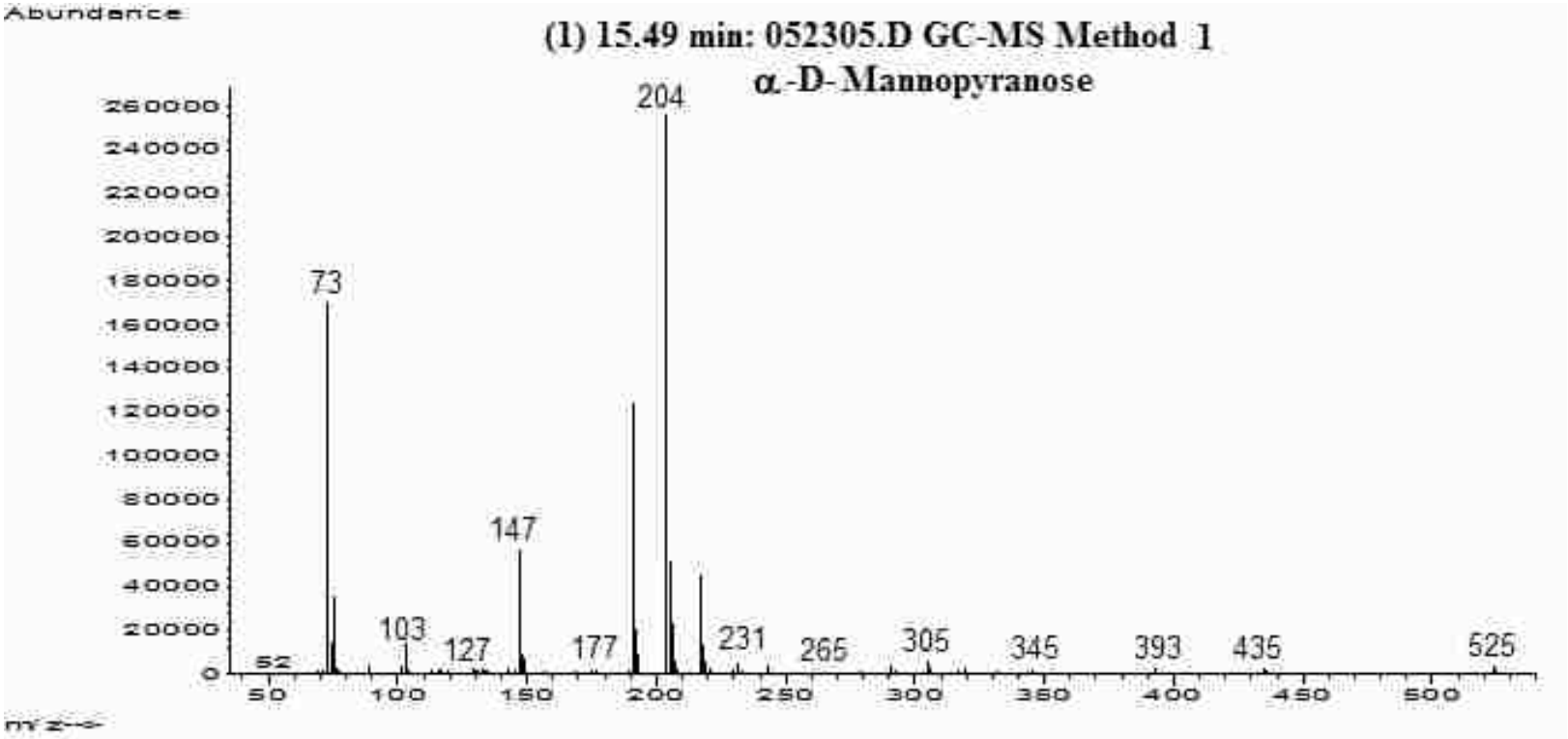

5.1.2 MS of peak (1) at 15.49 min, α-D-mannopyranose

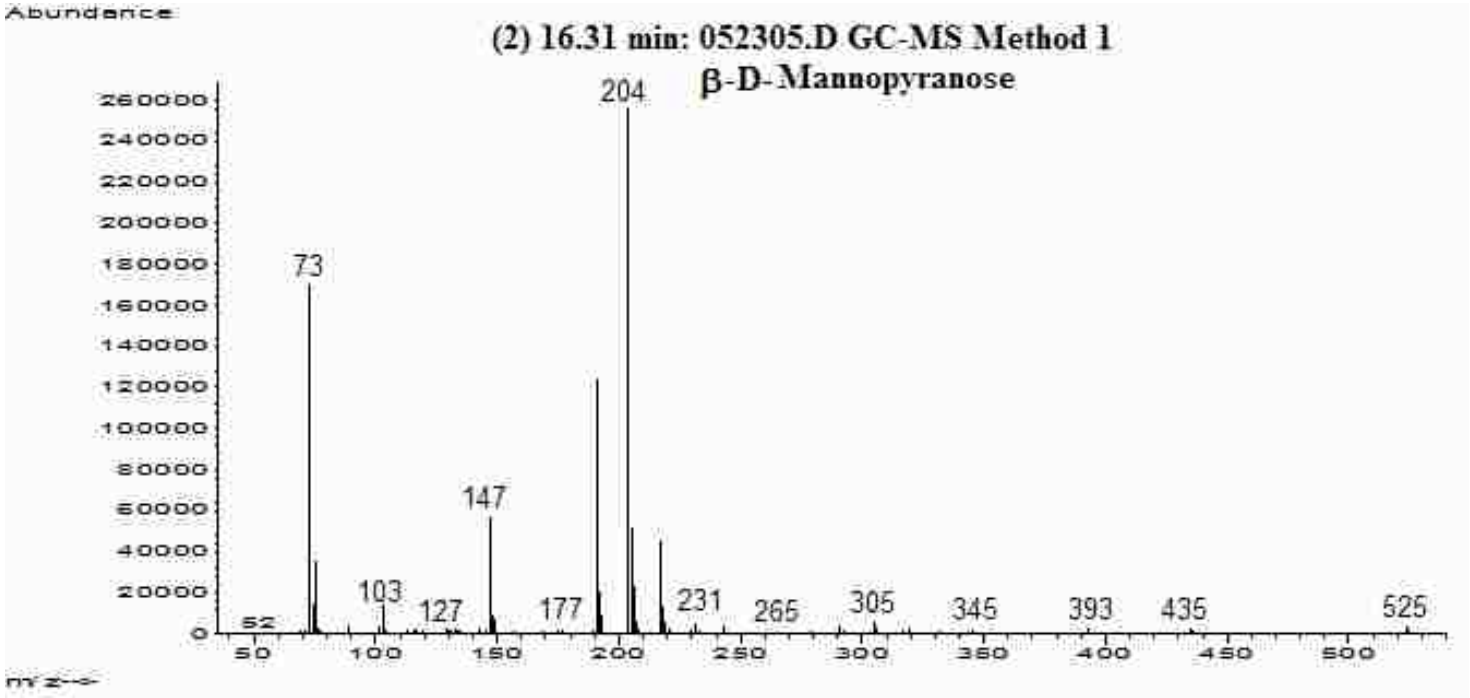

5.1.3 MS of peak (2) at 16.31 min, β-D-mannopyranose

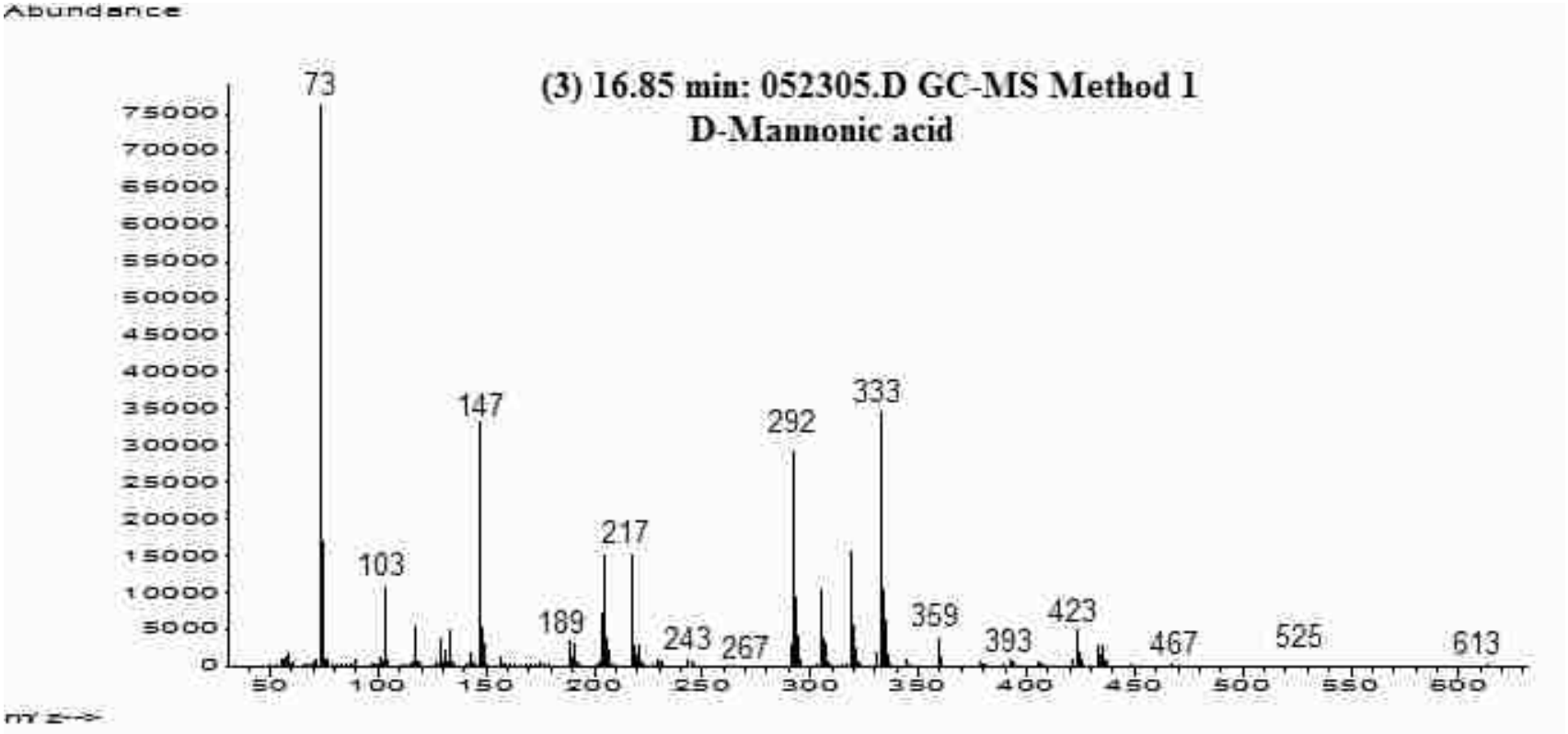

5.1.4 MS of peak (3) at 16.85 min, D-mannonic acid

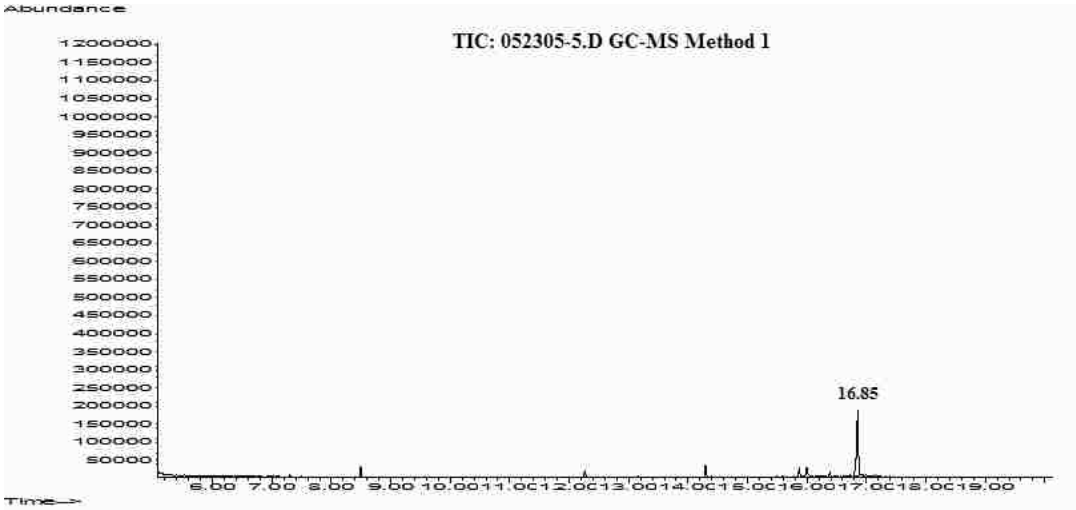

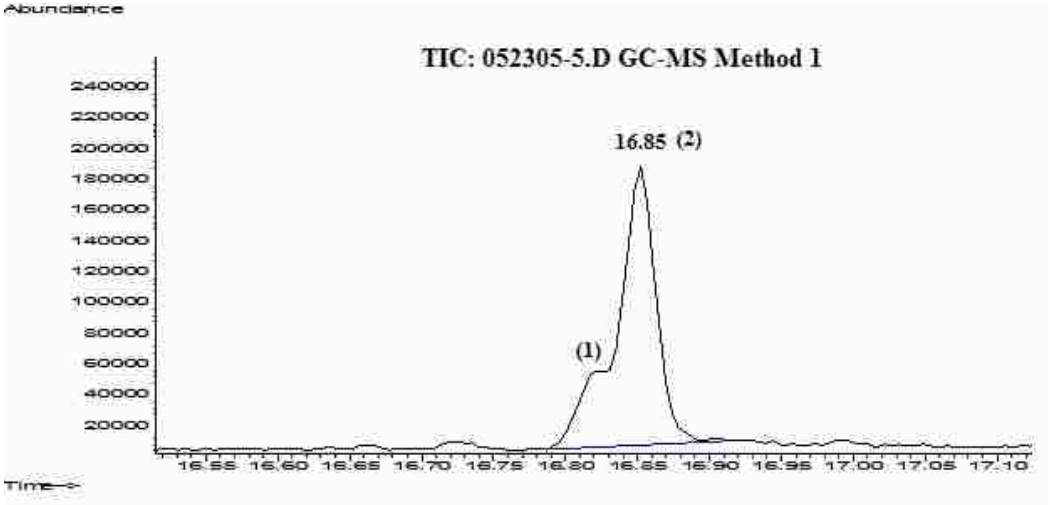

5.1.5 TIC of the final reaction mixture

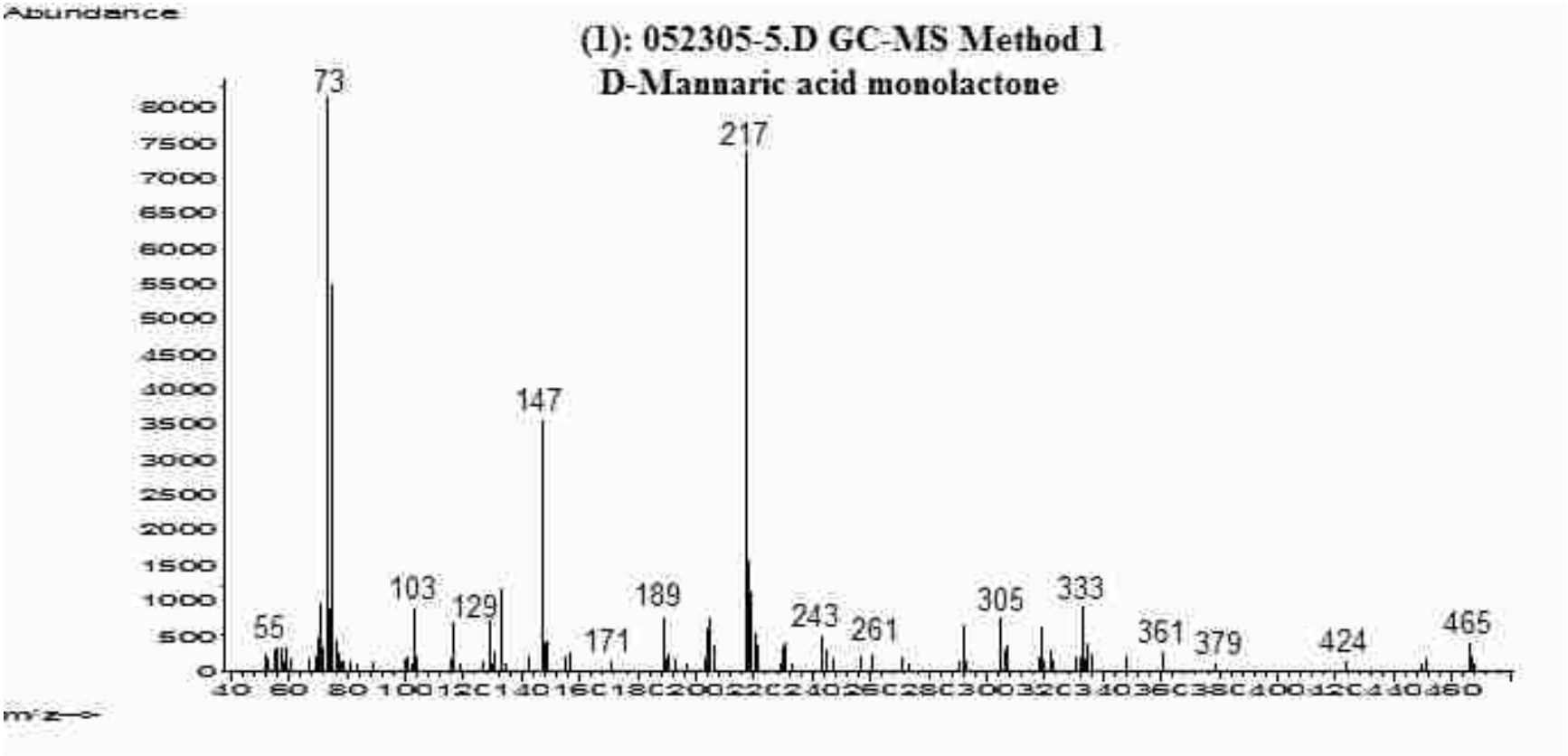

5.1.6 MS of peak (1), D-mannaric acid monolactone

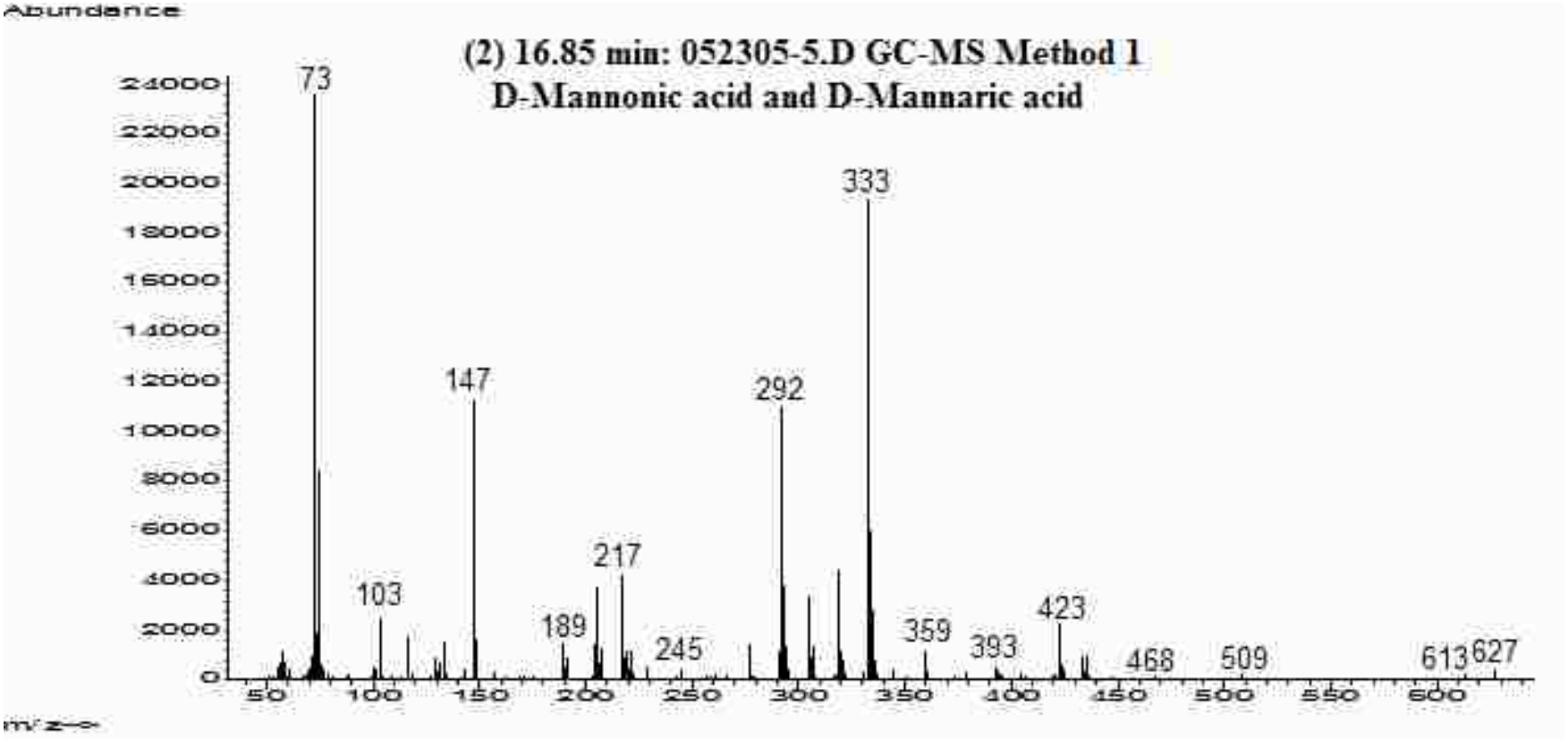

5.1.7 MS of peak (2) at 16.85 min, D-mannonic acid and D-mannaric acid

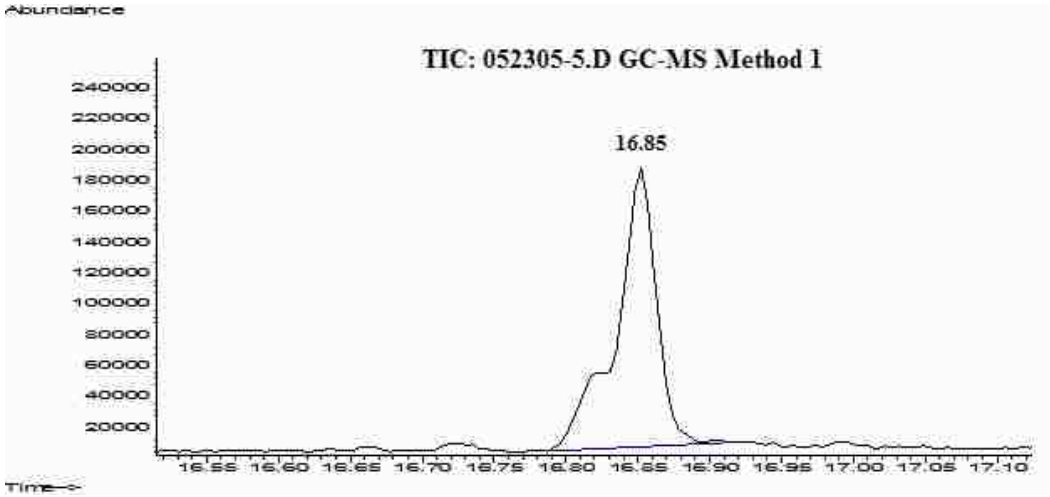

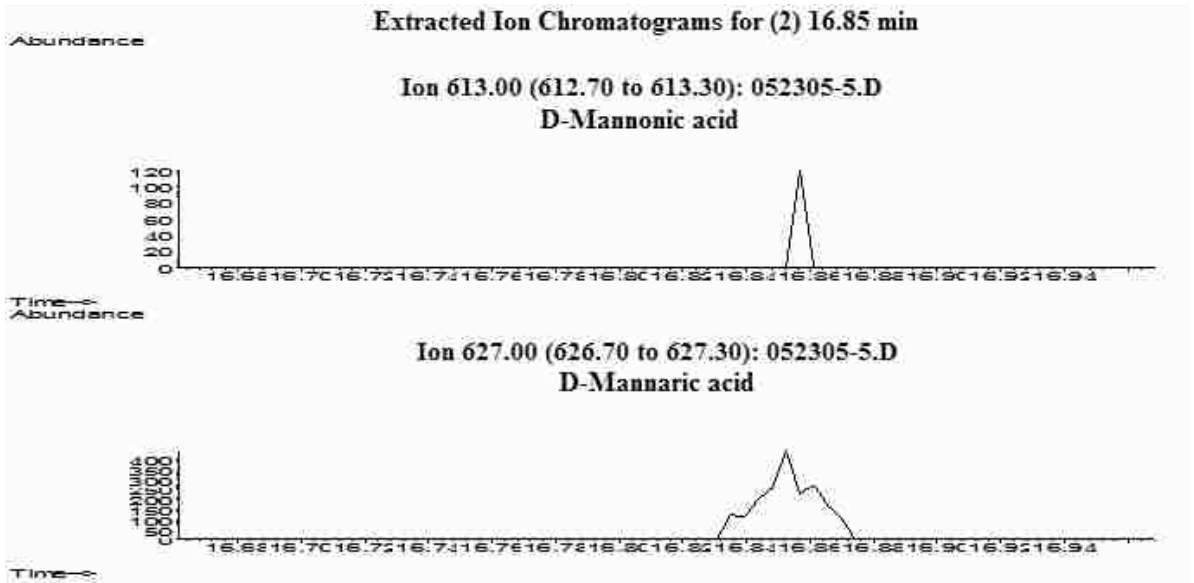

5.1.8 Extracted ion chromatogram of peak (2) at 16.85 min

5.2 Oxidation Experimental Method 4 Analyzed by GC-MS Method 1

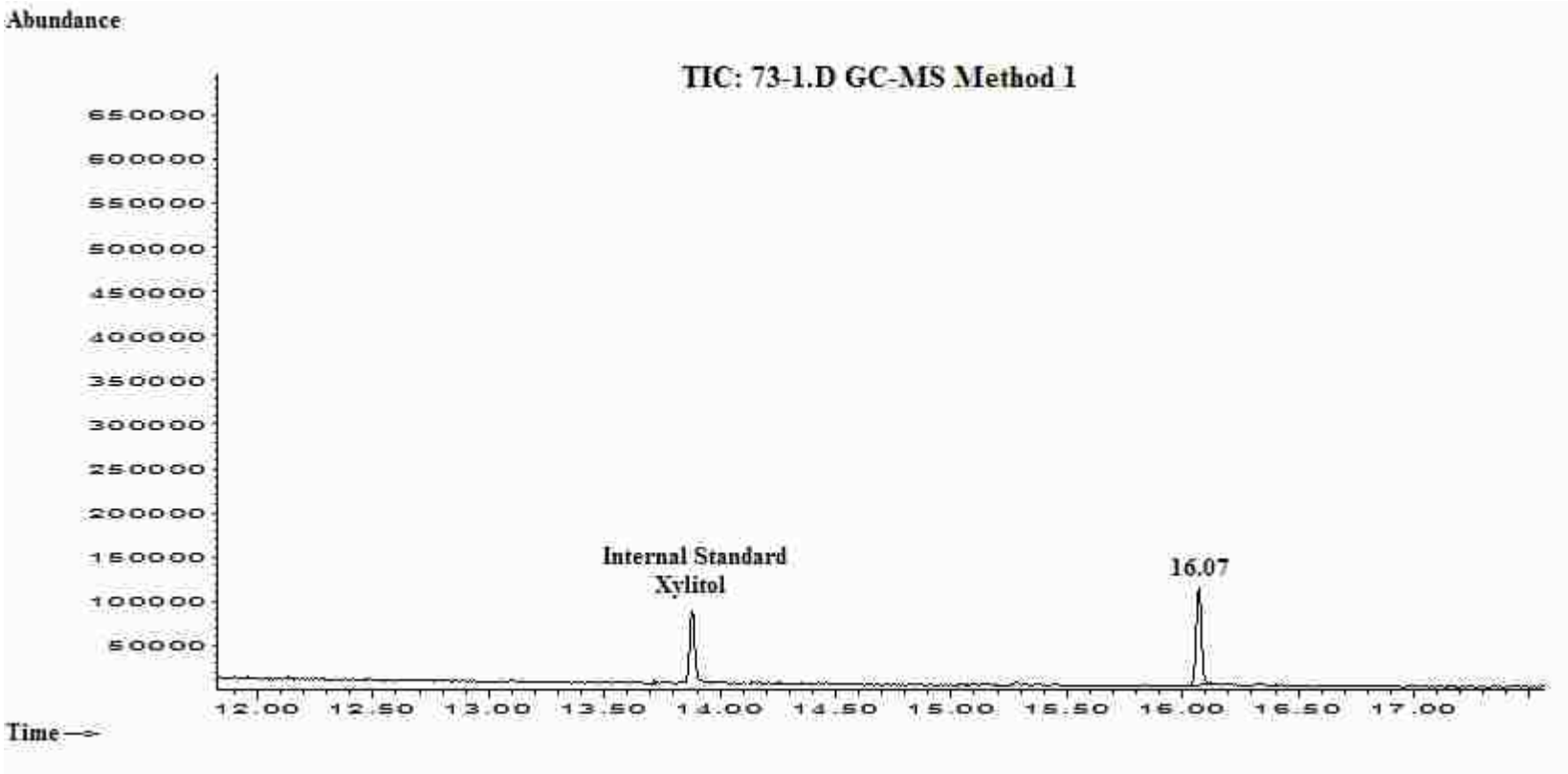

5.2.1 TIC after second addition of D-mannose solution (step 5)

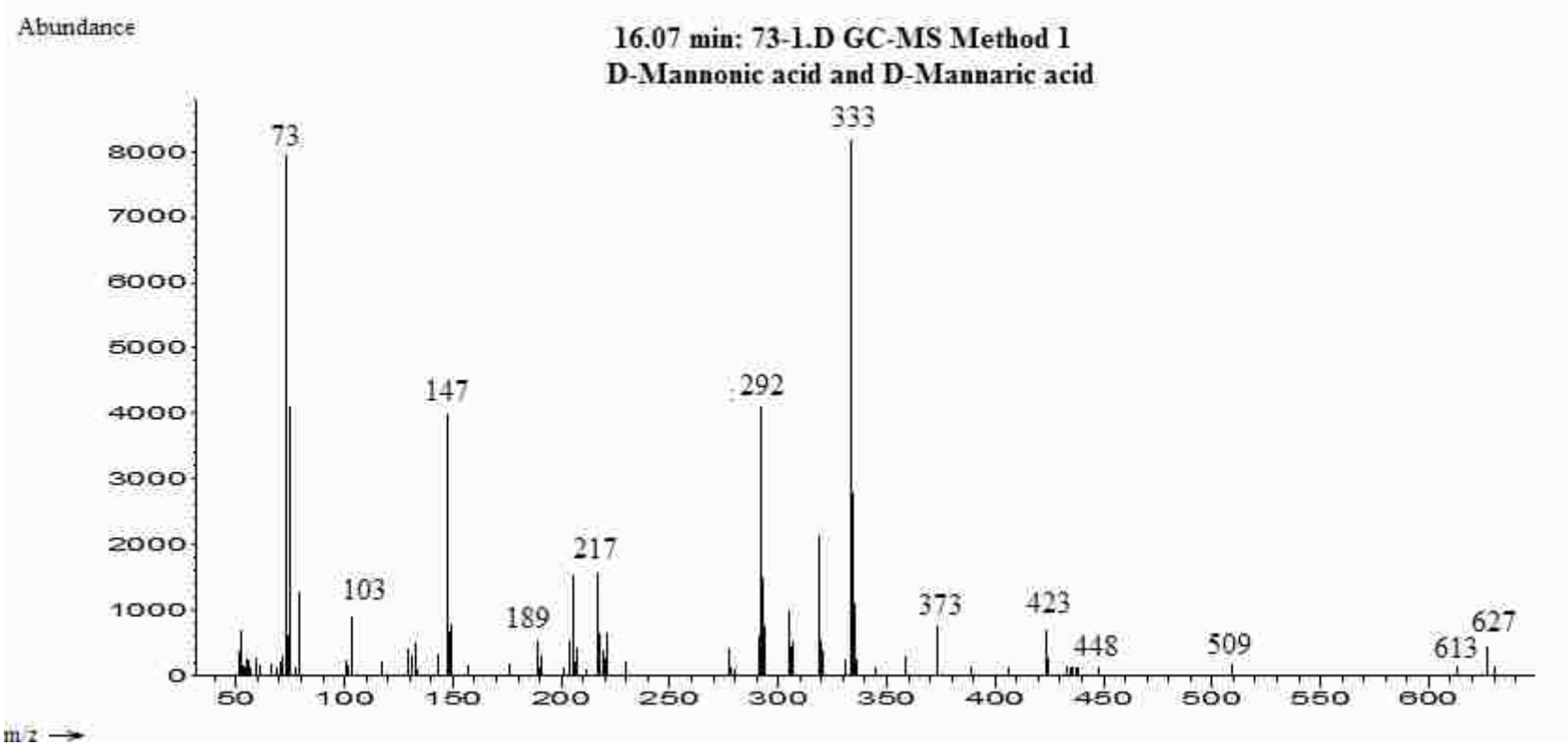

5.2.2 MS of peak at 16.07 min, D-mannonic acid and D-mannaric acid

5.3 Oxidation Experimental Method 4 Analyzed by GC-MS Method 2

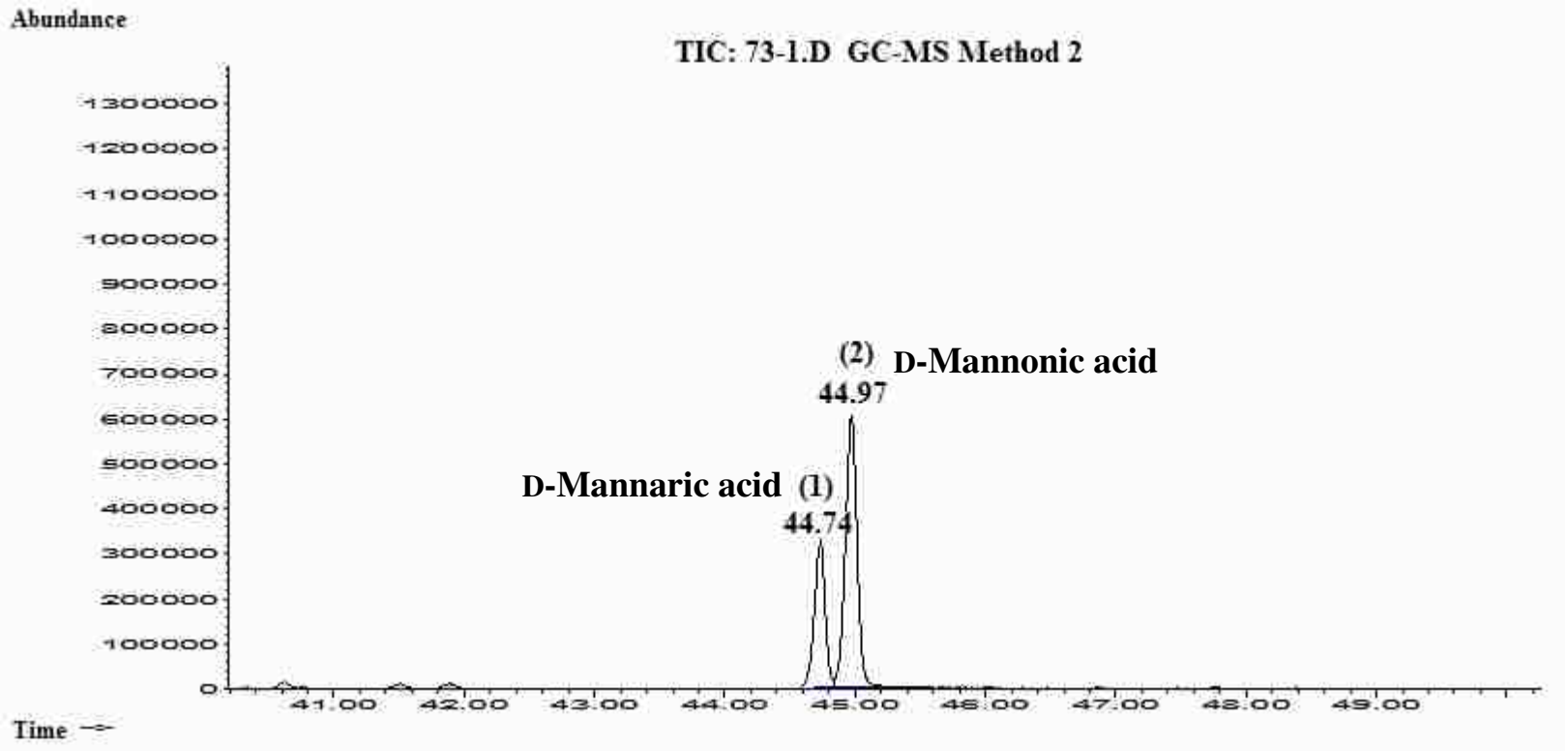

5.3.1 TIC after second addition of D-mannose solution (step 5)

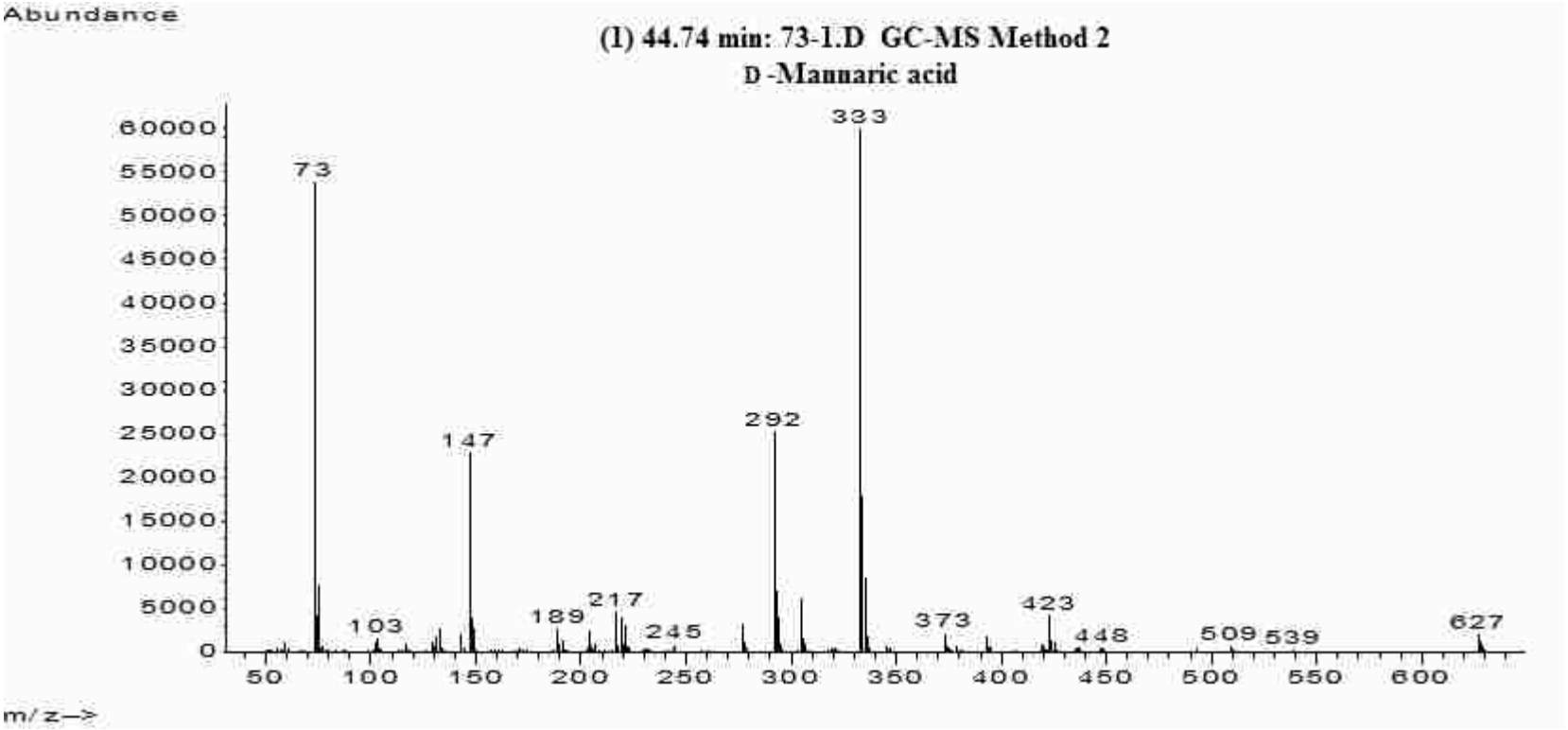

5.3.2 MS of peak (1) at 44.74 min, D-mannaric acid

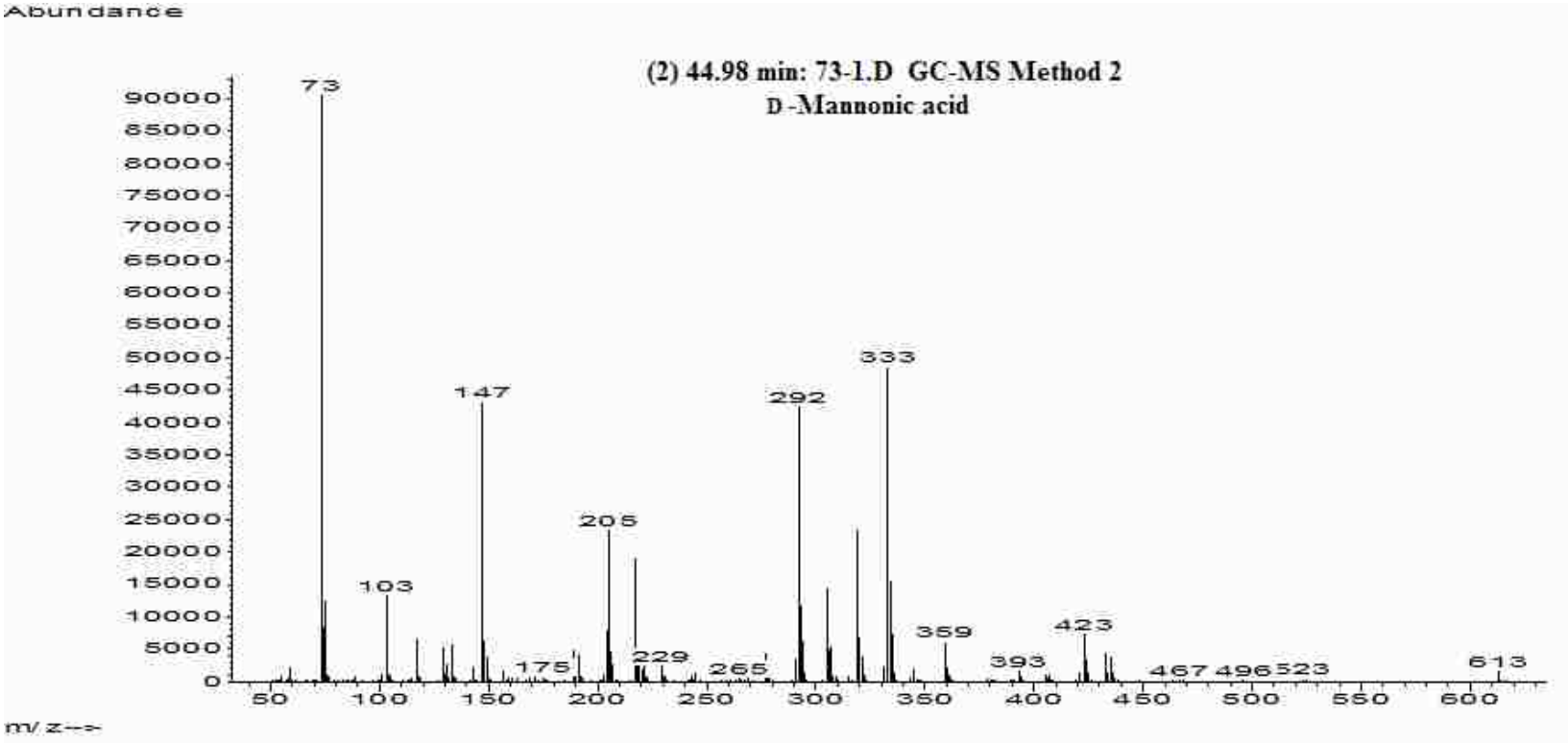

5.3.3 MS of peak (2) at 44.94 min, D-mannonic acid

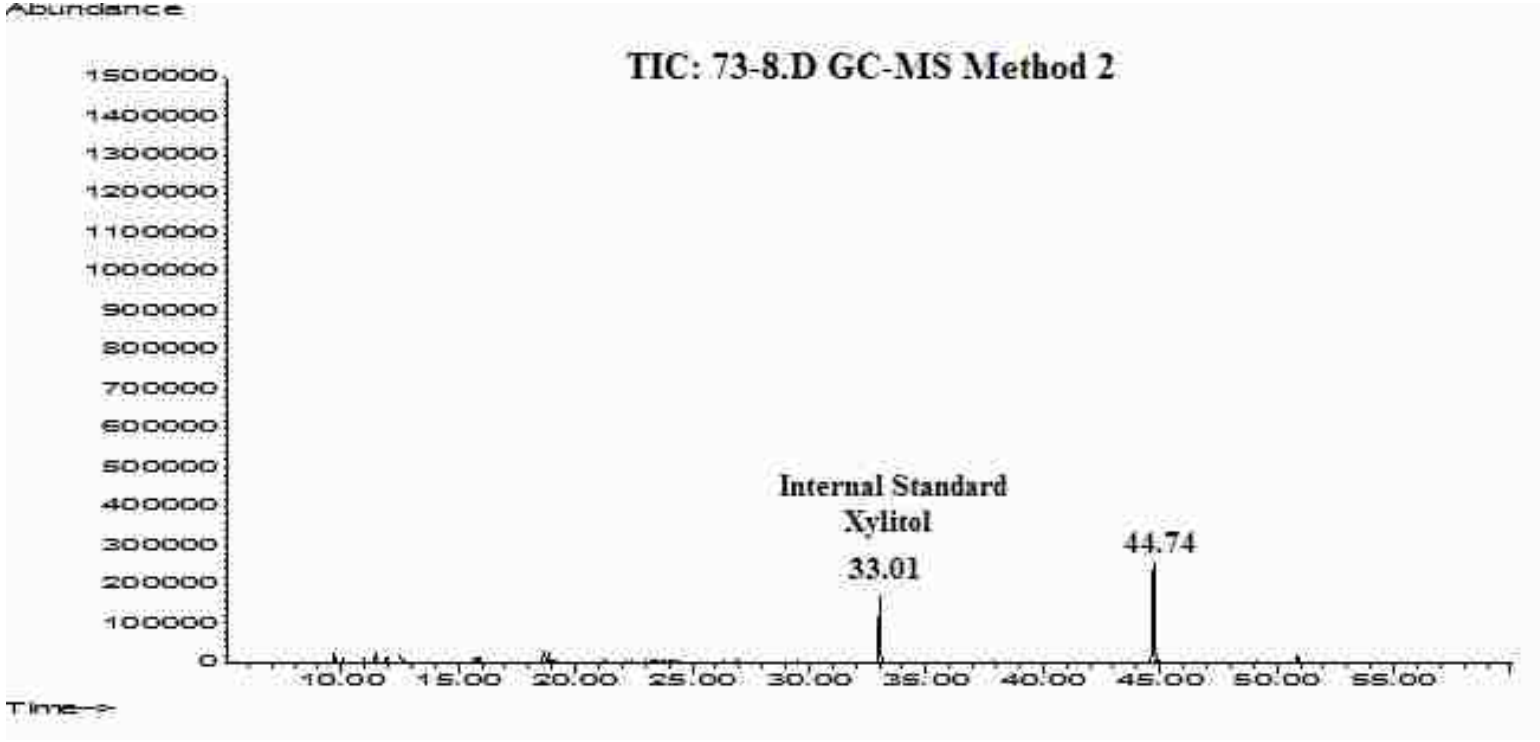

5.3.4 TIC of the final reaction mixture

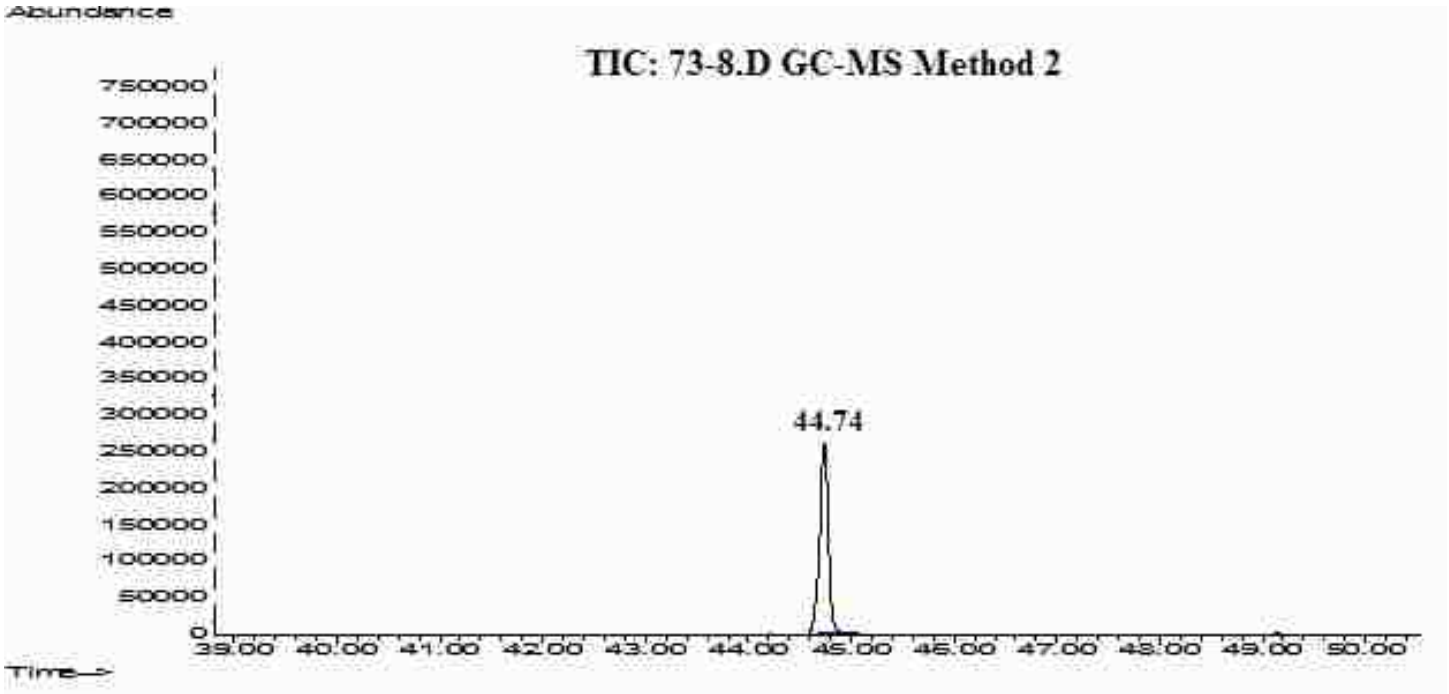

5.3.5 Expanded TIC of the final reaction mixture showing one peak at 44.74 min

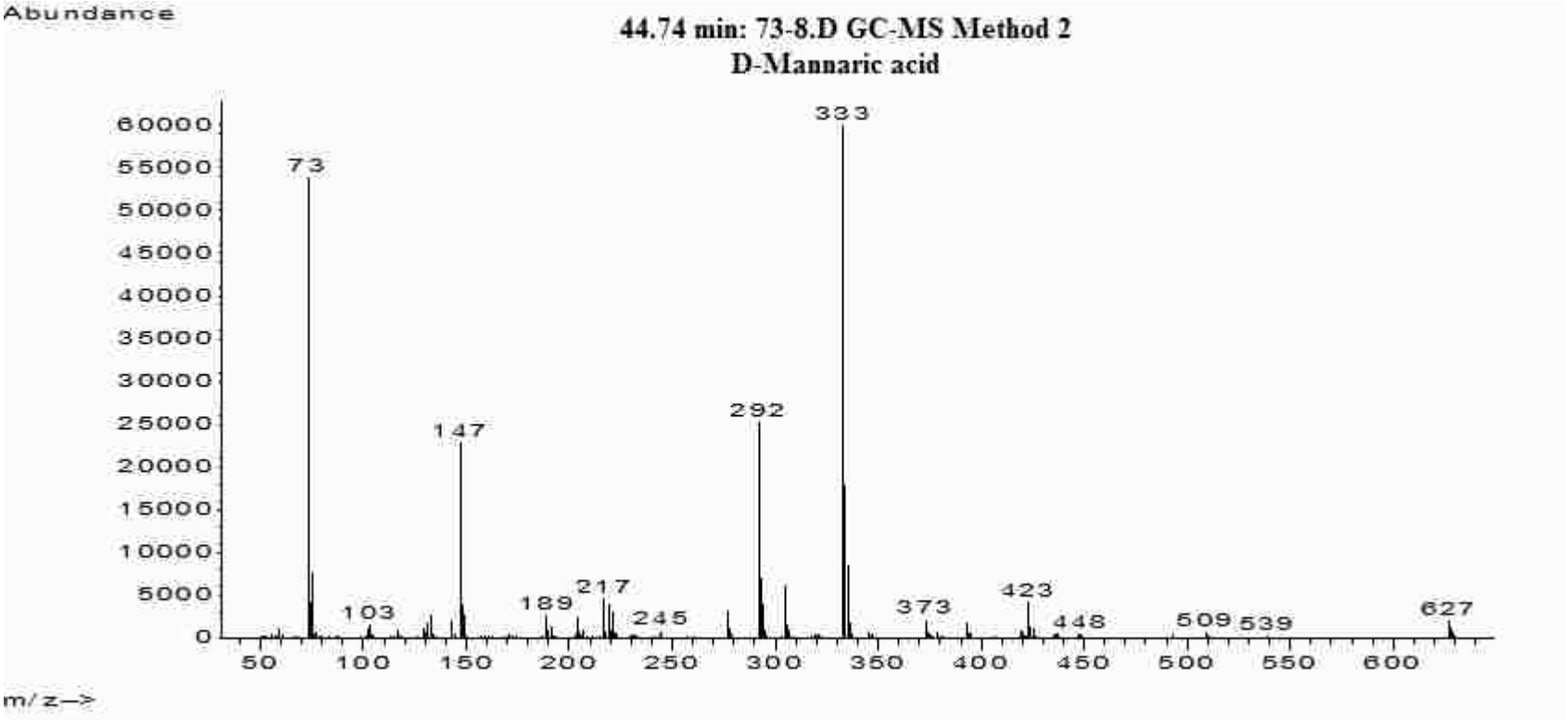

5.3.6 MS of peak at 44.74 min, D-mannaric acid

5.4 *N,N´*-dimethyl-D-mannaramide Analyzed by GC-MS Method 2

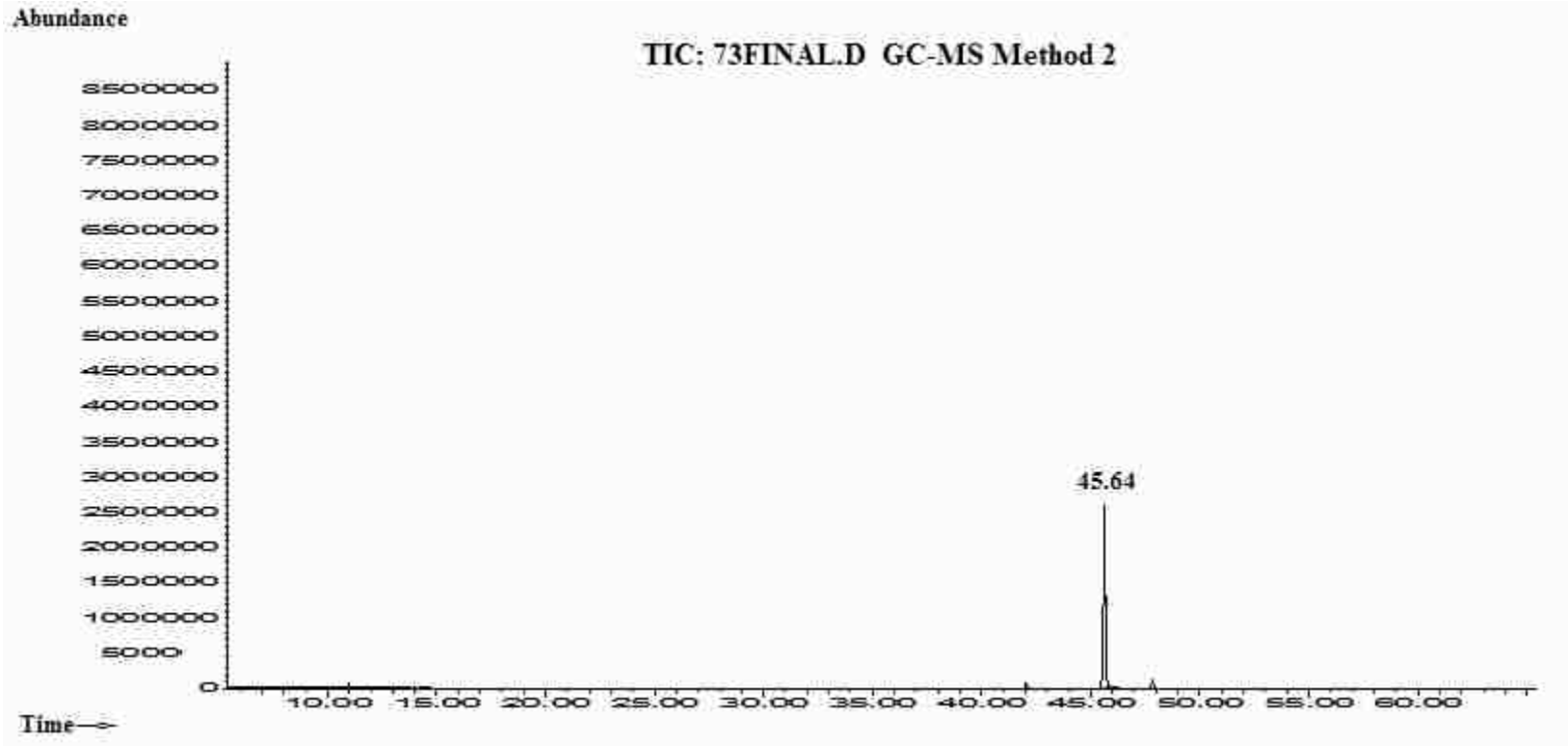

5.4.1 TIC of *N,N´*-dimethyl-D-mannaramide

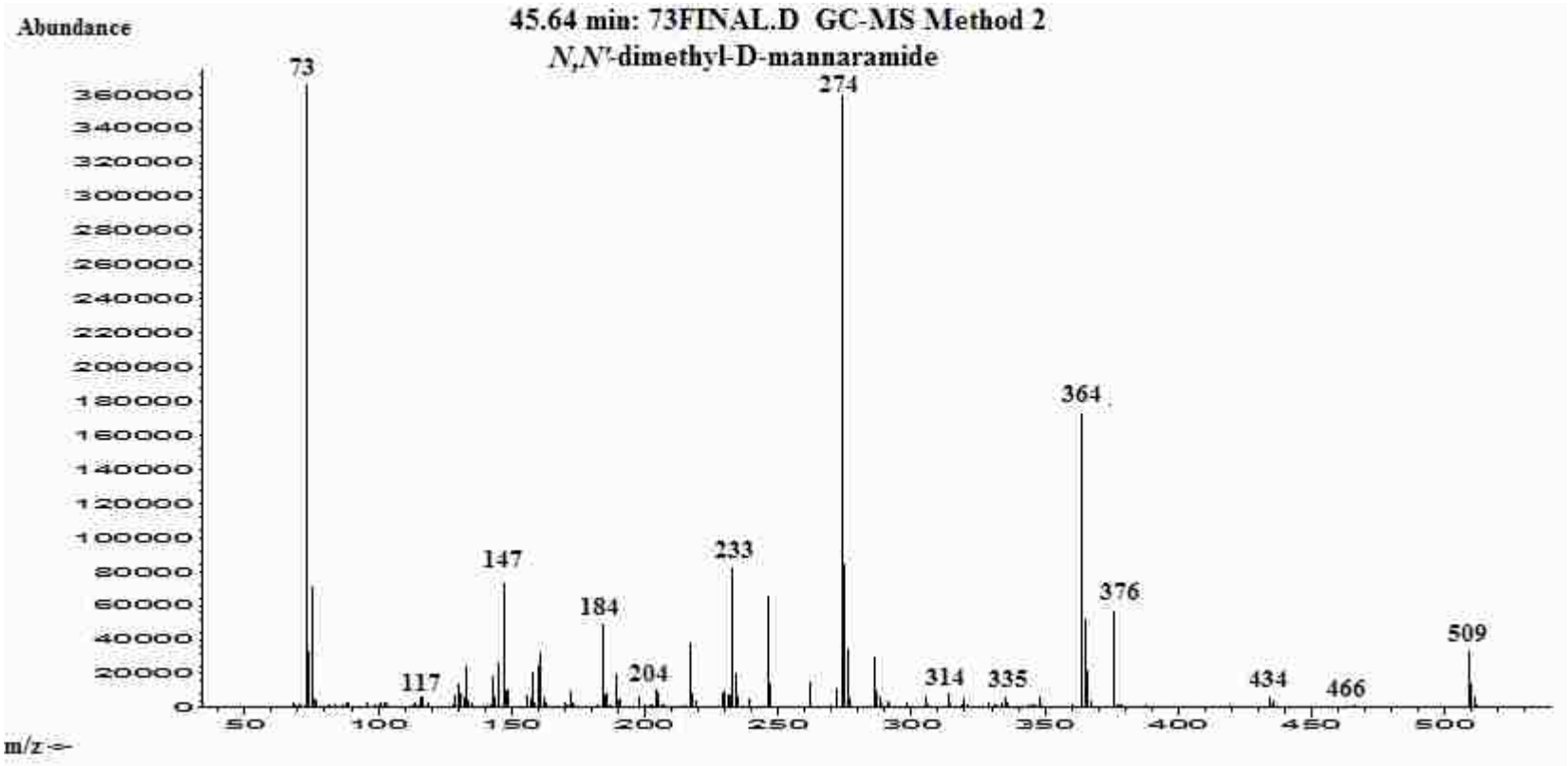

5.4.2 MS of peak at 45.64 min, *N,N´*-dimethyl-D-mannaramide

5.5 Complete X-Ray Crystal Data for *N,N´*-dimethyl-D-mannaramide (**9**)

Table 1. Crystal data and structure refinement for *N,N´*-dimethyl-D-mannaramide (**9**)

Identification code	CAC07_121bnew	
Empirical formula	C8 H16 N2 O6	
Formula weight	236.23	
Temperature	173(2) K	
Wavelength	1.54178 Å	
Crystal system	Monoclinic	
Space group	P2(1)	
Unit cell dimensions	a = 8.1098(3) Å	α= 90°.
	b = 5.6630(2) Å	β= 107.838(1)°.
	c = 11.8507(4) Å	γ = 90°.
Volume	518.09(3) $Å^3$	
Z	2	
Density (calculated)	1.514 Mg/m^3	
Absorption coefficient	1.119 mm^{-1}	
F(000)	252	
Crystal size	0.42 x 0.24 x 0.11 mm^3	
Theta range for data collection	3.92 to 65.97°.	
Index ranges	-9<=h<=9, -6<=k<=6, -13<=l<=13	
Reflections collected	3953	
Independent reflections	1541 [R(int) = 0.0095]	
Completeness to theta = 65.97°	96.3 %	
Absorption correction	Semi-empirical from equivalents	
Max. and min. transmission	0.8868 and 0.6507	

Refinement method	Full-matrix least-squares on F^2
Data / restraints / parameters	1541 / 1 / 152
Goodness-of-fit on F^2	1.093
Final R indices [I>2sigma(I)]	R1 = 0.0252, wR2 = 0.0676
R indices (all data)	R1 = 0.0253, wR2 = 0.0678
Absolute structure parameter	0.38(19)
Largest diff. peak and hole	0.143 and -0.200 e.$Å^{-3}$

Table 2. Atomic coordinates (x 10^4) and equivalent isotropic displacement parameters ($Å^2$x 10^3) for *N,N´*-dimethyl-D-mannaramide. U(eq) is defined as one third of the trace of the orthogonalized U^{ij} tensor.

	x	y	z	U(eq)
C(1)	4747(2)	2595(3)	2753(1)	15(1)
C(2)	3206(2)	3493(3)	1747(1)	16(1)
C(3)	3309(2)	2590(3)	547(1)	16(1)
C(4)	1819(2)	3612(3)	-454(1)	16(1)
C(5)	1818(2)	2655(3)	-1671(1)	16(1)
C(6)	359(2)	3867(3)	-2635(1)	16(1)
C(7)	-422(2)	7135(3)	-4041(2)	26(1)
C(8)	5768(2)	-297(4)	4347(2)	26(1)
N(1)	4442(2)	792(2)	3374(1)	18(1)
N(2)	806(2)	5753(2)	-3133(1)	21(1)
O(1)	6180(1)	3565(2)	2952(1)	21(1)
O(2)	3300(1)	5980(2)	1767(1)	20(1)
O(3)	3100(1)	96(2)	471(1)	22(1)
O(4)	229(1)	2932(2)	-277(1)	21(1)
O(5)	3458(1)	3111(2)	-1829(1)	19(1)
O(6)	-1158(1)	3130(2)	-2897(1)	23(1)

Table 3. Bond lengths [Å] and angles [°] for *N,N´*-dimethyl-D-mannaramide

C(1)-O(1)	1.2410(19)	O(5)-H(5A)	0.8400	O(6)-C(6)-C(5)	120.96(14)
C(1)-N(1)	1.326(2)			N(2)-C(6)-C(5)	116.10(13)
C(1)-C(2)	1.5267(19)	O(1)-C(1)-N(1)	124.00(13)	N(2)-C(7)-H(7A)	109.5
C(2)-O(2)	1.410(2)	O(1)-C(1)-C(2)	119.72(13)	N(2)-C(7)-H(7B)	109.5
C(2)-C(3)	1.538(2)	N(1)-C(1)-C(2)	116.28(13)	H(7A)-C(7)-H(7B)	109.5
C(2)-H(2)	1.0000	O(2)-C(2)-C(1)	106.98(12)	N(2)-C(7)-H(7C)	109.5
C(3)-O(3)	1.422(2)	O(2)-C(2)-C(3)	109.27(12)	H(7A)-C(7)-H(7C)	109.5
C(3)-C(4)	1.524(2)	C(1)-C(2)-C(3)	110.38(12)	H(7B)-C(7)-H(7C)	109.5
C(3)-H(3)	1.0000	O(2)-C(2)-H(2)	110.1	N(1)-C(8)-H(8A)	109.5
C(4)-O(4)	1.4213(17)	C(1)-C(2)-H(2)	110.1	N(1)-C(8)-H(8B)	109.5
C(4)-C(5)	1.541(2)	C(3)-C(2)-H(2)	110.1	H(8A)-C(8)-H(8B)	109.5
C(4)-H(4)	1.0000	O(3)-C(3)-C(4)	106.11(12)	N(1)-C(8)-H(8C)	109.5
C(5)-O(5)	1.4220(18)	O(3)-C(3)-C(2)	110.48(13)		
C(5)-C(6)	1.532(2)	C(4)-C(3)-C(2)	109.78(11)	H(8A)-C(8)-H(8C)	109.5
C(5)-H(5)	1.0000	O(3)-C(3)-H(3)	110.1	H(8B)-C(8)-H(8C)	109.5
C(6)-O(6)	1.2453(19)	C(4)-C(3)-H(3)	110.1	C(1)-N(1)-C(8)	123.33(13)
C(6)-N(2)	1.324(2)	C(2)-C(3)-H(3)	110.1	C(1)-N(1)-H(1)	118.3
C(7)-N(2)	1.451(2)	O(4)-C(4)-C(3)	108.71(12)	C(8)-N(1)-H(1)	118.3
C(7)-H(7A)	0.9800	O(4)-C(4)-C(5)	107.61(11)	C(6)-N(2)-C(7)	123.14(13)
C(7)-H(7B)	0.9800	C(3)-C(4)-C(5)	111.56(12)	C(6)-N(2)-H(2A)	118.4
C(7)-H(7C)	0.9800	O(4)-C(4)-H(4)	109.6	C(7)-N(2)-H(2A)	118.4
C(8)-N(1)	1.451(2)	C(3)-C(4)-H(4)	109.6	C(2)-O(2)-H(2B)	109.5
C(8)-H(8A)	0.9800	C(5)-C(4)-H(4)	109.6	C(3)-O(3)-H(3A)	109.5
C(8)-H(8B)	0.9800	O(5)-C(5)-C(6)	111.12(12)	C(4)-O(4)-H(4A)	109.5
C(8)-H(8C)	0.9800	O(5)-C(5)-C(4)	109.06(11)	C(5)-O(5)-H(5A)	109.5
N(1)-H(1)	0.8800	C(6)-C(5)-C(4)	108.59(12)		
N(2)-H(2A)	0.8800	O(5)-C(5)-H(5)	109.3		

O(2)-H(2B)	0.8400	C(6)-C(5)-H(5)	109.3		
O(3)-H(3A)	0.8400	C(4)-C(5)-H(5)	109.3		
O(4)-H(4A)	0.8400	O(6)-C(6)-N(2)	122.91(14)		

Symmetry transformations used to generate equivalent atoms:

Table 4. Anisotropic displacement parameters ($Å^2$x 10^3) for *N,N´*-dimethyl-D-mannaramide. The anisotropic displacement factor exponent takes the form: $-2\pi^2[h^2a^{*2}U^{11} + ... + 2 h k a^* b^* U^{12}]$

	U^{11}	U^{22}	U^{33}	U^{23}	U^{13}	U^{12}
C(1)	15(1)	17(1)	15(1)	-2(1)	6(1)	2(1)
C(2)	14(1)	15(1)	18(1)	2(1)	6(1)	0(1)
C(3)	15(1)	14(1)	18(1)	1(1)	5(1)	2(1)
C(4)	14(1)	15(1)	19(1)	2(1)	5(1)	-1(1)
C(5)	12(1)	17(1)	19(1)	2(1)	4(1)	1(1)
C(6)	16(1)	18(1)	16(1)	-2(1)	6(1)	0(1)
C(7)	22(1)	27(1)	27(1)	10(1)	4(1)	4(1)
C(8)	25(1)	30(1)	20(1)	9(1)	4(1)	7(1)
N(1)	16(1)	19(1)	17(1)	3(1)	3(1)	0(1)
N(2)	13(1)	24(1)	24(1)	7(1)	2(1)	0(1)
O(1)	14(1)	23(1)	24(1)	3(1)	4(1)	-1(1)
O(2)	18(1)	15(1)	26(1)	0(1)	7(1)	3(1)
O(3)	27(1)	13(1)	23(1)	2(1)	1(1)	5(1)
O(4)	12(1)	27(1)	24(1)	0(1)	7(1)	2(1)
O(5)	13(1)	24(1)	20(1)	0(1)	7(1)	2(1)
O(6)	14(1)	28(1)	24(1)	5(1)	1(1)	-2(1)

Table 5. Hydrogen coordinates (x 10^4) and isotropic displacement parameters ($Å^2$x 10^3) for *N,N´*-dimethyl-D-mannaramide.

	x	y	z	U(eq)
H(2)	2098	2965	1871	19
H(3)	4443	3045	440	19
H(4)	1907	5374	-449	19
H(5)	1607	912	-1701	20
H(7A)	-1401	6134	-4466	39
H(7B)	148	7751	-4599	39
H(7C)	-844	8454	-3670	39
H(8A)	6200	-1723	4063	38
H(8B)	5274	-719	4978	38
H(8C)	6725	816	4657	38
H(1)	3382	226	3187	21
H(2A)	1900	6190	-2903	25
H(2B)	2422	6537	1907	30
H(3A)	4009	-556	895	34
H(4A)	-360	4142	-256	31
H(5A)	3787	1912	-2117	28

Table 6. Torsion angles [°] for *N,N´*-dimethyl-D-mannaramide.

O(1)-C(1)-C(2)-O(2)	-40.35(17)
N(1)-C(1)-C(2)-O(2)	139.18(13)
O(1)-C(1)-C(2)-C(3)	78.44(17)
N(1)-C(1)-C(2)-C(3)	-102.03(14)
O(2)-C(2)-C(3)-O(3)	-176.12(12)
C(1)-C(2)-C(3)-O(3)	66.50(16)
O(2)-C(2)-C(3)-C(4)	-59.44(15)
C(1)-C(2)-C(3)-C(4)	-176.82(12)
O(3)-C(3)-C(4)-O(4)	60.76(15)
C(2)-C(3)-C(4)-O(4)	-58.64(15)
O(3)-C(3)-C(4)-C(5)	-57.75(15)
C(2)-C(3)-C(4)-C(5)	-177.15(11)
O(4)-C(4)-C(5)-O(5)	-174.57(12)
C(3)-C(4)-C(5)-O(5)	-55.40(15)
O(4)-C(4)-C(5)-C(6)	64.21(15)
C(3)-C(4)-C(5)-C(6)	-176.63(12)
O(5)-C(5)-C(6)-O(6)	156.78(14)
C(4)-C(5)-C(6)-O(6)	-83.27(17)
O(5)-C(5)-C(6)-N(2)	-25.11(18)
C(4)-C(5)-C(6)-N(2)	94.84(15)
O(1)-C(1)-N(1)-C(8)	-1.5(2)
C(2)-C(1)-N(1)-C(8)	179.03(14)
O(6)-C(6)-N(2)-C(7)	-0.6(2)
C(5)-C(6)-N(2)-C(7)	-178.64(15)

Symmetry transformations used to generate equivalent atoms:

Table 7. Hydrogen bonds for *N,N´*-dimethyl-D-mannaramide [Å and °].

D-H...A	d(D-H)	d(H...A)	d(D...A)	<(DHA)
N(1)-H(1)...O(6)#1	0.88	2.10	2.9600(17)	166.4
N(2)-H(2A)...O(1)#2	0.88	2.07	2.8697(16)	150.3
O(2)-H(2B)...O(6)#3	0.84	1.99	2.7781(15)	154.8
O(2)-H(2B)...O(4)#3	0.84	2.54	3.0716(15)	122.6
O(3)-H(3A)...O(5)#4	0.84	2.15	2.9822(15)	171.0
O(4)-H(4A)...O(3)#3	0.84	2.22	2.9094(15)	138.8
O(4)-H(4A)...O(4)#3	0.84	2.23	2.9556(6)	144.6
O(5)-H(5A)...O(1)#4	0.84	2.14	2.9536(16)	162.5
O(5)-H(5A)...O(2)#4	0.84	2.33	2.8738(14)	122.8

Symmetry transformations used to generate equivalent atoms:

#1 -x,y-1/2,-z #2 -x+1,y+1/2,-z #3 -x,y+1/2,-z

#4 -x+1,y-1/2,-z

5.6 Alkylenediammonium Mannarate ^{1}H NMR Spectra

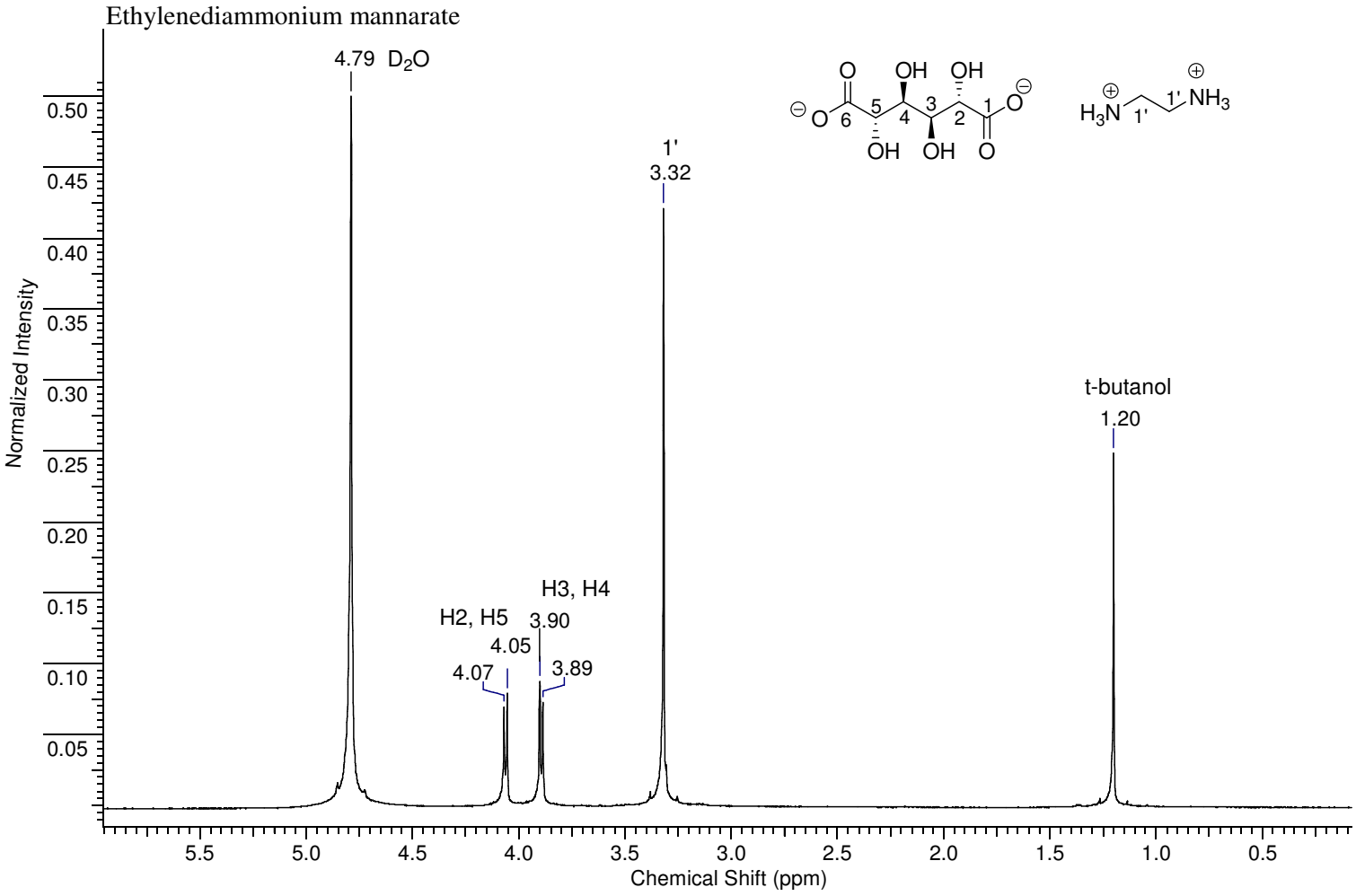

5.6.1 ^{1}H NMR of ethylenediammonium D-mannarate in D_2O

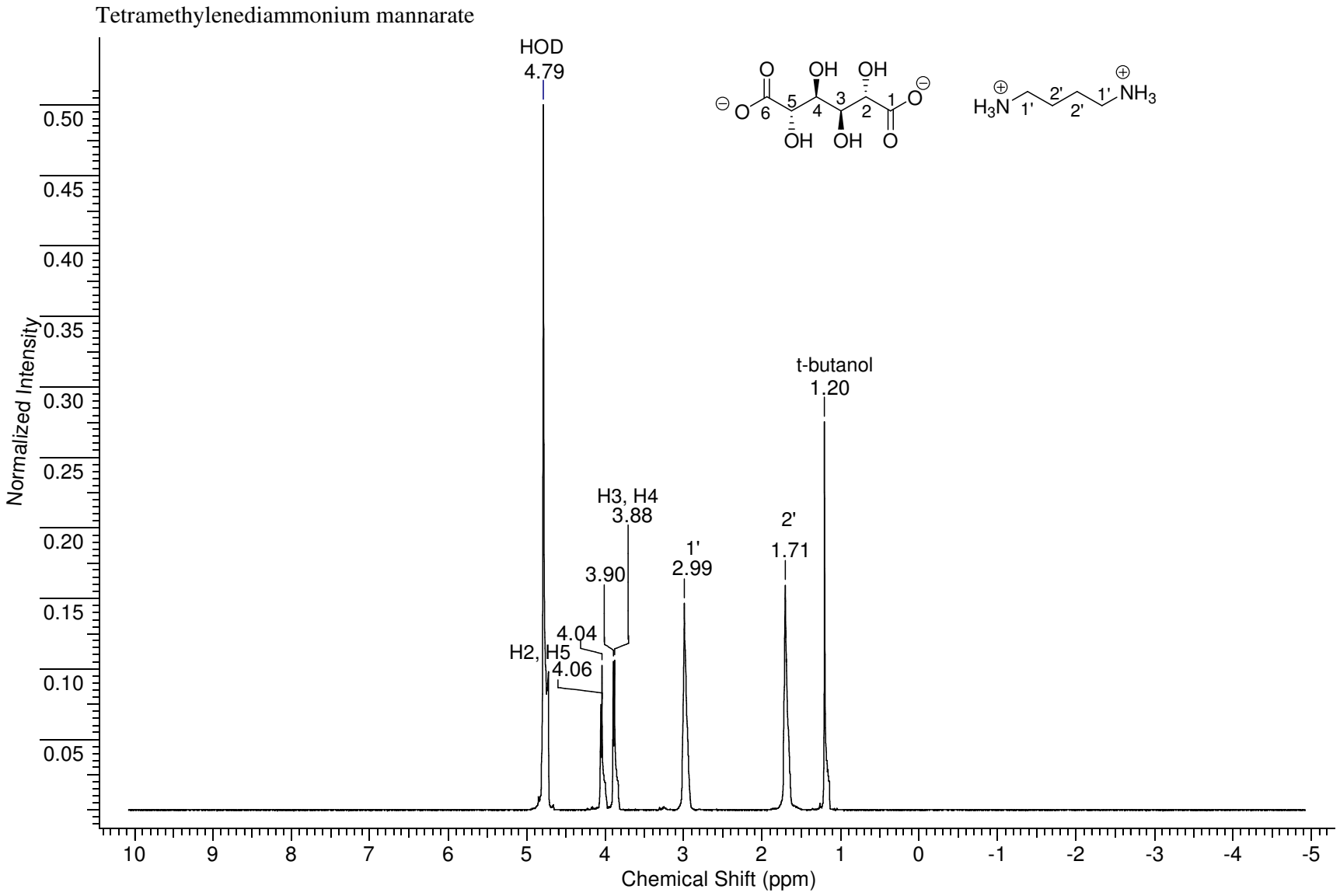

5.6.2 ^{1}H NMR of tetramethylenediammonium D-mannarate in D_2O

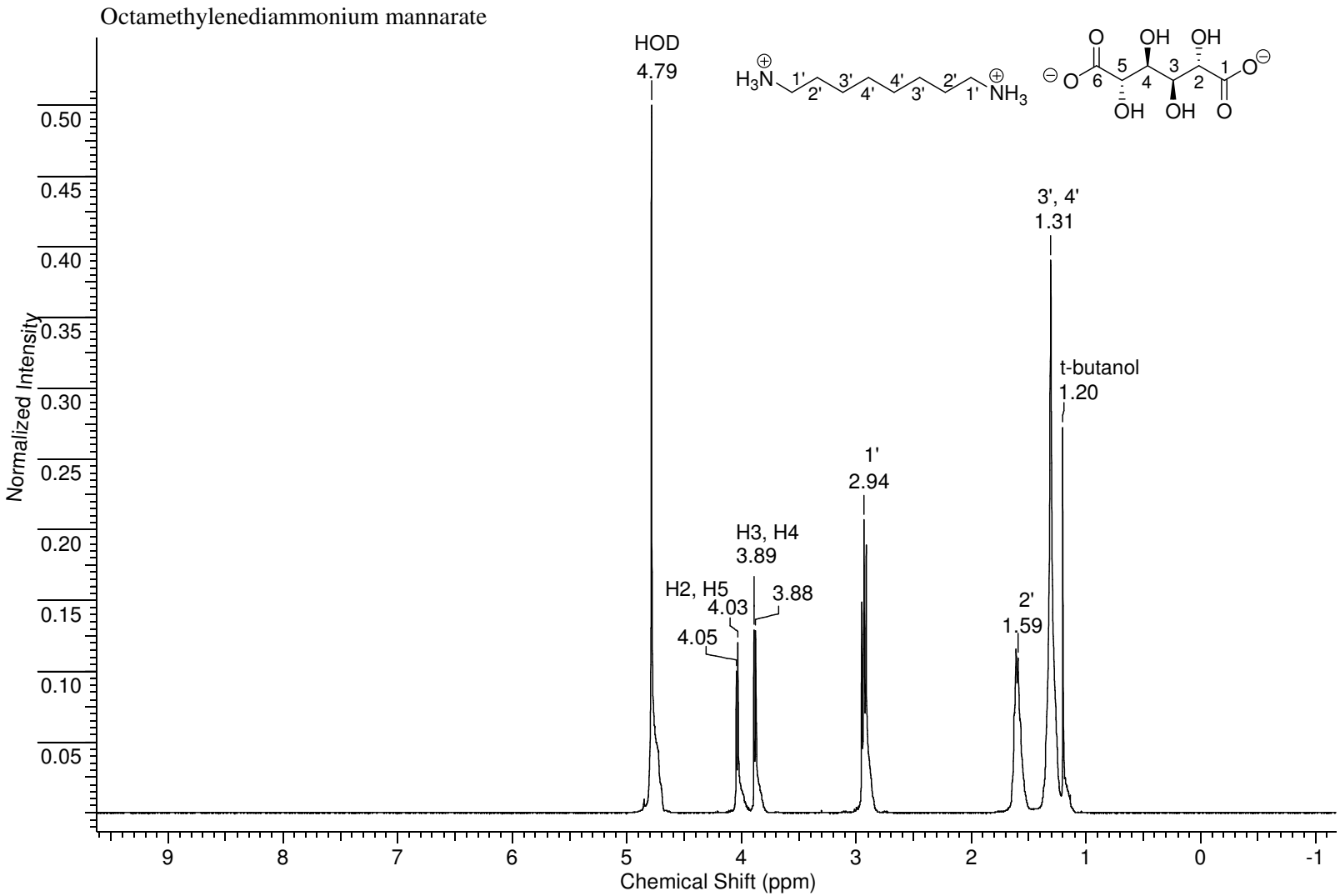

5.6.3 ^{1}H NMR of octamethylenediammonium D-mannarate in D_2O

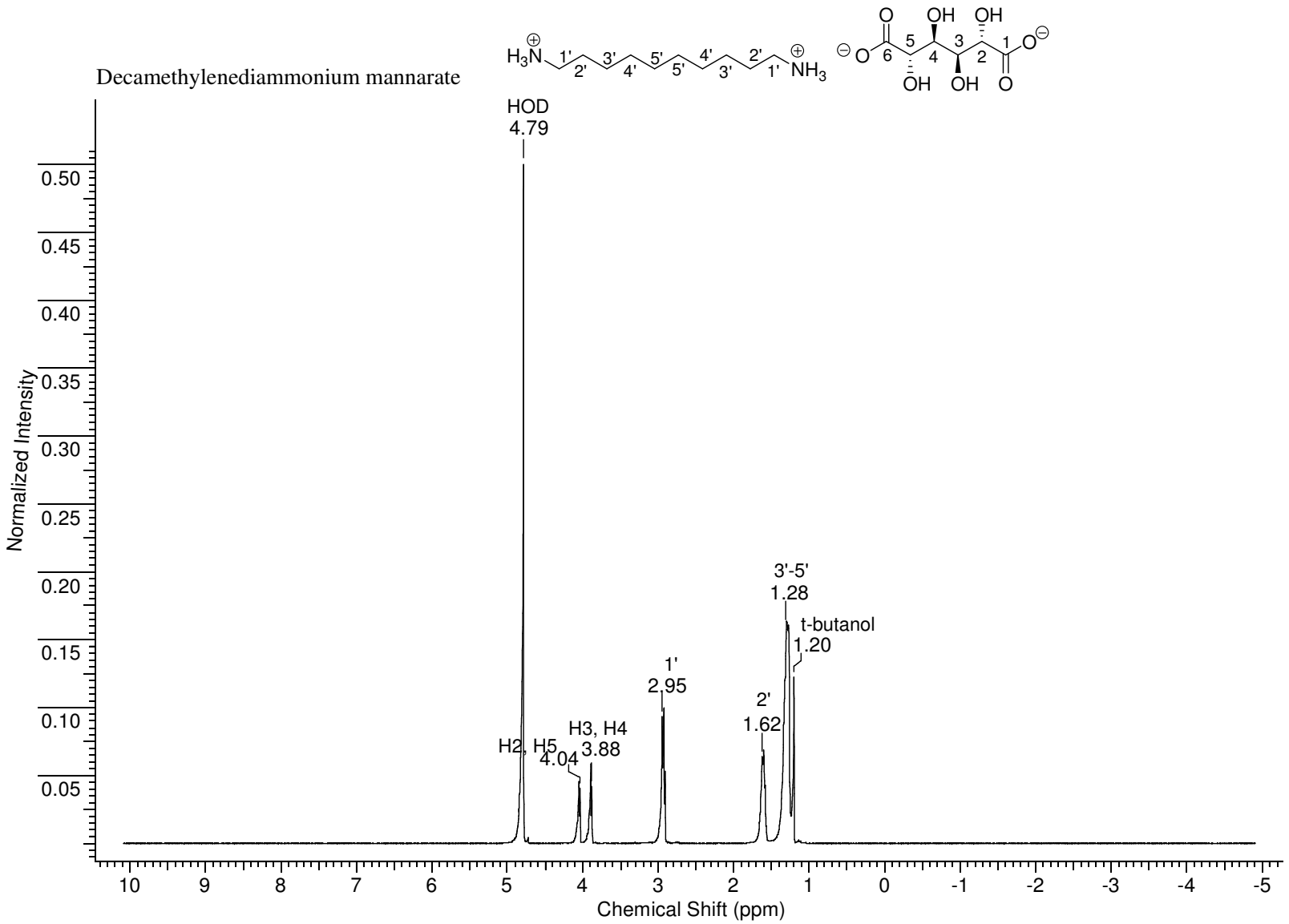

5.6.4 ^{1}H NMR of decamethylenediammonium D-mannarate in D_2O

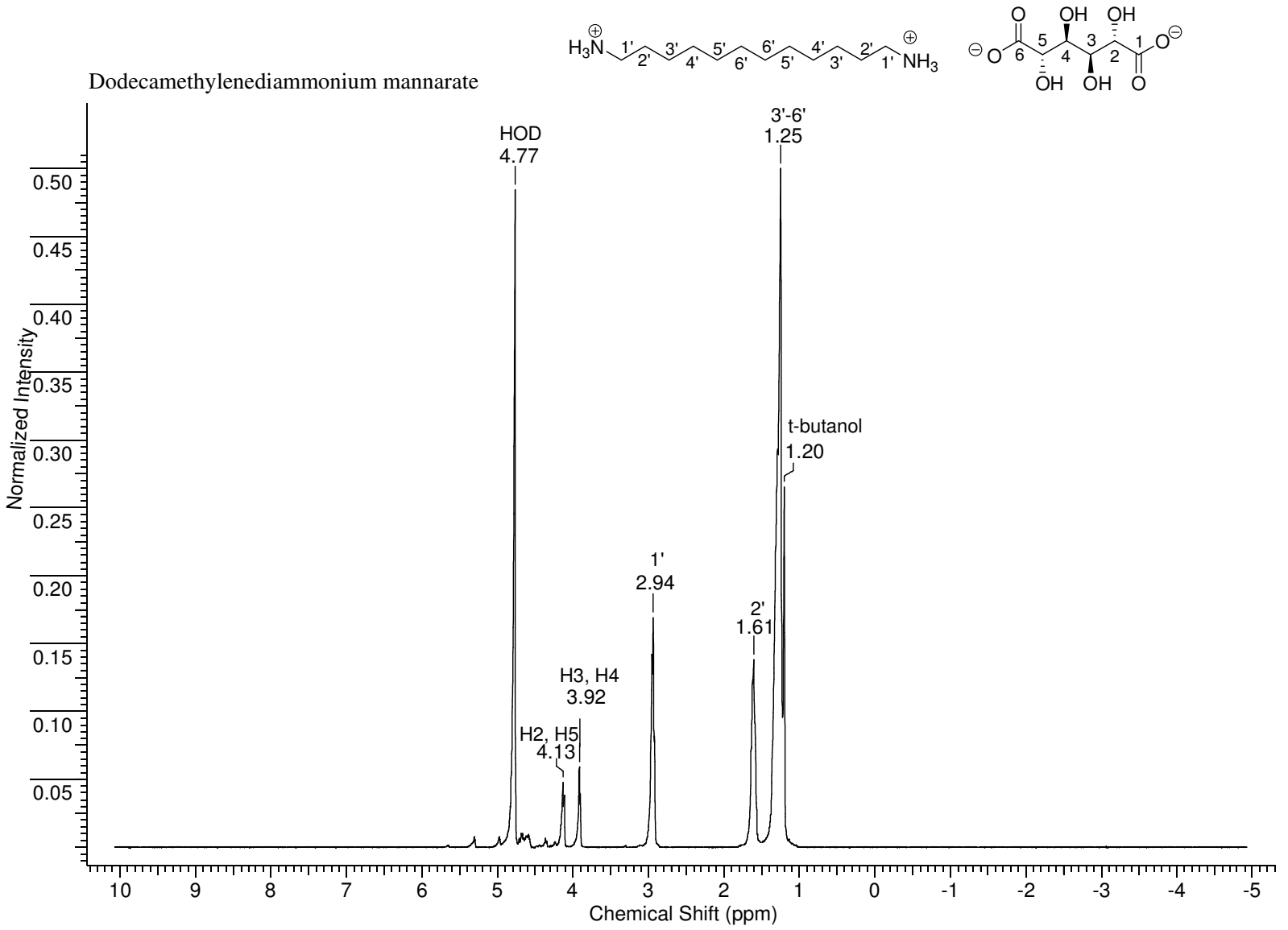

5.6.5 ^{1}H NMR of dodecamethylenediammonium D-mannarate in D_2O

5.7 Alkylene Diammonium Mannarate Ion Chromatographs

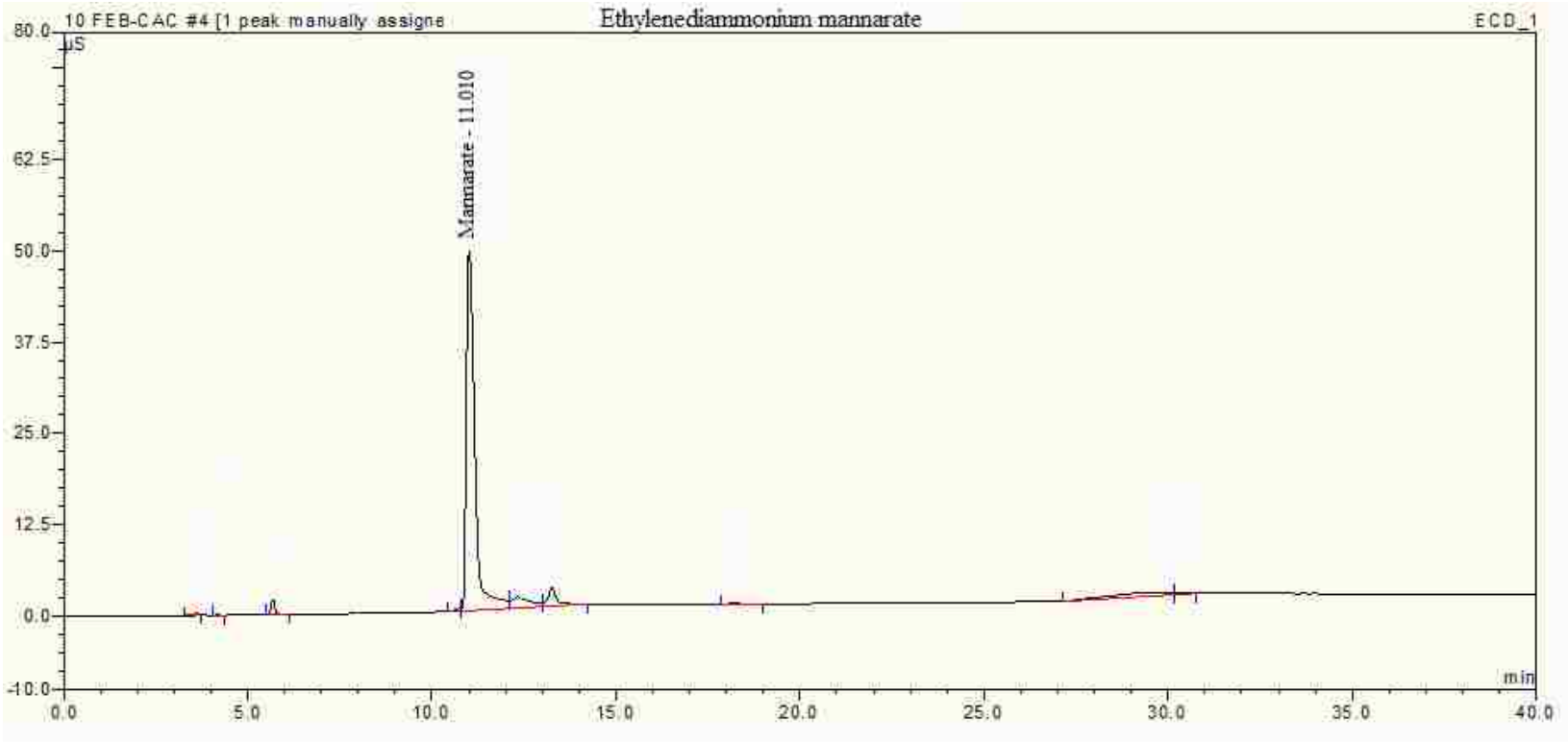

5.7.1 Ion chromatograph of ethylenediammonium D-mannarate

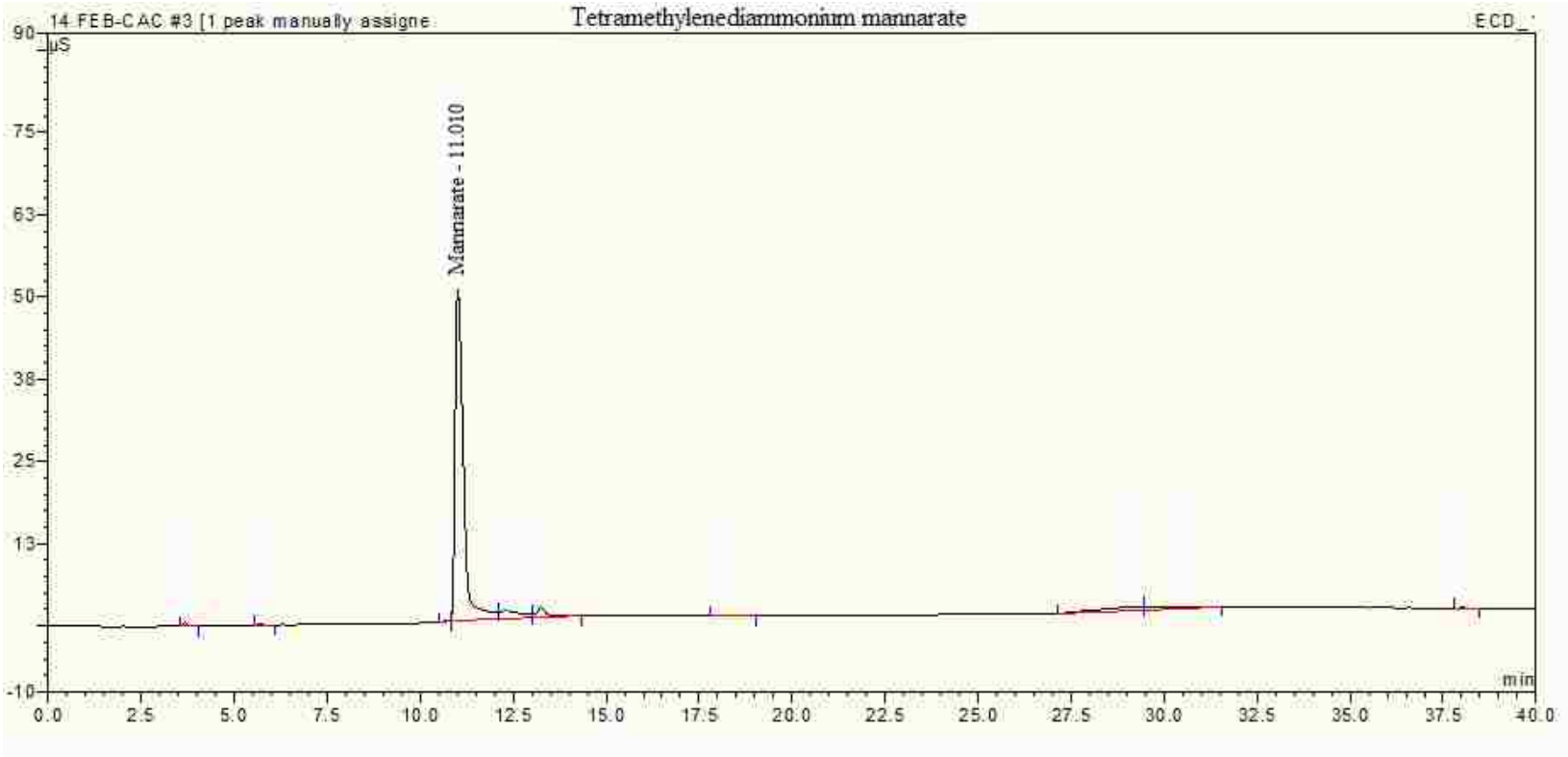

5.7.2 Ion chromatograph of tetramethylenediammonium D-mannarate

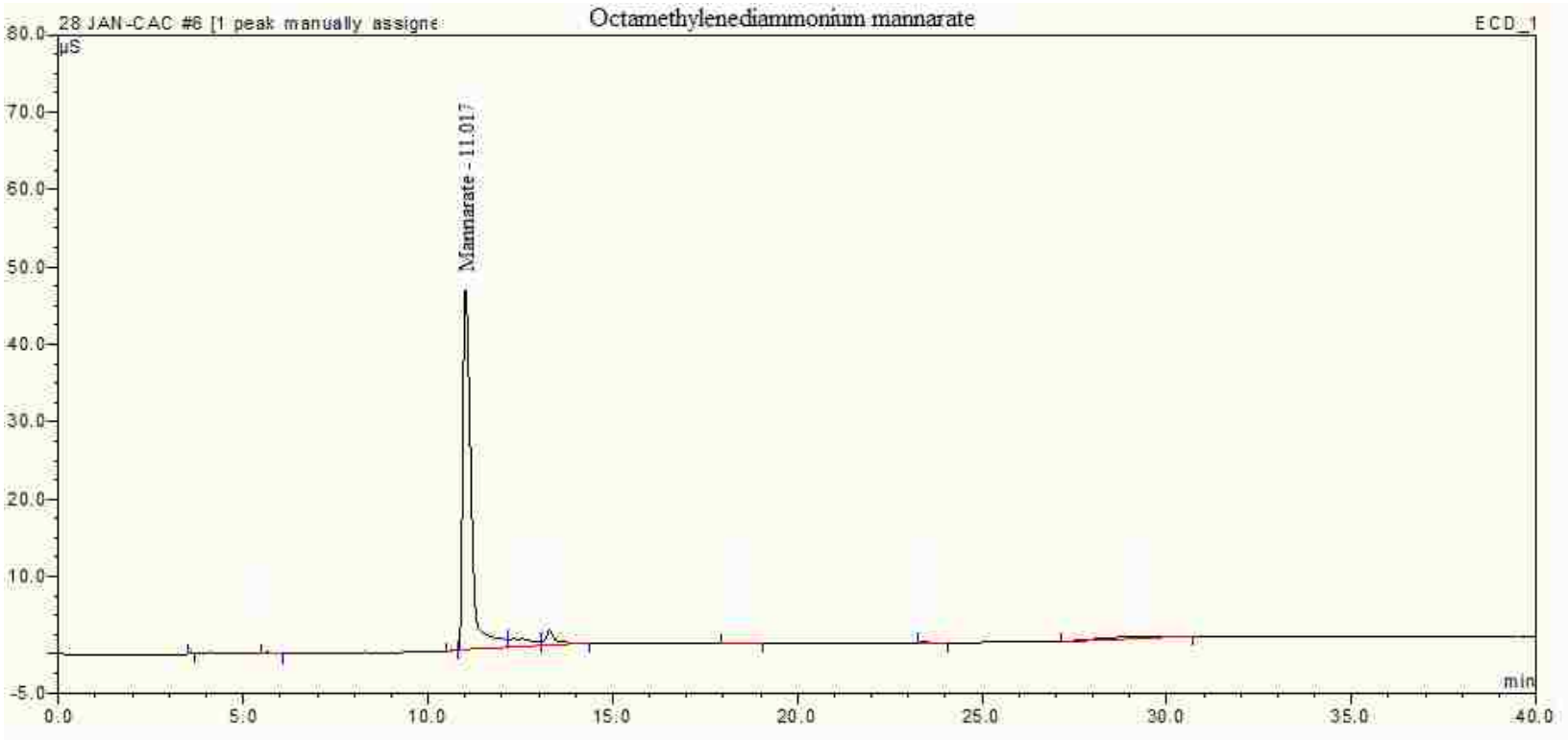

5.7.3 Ion chromatograph of Octamethylenediammonium D-mannarate

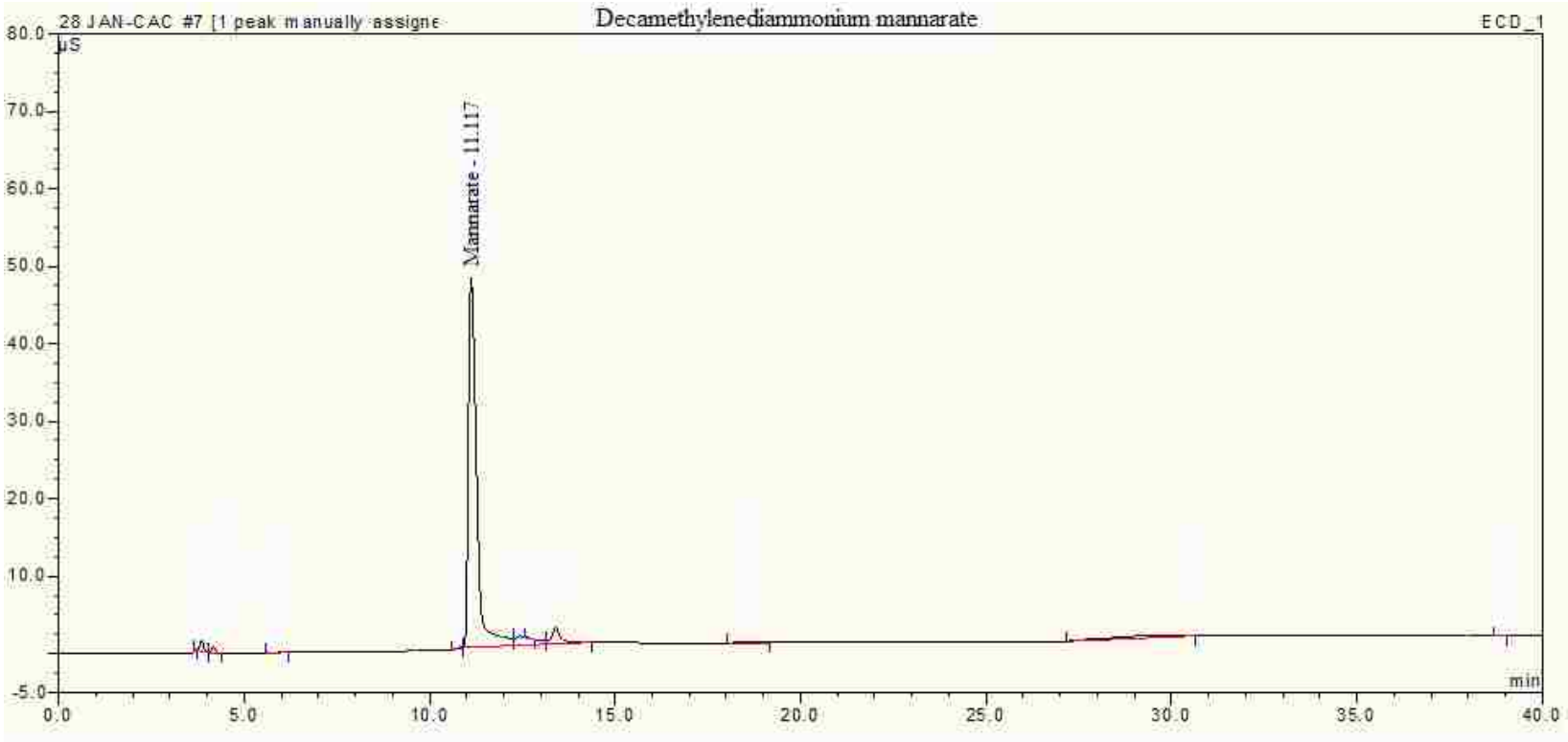

5.7.4 Ion chromatograph of decamethylenediammonium D-mannarate

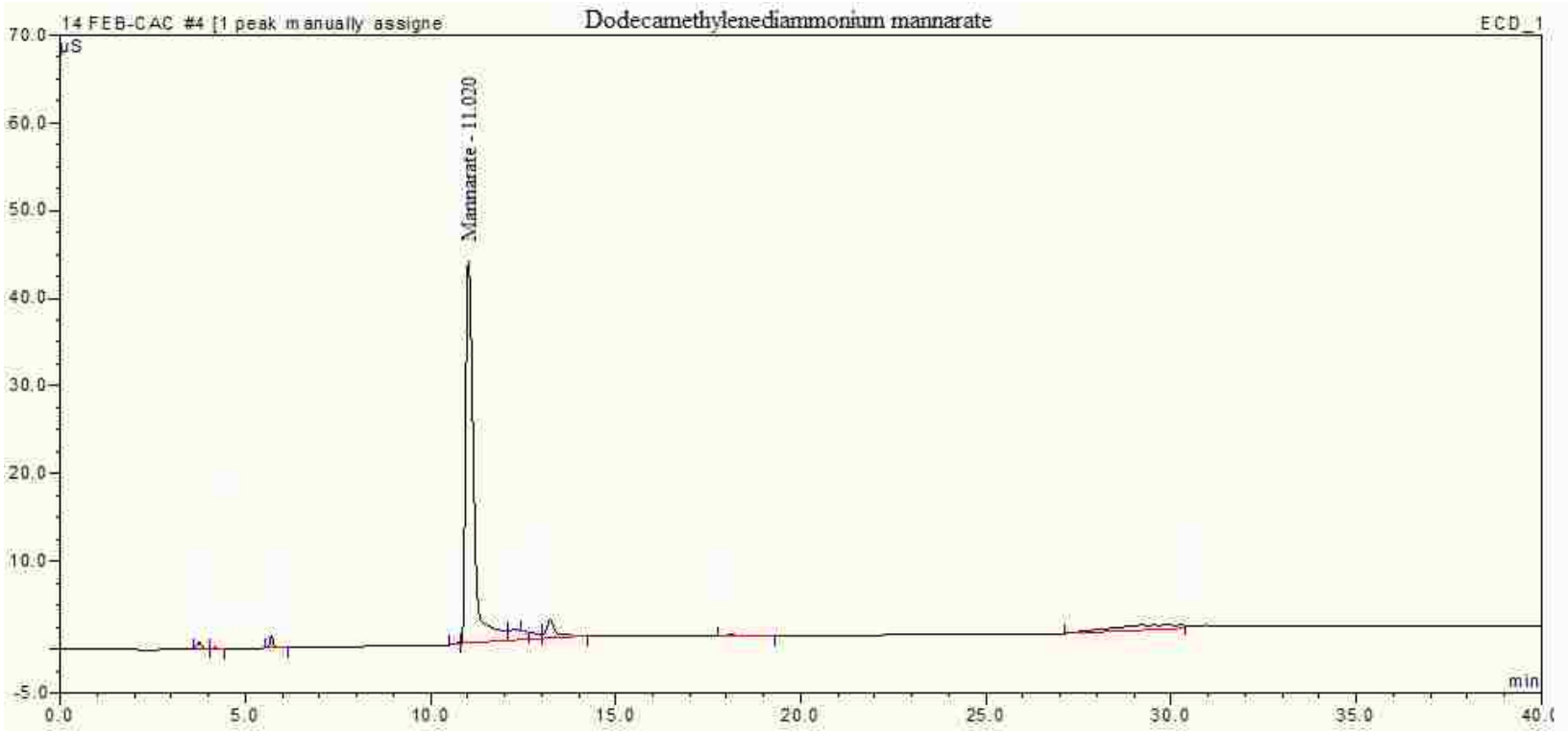

5.7.5 Ion chromatograph of dodecamethylenediammonium D-mannarate

5.8 Complete X-Ray Crystal Data for Octamethylenediammonium D-Mannarate (5d)

Table 1. Crystal data and structure refinement for Octamethylenediammonium D-mannarate (**5d**).

Identification code	cac0931as	
Empirical formula	C14 H30 N2 O8	
Formula weight	354.40	
Temperature	173(2) K	
Wavelength	1.54178 Å	
Crystal system	Orthorhombic	
Space group	P2(1)2(1)2(1)	
Unit cell dimensions	a = 5.44130(10) Å	α= 90°.
	b = 15.6027(3) Å	β= 90°.
	c = 20.8720(5) Å	γ = 90°.
Volume	1772.01(6) $Å^3$	
Z	4	
Density (calculated)	1.328 Mg/m^3	
Absorption coefficient	0.916 mm^{-1}	
F(000)	768	
Crystal size	0.27 x 0.25 x 0.16 mm^3	
Theta range for data collection	3.54 to 66.27°.	
Index ranges	-5<=h<=6, -18<=k<=15, -20<=l<=23	
Reflections collected	7699	
Independent reflections	2783 [R(int) = 0.0230]	
Completeness to theta = 66.27°	97.1 %	
Absorption correction	Semi-empirical from equivalents	
Max. and min. transmission	0.8673 and 0.7901	

Refinement method	Full-matrix least-squares on F^2
Data / restraints / parameters	2783 / 0 / 224
Goodness-of-fit on F^2	1.044
Final R indices [I>2sigma(I)]	R1 = 0.0249, wR2 = 0.0697
R indices (all data)	R1 = 0.0255, wR2 = 0.0702
Absolute structure parameter	0.04(14)
Extinction coefficient	0.00087(16)
Largest diff. peak and hole	0.146 and -0.117 e.$Å^{-3}$

Table 2. Atomic coordinates (x 10^4) and equivalent isotropic displacement parameters ($Å^2$x 10^3)
for octamethylenediammonium D-mannarate. U(eq) is defined as one third of the trace of the orthogonalized U^{ij} tensor.

	x	y	z	U(eq)
C(1)	-1784(3)	4025(1)	2360(1)	28(1)
C(2)	235(2)	3991(1)	2877(1)	22(1)
C(3)	-832(2)	3911(1)	3552(1)	22(1)
C(4)	1130(2)	3948(1)	4069(1)	22(1)
C(5)	24(2)	3813(1)	4740(1)	23(1)
C(6)	1981(3)	3784(1)	5271(1)	26(1)
C(7)	6187(3)	3568(1)	7021(1)	32(1)
C(8)	8524(3)	3402(1)	7394(1)	28(1)
C(9)	8100(3)	3516(1)	8112(1)	33(1)
C(10)	10423(3)	3423(1)	8512(1)	29(1)
C(11)	9950(3)	3635(1)	9213(1)	31(1)
C(12)	12199(3)	3552(1)	9644(1)	31(1)
C(13)	11711(3)	3907(1)	10311(1)	30(1)
C(14)	13936(3)	3861(1)	10746(1)	31(1)
N(1)	6552(2)	3408(1)	6325(1)	32(1)
N(2)	13522(2)	4366(1)	11339(1)	30(1)
O(1)	-1155(2)	4134(1)	1795(1)	50(1)
O(2)	-3972(2)	3930(1)	2527(1)	48(1)
O(3)	1722(2)	4736(1)	2818(1)	30(1)
O(4)	-2035(2)	3100(1)	3603(1)	27(1)
O(5)	2896(2)	3293(1)	3930(1)	27(1)

O(6)	-1658(2)	4486(1)	4867(1)	33(1)
O(7)	1349(2)	3946(1)	5833(1)	32(1)
O(8)	4145(2)	3577(1)	5115(1)	38(1)

Table 3. Bond lengths [Å] and angles [°] for octamethylenediammonium D-mannarate (Symmetry transformations used to generate equivalent atoms)

C(1)-O(1)	1.2393(17)	C(11)-C(12)	1.5245(19)	C(3)-C(2)-H(2)	108.2000
C(1)-O(2)	1.2491(18)	C(11)-H(11A)	0.9900	C(1)-C(2)-H(2)	108.2000
C(1)-C(2)	1.5414(17)	C(11)-H(11B)	0.9900	O(4)-C(3)-C(4)	107.61(10)
C(2)-O(3)	1.4214(15)	C(12)-C(13)	1.5218(19)	O(4)-C(3)-C(2)	108.43(10)
C(2)-C(3)	1.5278(17)	C(12)-H(12A)	0.9900	C(4)-C(3)-C(2)	112.61(10)
C(2)-H(2)	1.0000	C(12)-H(12B)	0.9900	O(4)-C(3)-H(3)	109.4000
C(3)-O(4)	1.4285(15)	C(13)-C(14)	1.5158(19)	C(4)-C(3)-H(3)	109.4000
C(3)-C(4)	1.5192(17)	C(13)-H(13A)	0.9900	C(2)-C(3)-H(3)	109.4000
C(3)-H(3)	1.0000	C(13)-H(13B)	0.9900	O(5)-C(4)-C(3)	107.44(10)
C(4)-O(5)	1.4322(15)	C(14)-N(2)	1.4839(17)	O(5)-C(4)-C(5)	110.46(10)
C(4)-C(5)	1.5382(17)	C(14)-H(14A)	0.9900	C(3)-C(4)-C(5)	111.50(10)
C(4)-H(4)	1.0000	C(14)-H(14B)	0.9900	O(5)-C(4)-H(4)	109.1000
C(5)-O(6)	1.4173(15)	N(1)-H(1A)	0.9100	C(3)-C(4)-H(4)	109.1000
C(5)-C(6)	1.5380(18)	N(1)-H(1B)	0.9100	C(5)-C(4)-H(4)	109.1000
C(5)-H(5)	1.0000	N(1)-H(1C)	0.9100	O(6)-C(5)-C(6)	109.54(10)
C(6)-O(7)	1.2492(16)	N(2)-H(2A)	0.9100	O(6)-C(5)-C(4)	108.75(10)
C(6)-O(8)	1.2637(18)	N(2)-H(2B)	0.9100	C(6)-C(5)-C(4)	112.91(11)
C(7)-N(1)	1.4869(18)	N(2)-H(2C)	0.9100	O(6)-C(5)-H(5)	108.5000
C(7)-C(8)	1.5134(19)	O(3)-H(3A)	0.8400	C(6)-C(5)-H(5)	108.5000
C(7)-H(7A)	0.9900	O(4)-H(4A)	0.8400	C(4)-C(5)-H(5)	108.5000
C(7)-H(7B)	0.9900	O(5)-H(5A)	0.8400	O(7)-C(6)-O(8)	123.38(13)
C(8)-C(9)	1.5258(19)	O(6)-H(6)	0.8400	O(7)-C(6)-C(5)	118.75(13)
C(8)-H(8A)	0.9900			O(8)-C(6)-C(5)	117.86(12)
C(8)-H(8B)	0.9900	O(1)-C(1)-O(2)	122.99(13)	N(1)-C(7)-C(8)	111.18(11)
C(9)-C(10)	1.522(2)	C(10)-C(11)-H(11B)	108.7000	H(14A)-C(14)-H(14B)	108.1000
C(9)-H(9A)	0.9900	C(12)-C(11)-H(11B)	108.7000	C(7)-N(1)-H(1A)	109.5000
C(9)-H(9B)	0.9900	H(11A)-C(11)-H(11B)	107.6000	C(7)-N(1)-H(1B)	109.5000

C(10)-C(11)	1.521(2)	C(13)-C(12)-C(11)	111.63(12)	H(1A)-N(1)-H(1B)	109.5000
C(10)-H(10A)	0.9900	C(13)-C(12)-H(12A)	109.3000	C(7)-N(1)-H(1C)	109.5000
C(10)-H(10B)	0.9900	C(11)-C(12)-H(12A)	109.3000	H(1A)-N(1)-H(1C)	109.5000
C(7)-C(8)-H(8A)	109.4000	C(13)-C(12)-H(12B)	109.3000	H(1B)-N(1)-H(1C)	109.5000
C(9)-C(8)-H(8A)	109.4000	C(11)-C(12)-H(12B)	109.3000	C(14)-N(2)-H(2A)	109.5000
C(7)-C(8)-H(8B)	109.4000	H(12A)-C(12)-H(12B)	108.0000	C(14)-N(2)-H(2B)	109.5000
C(9)-C(8)-H(8B)	109.4000	C(14)-C(13)-C(12)	113.10(12)	H(2A)-N(2)-H(2B)	109.5000
H(8A)-C(8)-H(8B)	108.0000	O(1)-C(1)-C(2)	118.32(12)	C(14)-N(2)-H(2C)	109.5000
C(10)-C(9)-C(8)	113.73(12)	O(2)-C(1)-C(2)	118.69(12)	H(2A)-N(2)-H(2C)	109.5000
C(10)-C(9)-H(9A)	108.8000	O(3)-C(2)-C(3)	111.34(11)	H(2B)-N(2)-H(2C)	109.5000
C(8)-C(9)-H(9A)	108.8000	O(3)-C(2)-C(1)	108.48(10)	C(2)-O(3)-H(3A)	109.5000
C(10)-C(9)-H(9B)	108.8000	C(3)-C(2)-C(1)	112.17(10)	C(3)-O(4)-H(4A)	109.5000
C(8)-C(9)-H(9B)	108.8000	O(3)-C(2)-H(2)	108.2000	C(4)-O(5)-H(5A)	109.5000
H(9A)-C(9)-H(9B)	107.7000	C(14)-C(13)-H(13A)	109.0000	C(5)-O(6)-H(6)	109.5000
C(11)-C(10)-C(9)	111.52(12)	C(12)-C(13)-H(13A)	109.0000	N(1)-C(7)-H(7A)	109.4000
C(11)-C(10)-H(10A)	109.3000	C(14)-C(13)-H(13B)	109.0000	C(8)-C(7)-H(7A)	109.4000
C(9)-C(10)-H(10A)	109.3000	C(12)-C(13)-H(13B)	109.0000	N(1)-C(7)-H(7B)	109.4000
C(11)-C(10)-H(10B)	109.3000	H(13A)-C(13)-H(13B)	107.8000	C(8)-C(7)-H(7B)	109.4000
C(9)-C(10)-H(10B)	109.3000	N(2)-C(14)-C(13)	110.73(11)	H(7A)-C(7)-H(7B)	108.0000
H(10A)-C(10)-H(10B)	108.0000	N(2)-C(14)-H(14A)	109.5000	C(7)-C(8)-C(9)	110.98(12)
C(10)-C(11)-C(12)	114.40(12)	C(13)-C(14)-H(14A)	109.5000		
C(10)-C(11)-H(11A)	108.7000	N(2)-C(14)-H(14B)	109.5000		
C(12)-C(11)-H(11A)	108.7000	C(13)-C(14)-H(14B)	109.5000		

Table 4. Anisotropic displacement parameters ($Å^2 x\ 10^3$) for octamethylenediammonium D-mannarate. The anisotropic displacement factor exponent takes the form: $-2\pi^2[\ h^2\ a^{*2}U^{11} + ...\ + 2\ h\ k\ a^*\ b^*\ U^{12}\ ]$

	U^{11}	U^{22}	U^{33}	U^{23}	U^{13}	U^{12}
C(1)	27(1)	34(1)	22(1)	1(1)	-5(1)	-1(1)
C(2)	21(1)	26(1)	20(1)	2(1)	-1(1)	1(1)
C(3)	20(1)	25(1)	21(1)	0(1)	-1(1)	2(1)
C(4)	21(1)	26(1)	20(1)	0(1)	1(1)	-1(1)
C(5)	22(1)	27(1)	20(1)	-1(1)	1(1)	1(1)
C(6)	29(1)	28(1)	20(1)	1(1)	-2(1)	-3(1)
C(7)	34(1)	33(1)	29(1)	-7(1)	-7(1)	5(1)
C(8)	28(1)	33(1)	23(1)	-3(1)	-4(1)	-1(1)
C(9)	34(1)	41(1)	24(1)	-7(1)	-4(1)	4(1)
C(10)	35(1)	31(1)	22(1)	0(1)	-3(1)	-1(1)
C(11)	36(1)	34(1)	24(1)	-3(1)	-5(1)	1(1)
C(12)	35(1)	34(1)	24(1)	-1(1)	-5(1)	3(1)
C(13)	32(1)	35(1)	24(1)	-2(1)	-6(1)	0(1)
C(14)	34(1)	34(1)	26(1)	0(1)	-8(1)	4(1)
N(1)	38(1)	33(1)	25(1)	3(1)	-13(1)	-6(1)
N(2)	34(1)	34(1)	23(1)	3(1)	-10(1)	1(1)
O(1)	38(1)	90(1)	22(1)	9(1)	-7(1)	-12(1)
O(2)	24(1)	90(1)	32(1)	0(1)	-6(1)	0(1)
O(3)	26(1)	34(1)	28(1)	5(1)	-2(1)	-6(1)
O(4)	21(1)	32(1)	27(1)	2(1)	-3(1)	-4(1)
O(5)	21(1)	40(1)	21(1)	-3(1)	-1(1)	6(1)

O(6)	29(1)	39(1)	31(1)	-6(1)	4(1)	9(1)
O(7)	43(1)	34(1)	18(1)	-1(1)	-1(1)	-3(1)
O(8)	25(1)	65(1)	25(1)	3(1)	-5(1)	4(1)

Table 5. Hydrogen coordinates (x 10^4) and isotropic displacement parameters ($Å^2$x 10^3) for octamethylenediammonium D-mannarate.

	x	y	z	U(eq)
H(2)	1289	3478	2793	27
H(3)	-2054	4379	3624	27
H(4)	1958	4520	4053	27
H(5)	-895	3258	4741	27
H(7A)	4865	3191	7184	38
H(7B)	5666	4170	7086	38
H(8A)	9819	3804	7249	34
H(8B)	9101	2812	7308	34
H(9A)	7390	4091	8188	40
H(9B)	6883	3086	8257	40
H(10A)	11038	2827	8478	35
H(10B)	11707	3810	8342	35
H(11A)	8647	3250	9376	37
H(11B)	9326	4230	9241	37
H(12A)	12665	2940	9678	37
H(12B)	13594	3864	9449	37
H(13A)	11181	4512	10273	36
H(13B)	10346	3581	10508	36
H(14A)	14266	3256	10860	38
H(14B)	15392	4087	10518	38

H(1A)	7856	3720	6183	48
H(1B)	5177	3566	6107	48
H(1C)	6847	2841	6260	48
H(2A)	13598	4936	11246	46
H(2B)	14699	4234	11632	46
H(2C)	12014	4240	11502	46
H(3A)	3199	4591	2773	44
H(4A)	-3424	3128	3429	40
H(5A)	3861	3240	4241	41
H(6)	-3044	4278	4952	50

Table 6. Torsion angles [°] for octamethylenediammonium D-mannarate.

O(1)-C(1)-C(2)-O(3)	53.01(17)
O(2)-C(1)-C(2)-O(3)	-127.91(15)
O(1)-C(1)-C(2)-C(3)	176.41(13)
O(2)-C(1)-C(2)-C(3)	-4.5(2)
O(3)-C(2)-C(3)-O(4)	-172.64(10)
C(1)-C(2)-C(3)-O(4)	65.58(13)
O(3)-C(2)-C(3)-C(4)	-53.68(14)
C(1)-C(2)-C(3)-C(4)	-175.45(10)
O(4)-C(3)-C(4)-O(5)	63.92(12)
C(2)-C(3)-C(4)-O(5)	-55.53(13)
O(4)-C(3)-C(4)-C(5)	-57.25(13)
C(2)-C(3)-C(4)-C(5)	-176.70(11)
O(5)-C(4)-C(5)-O(6)	178.35(10)
C(3)-C(4)-C(5)-O(6)	-62.26(13)
O(5)-C(4)-C(5)-C(6)	56.56(13)
C(3)-C(4)-C(5)-C(6)	175.95(10)
O(6)-C(5)-C(6)-O(7)	36.47(16)
C(4)-C(5)-C(6)-O(7)	157.82(12)
O(6)-C(5)-C(6)-O(8)	-145.00(12)
C(4)-C(5)-C(6)-O(8)	-23.65(17)
N(1)-C(7)-C(8)-C(9)	-176.63(11)
C(7)-C(8)-C(9)-C(10)	-175.75(12)
C(8)-C(9)-C(10)-C(11)	173.92(12)
C(9)-C(10)-C(11)-C(12)	179.76(12)

C(10)-C(11)-C(12)-C(13)	170.91(12)
C(11)-C(12)-C(13)-C(14)	-178.08(12)
C(12)-C(13)-C(14)-N(2)	168.71(12)

Symmetry transformations used to generate equivalent atoms:

Table 7. Hydrogen bonds for octamethylenediammonium D-mannarate [Å and °].

D-H...A	d(D-H)	d(H...A)	d(D...A)	<(DHA)
N(1)-H(1B)...O(8)	0.91	2.15	2.8576(14)	134.4
N(1)-H(1B)...O(7)	0.91	2.24	3.1262(16)	164.6
O(5)-H(5A)...O(8)	0.84	1.90	2.6036(13)	139.9
O(4)-H(4A)...O(2)	0.84	2.28	2.7994(14)	120.3
N(1)-H(1A)...O(7)#1	0.91	2.07	2.9278(17)	157.5
O(3)-H(3A)...O(2)#1	0.84	1.92	2.7278(15)	160.1
N(1)-H(1C)...O(5)#2	0.91	1.90	2.8044(15)	171.8
N(1)-H(1C)...O(4)#2	0.91	2.59	3.0606(15)	113.0
N(2)-H(2A)...O(7)#3	0.91	1.95	2.8375(15)	166.0
N(2)-H(2B)...O(2)#4	0.91	2.06	2.9101(15)	155.5
N(2)-H(2B)...O(1)#4	0.91	2.29	3.0705(16)	144.1
N(2)-H(2C)...O(1)#5	0.91	1.84	2.7410(17)	172.0
O(4)-H(4A)...O(5)#6	0.84	2.27	2.8577(13)	126.8
O(6)-H(6)...O(8)#6	0.84	1.91	2.7375(15)	167.8

Symmetry transformations used to generate equivalent atoms:

#1 x+1,y,z #2 x+1/2,-y+1/2,-z+1 #3 -x+3/2,-y+1,z+1/2

#4 x+2,y,z+1 #5 x+1,y,z+1 #6 x-1,y,z

5.9 Poly(Alkylene D-mannaramide) Prepolymer ^{1}H NMR Spectra

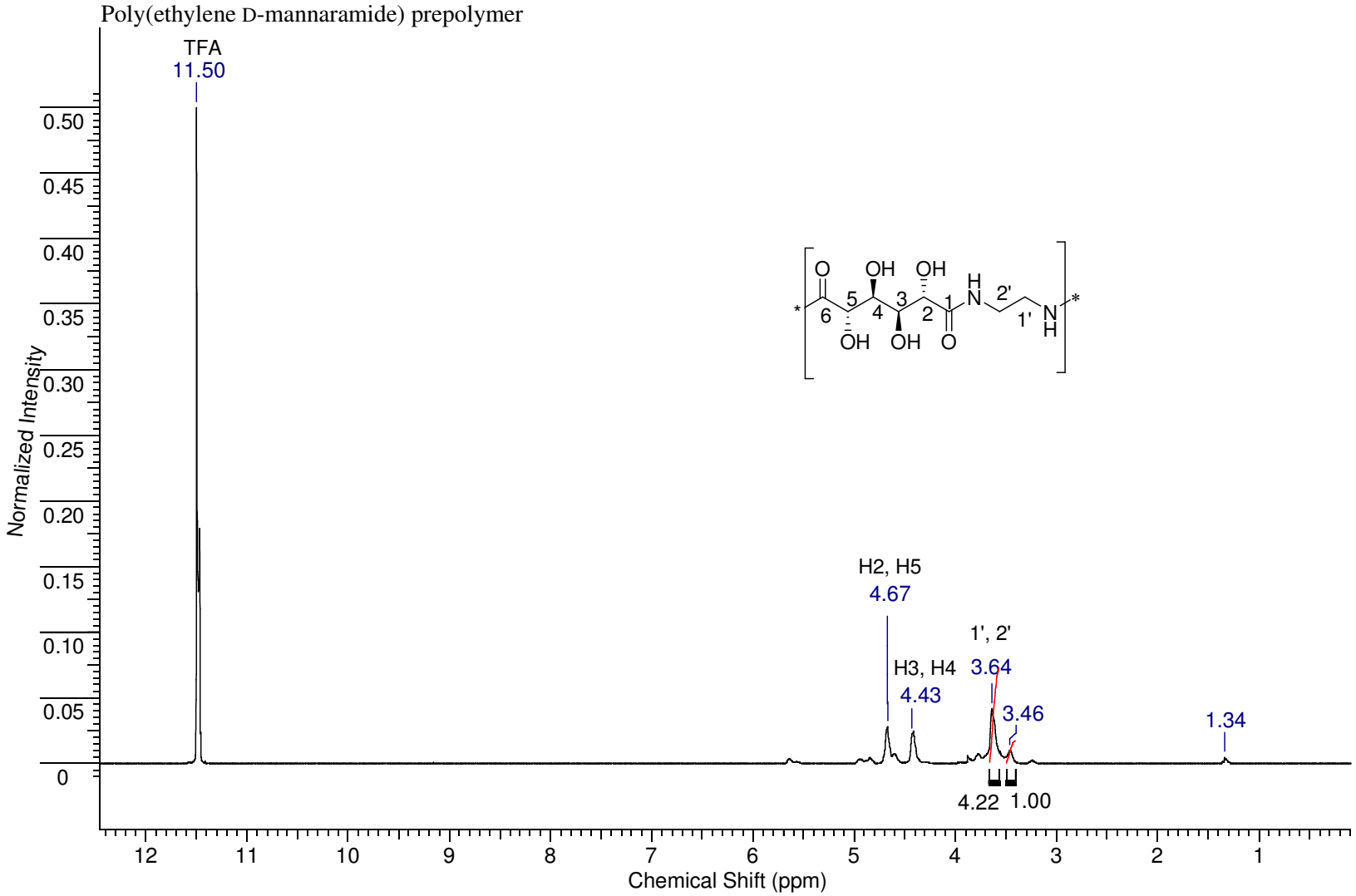

5.9.1 ^{1}H NMR of poly(ethylene D-mannaramide) prepolymer in TFA-*d1*

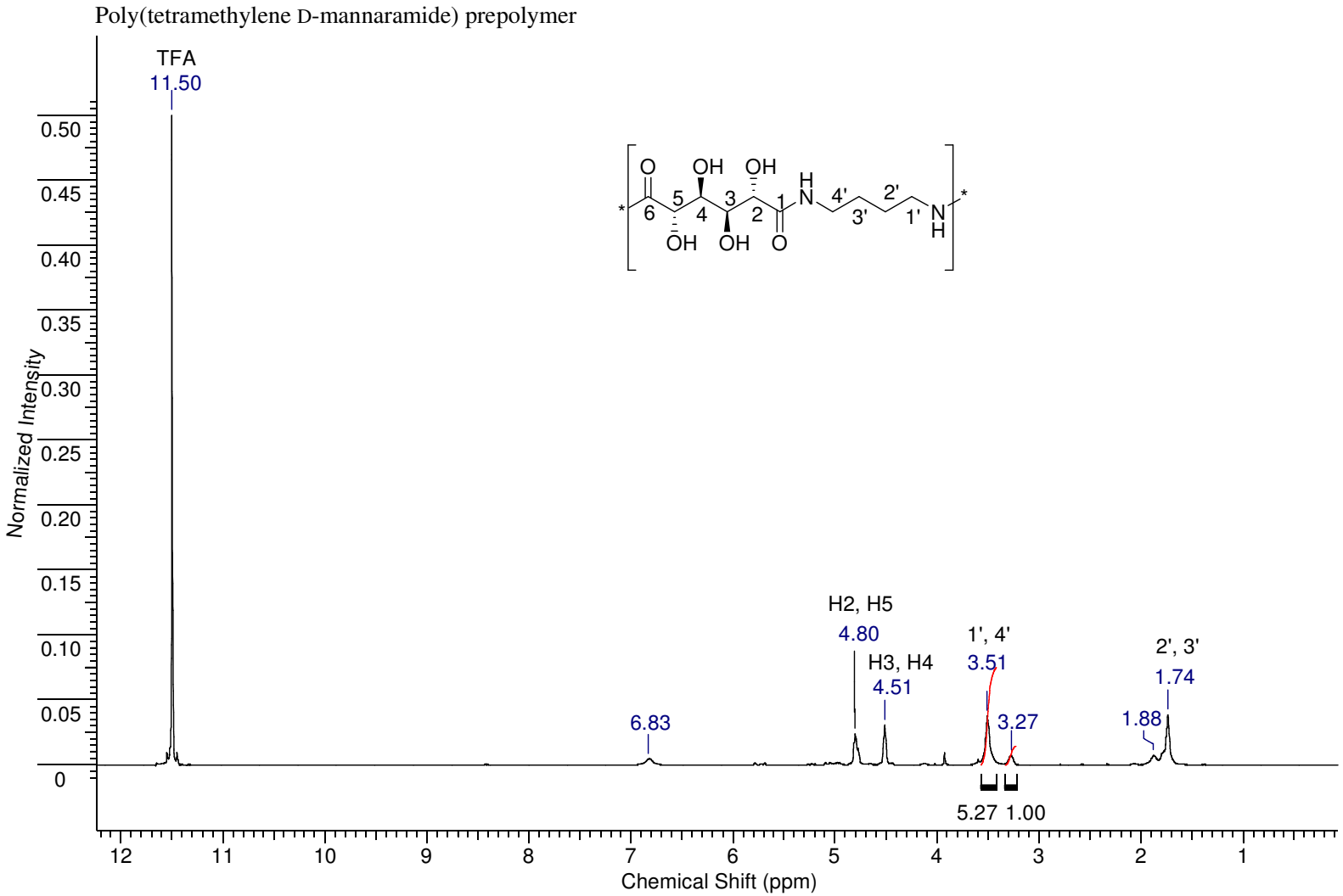

5.9.2 ^{1}H NMR of poly(tetramethylene D-mannaramide) prepolymer in TFA-*d1*

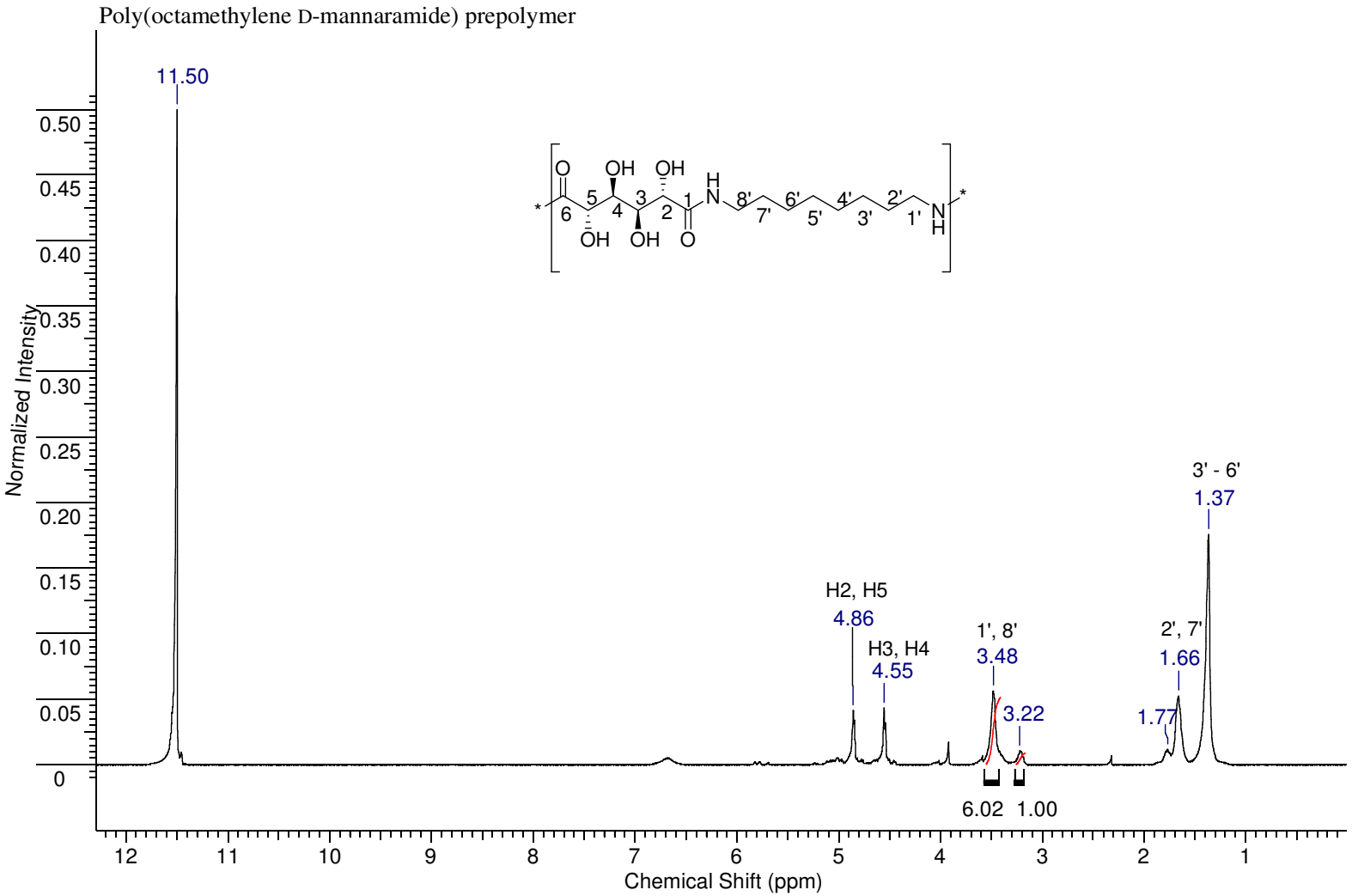

5.9.3 ^{1}H NMR of poly(octamethylene D-mannaramide) prepolymer in TFA-*d1*

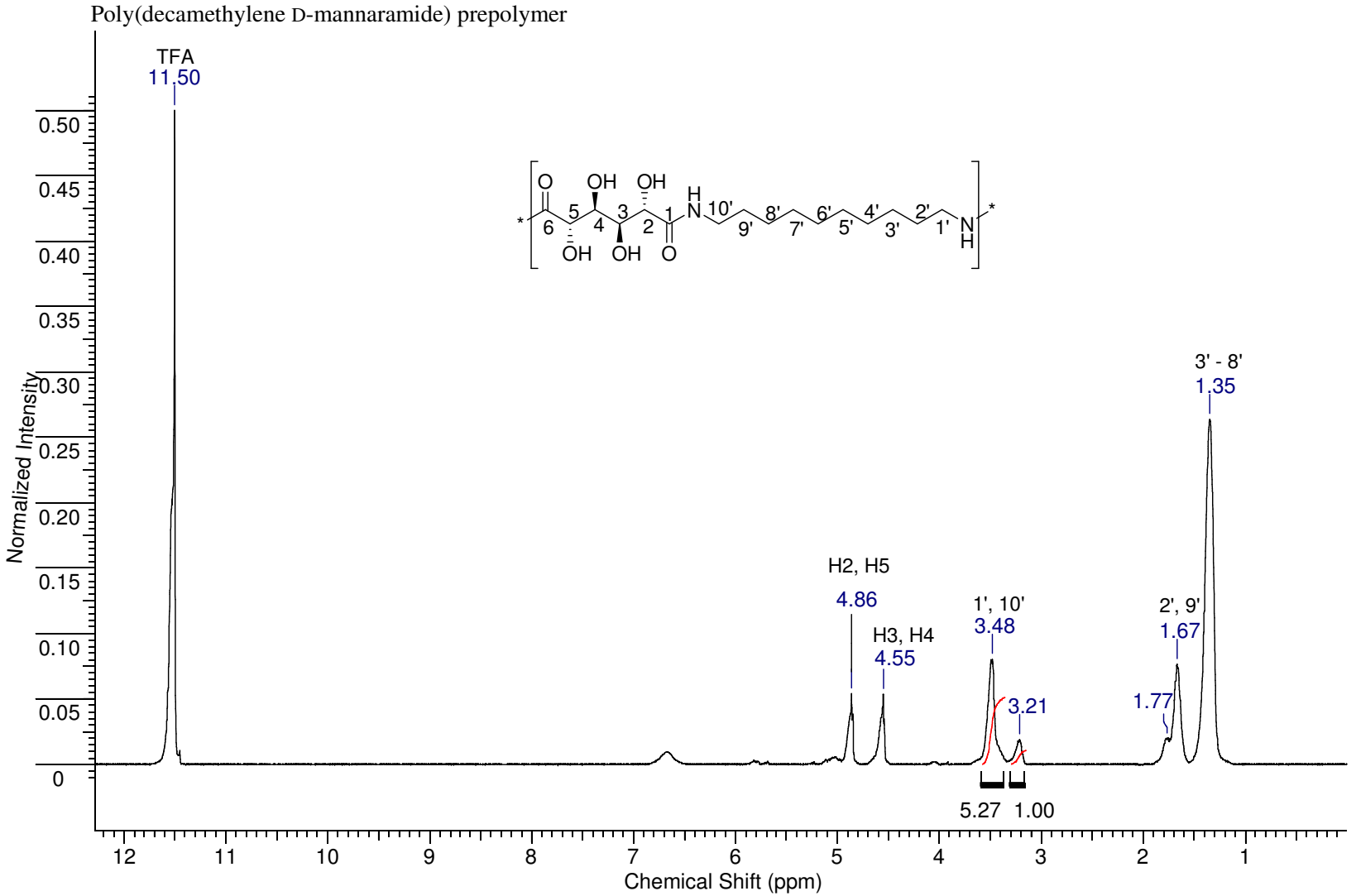

5.9.4 ^{1}H NMR of poly(decamethylene D-mannaramide) prepolymer in TFA-*d1*

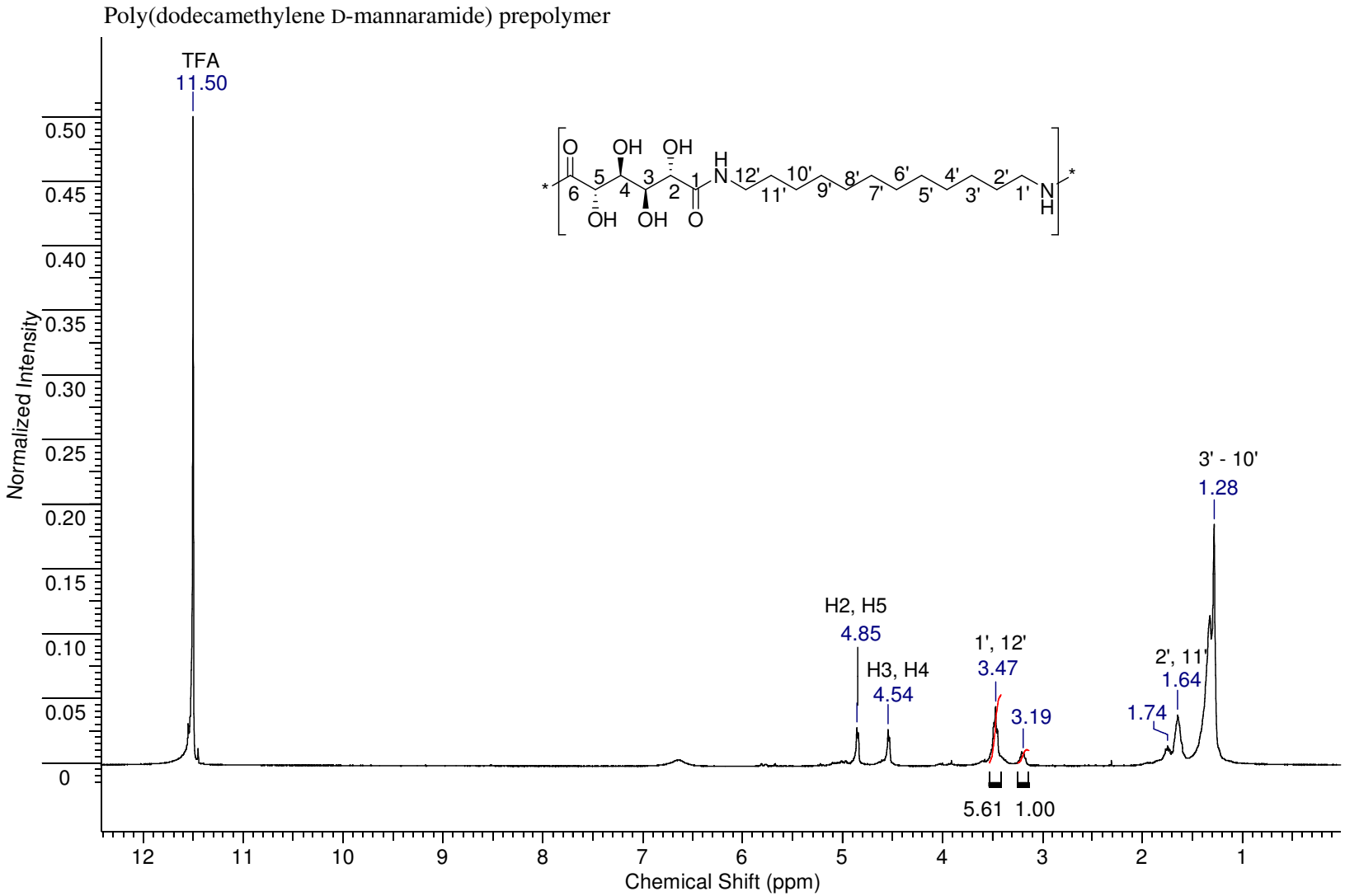

5.9.5 ^{1}H NMR of poly(dodecamethylene D-mannaramide) prepolymer in TFA-*d1*

5.10 Poly(Alkylene D-mannaramide) Postpolymer ^{1}H NMR Spectra

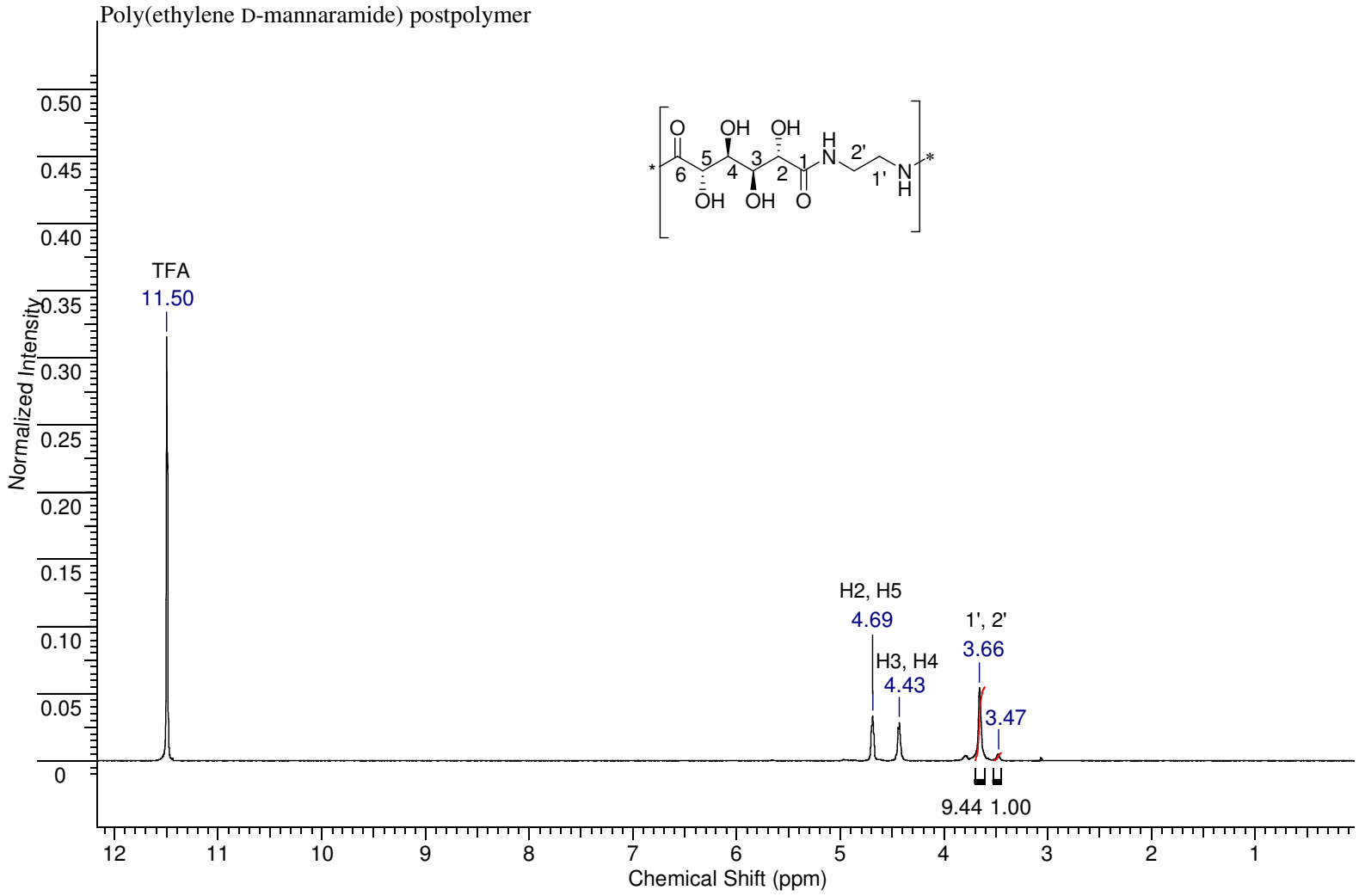

5.10.1 ^{1}H NMR of poly(ethylene D-mannaramide) postpolymer in TFA-*d1*

Poly(tetramethylene D-mannaramide) postpolymer

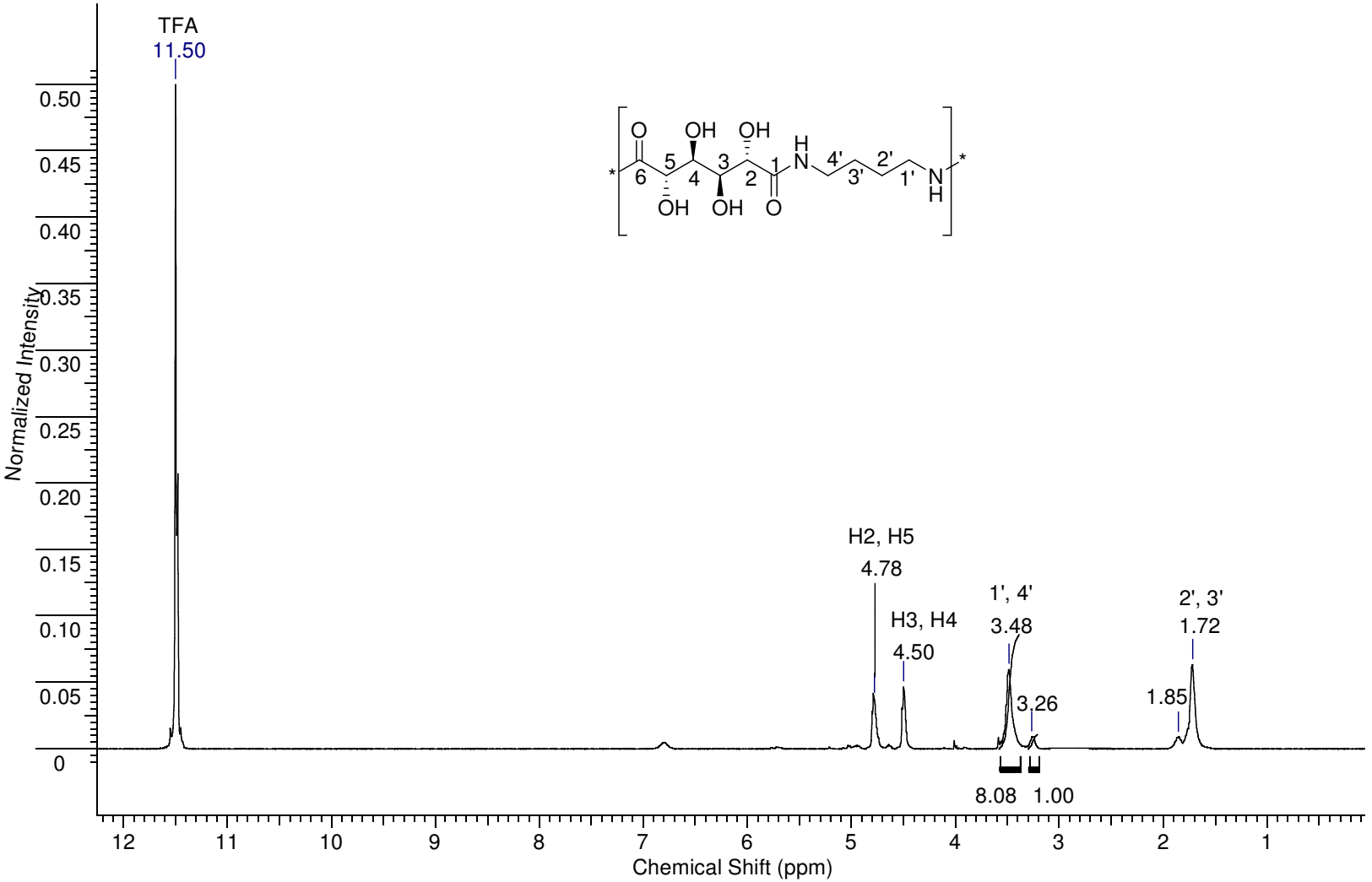

5.10.2 ^{1}H NMR of poly(tetramethylene D-mannaramide) postpolymer in TFA-*d1*

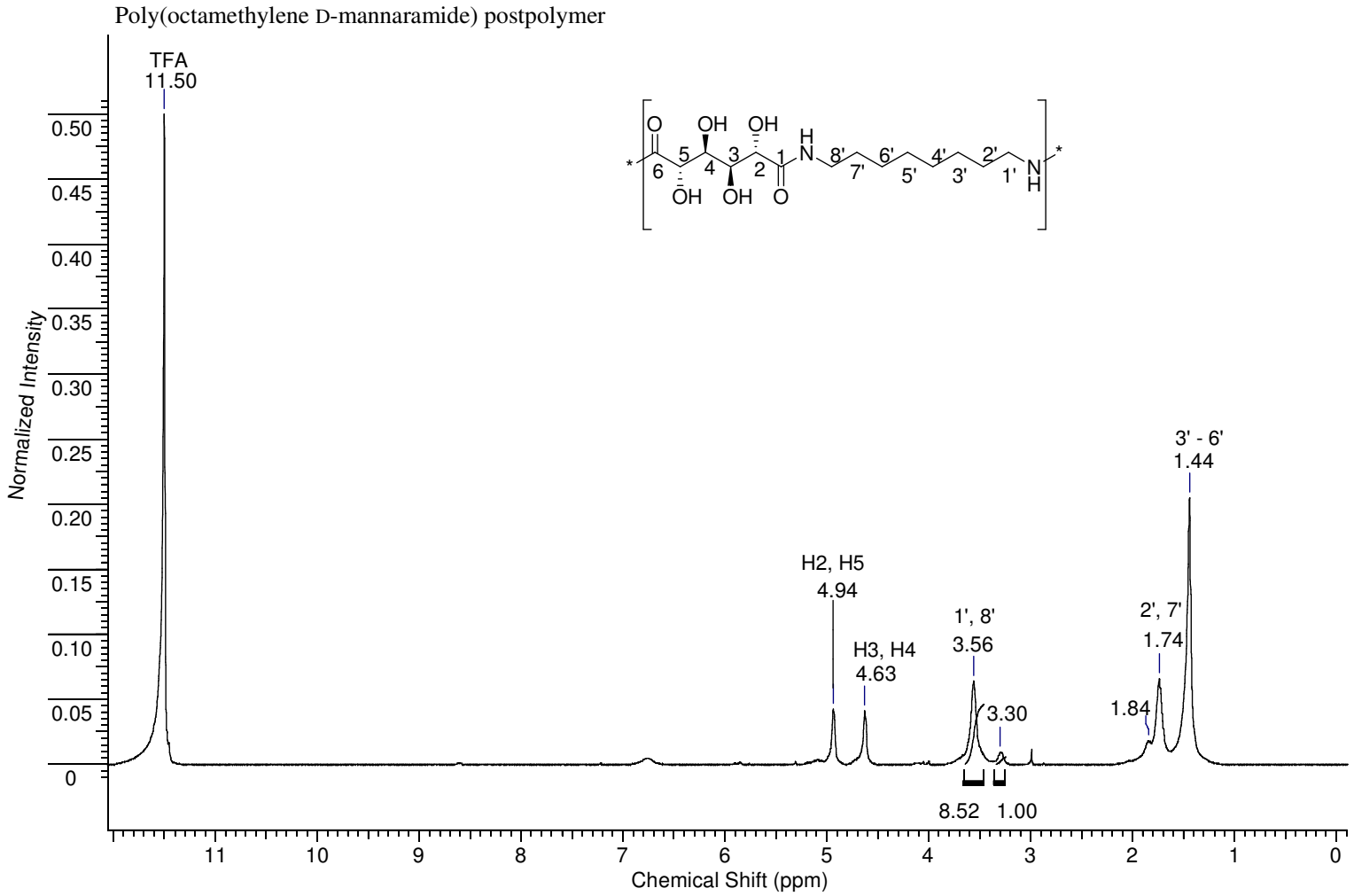

5.10.3 ^{1}H NMR of poly(octamethylene D-mannaramide) postpolymer in TFA-*d1*

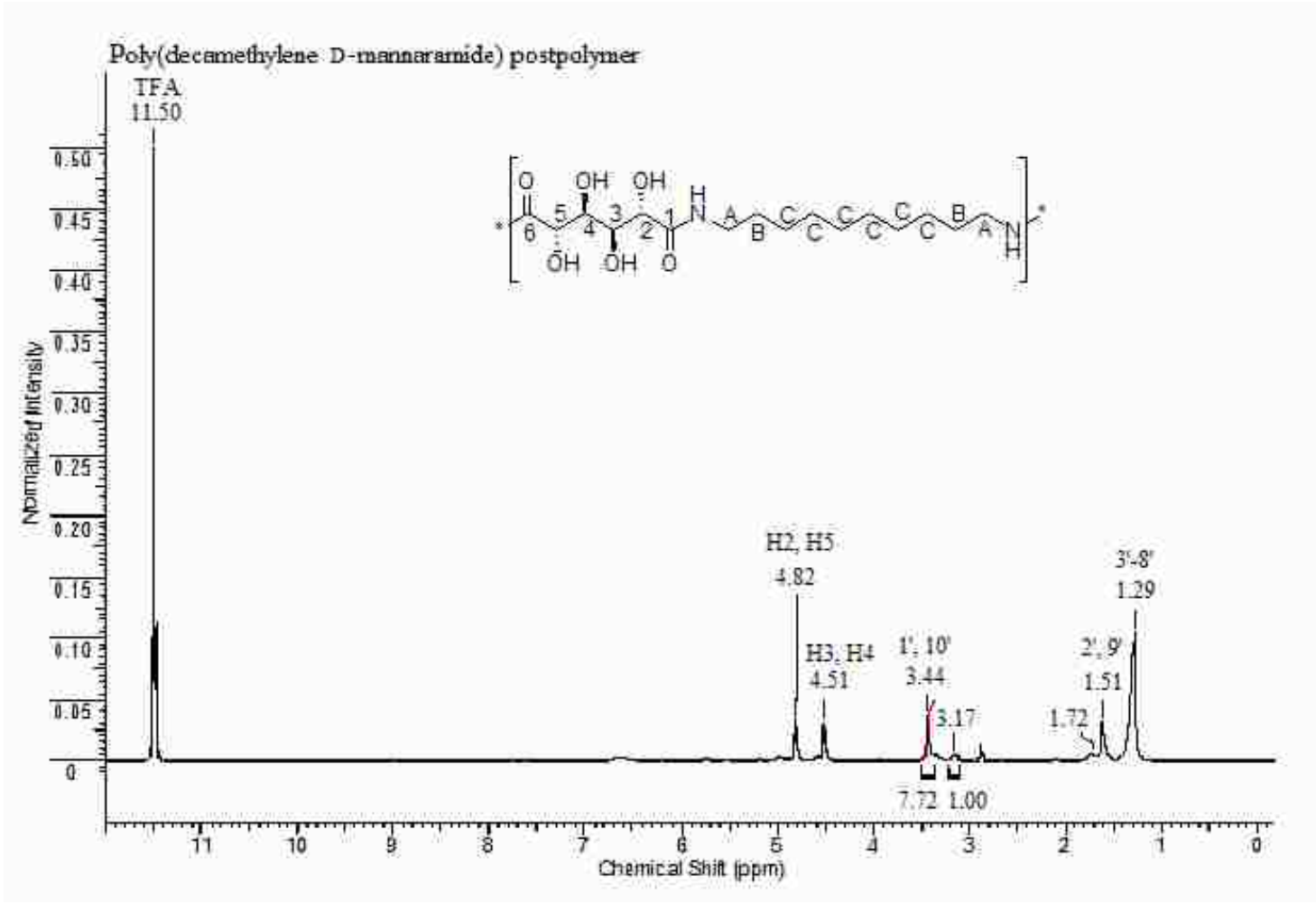

5.10.4 ^{1}H NMR of poly(decamethylene D-mannaramide) postpolymer in TFA-$_{d1}$

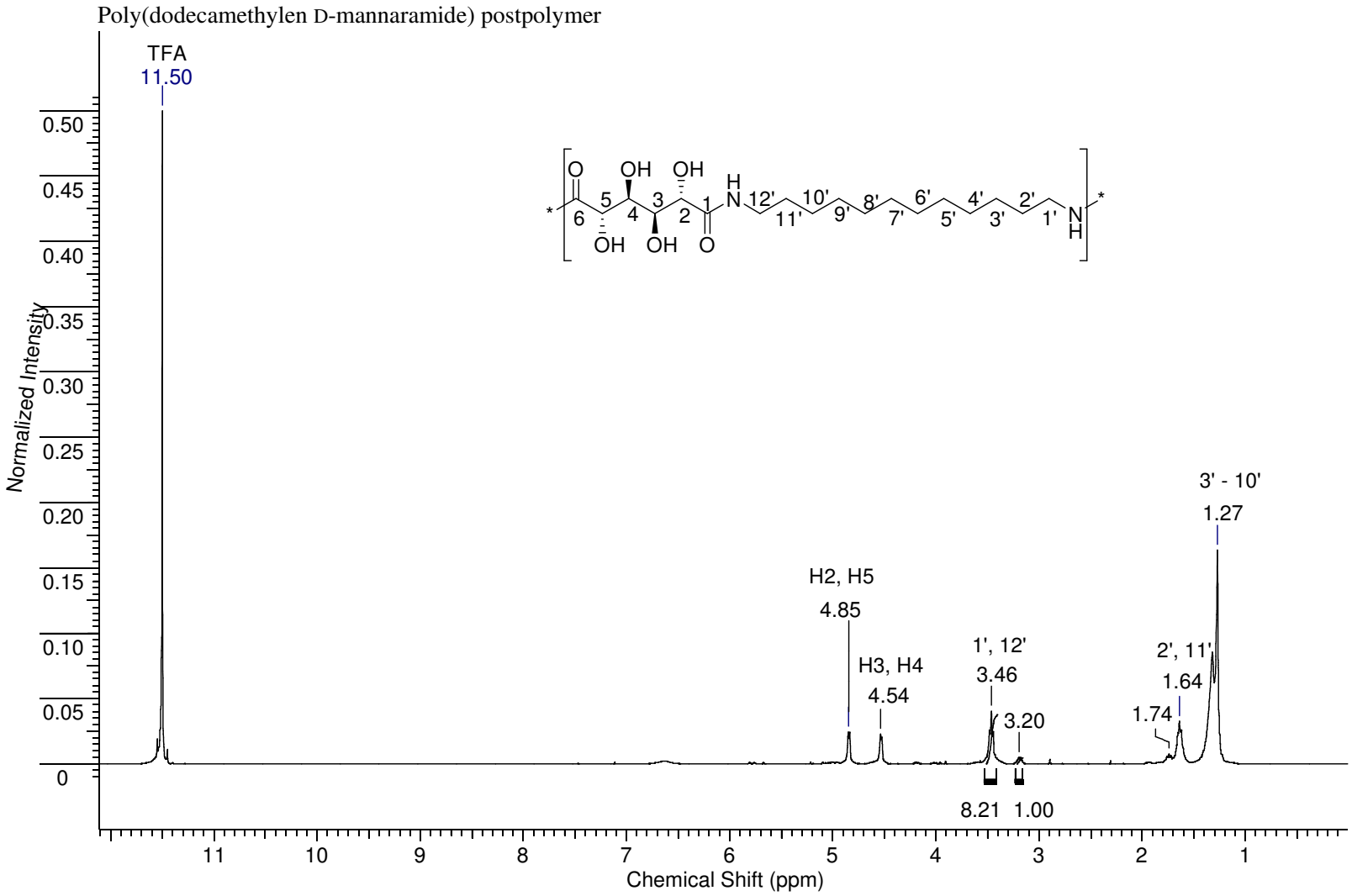

5.10.5 ^{1}H NMR of poly(dodecamethylene D-mannaramide) postpolymer in TFA-*d1*